Protein kinase D (PKD) mouse models – towards an understanding of the physiological role of PKD

EDITED BY DR MOHAMMAD MAHMOUD

Index

Summary

The three members of the protein kinase D (PKD) family, PKD1-3, have been identified as serine/threonine kinases with functions in fundamental cellular processes as diverse as adhesion and motility, proliferation and differentiation, membrane and protein trafficking, regulation of gene expression, apoptosis, and oxidative stress signaling. Numerous *in vitro* studies addressed cell context dependent activation and functional principles of the PKD isoforms. Thus, the molecular mechanisms of PKD regulation and functions are well understood today. However, research about the role of PKD family members *in vivo* is still in its infancy.

Due to its structural characteristics PKD3 is supposed to play a unique role among the three isoforms. In this study, the expression pattern of PKD3 during mouse development was investigated by immunohistochemistry. The expression is differentially regulated throughout early embryogenesis and organogenesis. Compared to other isoforms PKD3 is expressed more ubiquitously, implicating distinct and non-redundant functions within the PKD family.

To further elucidate the potential role of PKD *in vivo*, transgenic mice overexpressing dominant-negative PKD mutants in an inducible and tissue specific manner were generated. Several transgenic lines for each of the three isoforms were established, genetically characterized and analyzed concerning transgene inducibility, expression level, biodistribution, and subcellular localization. For PKD1 and PKD2 transgenic lines were identified to facilitate a considerable overexpression of dominant-negative PKD compared to endogenous PKD, which is required to create a "functional knockout".

To identify potential phenotypes provoked by skeletal muscle-specific transgene expression the response of mice to voluntary wheel running was studied. The running performance of mice expressing dominant-negative PKD1 was significantly decreased compared to control mice. Analysis of skeletal muscle fiber type composition after voluntary wheel running revealed that exercise-induced muscle remodeling was blocked in animals with transgene expression. Therefore, our data clearly indicate for the first time in a physiological *in vivo* model that PKD plays a fundamental role in the regulation of exercise-induced skeletal muscle remodeling.

Another functional consequence of transgene expression was observed in the brain. Overexpression of dominant-negative PKD1 in the hippocampus was found to interfere with neuronal Golgi morphology, a result which confirmed previous *in vitro* data. Together, these findings implicate a key role of PKD in the regulation of neuronal Golgi organization.

We conclude that the newly established transgenic mouse model serves as a valuable tool for the analysis of PKD functions in a physiological context and is useful for further studies in this field.

Zusammenfassung

Die drei Isoformen der Protein kinase D (PKD) Familie, PKD1-3, gehören zu den Serin/Threonin-spezifischen Proteinkinasen und regulieren vielfältige zelluläre Funktionen, wie beispielsweise Zelladhäsion und Zellbewegung, Proliferation und Differenzierung, Vesikeltransport, Genexpression, Apoptose und Reaktionen auf oxidativen Stress. Zahlreiche *in vitro* Studien beschäftigten sich mit den Prinzipien der Aktivierung und den Funktionen der PKD Isoformen mit der Folge, dass die molekularen Mechanismen der PKD Regulation heute in Grundzügen verstanden sind. Informationen über die Funktion der PKD-Isoformen im intakten Organismus (*in vivo*) sind allerdings kaum vorhanden.

Aufgrund ihrer strukturellen Besonderheiten wird davon ausgegangen, dass PKD3 eine besondere Funktion unter den drei Isoformen ausübt. In der vorliegenden Studie wurde die Expression von PKD3 in der embryonalen Mausentwicklung mit immunohistochemischen Methoden untersucht. In der frühen Embryonalentwicklung und Organogenese wird die Expression von PKD3 differenziell reguliert. Im Vergleich zu den anderen Isoformen erfolgt die PKD3-Expression allerdings eher ubiquitär, was eine individuelle und nicht-redundante Genfunktion innerhalb der PKD Familie vermuten lässt.

Um eine funktionelle Untersuchung von PKD unter physiologischen Bedingungen zu ermöglichen, wurden in dieser Arbeit außerdem transgene Mäuse hergestellt, in denen durch induzierbare und gewebsspezifische Überexpression dominant-negativer PKD-Varianten ein „funktioneller PKD-Knockout" herbeigeführt werden kann. Für jede der drei Isoformen wurden transgene Mauslinien etabliert, genetisch charakterisiert und bezüglich der Induzierbarkeit, des Expressionslevels, der gewebsspezifischen Verteilung und der subzellulären Lokalisation der modifizierten Proteine analysiert. Für PKD1 und PKD2 wurden transgene Mauslinien identifiziert, die eine deutliche Überexpression der dominant-negativen PKD Isoformen im Vergleich zum endogenen PKD Expressionslevel ermöglichen. Dies ist eine Voraussetzung für die Erzeugung eines „funktionellen PKD-Knockouts".

Um potentielle phänotypische Effekte, die durch Skelettmuskel-spezifische Transgenexpression hervorgerufen wurden, zu untersuchen, wurde das Verhalten der Mäuse in Laufradexperimenten analysiert. Es zeigte sich, dass die Laufleistung von Mäusen, die dominant-negatives PKD1 Protein exprimieren, im Vergleich zu Kontrollmäusen signifikant reduziert ist. Desweiteren zeigten Analysen der Fasertyp-Zusammensetzung, dass in Tieren mit Transgenexpression die Remodellierung des Muskels, welche normalerweise durch Training induziert wird, blockiert ist. Somit implizieren unsere Daten eine entscheidende Funktion von PKD in der Regulation dieses physiologischen Vorgangs.

Auch im Gehirn wurden Auswirkungen der Transgenexpression beobachtet. Überexpression dominant-negativer PKD1 führte hier auf zellulärer Ebene zu Veränderungen der Morphologie des Golgi-Apparates. Dieses Resultat ist in bester Übereinstimmung mit früheren Befunden aus *in vitro* Untersuchungen. Gemeinsam betrachtet weisen diese Ergebnisse auf eine wichtige Rolle von PKD in der Regulation und Organisation des Golgi-Apparates in Neuronen hin.
Zusammenfassend zeigen die Ergebnisse dieser Arbeit, dass diese neu generierten transgenen Mauslinien wertvolle Modellsysteme darstellen, mit denen sich die Bedeutung von PKD in physiologischen Zusammenhängen untersuchen lassen. Mit diesen Mauslinien eröffnen sich nun zahlreiche Möglichkeiten, gewebsspezifische und globale PKD-Funktionen *in vivo* zu analysieren.

Introduction

PKD classification and structure

The protein kinase D (PKD) family of serine/threonine protein kinases comprises 3 isoforms in mammals. The first member was identified in 1994, originally termed PKD or PKCμ (Johannes et al., 1994; Valverde et al., 1994), and is today referred to as PKD1 (gene name *PRKD1*, GeneID 18760 [*Mus musculus*], GeneID 5587 [*Homo sapiens*]). PKD1 is up to now the most extensively characterized member of the PKD family. Next, a kinase initially designated PKCv was described (Hayashi et al., 1999) and was attributed to a novel subgroup of the PKC family, together with PKCμ. Today PKCvis termed PKD3 (gene name *PRKD3*, Gene ID 75292 [*Mus musculus*], GeneID 23683 [*Homo sapiens*]). More recently PKD2 (gene name *PRKD2*, Gene ID 101540 [*Mus musculus*], GeneID 25865 [*Homo sapiens*]) has been discovered (Sturany et al., 2001).

PKD1, PKD2 and PKD3 are similar in their overall structure and exhibit a high degree of sequence homology (Figure 1). They share a modular structure containing a N-terminal regulatory domain and a conserved C-terminal catalytic domain, exhibiting high sequence homology for the three isoforms. The regulatory domains of both, PKD1 and PKD2 contain a stretch of highly hydrophobic amino acid residues (mainly alanine and proline), which is absent in PKD3. All three isoforms contain two cystein-rich zinc-finger domains (also called CRD1 and CRD2) separated by a linker region. In PKD2 this linker region contains a serine-rich stretch of amino acids. All PKDs possess an acidic domain rich in negatively charged amino acids (Gschwendt et al., 1997) and a pleckstrin homology (PH) domain.

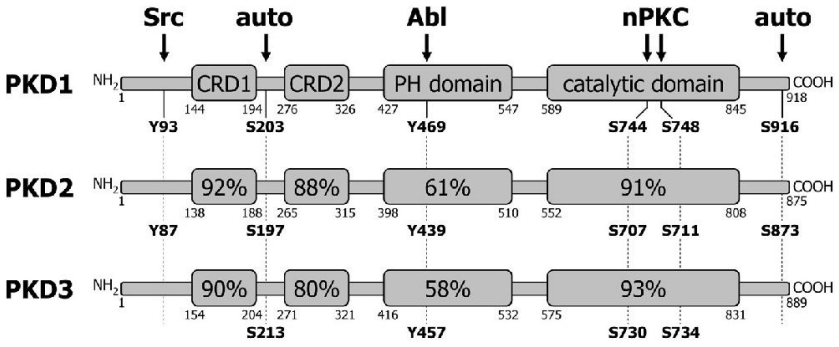

Figure 1 – Functional domains, conserved phosphorylation sites and upstream kinases of PKD isoforms. Amino acid numbering refers to mouse PKDs. Percentages indicating sequence homology of PKD2 and PKD3 domains with the corresponding PKD1 domains are specified. CRD1/CRD2 indicates cystein-rich, zinc finger-like domains; PH, pleckstrin homology domain. Modified from (Avkiran et al., 2008).

These structural properties distinguish PKDs from PKC isoforms (Rozengurt et al., 2005). Thus, the PKD family members are more closely related to the calcium/calmodulin-dependent protein kinase (CAMK) superfamily (Manning et al., 2002).

PKD structure-function relationship

The modular structure of PKD with its multiple subdomains is closely connected to its intracel-lular localization and regulation. Motives found to be structurally homologous to other kinases display functional homology by mediating translocation, activation and substrate specificity of the kinases. Studies on the structure – function relationship of PKD have been performed by mutating or deleting single subdomains and analyzing the activation or localization properties of the mutated proteins.

The C-terminal catalytic domain of PKDs is responsible for the serine/threonine kinase activity. In contrast, components of the regulatory domain exert an inhibitory effect on the catalytic activity, such that deletion or mutation of this domain renders PKDs constitutively active. To further characterize the sequence within the regulatory domain that mediates the inhibitory effect, conserved amino acids of the PH domain have been deleted, resulting in full activation of PKD1 (Iglesias and Rozengurt, 1998).

Similarly, PKD is fully activated when both CRDs are deleted (Iglesias and Rozengurt, 1999). However only CRD2 has an inhibitory effect on the catalytic activity of PKD, whereas CRD1 is involved in phorbol ester binding (Iglesias et al., 1998a; Iglesias and Rozengurt, 1999). Deletion of the N-terminal hydrophobic domain or the CRD1 domain completely abrogates Golgi localization, indicating a role of these subdomains in the recruitment of PKD to the Golgi (Hausser et al., 2002). During nuclear translocation, CRD2 is required for the nuclear import of PKD1 (Rey et al., 2001a). Nuclear export depends on the PH domain and on CRD1 (Auer et al., 2005; Rey et al., 2003).

Phosphorylation and regulation of PKD activity

A variety of mechanisms are involved in PKD phosphorylation and activation. Members of the PKC family directly interact with the PH domain of PKD and lead to the transphosphorylation of serine residues (S744 and S748 for mouse PKD1) located in the activation loop of the catalytic domain (Iglesias et al., 1998b; Waldron et al., 2001). Following activation loop phosphorylation the pleckstrin homology domain-mediated autoinhibitory effect is abolished and PKD can exert its full catalytic activity (Waldron and Rozengurt, 2003). PKD2 and PKD3 activation occurs in an analogue way by phosphorylation of serine residues in the activation loop

(S707 and S711 for mouse PKD2; S730 and S734 for mouse PKD3) (Matthews et al., 2003; Sturany et al., 2002).

The activation loop serines are preferentially phosphorylated by novel PKCs (such as PKCε, PKDδand PKCη), but not by atypical PKCs (Zugaza et al., 1996; Zugaza et al., 1997). However, classical PKCs, such as PKCα, can also contribute to activation loop phosphorylation (Wong and Jin, 2005). The PKC isoform responsible for PKD activation depends on cell context, type and stimuli. More than one isoform can be involved resulting in a functional redundancy.

Further upstream, the PKC-dependent PKD phosphorylation pathway requires phospholipase C (PLC) activation and diacylglycerol (DAG) production. Upon binding of growth factors or G-protein coupled receptor (GPCR) agonist to their respective receptors (Van Lint et al., 1998; Yuan et al., 2000) and in response to T cell receptor (TCR) or B cell receptor (BCR) engagement (Matthews et al., 2000b; Sidorenko et al., 1996) PLC becomes activated. Activated PLC is capable of catalyzing the hydrolysis of phosphatidylinositol-4,5-bisphosphate (PIP_2) into two important second messenger molecules, inositol-1,4,5-triphosphate (IP_3) and DAG. DAG, on the one hand, directly binds to the CRD1 domain of PKD and thereby targets PKD to the plasma membrane or to intracellular membranes. On the other hand, DAG activates novel PKC isoforms, which in turn, phosphorylate PKDs at the activation loop serines and causes their activation. Concurrently IP_3 leads to the release of Ca^{2+} from intracellular storages and contributes to Ca^{2+}-dependent activation of PKCs. Furthermore, substances like Bryostatin (Matthews et al., 1997), agents mimicking DAG like phorbol ester (Van Lint et al., 1995), neuropeptides such as bombesin, vasopressin, endothelin, bradykinin (Zugaza et al., 1997), oxidative stress (Storz et al., 2004; Waldron et al., 2004; Waldron and Rozengurt, 2000), ATP or P2X7 receptor activation (Bradford and Soltoff, 2002), and thrombin (Tan et al., 2003) can lead to PKC-dependent PKD activation.

Apart from that, $G_{\beta\gamma}$subunits can directly bind and activate PKD by interacting with the PH domain. This interaction is involved in the regulation of Golgi dynamics and protein secretion (Jamora et al., 1999).

An alternative mechanism of PKD activation occurs during the induction of apoptosis induced by genotoxic agents. Activated caspase 3 leads to proteolytic cleavage of PKD, resulting in the release of the catalytic domain from the regulatory domain and thereby activation of the kinase activity (Endo et al., 2000; Haussermann et al., 1999).

Moreover, during osteoblast differentiation the bone morphogenic protein 2 (BMP-2) can induce activation of PKD in a PKC-independent way, which finally leads to the activation of the stress mitogen-activated protein kinases JNK and p38 (Lemonnier et al., 2004).

Besides the transphosphorylation sites in the activation loop PKDs become phosphorylated at additional sites during *in vivo* activation. In PKD1 there are three further serines described as putative phosphorylation sites: Two are located in the regulatory domain (S203 and S255) and one in the C terminus (S916). S203 and S916 are autophosphorylation sites, which regulate interactions with 14-3-3 (Hausser et al., 1999; Vertommen et al., 2000) and PDZ proteins (Matthews et al., 1999b; Sanchez-Ruiloba et al., 2006), respectively. S255 is transphosphorylated downstream of a PKC-dependent pathway. Apart from serine phosphorylation PKD activity can also be enhanced upon tyrosine phosphorylation (at Y93 or Y469 for mouse PKD1) mediated by Src and Abl kinases induced by oxidative stress (Doppler and Storz, 2007; Storz et al., 2003). For PKD2 and PKD3 analogue serine and tyrosine phosphorylation sites have been mapped (Figure 1). Recently, an additional phosphorylation site (S244) has been mapped in human PKD2, which is targeted by casein kinase I and facilitates nuclear accumulation of the protein (von Blume et al., 2007).

In contrast to PKD1 and PKD2, PKD3 does not contain a PDZ motive associated with an autophosphorylation site at the C terminus (Sanchez-Ruiloba et al., 2006). Moreover, PKD3 lacks the relevant tyrosine residue targeted in response to oxidative stress (Doppler and Storz, 2007).

Subcellular localization of PKD

In response to specific stimuli the PKD isoforms can be recruited to a variety of subcellular compartments. The intracellular redistribution is regulated by the interaction of the regulatory subunits with other cellular proteins or lipids. Thus, the localization of PKD to specific compartments and the tight regulation of PKD activation have profound functional implications.

In resting cells, PKD is predominantly cytoplasmatic, with a smaller fraction being localized in the nucleus, at the Golgi or at mitochondria (Rozengurt et al., 2005). Moreover, PKD can be recruited to the cell surface in response to receptor activation, for example by growth factors, GPCR agonists, B cell receptor ligation and phorbol esters (Matthews et al., 2000a; Rey et al., 2001b), thereby leading to the activation of PKDs. Activated PKD returns to the cytosol, where it regulates major signaling pathways and remains active for hours (Matthews et al., 2000a).

Due to the presence of nuclear localization sequences (NLS) and a nuclear export signal (NES) within the regulatory domain, PKDs possess the ability to shuttle between the cytoplasm and the nucleus (Auer et al., 2005; Rey et al., 2001a; Rey et al., 2003). In the nucleus activated PKD phosphorylates class IIa HDACs, which are direct repressors of the myocyte enhancer factor 2 (MEF2) transcription factor (Dequiedt et al., 2005; Huynh and McKinsey,

2006; Matthews et al., 2006; Parra et al., 2005). The phosphorylation of HDACs promotes 14-3-3 binding and their nuclear export, thus enabling MEF2-dependent gene transcription (Potthoff and Olson, 2007).

Localization at the Golgi compartment is essential for the role of PKD in protein trafficking. At the trans-Golgi network (TGN) PKD regulates the fission of transport carriers specifically destined to the cell surface (Liljedahl et al., 2001; Prestle et al., 1996). Interestingly, the kinase activity seems to be dispensable for Golgi targeting, as kinase-inactive PKD also localizes to the TGN (Liljedahl et al., 2001). Golgi recruitment can be abolished by mutating the CRD1 domain or by reducing the level of DAG in the cell (Baron and Malhotra, 2002).

At the mitochondria PKD was identified as a sensor for oxidative stress signaling. In response to increased levels of reactive oxygen species (ROS) PKD is involved in the communication of signals to the nucleus leading either to NF-κB dependent gene transcription or to the induction of mitochondria-detoxifying enzyme MnSOD expression (Storz, 2007; Storz et al., 2005). Recently, it has been demonstrated that activation loop phosphorylated PKDs are associated with centrosomes, spindles and midbody suggesting a regulatory role of these activated kinases in mitosis and cell division (Papazyan et al., 2008).

Cellular functions of PKD

PKDs are known to participate in various cellular functions in fields as diverse as cell growth, DNA synthesis, proliferation, differentiation, migration, invasion, immune cell regulation, polarized cell growth, Golgi regulation and organization, oxidative stress signaling and cell death.

Proliferation, differentiation and transformation

The first correlation between PKD and cell proliferation was observed in keratinocytes from normal and neoplastic mouse epidermis. In primary cultures of these cells, PKD1 was shown to be highly expressed in basal dividing cells and low in differentiating cells (Rennecke et al., 1999). As PKD functions as pro-proliferative and/or anti-differentiative signal in keratinocytes it is proposed that differentiation inducers downregulate PKD to allow differentiation to proceed (Ernest Dodd et al., 2005).

In several cell types PKD appears to mediate proliferative effects of mitogens, such as PDGF, bombesin, vasopressin, endothelin and bradykinin (Zhukova et al., 2001; Zugaza et al., 1997). The fact that PKD promotes mitogenesis suggests the involvement of mitogen-activated protein kinase (MAPK) pathways in this process. Indeed, a role of PKD in the regulation of the MAPK p42 cascade and a modulation of ERK and JNK signal pathways has previ-

ously been described (Brandlin et al., 2002; Hausser et al., 2001). Presumably, PKD functions by phosphorylating the Ras-interacting protein RIN1 and thereby increases the association of RIN1 with 14-3-3 proteins. 14-3-3 binding of RIN1 leads to the release of its association with Ras. Free Ras protein in turn interacts with Raf, the proximal kinase of the ERK protein kinase cascade (Wang et al., 2002). Thus, PKD seems to act in a proproliferative manner through effects on the Ras/Raf/MEK/ERK-1/2 cascade (Bollag et al., 2004). Another group reports that PKD selectively potentiates mitogenesis by increasing the duration of ERK signaling (Sinnett-Smith et al., 2004).

Several studies indicated that PKD1 negatively interferes with the EGF receptor-mediated JNK activation. This inhibitory effect requires phosphorylation of the EGF receptor on two threonine residues (Bagowski et al., 1999). Furthermore, PKD1 phosphorylates alternative sites at the N-terminus of c-Jun (Hurd et al., 2002) thereby suppressing the EGF-induced, JNK-mediated phosphorylation of c-Jun at S63, which is crucial for its ability to mediate cell proliferation and differentiation (Hurd and Rozengurt, 2001). Conversely, recent findings suggest that PKD is involved in the BMP2-induced stimulation of JNK and p38, which is required for optimal differentiation of osteoblastic cells. In this context, PKD is activated via an exceptional PKC-independent mechanism (Lemonnier et al., 2004).

In endothelial cells, vascular endothelial growth factor (VEGF) stimulation leads to PKD activation, which induces ERK signaling and positively regulates endothelial cell proliferation (Wong and Jin, 2005). Another group demonstrated that upon VEGF stimulation PKD promotes the nuclear export of HDAC7 by phosphorylation and thereby activates transcription of VEGF responsive genes that control endothelial cell proliferation (Wang et al., 2008).

Though data from the literature suggest an association between PKD and cell proliferation, a direct causal relationship or downstream effector of PKD on cellular proliferation remains to be further investigated (Jaggi et al., 2007).

Cell motility, invasion and migration

PKD was related to cell invasiveness for the first time in 1999. PKD1 was found to form a complex with the actin binding protein cortactin and the focal adhesion protein paxillin in invadopodia of breast cancer cells. In contrast to its presence in invasive cells, this complex of proteins was not detectable in lysates from non-invasive cells that do not form invadopodia (Bowden et al., 1999). Invadopodia are actin-rich membrane protrusions involved in the proteolytic degradation of extracellular matrix components and are therefore correlated with the invasive potential of cancer cells.

Further evidence for a role of PKD in cell motility comes from studies with Kidins220/ARMS, the first physiological PKD substrate identified, a neuronal transmembrane protein localized at

neurite tips and growth cones (Iglesias et al., 2000). Kidins220/ARMS was moreover shown to be expressed in immature dendritic cells migrating on an extracellular matrix and thereby changing cyclically from a highly polarized morphology to a morphologically symmetrical shape (Riol-Blanco et al., 2004).

Besides, it was shown that PKD influences cell migration by regulating vesicular transport from the TGN to the plasma membrane. Interference of PKD function at the TGN inhibited directed cell motility and retrograde flow of surface markers and filamentous actin (Prigozhina and Waterman-Storer, 2004). Anterograde membrane transport mediated by PKD thus is a prerequisite for cell locomotion and lamellipodial dynamics.

In another study E-cadherin was identified as a novel substrate for PKD. In prostate cells, phosphorylation of E-cadherin by PKD was found to be associated with increased cellular aggregation and decreased cellular motility (Jaggi et al., 2005).

Further evidence for a negatively regulatory function of PKD in cell migration was obtained by observations of Eiseler et al. Overexpression of wildtype PKD displayed a reduced migratory potential whereas knockdown of PKD or overexpression of dominant-negative PKD enhanced cell migration. At the leading edge of migrating cells active PKD was found to be colocalized with F-actin, Arp3 and cortactin, suggesting a role of PKD in actin remodeling (Eiseler, 2006). In support of this, PKD directly interacts with F-actin and phosphorylates cortactin *in vitro* (Eiseler et al., 2007).

Corroborating the Eiseler (2006) data, recent findings demonstrated that in gastric cancer the promoter region of PKD1 is frequently hypermethylated, resulting in epigenetic downregulation of PKD1. A role of PKD in cell migration and metastasis in gastric cancer was proclaimed, as knockdown of PKD1 was shown to promote the invasiveness of cells (Kim et al., 2008a).

Protein transport and membrane trafficking

Soon after its identification, PKD has been found to be involved in secretion of glycoproteins (Prestle et al., 1996). Subsequently, a series of elegant studies from the Malhotra lab unravelleld details of PKD's role in secretion, vesiculation of the Golgi apparatus and membrane sorting of proteins. Thus, a fundamental role of PKD is suggested in regulating the detachment of cargo-containing tubular elements from the trans-Golgi network (TGN) (Liljedahl et al., 2001). Recruitment of PKD to the TGN occurs by an interaction with DAG and requires an intact CRD1 domain of PKD (Baron and Malhotra, 2002; Maeda et al., 2001). Activation of PKD at the TGN is mediated by interaction with $G_{\beta\gamma}$subunits of G-proteins (Jamora et al., 1999). Further studies revealed that specific $G_{\beta\gamma}$subunits, β1γ2 and β3γ2, are required that act in series with another kinase, the novel PKC isoform PKCη, to promote membrane fission at the TGN (Diaz Anel and Malhotra, 2005).

The three PKD isoforms are involved differentially in cargo trafficking. In non-polarized HeLa cells kinase-dead mutants of PKD1 and PKD2 were found to lead to an accumulation of the cell surface destined cargo within TGN tubules but had no effect on other transport pathways. In polarized MDCK kidney cells overexpression of kinase-dead PKD 1 or 2 led to the apical missorting of a basolateral destined exocytosis marker, possibly by the inhibition of a basolateral transport pathway. In contrast, overexpression of kinase-dead PKD3 seems to have no effect on apical or basolateral transport. The authors conclude that PKD activity is required only for the transport of proteins containing basolateral sorting information, and seems to be cargo specific (Yeaman et al., 2004). Moreover, siRNA mediated knockdown of PKD2 and PKD3 in Hela cells was shown to inhibit trafficking from the TGN, whereas constitutively active PKD promoted TGN vesiculation (Bossard et al., 2007). It was further proposed that PKD2 and PKD3 act as a dimer in the regulation of fission of exocytic carriers from the TGN to the cell surface (Bossard et al., 2007).

In 2002 Bankaitis proposed a model for the vesicle fission process: a vesicle budding machinery that deforms TGN membranes into short tubules is arranged by recruitment of effector molecules to the TGN-bound PKD (Bankaitis, 2002). A correlation between PKD and lipid kinases involved in this process has been proposed after the discovery of PKD-mediated phosphorylation of phosphatidylinositol-4-kinase IIIβ(PI4KIIIβ) *in vivo*. PKD1 and PKD2 have been shown to phosphorylate PI4KIIIβ, thereby stimulating lipid kinase activity and enhancing vesicular stomatitis virus G-protein transport to the plasma membrane (Hausser et al., 2005). Downstream of PKD-mediated PI4KIIIβ-phosphorylation, binding of 14-3-3 proteins has been found to preserve lipid kinase activity (Hausser et al., 2006).

In a further study the lipid transfer protein CERT, which mediates the nonvesicular transfer of ceramide from the endoplasmic reticulum to the Golgi complex, was identified as *in vivo* PKD substrate (Fugmann et al., 2007). PKD dependent CERT phosphorylation decreases the affinity towards its lipid target phosphatidylinositol-4-phosphate at Golgi membranes, thereby reducing ceramide transfer activity. In turn, CERT is also critical for PKD activation and PKD-dependent protein cargo transport to the plasma membrane (Fugmann et al., 2007).

Two recent reports deal with clinical implications of PKD functions at the Golgi. In neuroendocrine tumor cells PKD2 has been shown to control the release of chromogranin A secretory granules at the level of the Golgi apparatus; hence PKD could serve as a novel target to block hormone secretion in functional neuroendocrine tumors (von Wichert et al., 2008). Another group demonstrated that PKD is a key regulator of cardiomyocyte lipoprotein lipase secretion after diabetes and might therefore contribute to contractile dysfunctions in the course of disease (Kim et al., 2008c).

Apoptosis and cell survival

Besides its function in cell proliferation, PKD can also play an anti-apoptotic role in a cell context and apoptosis-inducing agent dependent manner. In transfected human and murine cell lines PKD expression was shown to reduce the sensitivity to TNF-induced apoptosis. The protection correlated with an enhanced expression of NF-kB dependent pro-survival genes (Johannes et al., 1998). In pancreatic tumor cells PKD has also been shown to prevent CD95-mediated apoptosis and to enhance proliferation. In cells overexpressing PKD1 an increased telomerase activity and an upregulation of the anti-apoptotic proteins c-FLIP and survivin have been detected (Trauzold et al., 2003).

Furthermore, PKD activation has been shown to protect from oxidative stress induced cell death. Oxidative stress initiated by H_2O_2 stimulation induces PKD activation via Src, PLC and PKCs (Waldron and Rozengurt, 2000). Storz and Toker propose a different model according to which activation of PKD by reactive oxygen species (ROS) is mediated by the Src-Abl pathway, leading to phosphorylation of tyrosine residues of PKD1 in the PH domain (Storz and Toker, 2003). Tyrosine phosphorylation of PKD1 in the PH domain promotes PKCδ-dependent phosphorylation of PKD activation loop serines (Storz et al., 2004). Thus, fully activated PKD1 mediates activation of IKKβand degradation of IκBα, resulting in NF-κB activation and cell survival. Conversely, upon H_2O_2 stimulation of endothelial cells PKD mediates induction of apoptosis through JNK activation. H_2O_2, but not TNF was reported to induce phosphorylation and translocation of PKD from the endothelial cell membrane to the cytoplasm, where it associates with the apoptosis signal-regulating kinase 1 (ASK1), a JNK upstream activator (Zhang et al., 2005).

PKD activation during caspase-mediated cleavage has been described previously (Endo et al., 2000; Haussermann et al., 1999). The expression of a caspase-resistant PKD1 mutant was shown to attenuate DNA damage-induced apoptosis (Vantus et al., 2004). Thus, PKD1 can act as an apoptosis inhibitory protein that, by caspase cleavage, can be transformed into an apoptosis sensitizing protein.

Recently, it was reported that PKD is a positive regulator of Bit1 apoptotic function. Bcl-2 inhibitor of transcription (Bit1) is a mitochondrial protein that induces caspase-independent apoptosis upon its release into the cytoplasm. The apoptotic function of Bit1 is primarily associated with anoikis and is inhibited by integrin-mediated cell attachment. PKD has been shown to contribute to the release of Bit1 from the mitochondria to the cytoplasm by phosphorylation of serine residues within the mitochondrial localization sequence of Bit1 (Biliran et al., 2008). Whether the PKD-mediated phosphorylation of Bit1 occurs at mitochondria or in

the cytoplasm remains to be investigated. In this line, it is of interest that oxidative stress induces the recruitment of PKD to mitochondria (Storz et al., 2005).

Organ specific functions of PKD

In addition to its pivotal role in common cellular processes, PKD seems to be of specific functional relevance for several organ systems like heart, vascular system, nervous system, immune system and bone.

Cardiac muscle

Several early studies demonstrated the presence of PKD proteins in the myocardium (Brooks et al., 1997; Haworth et al., 2000). Expression of PKD isoforms was confirmed in neonatal and adult rat ventricular myocytes and in adult mouse, rat, rabbit and human myocardium (Harrison et al., 2006; Haworth et al., 2007; Iwata et al., 2005; Roberts et al., 2005; Tsybouleva et al., 2004), with PKD1 being the major isoform in the heart (Avkiran et al., 2008). Moreover, there are indications that PKD expression in isolated myocytes and myocardial tissue underlies developmental regulation and decreases considerably in adulthood (Haworth et al., 2000). In disease, cardiac PKD expression has been shown to revert to the fetal phenotype, with increased PKD expression in the failing rat, rabbit and human myocardium (Avkiran et al., 2008; Harrison et al., 2006).

A variety of stimuli, like phorbol ester, FCS, norepinephrine, the α_1-adrenergic agonist phenylephrine, endothelin 1, angiotensin II and aldosteron have been shown to induce PKD activation in neonatal and adult ventricular myocytes (Harrison et al., 2006; Haworth et al., 2000; Haworth et al., 2007; Iwata et al., 2005; Roberts et al., 2005; Tsybouleva et al., 2004). In most cases PKD activation has been shown to be attenuated by PKC inhibition, proposing a key role for PKCs upstream of PKD activity in cardiac myocytes. Stimulation of neonatal rat cardiomyocytes with GPCR agonist and phorbol ester was shown to promote activation and translocation of PKD to the Z-discs (Iwata et al., 2005).

In cardiac myocytes PKD has been shown to interact with cardiac troponin I (cTnI), myosin-binding protein C (cMyBP-C), and telethonin, of which cTnI undergoes direct PKD-mediated phosphorylation resulting in reduced myofilament Ca^{2+} sensitivity (Cuello et al., 2007; Haworth et al., 2004). Furthermore, recent data underline that PKD activity is enhanced under conditions where PKA activity is attenuated, a counter-regulatory role that might allow PKD-mediated pathways greater significance for the control of contractile function in the presence of a pathological background such as heart failure (Haworth et al., 2007).

Prohypertrophic neurohormonal stimulation of neonatal rat ventricular myocytes was shown to mediate class II HDAC phosphorylation, which facilitates the binding of 14-3-3 proteins, nuclear export and cytosolic retention of these transcriptional inhibitors and thereby promotes MEF2-dependent pathological gene expression (Chang et al., 2004; McKinsey et al., 2000b; Zhang et al., 2002). PKD was identified as the kinase directly mediating class II HDAC phosphorylation (Huynh and McKinsey, 2006; Vega et al., 2004). Recently, the relevance of PKD signaling in pathological cardiac remodeling has also been supported by appropriate mouse models (Fielitz et al., 2008; Harrison et al., 2006).

Some cellular functions of PKD that have been unravelled in non-cardiovascular cells propose a role of PKD in regulating myocardial responses to ischemia. PKD was shown to mediate mitochondrial ROS detoxification via different pathways that all have been shown to play a role in protective mechanisms of myocardial ischemia (Bolli, 2007; Storz et al., 2004; Storz et al., 2005; Storz and Toker, 2003). Two known PKD substrates, the vanilloid receptor type 1 (Wang et al., 2004) and heat shock protein (HSP) 27 (Doppler et al., 2005), have furthermore been proposed to modulate the extent of myocardial ischemic injury (Hollander et al., 2004; Wang and Wang, 2005).

Recently, PKD was identified as a novel contraction-activated kinase linked to the GLUT4-mediated glucose uptake in cardiac myocytes. Contraction also induced cTnI phosphorylation, suggesting that the combined actions of PKD on cTnI and on GLUT4 translocation links accelerated contraction mechanics to increased energy production when the heart is forced to increase its contractile activity (Luiken et al., 2008).

Skeletal muscle

In skeletal muscle all three PKD isoforms are expressed with an exceptionally high level of PKD1 in slow twitch muscle fibers (Kim et al., 2008b). Skeletal muscle is composed of different muscle fibers types that vary in their physiological and metabolic parameters. In response to environmental demands, skeletal muscle remodels by activating signaling pathways to reprogram gene expression and sustain muscle performance (Bassel-Duby and Olson, 2006). Muscle remodeling has been shown to depend on phosphorylation of class II HDACs resulting in their export from the nucleus and activation of MEF2-dependent genes (McKinsey et al., 2000a). Though conclusive experimental evidence is still missing, PKD is widely accepted as skeletal muscle HDAC kinase (Bassel-Duby and Olson, 2006). Moreover, by the use of *in vivo* imaging techniques it was possible to demonstrate that a kinase-inactive PKD1 completely blocked motor nerve stimulation induced downstream gene transcription in skeletal muscle (Akimoto et al., 2008). Recent studies with transgenic and knockout mice confirm that PKD1

signaling cascades plays an important role in the control of skeletal muscle fiber types via its stimulatory activity on MEF2 (Kim et al., 2008b).

However PKDs are also supposed to carry out metabolic functions in skeletal muscle. For instance PKD3 has been shown to directly contribute to insulin-independent basal glucose uptake in skeletal muscle cells (Chen et al., 2005).

Vascular system

PKD is expressed in endothelial cells (Wong and Jin, 2005), vascular smooth muscle cells (Abedi et al., 1998) and platelets (Stafford et al., 2003). Moreover, PKD activity has been shown to be upregulated by physiological stimuli, like vascular endothelial growth factor (VEGF) (Wong and Jin, 2005) and H_2O_2 (Zhang et al., 2005) in endothelial cells; angiotensin II (Abedi et al., 1998; Tan et al., 2004), platelet-derived growth factor (Abedi et al., 1998), and thrombin (Tan et al., 2003) in vascular smooth muscle cells; and thrombin (Stafford et al., 2003) in platelets.

In endothelial cells, PKD was proposed to regulate proliferation (Wong and Jin, 2005), migration (Qin et al., 2006), and apoptosis (Zhang et al., 2005). However, the signaling pathways linking stimulation and downstream gene regulation are still under extensive investigation. A recent study demonstrated that, in endothelial cells, VEGF stimulates HDAC5 phosphorylation and nuclear export through a VEGF receptor 2/PLCγ/PKC/PKD-dependent pathway. Further downstream MEF2 transcriptional activation promotes expression of NR4A1, an orphan nuclear receptor involved in angiogenesis (Ha et al., 2008). In an analogue way, HDAC7 was shown to be phosphorylated by PKD upon VEGF stimulation in endothelial cells (Wang et al., 2008). Another group identified that HSP27, a known PKD substrate (Doppler et al., 2005), is directly phosphorylated by PKD upon VEGF stimulation in human umbilical vein endothelial cells (HUVEC) (Evans et al., 2008).

Pathologically more relevant is the angiotensin II (Ang II)-induced signaling pathway in vascular smooth muscle cells (VSMCs). Ang II stimulation induces PKD-mediated HDAC5 phosphorylation, nuclear export and MEF2-dependent gene transcription resulting in VSMC hypertrophy (Xu et al., 2007), which is implicated in the pathogenesis of hypertension, atherosclerosis and diabetes.

The transcription factor cAMP-response element-binding (CREB) protein has been shown to play a crucial role in Ang II-induced hypertrophy of VSMCs (Funakoshi et al., 2002). Interestingly, CREB protein is a PKD substrate (Johannessen et al., 2007). Moreover, PKD might influence vascular function indirectly by regulating the physiological actions of aldosterone in renal epithelial cells (Thomas et al., 2008).

Nervous system

In mice, all three PKD isoforms are expressed in neuronal tissue already at embryonic stages (Oster et al., 2006). However, until now only a few studies have addressed the functional relevance of PKD in neurons.

Interestingly, Kidins220/ARMS, an integral membrane protein, selectively expressed in brain and neuroendocrine cells, was the first physiological PKD substrate identified (Iglesias et al., 2000). The results of subsequent investigations now implicate a role of Kidins220/ARMS in neuronal differentiation (Bracale et al., 2007; Cortes et al., 2007), neurotrophin signaling (Arevalo et al., 2006), and neurotensin secretion (Li et al., 2008). However, additional findings are needed to delineate the underlying molecular mechanisms of these physiological processes.

Moreover, RIN1, another approved substrate of PKD, is expressed predominantly in a variety of neuronal cell types and tissues, with high levels in forebrain structures such as the cerebral cortex, hippocampus, amygdala and striatum (Bliss et al., 2006; Dhaka et al., 2003). Results from studies with RIN1 knockout mice propose a role of RIN1 as inhibitory modulator of neuronal plasticity in aversive memory formation (Dhaka et al., 2003). A recently published work demonstrated that RIN1 mediates EphA4 endocytosis in postnatal neurons after engagement of the EphA4 receptor with its cognate ligand ephrinB3 and thereby suppresses synaptic plasticity in the amygdala (Deininger et al., 2008).

There is one report indicating a role of PKD in neuronal development by showing that expression of a kinase-dead PKD variant in developing hippocampal neurons leads to a decrease in dendritic length and arborization (Horton et al., 2005). A more recently published article describes PKD as an essential regulator of early neuronal polarization (Yin et al., 2008). Contemporaneously, another group reported that PKD selectively regulates the trafficking of dendritic and axonal membrane proteins in mature neurons (Bisbal et al., 2008).

Another recent study identified PKD as one of the earliest markers of neuronal DNA damage, suggesting that signaling downstream of PKD may be critical for neuronal survival after genotoxic stress (Besirli and Johnson, 2006).

Immune system

Numerous *in vitro* studies provide evidence for a key role of PKD in TCR- and BCR-dependent signal transduction during activation of T and B cell mediated adaptive immune responses. B cells express PKD1 and PKD3 and both isoforms have been shown to be activated upon BCR engagement (Matthews et al., 2003). T cells predominantly express PKD1 which is activated upon TCR stimulation. Though, in T cells, B cells, and mast cells, PKDs are strongly activated

by antigen receptor stimulation but not by costimulatory receptors, chemokines or cytokines (Matthews et al., 2000b). In T cells, PKD appears to fulfill distinct functions in early T cell development, TCR rearrangement, T cell maturation, activation and selection (Marklund et al., 2003; Spitaler et al., 2006).

The class IIa histone deacetylase HDAC7 regulates negative selection of thymocytes by repressing the expression of Nur77, an orphan nuclear receptor involved in antigen-induced apoptosis (Dequiedt et al., 2003). Recently, it was demonstrated that TCR-induced nuclear export of HDAC7 and Nur77 expression is accomplished by PKD-mediated phosphorylation of HDAC7 (Dequiedt et al., 2005; Parra et al., 2005). Equally, in B cells PKD connects BCR activation and epigenetic control of chromatin by mediating phosphorylation and nuclear export of the class II histone deacetylases HDAC5 and HDAC7 (Matthews et al., 2006). With the help of a cellular knockout approach it was now possible to demonstrate that in DT40 B cells, PKD1 and PKD3 act at least in part redundant. Loss of either PKD1 or PKD3 had no impact on HDAC phosphorylation, but loss of both PKD1 and PKD3 abrogated antigen receptor-induced class II HDACs in DT40 B cells (Matthews et al., 2006).

Another substrate of PKD is the hematopoietic progenitor kinase 1 (HPK1). In lymphocytes HPK1 is recruited to the contact sites of antigen-presenting cell (APC)-T cell conjugates. Relocalization and clustering of HPK1 causes its activation, which is accompanied by PKD phosphorylation (Arnold et al., 2005). An additional protein family supposed to play a role in antigene receptor mediated activation of T lymphocytes are the Sly proteins (Beer et al., 2005; Beer et al., 2001). Sly 1 is specifically expressed in lymphocytes and has recently been shown to be a potential *in vivo* PKD substrate (Reis, 2007).

In mast cells PKD1 has been shown to be activated in response to innate, adaptive, and growth factor signals, likely via a PKC-independent pathway (Murphy et al., 2007).

A recent study provides evidence that PKD1 is involved in Toll-like receptor 9 (TLR) signaling in macrophages. After stimulation of TLR9, PKD1 interacts with the MyD88/IL-1R-associated kinase/TRAF6 complex and is required for activation of NF-κB and MAPKs and subsequent expression of cytokines (Park et al., 2008).

Bone tissue

During mouse embryogenesis PKD expression has been detected in developing bones (Ellwanger et al., 2008; Oster et al., 2006). Interestingly, studies on osteoblastic cell differentiation revealed a novel PKC independent mechanism of PKD activation. Bone morphogenetic protein 2 (BMP-2) has been shown to induce activation of the stress mitogen activated protein kinases JNK and p38 via a selective phosphorylation and activation of PKD (Lemonnier et al., 2004). This pathway, in addition to Smads, appears to be essential for the effect of BMP-

2 on osteoblastic cell differentiation. Another study addressed the signaling pathways activating Osterix (Osx), a critical gene for osteoblast differentiation and bone formation. In mesenchymal stem cells, it was demonstrated that BMP-2 and insulin growth factor I (IGF-I) induced phosphorylation of PKD1, which was required for Osx activation and bone mineralization (Celil and Campbell, 2005).

Transgenic mouse models

By the use of transgenic technologies, a characteristic genetic sequence can be evaluated within the specific genomic background of a whole organism.

As mice are highly comparable to humans in respect to physiology, organ systems, tissues and even behavioural traits, and as most genes are conserved, mice are the most widely used model organisms in biomedical research. Consequently, mice are unique in offering the possibility to understand the genotype-phenotype relationship that is relevant for unravelling the biologic role of a gene *in vivo*. Genetically engineered mouse models have been established for a variety of human disorders like cancer or cardiovascular diseases. Moreover, mouse models are used to study gene functions which are still unknown or only predicted *in vivo*.

Methods of manipulating the mouse genome

For the generation of genetically modified mice in biomedical research two major techniques are widely used. With the first technique, transgenic DNA sequences of variable length and origin can be introduced into the mammalian genome by pronuclear microinjection of fertilized oozytes. The method was firstly described by Gordon and colleagues in 1980 and is today referred to as the "conventional transgenics" technique (Gordon et al., 1980). This experimental modification of the animal germ line (transgenesis) was initially established in mice. Conventional transgenic mice containing additional foreign DNA are generally named gain-of-function mutations. However, functional knockout animals can be obtained by integration of transgenic constructs, which drive the expression of dominant-negative proteins (Metsaranta et al., 1992; Peters et al., 1994; Stacey et al., 1988). Besides, transgenic constructs encoding antisense RNAs have been successfully used to inhibit the expression of endogenous genes (Erickson, 1999; Sokol and Murray, 1996). Furthermore, RNA interference can be applied to animals and has already been reported to knockdown gene expression in transgenic mice (McCaffrey et al., 2002; Spankuch and Strebhardt, 2005).

For temporal and inducible expression of conventional transgenes several systems are available (Lewandoski, 2001). The most popular method is the tetracycline-dependent gene expression system, which is explicitly outlined in the following chapter.

From a geneticist's point of view conventional transgenic mice expressing novel or additional genes represent gain-of-function mutations. Loss of function mutations can be generated by random insertional mutations (Woychik and Alagramam, 1998) or by gene targeting (Brinster et al., 1989). Though, homologous integration after pronucleus injection is a rather rare event. However, human genetic diseases are more often characterized by loss-of-function mutations or by homozygous recessive gene mutations, which are both beyond the reach of conventional transgenesis.

A milestone for the establishment of the second technique, the "gene targeting" technique, was the demonstration of feasibility of interrupting a targeted gene by a neomycin gene in mouse embryonic stem (ES) cells (Mansour et al., 1988). Transfection of ES cells permits the selection of rare recombination events, allowing the investigator to identify cells in which homologous recombination between the gene of interest and the transforming DNA has taken place. From previous studies it was already known that mouse ES cells derived from blastocyst stage embryos are capable of contributing to many different tissues in chimeras, including the germ line (Bradley et al., 1984). Other studies demonstrated that ES cells conserve their pluripotency when injected into host blastocysts and returned to a foster mother even after genetic modification by viral infections or transfections with foreign DNA (Gossler et al., 1986; Robertson et al., 1986).

Nowadays it is possible to generate both loss-of-function (knockout) and gain-of-function (knock-in) models by the gene targeting technique (Hanks et al., 1995). Additionally, conditional genetic manipulations or tissue-specific knockouts using site-specific DNA recombinases are today routine to circumvent early lethality caused by some constitutive mutations (Nagy, 2000). By the use of the Cre-LoxP system it is possible to restrict genetic changes accomplished by homologous recombination to specific cell types or developmental stages, allowing spatio-temporal control of gene mutations. The power and spectrum of this system was further increased with the development of various reporter mouse lines to monitor either endogenous gene expression or Cre-mediated excision (Mao et al., 1999; Novak et al., 2000; Srinivas et al., 2001).

A completely different approach for the development of mouse models and for the detection of specific phenotypes makes use of random mutagenesis. Random mutations can be introduced by chemical agents, by transposons or proviral elements (Hrabe de Angelis et al., 2000; Mikkers and Berns, 2003; Takeda et al., 2007). Gene trapping is a high throughput approach to introduce insertional mutations across the genome and tag the insertion site with

a reporter sequence (Stanford et al., 2001). This technique facilitated the generation of large public gene trap libraries of mutagenized ES cell clones in the past few years (Yamamura and Araki, 2008).

Another alternative strategy for studying the role of genes in mice makes use of techniques from the field of gene therapy. Adenoviruses or adeno-associated viruses can infect most non-dividing cells and can therefore be used to assess gene function readily *in vivo*. An important advantage is that adenovirus mediated gene transfer can be used for local delivery of transgenes in a variety of genetic backgrounds without spending time on transgenic techniques and breeding (Buch et al., 2008; Mochizuki et al., 2002).

Conditional transgene expression with the Tet system

The tetracycline controlled gene expression system (Tet system) has developed into an efficient tool for the study of gene functions *in vivo*. The Tet system is composed of an activator and a responder construct. The activator transgene, a fusion protein comprising the prokaryotic tetracycline repressor (TetR) fused to the transcription activation domain of herpes simplex virus protein VP16. TetR can bind both, a 19 bp sequence called tet operator (tetO) that is not present in the mammalian genome, and the antibiotic tetracycline or its analogue doxycycline (Gossen et al., 1995). The responder construct comprises the tetO sequence, as cognate binding site of TetR, combined with a minimal promoter ligated to the sequence of the gene of interest. The expression of the engineered activator transgene does not cause ectopic activation of endogenous genes, but selectively activates tetO transgenes that are dependent on the presence or absence (tet-ON and tet-OFF systems, respectively) of tetracycline (Figure 2). As tetracycline or doxycycline can be administered or withdrawn at any time during the lifespan of animals, the Tet system allows the regulation of individual gene activities in complex genetic systems in a truly conditional manner (Schönig and Bujard, 2002; Shin et al., 1999).

The original Tet system has been further developed and modified over the years. Most notably was the generation of the so called reverse tetracycline transactivator rtTA. The exchange of three amino acids within the tetR resulted in fundamentally altered binding properties towards tetO. The conventional tetR or tTA activates transcription in the absence of doxycycline (Figure 2A) whereas rtetR or rtTA activates transcription in the presence of doxycycline (Figure 2B).

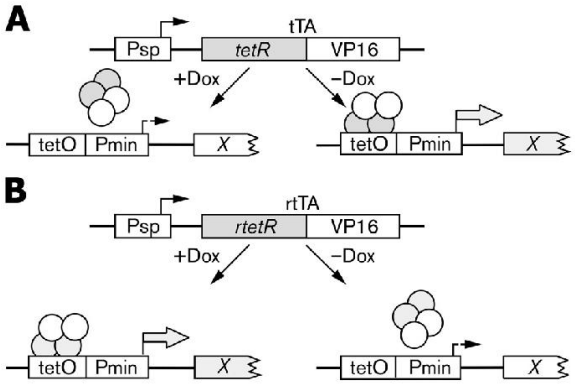

Figure 2 – Schematic outline of tetracycline regulatory systems. Activation principle of (A) tet-OFF and (B) tet-ON system. The transactivator constructs (tTA and rtTA) are composed of the prokaryotic sequence of the repressor and a proportion of the protein 16 of herpes simplex virus that functions as a strong transcriptional activator. (A) tTA binds in the absence but not in the presence of doxycycline (Dox) to the tet operator sequence (tetO) and activates transcription from a minimal human cytomegalovirus (hCMV) promoter (P_{min}). (B) rtTA requires doxycycline (Dox) for binding to tetO and thus for transcriptional activation. Modified from (Kistner et al., 1996).

Tetracycline and doxycycline belong to a class of compounds that have been investigated in detail because of their importance as antibiotics in veterinary and human medicine. The high affinity to tetR and rtetR as well as the excellent tissue penetration and pharmacokinetic properties make doxycycline a favorable effector molecule. Doxycycline is preferably administered in the drinking water of the animals, though it is also possible to supply it in higher doses in the food (Mansuy and Bujard, 2000). Even prolonged exposure of mice to doxycycline has not yielded any adverse effects (Kistner, 1996). Moreover, since doxycycline passes the placenta and is also present in the milk of feeding mothers, Tet systems can be used for the regulated gene expression during embryogenesis and development (Fedorov et al., 2001).

Results and Discussion

Since the identification, cloning and characterization of the first PKD isoform in the early 1990s, substantial efforts have been made to unravel the multiple cellular functions of PKD family members. Still, most of our knowledge about PKD function comes from studies in cultured or often transformed cell lines. One early study addressed the role of PKD in T cell differentiation by the use of transgenesis to target active PKD to different compartments in pre-T cells (Marklund et al., 2003). Apart from that, there were no reports in the literature about genetically modified mouse models specifically designed to provide insight into PKDs role *in vivo* at the time of starting this PhD project.

In the meantime, experimental data from primary human and mouse cells and from PKD mouse models began to accumulate (Bossuyt et al., 2008; Fielitz et al., 2008; Kim et al., 2008b; Kim et al., 2008c; Yin et al., 2008). In addition, several recent research articles suggest that PKD is causally involved in certain human diseases (Kim et al., 2008a; Kim et al., 2008c). Therefore, PKD family members represent putative targets for novel therapeutic approaches (Chen et al., 2008; Jaggi et al., 2007).

Most of the studies about PKD function have been focused on PKD1. However, structural differences among the three isoforms imply distinct functional properties. Indeed, functional differences between the three isoforms were demonstrated concerning specific activation pathways, substrate phosphorylation or subcellular localization (Doppler and Storz, 2007; Hausser et al., 2005; Li et al., 2008; Lu et al., 2007).

One objective of this thesis was to gain further insights into isoform selective or redundant functions of PKD1, PKD2 and PKD3, respectively. On the basis of these findings, it was the second aim of this work to establish an appropriate mouse model to study PKD function *in vivo*. Thus, transgenic mice, which overexpress dominant-negative PKD isoforms in an inducible and tissue specific manner were generated and provide a new tool to study the physiological role of PKD in mice. As first examples to proof the usefulness of the developped model system, we studied PKD's potential functions in muscle and brain. Specifically efforts focussed on a better understanding of PKD´s role in muscle remodeling and neuronal Golgi organization.

Expression and potential *in vivo* function of PKD isoforms during mouse embryogenesis

In adult mouse or human tissue, northern analysis revealed a broad expression of PKD3 in a variety of tissues and organs, whereas PKD1 and PKD2 mRNAs seemed to be restricted to

several specific organs (Hayashi et al., 1999; Johannes et al., 1994; Sturany et al., 2001; Valverde et al., 1994). Other reports suggest that the PKD isoforms may regulate both housekeeping functions and stimulus-induced gene expression patterns *in vivo* in a cell type and isoform-specific manner (Matthews et al., 2006).

Knowledge about the endogenous expression of a protein of interest is a prerequisite for functional analysis *in vivo*. To get an idea about where and when PKD isoforms might play a role in mouse development, we examined PKD expression during mouse embryogenesis. In this study we performed a detailed analysis of PKD3 expression by immunohistochemistry. We focused on this isoform since it is supposed to play an unique role among the three PKD isoforms, presumably due to its specific structural characteristics (Doppler and Storz, 2007; Sanchez-Ruiloba et al., 2006). For immunohistochemistry we used an antibody raised against a C-terminal epitope of human PKD3, which was previously shown to be PKD3 specific. Earlier studies in the lab revealed that other PKD antibodies available are either cross-reactive or not applicable for immunohistochemistry on mouse tissue (Ellwanger, 2004).

In early embryogenesis, PKD3 expression was found to be most prominent in the heart suggesting an important role of the kinase in fetal cardiac myocytes. In the course of gestation the expression in the heart remains constant or slightly decreases. This result is in agreement with other reports in the literature, describing high expression levels of all three PKD isoforms in the fetal heart followed by a developmental decline in abundance (Haworth et al., 2000). Recent studies implicated a key role of PKD in cardiac hypertrophy and heart failure (Backs and Olson, 2006; Fielitz et al., 2008). Interestingly, pathological cardiac remodeling was shown to be associated with reactivation of fetal cardiac genes and among others an upregulation of PKD expression levels (Bossuyt et al., 2008; McKinsey, 2007). Several reports indicate that the three PKD isoforms act, at least in part, redundant in hypertrophic signaling pathways (Fielitz et al., 2008; Matthews et al., 2006; Vega et al., 2004).

Apparent PKD3 expression was also observed in the developing skeleton. Cartilage primordia of the scull or developing nasal or costal bones as well as domains along the axis, where scle-rotomic material is condensed, showed for instance striking PKD3 expression.

Remarkably, PKD activation has been experimentally observed in the context of osteoblast differentiation *in vitro* (Celil and Campbell, 2005; Lemonnier et al., 2004). However, from the present state of knowledge, it is not possible to attribute this function to a specific PKD isoform.

Starting at stage E12.5 of mouse embryonic development, PKD3 is progressively expressed in neuronal cells as well as in the connective tissue and in skeletal muscle. An interesting polarized distribution of PKD3 expression in skeletal muscle was found in cross sections at stage E16.5, indicating potential function of the kinase in the regulation of sarcomerogenesis or

myoblast fusion, which occur during this phase of embryonic development (Gautel et al., 1998).

Apart from that, we were able to uncover further histological details about PKD3 expression patterns during organogenesis (as explicitly illustrated and discussed on page 34 et seq.) which might be of relevance for future studies in the field.

Finally, our study revealed that PKD3 expression patterns are differentially regulated during early mouse embryogenesis. Yet, from embryonic stage E13.5 onwards, PKD3 is more or less ubiquitously expressed. This is in agreement with the expression pattern of PKD3 observed in adult organs and tissues, suggesting a basic housekeeping function of the kinase (Hayashi et al., 1999).

Our results furthermore confirm previous data, showing a differential expression of all three PKD isoforms during embryogenesis (Oster et al., 2006). In this study, mouse embryonic expression patterns were visualized by in situ hybridization using isoform specific probes. Thus, Oster and colleagues provided supplementary information about isoform specific expression patterns. In some organs and developmental stages the three PKD family members have a strikingly different transcriptional activity whereas other tissues express all three PKD isoforms, implying either complementary or redundant functions of the PKDs (Oster et al., 2006).

Establishment of a transgenic mouse model to study the role of PKDs *in vivo*

One main goal of this study was to establish an appropriate PKD mouse model to study the physiological role of PKDs *in vivo*. Transgenic mice carrying EGFP-fused kinase-dead variants of PKD1, PKD2 or PKD3 under the control of the tetracycline responsive element were successfully generated in this work. For each construct, several transgenic mouse lines were obtained that were genetically stable and transmit the genetic alteration to their progeny. In double-transgenic animals, generated by crossing hemizygous Tg(tetO-PKDkd-EGFP) animals with mice hemizygous for a reverse tetracycline transactivator, transgene expression was demonstrated to be inducible in a doxycycline dependent manner. In conclusion, the transgenic strategy worked well and was successfully used to study phenotypes provoked by transgenic overexpression of kinase-dead PKDs (as discussed in the following two chapters).

However, one point has to be further discussed concerning the transgenic animals.

An important goal of the establishment of transgenic lines is to minimize the potential confounding influence of background genes from breeder parents (Crawley, 2007; Keverne et al., 1996). Transgene expression in an inhomogeneous genetic background can cause phenotypic variations and complicates the interpretation of experimental results (Gerlai, 1996). It is

therefore recommended to backcross newly established transgenic mice into an appropriate inbred background and thereby develop a so called congenic strain (Markel et al., 1997; Wong, 2002). The choice of genetic background should be determined according to the expected phenotype or according to the planned experimental application (Yoshiki and Moriwaki, 2006). However, a common disadvantage of inbred strains is their reduced reproductive capacity.

The transgenic animals generated in this study were established in the outbred background CD1. Transactivator strains were obtained in a mixed NMRI/B6 background and were successively backcrossed to CD1 to make use of the excellent breeding performance of this strain. Since backcrossing to obtain congenic strains is very time intensive, we immediately used transgenic founder animals with mixed genetic background for functional analysis. On the one hand this strategy was straightforward but on the other hand we had to cope with the drawbacks of an undefined genetic background. For the evaluation of experimental data obtained with these mice we therefore have to keep in mind that the detected phenotype might not be exclusively attributed to transgene expression and that genetic background effects can suppress or exacerbate an observed phenotype (Montagutelli, 2000; Valdar et al., 2006).

Hence, littermates were used whenever possible as control animals to limit the variances of the genetic background among the animals used for an experiment.

Role of PKD in muscle remodeling

The functional characterization of the newly generated transgenic mice was a crucial part of this thesis. Transgenic PKD1kd-EGFP expression in the background of the CMV/β-actin rtTA strain (Wiekowski et al., 2001) was shown to be highly upregulated in skeletal muscle upon doxycycline treatment. Moreover, fluorescence microscopy revealed a continuously uniform distribution within the skeletal muscle and an enrichment of the protein in the nuclei of myofibers. Despite the strong overexpression of PKDkd-EGFP, which should induce dominant-negative effects, those mice did not display any phenotypic abnormalities in comparison to control littermates. In the absence of natural stress conditions, laboratory mice, which have not been under any selective pressure since the early 1900s, often come up with only very subtle effects due to genomic mutations (Hofker and Deursen, 2003). The best option for discovering gene function in such a case is to increase the stress on the system e.g. by changing the environmental conditions. To approach this issue, we provided the mice access to running wheels. Hence, we investigated the role of PKD in exercise-induced muscle remodeling. Skeletal muscle consists of type I and type II fibers, exhibiting different metabolic and contractile properties. The fiber type composition of a muscle is highly dynamic and can be modified in response to environmental demands (Potthoff et al., 2007a). Voluntary wheel

running experiments demonstrated that the running performance of mice overexpressing dominant-negative PKD1 was significantly decreased compared to control mice. In line with this, analysis of skeletal muscle fiber type composition after voluntary wheel running revealed that exercise-induced muscle remodeling was blocked in animals with transgene expression. Therefore, our data indicate that PKD is a key regulator of exercise-induced skeletal muscle remodeling *in vivo*.

PKD was previously described as a class IIa HDAC kinase involved in hypertrophic cardiac remodeling (Vega et al., 2004). A similar role of PKD was proposed for the signaling pathways mediating skeletal muscle remodeling (Bassel-Duby and Olson, 2006). Recently, overexpression of a constitutively active mutant of PKD1 has been shown to alter the muscle fiber type composition in skeletal muscle *in vivo*. However, in the same study, deletion of PKD1 had no effect on muscle fiber type composition (Kim et al., 2008b). This result is in agreement with our hypothesis that PKD is involved in exercise-induced muscle remodeling. If constitutively active PKD is overexpressed as a transgene, the endogenous signaling pathway leading to the activation of muscle remodeling is bypassed.

Though, the physiological effect of voluntary wheel running on muscle performance and on the fiber type composition after voluntary exercise is indisputable, but molecular analyses of the underlying mechanism is still missing. Yet, based on our results, we propose the following model: overexpressed PKD1kd-EGFP blocks class IIa HDAC phosphorylation by competing with the endogenous PKDs and possibly other redundant HDAC kinases; class IIa HDACs remain in the nucleus, where they directly interact with the transcription factor MEF2 thereby inhibiting transcription of muscle remodeling genes. Numerous *in vitro* studies support the existence of this signaling pathway in skeletal muscle remodeling (Berdeaux et al., 2007; Liu et al., 2005; McKinsey et al., 2000a; Vega et al., 2004).

To quantitate the levels of total HDAC5 and phosphorylated HDAC5 in skeletal muscle lysates, we performed immunoprecipitation and Western blot analysis. However, we failed to detect differences (data not shown). One problem might be that the method is not sensitive enough to detect variances in a whole muscle lysate, since only single fibers are affected from the remodeling. Thus, the biochemical analysis of the phenotype remains challenging.

Apart from that, complementary tests to support the muscle remodeling phenotype are worth considering. Forced running experiments, force transducer measurements with isolated muscles or tests for impaired motor functions like open field locomotion are conceivable. Furthermore, studies using metabolic cages to measure food and liquid uptake, as well as oxygen and carbon dioxide consumption could be useful to reveal changes in the metabolic properties of the mice. In myotubes, PKD3 has been shown to be involved in the regulation of glucose uptake (Chen et al., 2005). From the present state of knowledge we can not ex-

clude that transgene expression also interferes with the metabolism and thereby contributes to the observed phenotype. However, in mice with skeletal muscle-specific overexpression of constitutively active PKD1, no alterations in the metabolic properties were detected (Kim et al., 2008b).

In cardiac myocytes an interaction of PKD with myofilament proteins has been demonstrated and cTnI has been identified as a specific PKD substrate involved in the regulation of myofilament Ca^{2+} sensitivity (Cuello et al., 2007; Haworth et al., 2004). A similar role of PKD in skeletal myocytes has not been discovered, yet it has to be taken into account that PKD might regulate muscle function and contraction properties also at the level of myofilament proteins.

Role of PKD in neuronal Golgi organization

Recently, our lab started to study PKD functions in mouse primary hippocampal neurons. All three PKD isoforms are expressed in the central nervous system already at embryonic stages in mice (Ellwanger et al., 2008; Oster et al., 2006). However, only a few studies have so far addressed the functional role of PKD in neurons implicating an involvement of PKD activity in the regulation of early dendritic development (Horton et al., 2005), neuronal polarization (Yin et al., 2008), or selective transport of dendritic proteins (Bisbal et al., 2008).

Since neurons are strongly polarized, they require an effective and strictly regulated intracellular transport machinery to provide the huge membrane surface and to establish and maintain the functional and structural asymmetry of the cells (Jareb and Banker, 1997; Zmuda and Rivas, 1998). Mature hippocampal neurons were found to have a thread-like, perinuclear Golgi structure, which usually extends into the main dendrite(s) (Horton et al., 2005). Transfection of mature hippocampal neurons either with fluorescently-tagged wild type PKD1 or with constitutively active PKD1 revealed that both proteins are selectively enriched at the TGN and do not interfere with its thread-like morphology. Moreover, introduction of a PKD reporter pointed out that endogenous PKD is highly active at the Golgi complex and in dendrites but not in the axon. Interestingly, the endogenous PKD1 level of primary hippocampal neurons increased considerably after plating, suggesting a potential role of PKD in neuronal development and neurite differentiation.

Transfection of mature hippocampal neurons with fluorescently tagged kinase-dead PKD1 led to the disruption of the neuronal Golgi complex. Another striking functional consequence was the severe shrinkage of the dendritic tree within 20 hours following transfection. Vice versa constitutively active PKD provoked an increase of the dendritic arborization. These results are in line with and extend previous observations where ectopic overexpression of kinase-dead

PKD1 was shown to inhibit dendritic outgrowth of hippocampal neurons in an early differentiation state (Horton et al., 2005).

All these *in vitro* experiments were based on the transfection of primary hippocampal neurons from wildtype mice. With the use of transgenic mice specifically overexpressing kinase-dead PKD in neurons, we aimed at a confirmation of these results *in vivo*. Double transgenic animals were generated by crossing Tg(tetO-PKD1kd-EGFP) mice with mice carrying rtTA2 under the control of the forebrain specific CaMKIIαpromoter (Michalon et al., 2005). After 2-4 weeks of doxycycline treatment transgene expression was analyzed. Notably, PKD1kd-EGFP was not uniformly expressed within the forebrain neurons. However, elevated transgene lev-els were detected in the hippocampal neurons, especially in the dentate gyrus (DG) and CA3 region. On a subcellular level, PKD1kd-EGFP was concentrated in the perinuclear region and in proximal dendrites. Furthermore, costaining with a trans-Golgi marker revealed that PKD1kd-EGFP was enriched at TGN structures, which presented with a fragmented pheno-type. Similar findings were obtained with primary hippocampal neurons from double trans-genic mice upon doxycycline treatment (data not shown). Thus, *in vivo* and *ex vivo* observa-tions are in full accordance with the results obtained with transfected hippocampal neurons and provide direct evidence that PKD activity is crucially involved in the maintenance of den-dritic arborization and Golgi structure of hippocampal neurons.

Very recently, another group reported about the requirement of PKD at the Golgi apparatus for the establishment and maintenance of neuronal polarity (Yin et al., 2008). Compared to our study, these authors addressed very early events of neuronal polarization. Loss of function of PKD directly after plating, mediated by chemical kinase inhibitors, RNA interference or by overexpression of dominant-negative PKD, was shown to disrupt polarized membrane trafficking and apparently induced multiple axon formation (Yin et al., 2008). Additionally, Yin and colleagues were able to show distinct functional properties of the PKD isoforms, by demonstrating that PKD1 and PKD2 are essential for neuronal polarization whereas PKD3 is dispensable in this context (Yin et al., 2008). Moreover, they applied PKD mutants with defective Golgi binding motifs and performed rescue experiments, which suggested that neuronal polarization selectively depends on PKD activity at the Golgi, but no other cell compartment (Yin et al., 2008).

The results of Yin et al (2008) are contradictory to preliminary observations made in our lab with DIV2 transfected primary hippocampamal neurons. According to our data, dominant-negative PKD1 reduced axonal as well as total neurite length, while expression of the constitutively active PKD1 mutant led to a decrease in side-branches and enhanced Tau1-immunostaining in all neurites (Katalin Czöndör and Katalin Schlett, unpublished results). Since Tau1 selectively marks axons already at this developmental stage (Mandell and Banker,

1996), our data also indicate that PKD activity interferes with early axon/dendrite specification. A latest report provided additional details on the polarized activity of PKD in neurons (Bisbal et al., 2008). Impaired PKD activity was shown to selectively alter intracellular trafficking with the consequence that dendritic but not axonal membrane proteins are mispackaged and mistargeted (Bisbal et al., 2008). These data are in full accordance with our own results indicating a prominent role in of PKD in maintaining dendrite structure. However, in light of the Yin lab data it is also clear that further studies are required to elucidate apparent discrepancies and to scrutinize the specific role of PKD in induction and maintenance of neuronal polarization and in neuronal functions.

Further, to which extend PKD-mediated phosphorylation of the neuronal substrates RIN1 (Wang et al., 2002) and Kidins220/ARMS (Iglesias et al., 2000) is involved in the regulation of physiological processes has to be determined in future studies.

Evaluation of PKD functions in other PKD mouse models

Contemporaneously with this study, two other PKD mouse models have been independently developped and first results published.

The group of Eric Olson investigated the role of PKD *in vivo* using a knockout approach. They designed a floxed *PRKD1* allele by inserting LoxP sites upstream of exon 12 and downstream of exon 14 (Fielitz et al., 2008). The floxed sequence encodes parts of the catalytic domain of PKD1 including the ATP binding motif that is essential for kinase function. To assess the consequences of a complete loss-of-function mutation of PKD1 they used a Cre transgenic mouse line, which activates Cre recombinase at the zygote stage (Sakai and Miyazaki, 1997). They reported that homozygous deletion of PKD1 at this early stage of development causes embryonic lethality, however with an incomplete penetrance (Fielitz et al., 2008). Specific developmental defects attributable to the lack of PKD1 and causal for the embryonic lethality have not been described in this study.

In addition to the conditional PKD1 knockout mouse (Fielitz et al., 2008), conventional transgenic mice overexpressing constitutively active PKD in cardiac muscle (Harrison et al., 2006) or skeletal muscle (Kim et al., 2008b) were generated. Interestingly, these mice were analyzed on the background of muscle dynamics and remodeling which was also addressed in this study. Ectopic overexpression of constitutively active PKD1 in heart or skeletal muscle *in vivo* was shown to cause cardiac hypertrophy and conversion of skeletal muscle fiber types, respectively (Harrison et al., 2006; Kim et al., 2008b).

In contrast, mice with cardiac specific deletion of PKD1 (PKD1 cKO) were indistinguishable from their wildtype littermates. Moreover, the hearts of WT and PKD1 cKO mice were compa-

rable in size and morphology (Fielitz et al., 2008). However, a phenotype became apparent after exposing the animals to stress cues that normally lead to cardiac hypertrophy, fibrosis and fetal gene activation. Mice lacking cardiac PKD1 showed an attenuated response to cardiac stress signals (Fielitz et al., 2008). Likewise, we did not detect any obvious differences between mice with and without expression of dominant-negative kinase-dead PKD1 in skeletal and cardiac muscle under non-stressed conditions. Though, we would expect a similar response in the heart, as observed for skeletal muscle, of mice overexpressing dominant-negative PKD1 upon application of appropriate stress conditions. Since the techniques to induce cardiac stress (thoracic aortic constriction or chronic angiotensin II stimulation using osmotic minipumps) are not established in our lab, we were not able to experimentally confirm this assumption.

Very similar effects were also described for MEF2D knockout mice upon induction of cardiac stress, confirming the hypothesis that this transcription factor drives pathological cardiac remodeling *in vivo* downstream of PKD1 (Kim et al., 2008d).

Comparing PKD mouse models

As described above, both conditional PKD1 knockout mice and inducible transgenic mice overexpressing dominant-negative PKDs are available meanwhile, it is timely to compare the two approaches.

Knockout versus dominant-negative approach

From a technical point of view both approaches require two mouse strains. In case of conditional knockout mice, one mouse strain harbors the floxed or FRP-flanked gene segment generated by gene targeting in ES cells and a second strain (the so called 'deleter strain') expresses site specific recombinases like Cre or FLP in one or several organs and either constitutively or upon induction (Kühn and Schwenk, 2002). For the inducible dominant-negative transgene approach, one mouse strain is required that carries the dominant-negative protein under the control of the tetracycline responsive element; a second mouse strain expresses the reverse tetracycline transactivator under the control of a tissue specific promoter.

The expression level of conventional transgenic mice depends on the site and frequency of transgene integration (as described in the Supplement section on page 92 et seq.). Most deleter strains are generated with conventional transgenic techniques, thus the expression of the recombinase is determined by the promoter used and by position effects of the integration site. Hence, the expression level of the recombinase determines the efficiency of gene deletion. Furthermore, the recombination efficiency is also influenced by the genomic integra-

tion site of the floxed or FRP-flanked gene segment (Baubonis and Sauer, 1993). As a consequence, one weakness of the current standard method to derive conditional knockout mice is insufficient recombination efficiency leading to hypermorphic mutants.

In mice with conditional cardiac specific deletion of PKD1 a fivefold reduction of mRNA levels was displayed (Fielitz et al., 2008). Nevertheless, a truncated mRNA composed of exon 1 to 11 was still transcribed and attested by rtPCR in lysates from knockout hearts. Low protein levels of PKD1 were moreover detectable in heart lysates from knockout mice. Thus, the authors claim that residual expression most likely reflects PKD1 expression in fibroblasts, endothelial smooth muscle cells and immune cells within the heart (Fielitz et al., 2008). However, one cannot rule out the possibility that the residual PKD expression results from incomplete recombination efficiency in the cardiomyocytes. The situation looks even worse for the mice with skeletal muscle-specific deletion of PKD1. In the soleus about 30% of the wildtype mRNA level was still present and in other muscle groups even up to 50% (Kim et al., 2008b), indicating that the recombination of the floxed PKD1 alleles was far from being complete. One should keep in mind that even low percentage of intact genes can be sufficient to carry out essential gene functions and prevent the obvious manifestation of pathophysiological phenotypes. This might also explain the only very subtle effects of the muscle-specific PKD1 deletion regarding fatigue resistance during repetitive contractions (Kim et al., 2008b).

The following considerations brought us to the decision that a dominant-negative transgene approach is favorable to study the role of the multifunctional kinase family PKD. It is widely accepted that the individual PKDs act, at least in part, functionally redundant. Moreover, the expression patterns of the distinct isoforms have been shown to be partially overlapping. Thus, a knockout of one PKD family member could conceivably be compensated by the presence of a redundant PKD isoform. To study PKD function in such a case it would be necessary to target all three PKD isoforms and create double or triple knockout animals. Compared to this, the transgenic overexpression of one single kinase-dead PKD isoform can exert a dominant-negative effect on all PKD isoforms that might have redundant functions. However, with a kinase-dead mutant it is not possible to assess functions that depend on mechanisms independent from the kinase activity (e.g. scaffolding function). Thus the phenotype of a mouse overexpressing dominant-negative PKD is not necessarily expected to be equal to the phenotype of a PKD knockout mouse. Such discrepancies have been described for several kinases (Knight and Shokat, 2007; Madeddu et al., 2008).

General evaluation of the functional PKD knockout mouse model

The Tet system is currently the best approved system for inducible transgene expression (Schönig and Bujard, 2002). For our transgenic approach the tetracycline activation principle

turned out to be very well applicable. Doxycycline administration induced a strong upregulation of transgene expression in a variety of organs depending on the tissue specificity of the promoter used in the transactivator strain. Only in the brain doxycycline induced transgene expression was more problematic. Even though doxycycline penetrates the blood brain barrier fairly well, the concentration achieved in this compartment of the mouse body is considerably low compared with serum levels (Mansuy et al., 1998b). Accordingly, rather high concentrations of doxycycline in the food of the animals (approximately 6mg of Dox/g of food) are needed for full activation of rtTA (Malleret et al., 2001; Mansuy and Bujard, 2000; Mansuy et al., 1998a). Though, compared to the expression pattern described in the original publication of the used transactivator mice (Michalon et al., 2005), we observed only a very patchy expression in the forebrain, even after treating the animals with high concentrations of doxycycline for more than 4 weeks. This discrepancy can most likely be explained by integration effects of the responder transgene. It is therefore crucial that for each single application the combination of transactivator and responder line has to be well coordinated. For the characterization of transactivator strains several indicator mouse lines expressing luciferase or β-galactosidase are available (Kistner, 1996; Kistner et al., 1996). Patchy expression of the transactivator in a specific organ or tissue will never enable uniform expression of a responder transgene.

With the random integration approach, it is possible to generate mouse lines in which a very stringent control and a wide window of regulation of a transgene of interest can be achieved. However, several transgenic lines for each constructs have to be generated, combined with suitable transactivator strains and characterized for controlled induction and pattern of transgene expression.

In our study appropriate transactivator strains were selected, combined with newly generated PKDkd-EGFP responder mice and transgene expression was extensively characterized. Tissue specific overexpression of kinase-dead PKD was shown to interfere with endogenous PKD functions, like Golgi organization and regulation of muscle remodeling, and can therefore be regarded as functioning dominant-negative.

In conclusion, a new transgenic mouse model of inducible interference with PKD function has been established, which serves as a valuable tool for the analysis of PKD's *in vivo* role. With the muscle and brain specific expression of the transgene not only proof of concept of the transgenic model was obtained, but already novel insights into organ specific PKD functions. It is apparent from these initial results that the established dominant-negative PKD mouse model is useful for a wide spectrum of further applications addressing *in vivo* PKD functions.

Publication manuscripts

Expression patterns of protein kinase D 3 during mouse embryogenesis

Kornelia Ellwanger, Klaus Pfizenmaier, Sylke Lutz and Angelika Hausser*

Institute of Cell Biology and Immunology, University Stuttgart, Stuttgart, Germany

*Corresponding author

BMC Developmental Biology 2008, **8**:47
Received: 11 January 2008
Accepted: 25 April 2008
Published: 25 April 2008

Abstract

Background: The PKD family of serine/threonine kinases comprises a single member in *Drosophila* (dPKD), two isoforms in *C. elegans* (DKF-1 and 2) and three members, PKD1, PKD2 and PKD3 in mammals. PKD1 and PKD2 have been the focus of most studies up to date, which implicate these enzymes in very diverse cellular functions, including Golgi organization and plasma membrane directed transport, immune responses, apoptosis and cell proliferation. Concerning PKD3, a role in the formation of vesicular transport carriers at the trans-Golgi network (TGN) and in basal glucose transport has been inferred from *in vitro* studies. So far, however, the physiological functions of the kinase during development remain unknown.

Results: We have examined the expression pattern of PKD3 during the development of mouse embryos by immunohistochemistry. Using a PKD3 specific antibody we demonstrate that the kinase is differentially expressed during organogenesis. In the developing heart a strong PKD3 expression is constantly detected from E10 to E16.5. From E12.5 on PKD3 is increasingly expressed in neuronal as well as in the supporting connective tissue and in skeletal muscles.

Conclusions: The data presented support an important role for PKD3 during development of these tissues.

Background

The protein kinase D (PKD) family of serine/threonine kinases comprises a single member in *Drosophila* (Maier et al., 2006; Maier et al., 2007), two isoforms in *C. elegans* (Feng et al., 2006a; Feng et al., 2006b) and three members, PKD1 (PKCμ), PKD2 and PKD3 (PKCν) in mammals. The three mammalian isoforms share similar structural modules. They consist of an N-terminal regulatory domain and a C-terminal kinase domain. While PKD1 and PKD2 posses an alanine/proline-rich region at their N–terminus, in PKD3 this hydrophobic domain is absent. All isoforms contain two cysteine-rich domains (CRD) separated by a long linker region, an acidic region consisting of negatively charged amino acids and a pleckstrin homology domain (PH). These characteristic motifs are also important for the regulation of enzyme activity and localization within cells. The PKD enzymes have recently been implicated in very diverse cellular functions, including Golgi organization and plasma membrane directed transport, metastasis, immune responses, apoptosis and cell proliferation (for an overview see (Wang, 2006)). PKD3 was originally identified in 1999 (Hayashi et al., 1999). Northern blot analysis revealed a ubiquitous expression of the protein in a wide variety of human tissues suggesting a basic housekeeping function (Hayashi et al., 1999). *In vitro* studies propose a potential role of the kinase in signaling events of GPCR agonists which induced a rapid activation of PKD3 by a protein kinase C (PKC)-dependent pathway (Rey et al., 2003). PKD3 can also be activated by bombesin in a Rac and Gαdependent mechanism (Yuan et al., 2005; Yuan et al., 2006). Moreover, PKD3 was implicated to play a role in B cell antigen receptor signaling by phosphorylating class II HDAC5 and 7 thereby promoting nuclear export of these proteins (Matthews et al., 2003; Matthews et al., 2006). Activation of PKD3 in these cells involves the phosphorylation of the activation loop serines which is mediated by a DAG-PLC-PKC-dependent pathway. Putative upstream kinases for PKD3 are PKCε, PKCη or PKCθ(Matthews et al., 2003). According to the localization of the kinase at the trans-Golgi network (TGN) (Hausser et al., 2005), a function in the formation of exocytotic transport carriers has been described (Yeaman et al., 2004). Recently, it could be demonstrated that PKD3 and PKD2 dimerize at the TGN and regulate membrane fission (Bossard et al., 2007). How-ever, there is also substantial evidence that PKD3 has a distinct and non-redundant function within the PKD family. Compared to PKD1 and 2, PKD3-specific direct substrates at the TGN have not been identified yet (Fugmann et al., 2007; Hausser et al., 2005). A PDZ domain identified in PKD1 and 2 is lacking in PKD3 (Sanchez-Ruiloba et al., 2006). Moreover, PKD1 and PKD2, but not PKD3, are targets for PKCδin response to oxidative stress, because PKD3 lacks the relevant tyrosine residue that generates a PKCδinteraction motif (Doppler and

Storz, 2007). PKD3 also localizes to vesicular structures that are part of the endocytic compartment. This localization may be mediated by the interaction of PKD3 with the vesicle-associated membrane protein VAMP2 (Lu et al., 2007). In L6 skeletal muscle cells, a specific role for PKD3 in basal glucose uptake could be demonstrated (Chen et al., 2005).

The functional activities of PKD3 described so far are derived from *in vitro* studies performed with established cell lines. Transgenic mouse models, which allow interference with endogenous PKD3, are not available. Consequently, the *in vivo* functions of PKD3 remain unknown so far. In a recent report, Oster and colleagues described the expression of PKD isoforms during mouse embryogenesis using *in situ* hybridization techniques (Oster et al., 2006). In early stages of development, PKD3 mRNA was clearly detected in the heart, nasal processes and limb buds. During later stages of development, PKD3 transcript was more or less ubiquitously present. In an independent study, we have investigated the expression of PKD3 protein by immunohistochemistry on sagittal sections of mouse embryos using a PKD3 specific antibody. We here describe PKD3 protein expression in developmental stage E10 through E16.5 of the mouse.

Results and Discussion

Specificity of the PKD3 antibody

The affinity purified polyclonal PKD3 specific antibody used in this study was generated by immunization of rabbits with a peptide corresponding to the C-terminal epitope of human PKD3 (amino acids 875 to 890). This epitope is conserved in the mouse orthologous gene, but not present in PKD1 or PKD2 isoforms (Fig. 1A). To demonstrate that the antibody is specific for PKD3 and not cross-reactive with PKD1 and PKD2, we performed Western blot analysis. Total cell lysates of HEK293T cells transiently transfected with plasmids encoding GFP-tagged human PKD1, GFP-tagged human PKD2, and human Flag-tagged PKD3 were analyzed (Fig. 1B). The PKD3-specific antibody detected Flag-PKD3, migrating at about 120 kDa, and endogenous PKD3, migrating at about 105 kDa, but not PKD1 or PKD2, thus demonstrating the specificity of the reagent. Since no PKD3 mutants are available, the antibody could not be tested in a PKD3 deficient background. We have therefore applied several approaches to confirm specificity of the PKD3 antibody used here; control staining procedures performed without the primary antibody or with rabbit preimmune-serum were all negative. Various antibody dilutions (1:500 – 1:2000) had no effect on the staining pattern (data not shown). In addition, we performed staining with either Flag-specific mouse monoclonal or GFP-specific rabbit polyclonal antibodies that was negative, too (Fig. 1C).

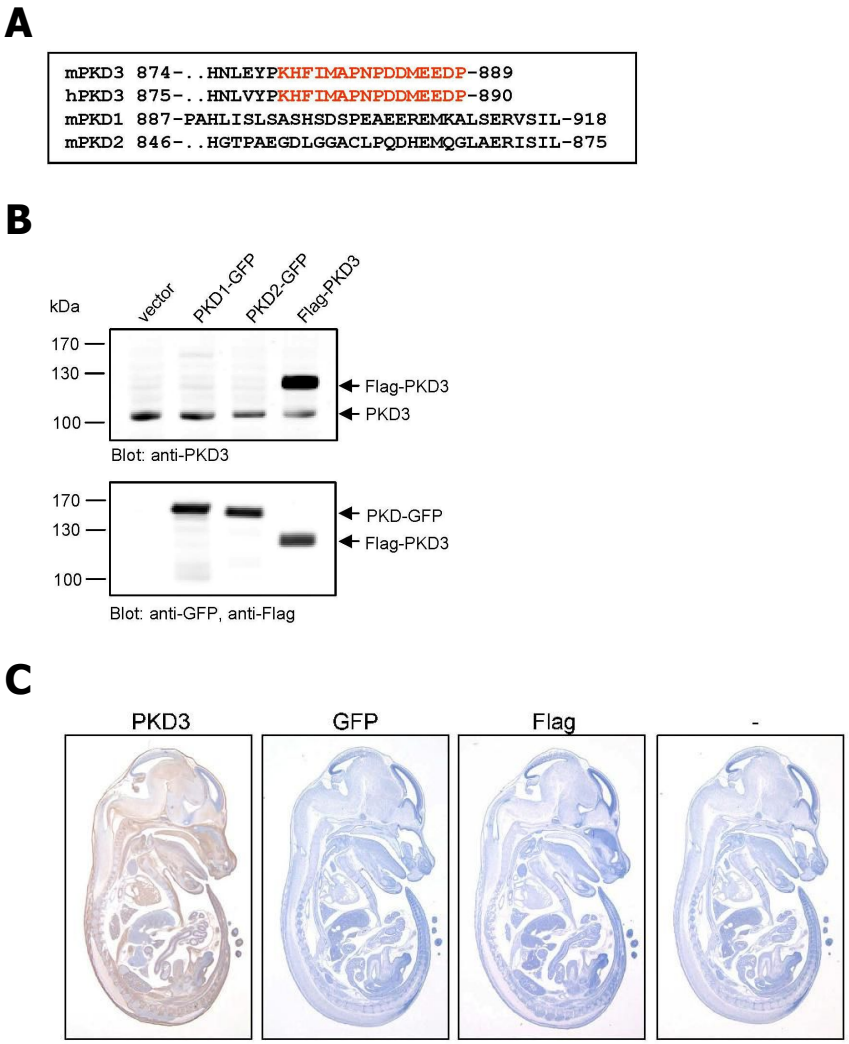

Figure 1 – Specificity of the PKD3 antibody. A: Sequence alignment of mouse PKD3 with human PKD3, mouse PKD1 and PKD2. The sequence of PKD3 used for peptide synthesis and immunization of mice is marked in red. **B**: HEK293T cells were transfected with the indicated plasmids, whole cell lysates were prepared and Western blot analysis was performed with the indicated antibodies. **C:** Immunohistochemistry on sagittal sections (6 µm) of E14.5 mouse embryos. Sections incubated with mouse Flag- and rabbit GFP-specific antibodies (both 0.5 µg/ml), respectively or without primary antibody (-) were negative and used as control. Section incubated with rabbit anti-PKD3 antibody (1:2000) displayed specific staining.

PKD3 expression in early and later stages of development

Performing immunohistochemistry on paraffin sections of mouse embryos at developmental stage E10 – E16.5 we obtained histological details of PKD3 expression.

In E10.0 the most prominent expression was evident in the developing heart (Fig 2C, D and E). Cells forming the ventricular and atrial chambers showed a strong staining (Fig. 2E and I). This strong expression in the heart was visible from early to late stages of embryonic development (Fig. 2-7). Recent work suggests an important role for the PKD kinase family in car-

diac myocytes. The expression of PKD1 and PKD2 or PKD3 was demonstrated in neonatal and adult rat ventricular myocytes as well as adult mouse, rat, rabbit, and human myocardium (for an overview see (Avkiran et al., 2008)). Of note, the PKD expression seems to be subject to developmental regulation and declines significantly in adulthood (Haworth et al., 2000). Furthermore, studies with transgenic mice revealed a role for PKD1 in pathological cardiac remodeling. Cardiac-specific expression of a constitutive active PKD1 *in vivo* caused hypertrophy, chamber dilation, and impaired systolic function (Harrison et al., 2006). Conversely, mice with a cardiac specific PKD1 knockout demonstrated an impaired response to stress signals that normally lead to cardiac hypertrophy, fibrosis and fetal gene activation (Fielitz et al., 2008). There is substantial evidence that this phenotype is associated with the PKD-mediated phosphorylation of class II HDAC5. However, each PKD isoform is capable of phosphorylating class II HDACs on the serines that mediate nuclear export via interaction with 14-3-3 proteins (Huynh and McKinsey, 2006; Matthews et al., 2006), suggesting that PKD family members could act redundant. Although the diminished hypertrophic response of PKD1 cardiac knockout mice indicates that PKD2 and 3 cannot fully compensate for the loss of PKD1 it is likely that the residual hypertrophy and fetal gene activation in these animals reflects redundant functions of cardiac PKD2 and 3.

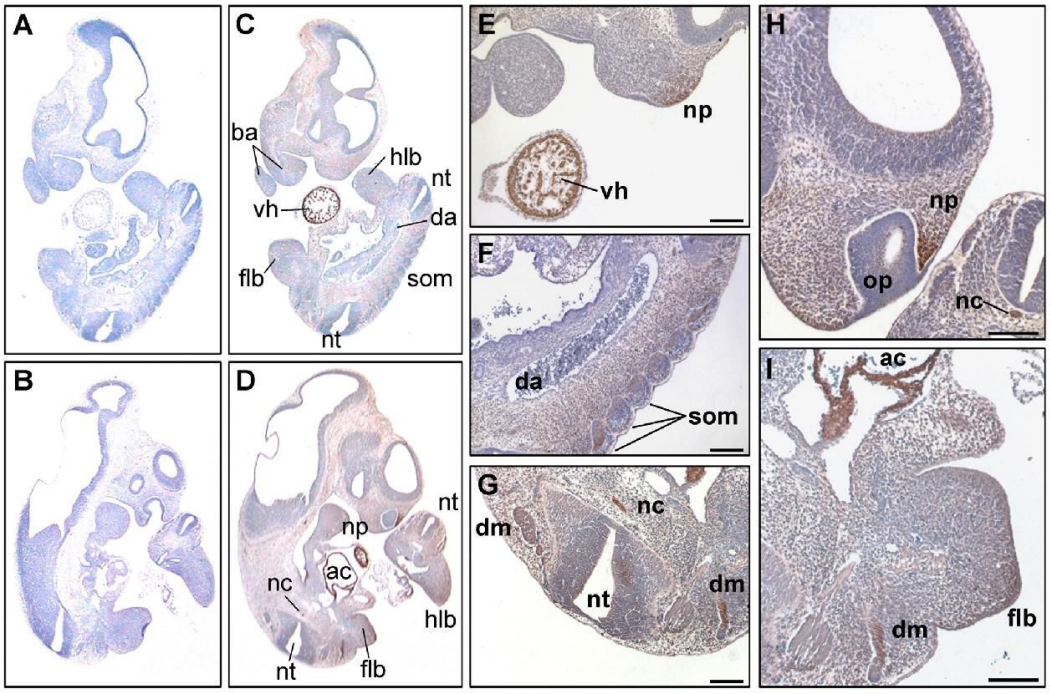

Figure 2 – PKD3 expression at embryonic stage E10. Immunohistochemistry was performed on sagittal sections (6 µm) of E10 mouse embryos. (A) - (B) Control sections incubated without primary antibody. (C) - (I) Sections incubated with anti-PKD3 antibody (1:2000). ac: atrial chamber, ba: branchial arch, da: dorsal aorta, dm: dermamyotome, flb: forelimb bud, hlb: hindlimb bud, nc: notochord, np: nasal process, nt: neural tube, op: olfactory pit, som: somites, vh: ventricular chamber of heart. Scale bars: 100 µm.

In addition, PKD3 was expressed in the nasal processes (Fig. 2D, E and H) and forelimb buds (Fig. 2I). These observations are in line with previously published data on mRNA distribution at this stage (Oster et al., 2006). On top of this, an obvious PKD3 expression was also visible in the embryonic mesoderm. Especially somite derived structures forming the dermamyotome (Fig. 2F, G and I) and the notochord (Fig. 2G, H) were PKD3 positive. Of note, PKD3 was not expressed in erythrocytes present in the atrium and the dorsal aorta (Fig. 2F and I). In contrast to *in situ* hybridization studies (Oster et al., 2006) PKD3 protein could not be detected in the forebrain or midbrain region at this stage. This might be due to low levels of PKD3 mRNA at this stage (Oster et al., 2006), which might result in low protein levels that are difficult to detect and/or additional regulation of PKD3 expression at the posttranscriptional level in this tissue.

In embryonic stage E11.5 PKD3 expression was detectable in additional tissues (Fig. 3C and D). Parts of the head region near the developing base of the scull and nasal process (Fig. 3E) were positive for PKD3 protein. PKD3 expression was visible in and along the notochord, where sclerotomic material is condensed to form the centrum of the axis (Fig. 3H and J).

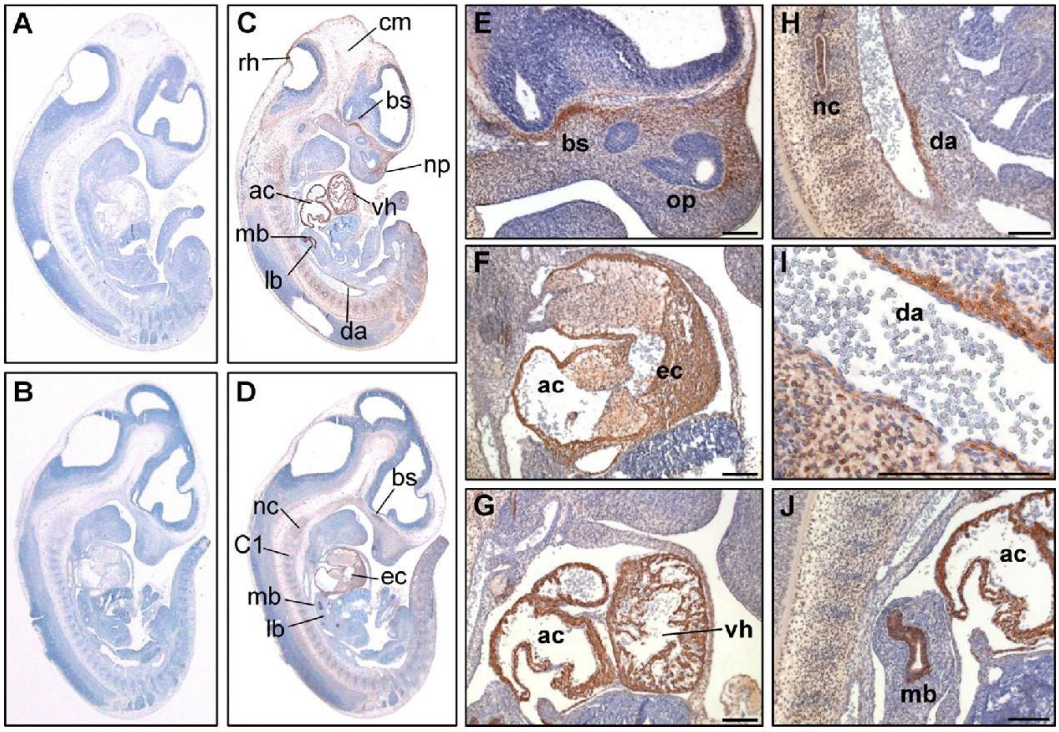

Figure 3 – PKD3 expression at embryonic stage E11.5. Immunohistochemistry was performed on sagittal sections (6 µm) of E11.5 mouse embryos. (A) - (B) Control sections incubated without primary antibody. (C) - (J) Sections incubated with anti-PKD3 antibody (1:2000). ac: atrial chamber, bs: cartilage primordium of base of the skull, C1: condensation of sclerotomic material forming centrum of axis, cm : cephalic mesenchyme, da: dorsal aorta, ec: endocardial cushion tissue lining the atrioventricular canal, lb: lung bud, mb: main bronchus, nc: notochord, np: nasal process, op: olfactory pit, rh: roof of hindbrain, vh: ventricular chamber of heart. Scale bars: 100 µm.

A strong PKD3 expression was detected in the bronchus of the lung bud (Fig. 3J) restricted to the cytoplasm of the epithelium. PKD3 expression in the cardiac muscle cells was still obvious (Fig. 3F, G). Moreover, PKD3 was expressed in the wall of the dorsal aorta at this stage (Fig. 3H and I).

In embryonic stage E12.5 more cytological details of PKD3 expression were visible (Fig. 4C, D). PKD3 was detected in the cartilage primordium of nasal bones (Fig. 4E), the temporal bones (Fig. 4J) and the vertebra (Fig. 4F). PKD3 expression was still detectable in the notochord (Fig. 4F and F``) and in cardiomyocytes forming the ventricular and atrial chambers but was absent from the atrio-ventricular bulbar cushion tissue (Fig. 4G). Further, the membrane of the oesophagus showed a strong PKD3 expression (Fig. 4F and F´). Within the lung strong PKD3 expression was found in epithelial cells of segmental bronchii (Fig. 4H). PKD3 expression is also observed in the urogenital ridge surrounding the lumen of the urogenital sinus (Fig. 4I). Moreover, PKD3 expression now became detectable in the developing brain, with a prominent staining of the outer layer of the choroid plexus within the fourth ventricle (Fig. 4K). In the stomach, the mucous membrane was PKD3 positive (Fig. 4L).

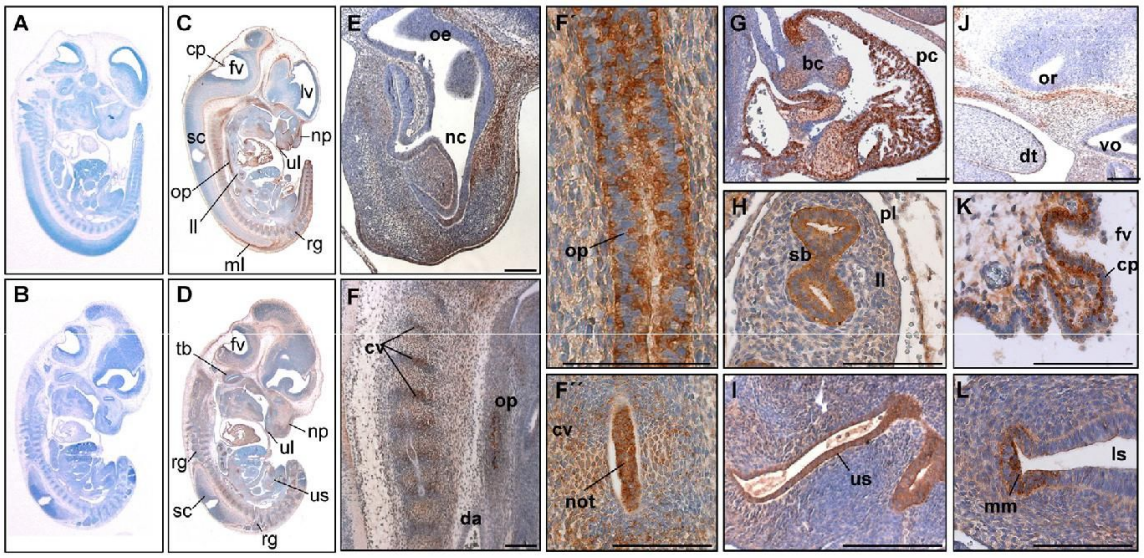

Figure 4 – PKD3 expression at embryonic stage E12.5. Immunohistochemistry was performed on sagittal sections (6 µm) of E12.5 mouse embryos. (A) - (B) Control sections incubated without primary antibody. (C) - (L) Sections incubated with anti-PKD3 antibody (1:2000). bc: atrio-ventricular bulbar cushion tissue, cp: origin of choroid plexus, cv: cartilage primordium of vertebra, da: descending (thoracic) aorta, dt: dorsum of tongue, fv: fourth ventricle, ll: left lung, ls: lumen of stomach, lv: lateral ventricle, ml: marginal layer of spinal cord, mm: mucous membrane, nc: nasal cavity, not: notochord, np: nasopharynx, oe: olfactory epithelium, op: oesophagus, or: optic recess of diencephalon, pc: pericardial cavity, pl: pleural cavity, rg: root ganglia, sb: segmental bronchus, sc: spinalcord, tb: cartilage primordium of temporal bone, ul: upper lip, us: urogenital sinus, vo: vomeronasal organ. Scale bars: 100 µm.

In embryonic stage E13.5 PKD3 was found to be more or less ubiquitously expressed (Fig. 5C and D). In addition to PKD3 positive structures like cardiomyocytes (Fig. 5E), the protein could also be detected in further muscle structures: Skeletal muscle cells of the neck region (Fig. 5F) as well as muscles of the tongue (Fig. 5G and G´) showed strong PKD3 expression. In the lung, the epithelial layer of the segmental but not the main bronchi was positive (Fig. 5H, H´). A prominent PKD3 expression could be detected in the middle layer (submucosa) of the stomach, but not the inner layer (mucosa) (Fig. 5I and I´). Prominent sites of PKD3 expression were also detected in the marginal layer of the spinal cord (Fig. 5J) and the choroid plexus within the fourth ventricle (Fig 5K and K´). Expression of PKD3 was also detected in developing bones. Especially the cartilage primordium of turbinate bones (Fig. 5L) and osteoblasts in the vertebrae which secrete bone material into previously existing cartilage matrix were intensively stained (Fig. 5M and M´). The membranous layer surrounding cartilage during ossification, the perichondrium, was also positive for PKD3 expression (Fig. 5M´). Of note, the ventricular zone of the neocortex as well as the liver was negative (Fig 5C and D).

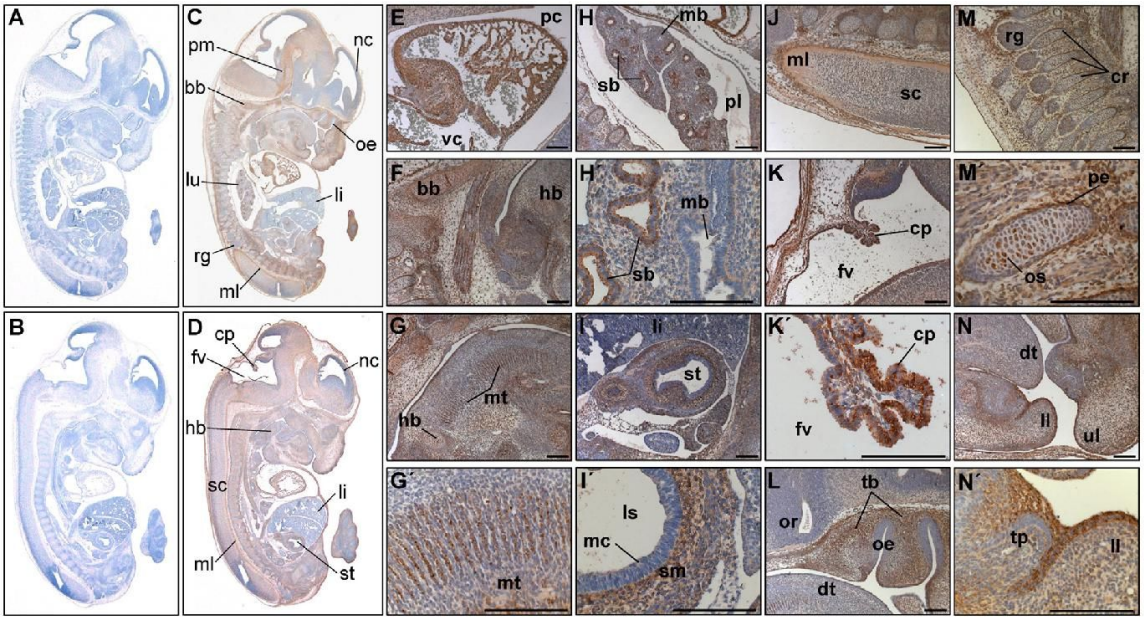

Figure 5 – PKD3 expression at embryonic stage E13.5. Immunohistochemistry was performed on sagittal sections (6 µm) of E13.5 mouse embryos. (A) - (B) Control sections incubated without primary antibody. (C) - (N´) Sections incubated with anti-PKD3 antibody (1:2000). bb: cartilage primordium of basioccipital bone (clivus), cp:choroid plexus, cr: cartilage primordium of ribs, dt: dorsum of tongue, fv: fourth ventricle, hb: cartilage primordium of body of hyoid bone, li: liver, ll: lower lip, ls: lumen of stomach, lu: lung, mb: main bronchus, mc: mucosal lining, ml: marginal layer of spinal cord, mt: muscle mass of the tongue, nc: neocortex, oe: olfactory epithelium, or: optic recess of diencephalon, os: osteoblasts, pc: pericardial cavity, pe: perichondrium, pl: pleural cavity, pm: pons-midbrain junction, rg: root ganglion, sb: segmental bronchus, sc: spinal cord, sm: submucosa, st: stomach, tb: cartilage primordium of turbinate bones, tp: tooth primordium, ul: upper lip, vc: vena cava. Scale bars: 100 µm.

PKD3 expression in osteoblasts was even more prominent in stage E14.5 in developing bones of the spinal column (Fig. 6G). The nucleus pulposus in the middle of the spinal disc was also intensively stained (Fig. 6H, H´). Skeletal muscle cells of the diaphragm (Fig. 6I, I´) also showed a strong PKD3 expression. Oster and colleagues failed to detect elevated levels of PKD3 mRNA in skeletal muscle by *in situ* hybridization [20]. The reason for this seeming discrepancy is unclear and might be of technical nature or reflect the fact that the level of mRNA does not necessarily correlate with the protein level.

In this stage we found a strong expression in the kidney capsule (Fig. 6J, J´), in terminal bronchioles of the lung (Fig. 6K), in the nuclei of distinct cells of the liver (Fig. 6L) as well as in the middle layer of the duodenum (Fig. 6M). In the brain, PKD3 expression was ubiquitously detected with exception of the neocortex, which was negative (Fig. 6D, E, F). Interestingly, in the medulla oblongata distinct nerve tracts were intensively stained for PKD3 (Fig. 6N); moreover, the choroid plexus within the fourth and lateral ventricle was also positive (Fig. 6E, O). In accordance with published data on PKD3 mRNA expression [20] the inner layer of the retina shows a weak PKD3 specific staining, whereas the extrinsic ocular muscle displays a strong expression of PKD3 (Fig. 6P). Interestingly, cells within the olfactory epithelium displayed a strong PKD3 signal within the nuclei (Fig. 6Q). The root sheath of the Whisker follicles showed a steady PKD3 expression in E14.5 and E16.5 (Fig. 6R, R´, and 7H). Furthermore, the suprabasal layer of the epidermis as well as underlying connective tissue (Fig. 6S) are positive for PKD3. The epidermal staining was impressively evident in the mouth region where PKD3 negative endoderm and PKD3 positive ectoderm derived epidermal layers came into direct contact (Fig. 6T). PKD3 is also expressed in the first primordium of the upper molar tooth (Fig. 6U), which is formed by an incorporation of dental epithelium.

Figure 6 – PKD3 expression at embryonic stage E14.5. Immunohistochemistry was performed on sagittal sections (6 µm) of E14.5 mouse embryos. (A) - (C) Control sections incubated without primary antibody. (D) - (U) Sections incubated with anti-PKD3 antibody (1:2000). bl: basal layer of epidermis, ce: cerebellum, cp: choroid plexus, du: duodenum, il: inner layer of retina, kc: kidney capsule, ki: kidney, ld: lumen of duodenum, le: lens, li: liver, lv: lateral ventricle, mb: main bronchus, md: muscle of diaphragm, mf: muscle fibers, ml: marginal layer of spinal cord, mo: medulla oblongata, mr: medulla renalis, mt: primordium of upper molar tooth, mu: muscularis layer of duodenum, nb: cartilage primordium of the nasal bone, nc: nasal cavity, nl: neural layer of retina, np: nucleus pulposus in the central region of future invertebral disc, oe: olfactory epithelium, op: oesophagus, or: oropharynx, rg: root ganglia, rp: renal pelvis, sc: spinal cord, scl: sclera, sl: suprabasal layer of epidermis, sm: submucosal layer of duodenum, sp: cartilage primordium of spinal column, st: stomach, tb: terminal bronchus, th: thymus, tt: tip of the tongue, ul: upper lip, vi: primordia of follicles of vibrissae. Scale bars: 100 µm.

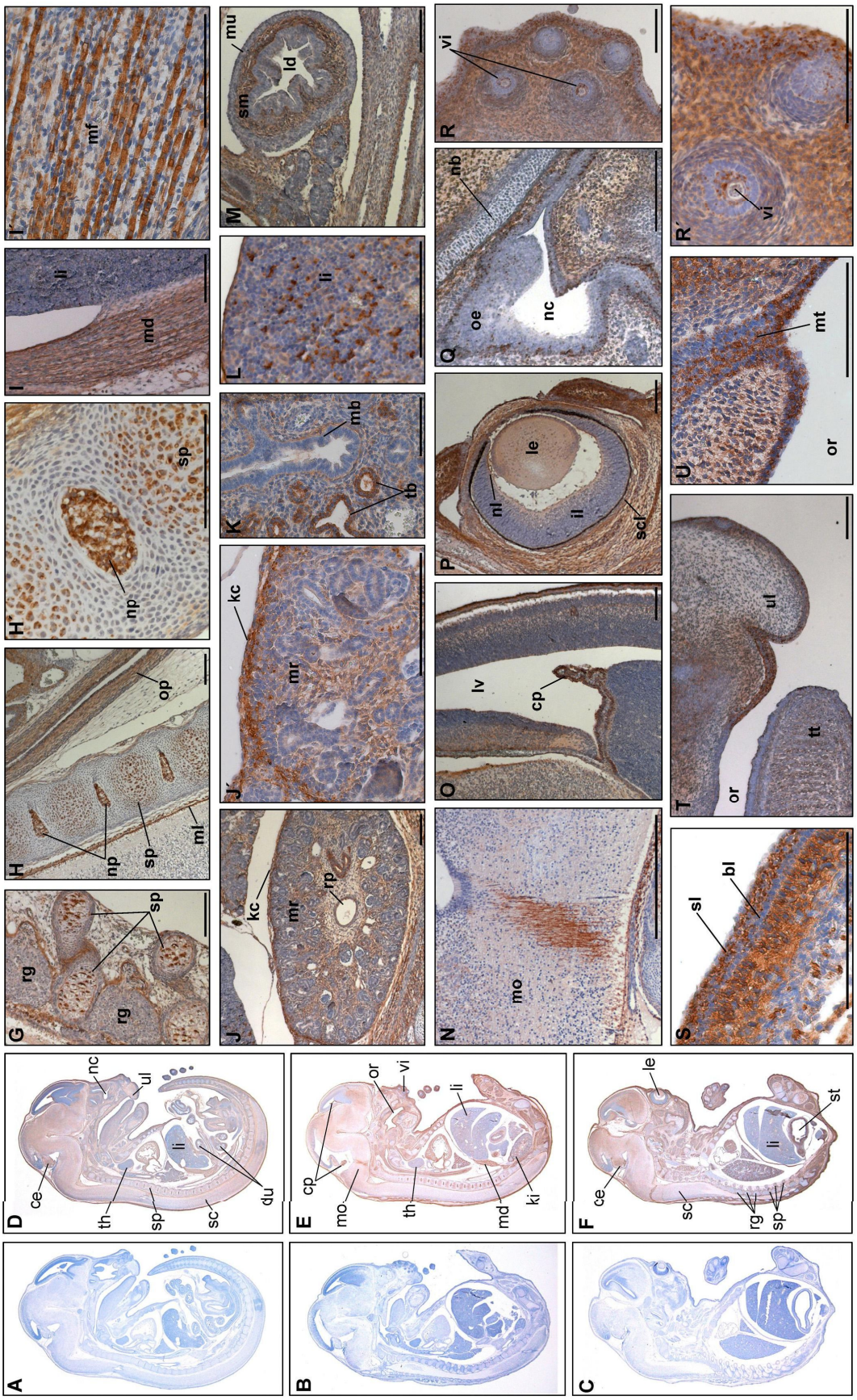
A
B
C
D
ce
nc
ul
th
li
sp
sc
du
E
cp
or
vi
mo
th
li
md
ki
F
le
ce
st
sc
li
rg
sp
G
rg
sp
rg
H
op
np
sp
ml
H´
sp
np
I
li
md
I´
mf
J
kc
mr
rp
J´
kc
mr
K
mb
tb
L
li
M
mu
sm
ld
N
mo
O
lv
cp
P
le
nl
il
scl
Q
nb
oe
nc
R
vi
R´
vi
S
sl
bl
T
or
ul
tl
U
mt
or

PKD3 was found to be more ore less ubiquitously expressed in embryonic stage E16.5 (Fig. 7C and D). Particularly strong PKD3 expression was detected in nerve tracts in the pons (Fig. 7E) and the choroid plexus of the lateral and fourth ventricle (Fig. 7F, G). The middle layer (submucosa) but not the mucosa or the muscle layer (Fig. 7I) demonstrated PKD3 expression. In contrast to E13.5, the submucosa of the stomach showed only a weak PKD3 expression, however, smooth muscle cells in the muscularis layer of the stomach were still PKD3 negative (Fig. 7J, J´). Within the liver PKD3 expression seemed to be further increased (Fig. 7C, D), which is in accordance with high mRNA levels detected by *in situ* hybridization in E18.5 (Oster et al., 2006). The strong PKD3 expression in the kidney capsule (Fig. 7K) and in the terminal bronchi of the lung (Fig. 7L) detected in E14.5 was even more evident. In the region of the lower lip, the intensive staining of the suprabasal layer of the epidermis was

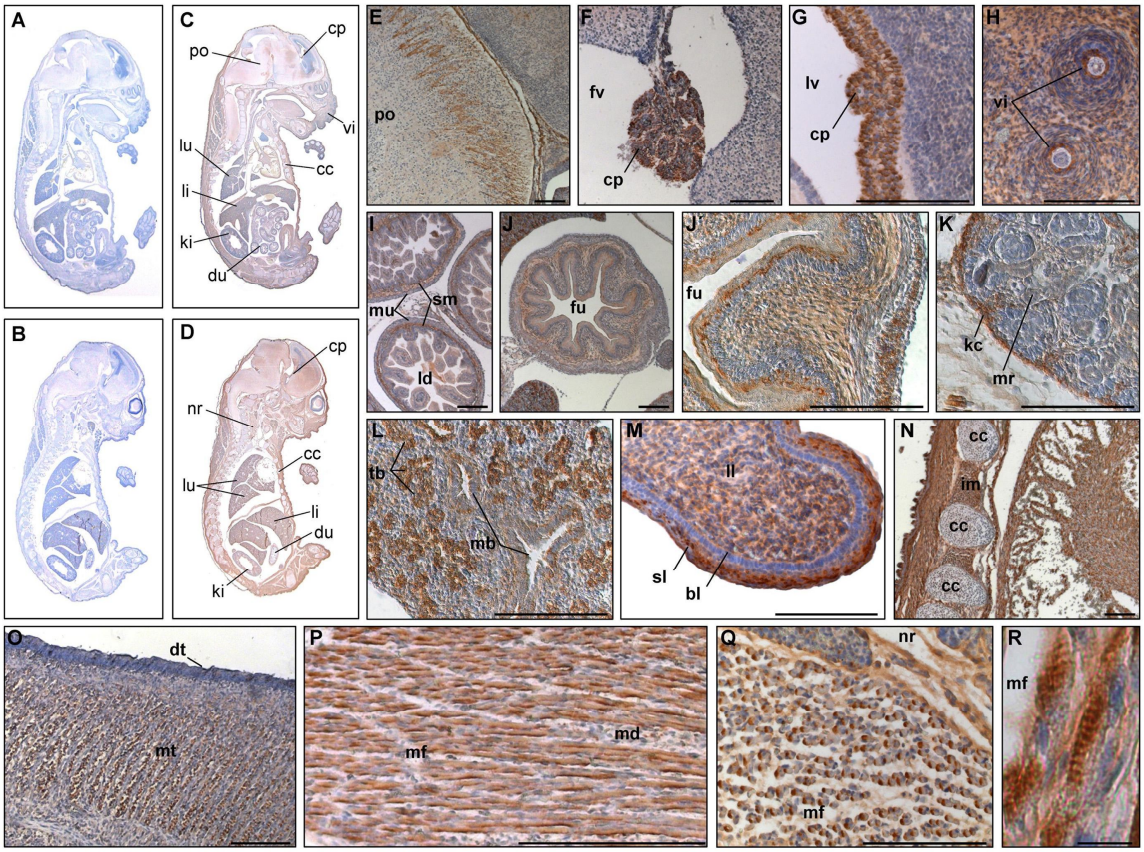

Figure 7 – PKD3 expression at embryonic stage E16.5. Immunohistochemistry was performed on sagittal sections (6 µm) of E16.5 mouse embryos. (A) - (B) Control sections incubated without primary antibody. (C) - (Q) Sections incubated with anti-PKD3 antibody (1:2000). bl: basal layer of epidermis, cc: costal cartilage, cp: choroid plexus, dt: dorsum of tongue, du: duodenum, fu: fundus region of stomach, fv: fourth ventricle, im: intercostal muscle, kc: kidney capsule, ki: kidney, ld: lumen of duodenum, li: liver, ll: lower lip, lu: lung, lv: lateral ventricle, mb: main bronchus, md: muscle fibers of diaphragm, mf: muscle fibers, mr: medulla renalis, mt: muscle mass of the tongue, mu: muscularis layer, nr: neck region, po: pons, sl: suprabasal layer of epidermis, sm: submucosal layer, tb: terminal bronchus, vi: primordia of follicles of vibrissae. Scale bars: 100 µm (E) - (Q), 10 µm (R).

obvious (Fig. 7M). All skeletal muscle cells within the embryo showed a strong PKD3 expression (Fig 7 N-R) e.g. intercostal muscle cells (Fig. 7N) and the transverse muscle fibers of the tongue (Fig. 7O). Interestingly, PKD3 distribution in skeletal muscle cells of the diaphragm (Fig. 7P) and the neck region (Fig. 7Q) is polarized, especially visible in cross-sections (Fig. 7Q). Of note, PKD3 was not detected in smooth muscle cells and in the thymus at this stage. Interestingly, Oster and colleagues could detect PKD3 mRNA in the thymus at E18.5 (Oster et al., 2006). In line with this, Western blot analysis revealed a strong PKD3 expression in the thymus of adult animals (unpublished observation K. Ellwanger), suggesting an increase in the expression level of PKD3 protein in neonatal mice.

Conclusion

The expression pattern of PKD3 reveals a tissue selective expression at stage E10, which became more abundant and distributed later on during embryonic development. Our data are in accordance with previously published results on PKD3 mRNA levels using *in situ* hybridization analysis (Oster et al., 2006). On top of that, we provide a comprehensive study on the expression pattern of PKD3 during organogenesis discovering additional histological details. The strong expression of PKD3 in specific tissues, e.g. cardiac and skeletal muscle, points to an important role for this kinase in the development of these tissues. PKD3 has been implicated in the regulation of secretory transport processes at the Golgi compartment (Bossard et al., 2007; Yeaman et al., 2004) as well as regulation of basal glucose uptake in skeletal muscle cells (Chen et al., 2005), both of which are important processes during organogenesis. Moreover, PKD3 has been shown to regulate the nuclear localization and thus activity of its physiological substrates class II HDAC5 and 7 (Matthews et al., 2006). Interestingly, class II HDAC proteins play an important role in heart development and function (Chang et al., 2004; Zhang et al., 2002). It will now be exciting to investigate the potential function of PKD3 in these tissues using transgenic mouse models, interfering with endogenous PKD3 function by overexpression of a dominant-negative protein or deletion of the PKD3 gene (knockout).

Methods

Antibodies

The primary antibody used in this study was an affinity-purified PKD3 specific polyclonal antibody raised in rabbits against a C-terminal epitope of human PKD3 (amino acids 875-890). The mouse monoclonal GFP- and Flag-specific antibodies were obtained from Roche Biosciences and Sigma-Aldrich, respectively. The rabbit polyclonal GFP-specific antibody was from Santa Cruz Biotechnology. The secondary IRdye-conjugated antibodies were from Li-COR

Biosciences. Transfection of HEK293T cells was performed as described in (Hausser et al., 2005).

Animals

C57BL/6 mice were time mated and pregnant females were sacrificed to collect the embryos at different stages (E10 - E16.5). The finding of a vaginal plug at noon was considered as E0. The fetuses were isolated from the uterus and dissected free of embryonic membranes in ice-cold PBS. All animal experiments carried out in this study were approved by the ethical committee at the University of Stuttgart.

Western blot

Cells were harvested and lysed in lysis buffer (20 mM Tris (pH7.4), 150 mM NaCl, 1 mM EDTA, 1 mM EGTA, and 1 % Triton X-100, plus protease and phosphatase inhibitors). Equal amounts of protein were subjected to a 4-12% NuPAGE Bis-Tris-Gel (Invitrogen, Germany), blotted onto a nitrocellulose membrane and blocked with 0.5% blocking buffer (Roche Biosciences, Germany). Incubation with primary antibodies was performed in blocking buffer at 4 °C overnight. After washing with PBS, samples were incubated with secondary IRdye680-conjugated anti-mouse or IRdye800-conjugated anti-rabbit IgG antibodies in blocking buffer for 1 h at room temperature. The detection was performed on an Odyssey Infrared Imaging System (Li-COR Biosciences, Germany).

Immunohistochemistry

After fixation embryos were dehydrated through a graded ethanol series and into a 50:50 mixture of ethanol:Histoclear (Carl Roth GmbH, Karlsruhe, Germany). Tissue was then incubated in Histoclear for 1-3 hours and transferred into a 50:50 mixture of Histoclear:Paraplast (Carl Roth GmbH, Karlsruhe, Germany) at 42°C, where it was incubated over night. Embryos were transferred into pure Paraplast preheated to 60°C and incubated for 1-3 days. Serial sagittal sections were cut at a thickness of 10 µm on a microtome and floated on a 40°C water bath. Sections were dewaxed in 3 changes of Roticlear for 10 minutes each and incubated in isopropanol and ethanol 15 minutes each. Slides were rehydrated through a reverse series of ethanol dilutions in PBS and finally washed in PBS. Endogenous peroxidase activity was quenched by incubation in PBS containing 0.3 % H_2O_2 for 30 minutes. Slides were rinsed with PBS for 10 minutes and then incubated with 5 % normal goat serum in a humidified chamber to block unspecific binding sites. Primary antiserum diluted in 1.5 % normal goat serum was applied. Slides were incubated in the humidified chamber at 4°C over night.

Immunohistochemical staining was performed using the Vectastain Elite ABC Kit (rabbit IgG) (Vector Laboratories, Burlingame, CA, USA). To remove non-specifically bound antibody, slides were washed three times in PBS for 10 minutes each time. Subsequently, sections were incubated with biotinylated goat anti-rabbit IgG diluted 1:200 in 1.5 % normal goat serum for 1 hour at room temperature. In case of the mouse monoclonal Flag-specific antibody, a bio-tin-SP-conjugated goat anti-mouse IgG (Jackson Immunoresearch, West Grove, PA, USA) diluted 1:500 in 1.5 % normal goat serum was used as secondary antibody. After the slides had been rinsed in PBS as before, immunoperoxidase staining was performed. Sections were incubated with the Vectastain Elite ABC reagent (prepared 30-60 minutes before use) for 30 minutes and washed three times with PBS for 5 minutes each time. For peroxidase visualiza-tion the DAB Substrate Kit for peroxidase (Vector Laboratories, Burlingame, CA, USA) was used. Color development was stopped by rinsing the sections in water for 5 minutes. Sections were counterstained with hematoxylin for 1 minute and coverslipped with Mowiol (Poly-sciences, Warrington, PA, USA) or Eukitt (EMS, Fort Washington, PA, USA).

Microscopy and image processing

Stained sections were analyzed using a widefield microscope (Zeiss Axiovert 200M) equipped with the AxioCam HRC (Zeiss, Germany) and an Achroplan 10x/0,25 Ph1 or a LD Achroplan 40x/0,60 Korr Ph2 (DICIII) objective. Images were further processed with Axiovision software version 4.5 (Zeiss, Germany).

Author's contribution

KE carried out the immunohistochemistry, analyzed the data and helped to draft the manuscript. SL purified the anti-PKD3 polyclonal immune serum. KP was involved in conception of study, data interpretation and manuscript writing. AH designed the study, analyzed and interpreted the data, and drafted the manuscript. All authors read and approved the final manuscript.

Acknowledgements

We would like to thank Vivek Malhotra for providing us with the anti-PKD3 polyclonal serum, Katalin Schlett for the biotinylated goat anti-mouse IgG, Olaf Selchow, Franz Brümmer and Martin Pfannkuchen for support with microscopy, Gisela Link for excellence technical assistance and Heinz Streble for insightful discussions. This work was supported by grants from the Landesstiftung Baden-Württemberg and the Deutsche Forschungsgemeinschaft (HA3557/2-1) to A. Hausser.

References

Avkiran, M., Rowland, A. J., Cuello, F., and Haworth, R. S. (2008). Protein kinase d in the cardiovascular system: emerging roles in health and disease. Circ Res *102*, 157-163.

Bossard, C., Bresson, D., Polishchuk, R. S., and Malhotra, V. (2007). Dimeric PKD regulates membrane fission to form transport carriers at the TGN. J Cell Biol *179*, 1123-1131.

Chang, S., McKinsey, T. A., Zhang, C. L., Richardson, J. A., Hill, J. A., and Olson, E. N. (2004). Histone deacetylases 5 and 9 govern responsiveness of the heart to a subset of stress signals and play redundant roles in heart development. Mol Cell Biol *24*, 8467-8476.

Chen, J., Lu, G., and Wang, Q. J. (2005). Protein kinase C-independent effects of protein kinase D3 in glucose transport in L6 myotubes. Mol Pharmacol *67*, 152-162.

Doppler, H., and Storz, P. (2007). A novel tyrosine phosphorylation site in protein kinase D contributes to oxidative stress-mediated activation. J Biol Chem *282*, 31873-31881.

Feng, H., Ren, M., and Rubin, C. S. (2006a). Conserved domains subserve novel mechanisms and functions in DKF-1, a Caenorhabditis elegans protein kinase D. J Biol Chem *281*, 17815-17826.

Feng, H., Ren, M., Wu, S. L., Hall, D. H., and Rubin, C. S. (2006b). Characterization of a novel protein kinase D: Caenorhabditis elegans DKF-1 is activated by translocation-phosphorylation and regulates movement and growth in vivo. J Biol Chem *281*, 17801-17814.

Fielitz, J., Kim, M. S., Shelton, J. M., Qi, X., Hill, J. A., Richardson, J. A., Bassel-Duby, R., and Olson, E. N. (2008). Requirement of protein kinase D1 for pathological cardiac remodeling. Proc Natl Acad Sci U S A *105*, 3059-3063.

Fugmann, T., Hausser, A., Schoffler, P., Schmid, S., Pfizenmaier, K., and Olayioye, M. A. (2007). Regulation of secretory transport by protein kinase D-mediated phosphorylation of the ceramide transfer protein. J Cell Biol *178*, 15-22.

Harrison, B. C., Kim, M. S., van Rooij, E., Plato, C. F., Papst, P. J., Vega, R. B., McAnally, J. A., Richardson, J. A., Bassel-Duby, R., Olson, E. N., and McKinsey, T. A. (2006). Regulation of cardiac stress signaling by protein kinase d1. Mol Cell Biol *26*, 3875-3888.

Hausser, A., Storz, P., Martens, S., Link, G., Toker, A., and Pfizenmaier, K. (2005). Protein kinase D regulates vesicular transport by phosphorylating and activating phosphatidylinositol-4 kinase IIIbeta at the Golgi complex. Nat Cell Biol *7*, 880-886.

Haworth, R. S., Goss, M. W., Rozengurt, E., and Avkiran, M. (2000). Expression and activity of protein kinase D/protein kinase C mu in myocardium: evidence for alpha1-adrenergic receptor- and protein kinase C-mediated regulation. J Mol Cell Cardiol *32*, 1013-1023.

Hayashi, A., Seki, N., Hattori, A., Kozuma, S., and Saito, T. (1999). PKCnu, a new member of the protein kinase C family, composes a fourth subfamily with PKCmu. Biochim Biophys Acta *1450*, 99-106.

Huynh, Q. K., and McKinsey, T. A. (2006). Protein kinase D directly phosphorylates histone deacetylase 5 via a random sequential kinetic mechanism. Arch Biochem Biophys *450*, 141-148.

Lu, G., Chen, J., Espinoza, L. A., Garfield, S., Toshiyuki, S., Akiko, H., Huppler, A., and Wang, Q. J. (2007). Protein kinase D 3 is localized in vesicular structures and interacts with vesicle-associated membrane protein 2. Cell Signal *19*, 867-879.

Maier, D., Hausser, A., Nagel, A. C., Link, G., Kugler, S. J., Wech, I., Pfizenmaier, K., and Preiss, A. (2006). Drosophila protein kinase D is broadly expressed and a fraction localizes to the Golgi compartment. Gene Expr Patterns *6*, 849-856.

Maier, D., Nagel, A. C., Gloc, H., Hausser, A., Kugler, S. J., Wech, I., and Preiss, A. (2007). Protein kinase D regulates several aspects of development in Drosophila melanogaster. BMC Dev Biol *7*, 74.

Matthews, S. A., Dayalu, R., Thompson, L. J., and Scharenberg, A. M. (2003). Regulation of protein kinase Cnu by the B-cell antigen receptor. J Biol Chem *278*, 9086-9091.

Matthews, S. A., Liu, P., Spitaler, M., Olson, E. N., McKinsey, T. A., Cantrell, D. A., and Scharenberg, A. M. (2006). Essential role for protein kinase D family kinases in the regulation of class II histone deacetylases in B lymphocytes. Mol Cell Biol *26*, 1569-1577.

Oster, H., Abraham, D., and Leitges, M. (2006). Expression of the protein kinase D (PKD) family during mouse embryogenesis. Gene Expr Patterns *6*, 400-408.

Rey, O., Yuan, J., Young, S. H., and Rozengurt, E. (2003). Protein kinase C nu/protein kinase D3 nuclear localization, catalytic activation, and intracellular redistribution in response to G protein-coupled receptor agonists. J Biol Chem *278*, 23773-23785.

Sanchez-Ruiloba, L., Cabrera-Poch, N., Rodriguez-Martinez, M., Lopez-Menendez, C., Jean-Mairet, R. M., Higuero, A. M., and Iglesias, T. (2006). Protein kinase D intracellular localization and activity control kinase D-interacting substrate of 220-kDa traffic through a postsynaptic density-95/discs large/zonula occludens-1-binding motif. J Biol Chem *281*, 18888-18900.

Wang, Q. J. (2006). PKD at the crossroads of DAG and PKC signaling. Trends Pharmacol Sci *27*, 317-323.

Yeaman, C., Ayala, M. I., Wright, J. R., Bard, F., Bossard, C., Ang, A., Maeda, Y., Seufferlein, T., Mellman, I., Nelson, W. J., and Malhotra, V. (2004). Protein kinase D regulates basolateral membrane protein exit from trans-Golgi network. Nat Cell Biol *6*, 106-112.

Yuan, J., Rey, O., and Rozengurt, E. (2005). Protein kinase D3 activation and phosphorylation by signaling through G alpha q. Biochem Biophys Res Commun *335*, 270-276.

Yuan, J., Rey, O., and Rozengurt, E. (2006). Activation of protein kinase D3 by signaling through Rac and the alpha subunits of the heterotrimeric G proteins G12 and G13. Cell Signal *18*, 1051-1062.

Zhang, C. L., McKinsey, T. A., Chang, S., Antos, C. L., Hill, J. A., and Olson, E. N. (2002). Class II histone deacetylases act as signal-responsive repressors of cardiac hypertrophy. Cell *110*, 479-488.

Protein kinase D is essential for exercise-induced skeletal muscle remodeling *in vivo*

Kornelia Ellwanger[1], Sylke Lutz[1], Jenni Raasch[1,2], Maria T. Wiekowski[3], Klaus Pfizenmaier[1], Angelika Hausser[1*]

[1]Institute of Cell Biology and Immunology, University of Stuttgart, Allmandring 31, 70569 Stuttgart, Germany

[2]present address: Institute of Neuropathology, Georg August University, 37099 Göttingen, Germany

[3]Department of Immunology, Schering-Plough Research Institute, 2015 Galloping Hill Road, Kenilworth, NJ 07033, USA

[*]Corresponding author

Abstract

Skeletal muscle responds to exercise by activation of signaling pathways which coordinate gene expression to sustain muscle performance. Activation of transcription factor MEF2 controlling myosin heavy chain genes promotes the transformation from fast-twitch into slow-twitch fibers. Tight regulation of MEF2 activity by direct interaction with class IIa HDACs is thus an important feature. Protein kinase D (PKD) is a direct upstream kinase of skeletal muscle class IIa HDACs mediating their nuclear export and thus derepression of MEF2. A role for PKD in exercise-induced skeletal muscle remodeling has not been described. We created transgenic mice with an inducible and conditional expression of a dominant-negative PKD1kd protein in skeletal muscle to assess impairment of PKD function on muscle function. Voluntary wheel running experiments demonstrate that mice expressing PKD1kd exhibit altered muscle fiber composition and decreased running performance. Our data thus support an essential role for PKD in skeletal muscle remodeling *in vivo*.

Introduction

Skeletal muscle is composed of a heterogenous population of myofibers which differ in their metabolic and contractile properties and are classified based on their expression of myosin heavy chain genes. Type I fibers (slow-twitch fibers) express myosin heavy chain type I, exert a slow contraction, are oxidative and rich in mitochondria and myoglobin, and have a high resistance to fatigue whereas the fast-twitch or type II fibers express myosin heavy chain type II, exert quick contraction, fatigue rapidly, and exert a glycolytic (type IIb) or oxidative (type IIa) metabolism. Physiological signals such as exercise induce signal transduction pathways which promote adaptive changes in the protein composition and cytoarchitecture of myofibers thus transforming preexisting type II fast-twitch fibers into type I slow-twitch fibers (Potthoff et al., 2007a). One important transcription factor which is involved in the regulation of myofiber remodeling is myocyte enhancer factor 2 (MEF2) (Potthoff and Olson, 2007; Potthoff et al., 2007a). There is substantial evidence that MEF2 is a key regulator of skeletal muscle development and myofiber remodeling. MEF2 is preferentially activated in slow, oxidative fibers to support calcium-dependent signaling pathways that promote fiber type remodeling (Potthoff and Olson, 2007). Moreover, skeletal muscles of MEF2 knockout mice demonstrate a reduction in type I fibers. Conversely, expression of a constitutive-active MEF2 protein increases the number of slow-twitch fibers in skeletal muscle and thus exercise endurance and muscle performance (Potthoff et al., 2007b). Transcriptional activity of MEF2 is inhibited by its direct interaction with members of the class IIa histone deacetylases (HDACs), which repress the ability of MEF2 to bind DNA (Potthoff and Olson, 2007). Class IIa HDACs family members are HDACs 4, 5, 7 and 9. The activity of class IIa HDACs towards MEF2 is highly controlled by phosphorylation on conserved serine residues. Phosphorylation at these sites induces binding of HDACs to 14-3-3 proteins, thereby mediating unmasking and masking of nuclear export and nuclear localization sequences, respectively. The phosphoryla-tion-dependent interation with 14-3-3 proteins results in the retention of class IIa HDACs in the cytoplasm, the release of MEF2, and thus derepression of downstream target genes (Zhang et al., 2002). Such a phosphorylation-dependent nuclear export of class IIa HDACs was demonstrated for HDAC5 in cultured myoblasts upon initiation of the muscle differentia-tion program (McKinsey et al., 2000a). In addition, HDAC4 and HDAC7 translocate from the nucleus to the cytoplasm in a signal-dependent manner in cultured adult skeletal muscle (Liu et al., 2005) and during MEF2-mediated differentiation of mouse myoblasts (Dressel et al., 2001), respectively.

Several serine/threonine kinases can phosphorylate class IIa HDACs at the 14-3-3 binding sites, including Ca^{2+}-calmodulin dependent protein kinase CaMKII (Backs et al., 2008; Backs et al., 2006), the AMPK family kinase Mark2 (Chang et al., 2005), and the salt-induced kinase Sik1 (Berdeaux et al., 2007). In an elegant screen Chang and co-workers could identify protein kinase D (PKD) as a class IIa HDAC kinase (Chang et al., 2005). The PKD family of serine/threonine specific kinases consists of three isoforms, PKD1, PKD2, and PKD3. PKD activity is regulated by the second messenger lipid diacylglycerol (DAG) and nPKC-dependent activating phosphorylation. PKD family members have been implicated in various cellular functions including membrane traffic, apoptosis, and migration (for review see (Wang, 2006)). Recent work demonstrated a functional interplay between PKD and HDACs in agonist-dependent cardiac hypertrophy. Vega and coworkers could show that PKD1 directly phosphorylates HDAC5 thereby promoting binding of 14-3-3 proteins and nuclear export (Vega et al., 2004). The ability of PKD to phosphorylate and inhibit HDAC5 directly correlates with pathological remodeling of the heart: Expression of a constitutive-active PKD1 or excessive activation of PKD1 leads to cardiac remodeling, heart failure, and death (Harrison et al., 2006). Conversely, heart-specific deletion of PKD1 diminishes hypertrophy and pathological remodeling in response to pressure overload and chronic adrenergic signaling (Fielitz et al., 2008). Interestingly, all four class IIa HDACs contain the PKD substrate sequence and recently it was demonstrated that PKD1 is also able to directly phosphorylate HDAC4, 7 and 9 (Chang et al., 2005; Dequiedt et al., 2005; Parra et al., 2005; Vega et al., 2004). In addition, besides PKD1 also PKD2 and PKD3 are capable of phosphorylating class IIa HDACs *in vitro* and in a cellular context (Huynh and McKinsey, 2006; Matthews et al., 2006) indicating that the individual PKD isoforms are functionally redundant. Very recently, Kim and colleagues reported a role for PKD1 in MEF2-dependent skeletal muscle function (Kim et al., 2008b). The authors demonstrated that skeletal muscle-specific overexpression of a constitutive-active PKD1 promotes phosphorylation of HDAC4 and 5, the formation of slow-twitch fibers, and an increase in the levels of specific contractile proteins. In addition, skeletal muscle of these mice displayed fatigue resistance in an *ex vivo* muscle contraction model. However, although the skeletal muscle-specific knockout of PKD1 resulted in an increase in susceptibility to fatigue, no changes in fiber type composition were observed. To explain these findings, it was argued that in skeletal muscle besides PKD1, PKD2 and PKD3 are expressed, thus likely compensating the loss of PKD1 (Kim et al., 2008b).

Here we report the generation of transgenic mice which express a dominant-negative PKD1kd-GFP variant in a conditional and inducible manner under the control of the CMV/β-actin promotor. In these mice, doxycycline treatment induced a strong expression of PKD1kd-GFP predominantly in skeletal muscle. Fluorescence microscopy of cryosections demonstrated

a uniform expression of PKD1kd-GFP in skeletal muscle with a dominant localization of the protein in the nuclei. Voluntary wheel running experiments revealed that running performance of mice expressing the dominant-negative PKD1 variant was significantly decreased compared to control mice. In line with that, analysis of skeletal muscle fiber composition after voluntary wheel running demonstrated that, compared to control animals, mice expressing PKD1kd-GFP contained a significantly lower amount of type IIa fibers whereas the amount of type IIb fibers was increased. Based on our data, we conclude that expression of a dominant-negative PKD1-GFP is sufficient to inhibit MEF2-dependent skeletal muscle remodeling induced by voluntary wheel running and demonstrate for the first time an essential role for PKD-mediated signaling in exercise-induced skeletal muscle remodeling.

Material and methods

Transgenic mice

For the generation of Tg(tetO-PKD1kd-EGFP) mice the cDNA encoding EGFP-tagged human kinase-dead (kd) PKD1 (K612W) (Hausser et al., 2002) was inserted into the multiple cloning site of pBI-5 (Baron et al., 1995) via SalI and EcoRV restriction sites. The construct contains a downstream rabbit ß-globin intron/polyadenylation signal. The construct for microinjection containing the tet-operator, hCMV promoter sequences, PKD1kd-GFP, and β-globin was excised from prokaryotic vector sequences via NarI and BsrBI restriction sites (Fig. 1B). Pronucleus microinjection was performed by standard procedures (Nagy, 2003). Tail DNA from founder mice was digested with EcoRV and analyzed by Southern blotting with a 577-bp EGFP probe (Fig. 1C). Genotyping was routinely performed by PCR using a primer pair specific for mouse and human PKD1 (forward: 5'- TTG GTC GTG AGA AGA GGT CAA ATT C -3'; reverse: 5'- CAC CAA GGC AGT TGT TTG GTA CTT T-3'). A 246-bp fragment was indicative of transgenic human PKD1kd and a 399-bp fragment of endogenous mouse PKD1 (Fig. 1D). Genomic DNA was obtained from tail tips. PCR was performed in 20 µl reaction mixture containing standard buffer and 0.5 µM of each primer. The cycling conditions consisted of an initial 2-min denaturing step at 95°C, followed by 36 cycles of 45 sec at 95°C, 45 sec at 60°C, and 60 sec at 72°C. Genotyping of rtTA mice was performed according to (Wiekowski et al., 2001). All animal handling and experiments carried out in this study were approved by the Regierungspräsidium Stuttgart and complied with local guidelines and regulations for the use of experimental animals (35-9185.81/0209, 35-9185.81/0247).

Conditional expression of PKD1kd-GFP in transgenic mice

To induce transgene expression double transgenic mice were supplied with a solution of 2 mg/ml doxycycline hyclat (Fagron GmbH Co. KG, Barsbüttel) and 5% sucrose in sterile ddH_2O as drinking water. Doxycycline-containing drinking water was protected from light and replaced every 3-4 days. Control animals were either single or non-transgenic animals treated with doxycycline-drinking water or double transgenic animals treated with drinking water containing 5% sucrose without doxycycline.

Antibodies

Commercially available antibodies used were: anti-GFP mouse monoclonal antibody (Roche Applied Science, Germany) anti-PKCμ C20 rabbit polyclonal antibody (Santa Cruz, CA, USA), anti-phospho-PKD1 (Ser916) rabbit polyclonal (Cell Signaling, MA, USA), anti-PKD2 rabbit polyclonal antibody (Calbiochem, Germany), anti-tubulin-αAb-2 mouse monoclonal antibody (Neomarkers, Fremont, CA, USA), and anti-transferrin receptor mouse monoclonal antibody (Zymed Laboratories, CA, USA). Mouse monoclonal anti-PKD1 antibody JP2 (Johannes et al., 1995) and rabbit polyclonal anti-PKD3 antibody (Ellwanger et al., 2008) have been described before. Mouse monoclonal antibodies against myosin heavy chain (MHC) type I and type IIa were purified from the supernatant of the hybridoma cell lines BA-D5 and SC-71, respectively (both German Collection of Microorganisms and Cell Cultures, Braunschweig, Germany) according to the manufacturer's protocol. Fluorescently labeled secondary antibodies for immunofluorescence were Alexa546 coupled goat anti-mouse IgG (Invitrogen, Karlsruhe, Germany) and NL637 coupled donkey anti-mouse IgG (R&D Systems, Inc., MN, USA). The secondary IRdye-conjugated antibodies for Western blotting were from Li-COR Biosciences.

Protein extraction from tissue and Western blotting

For Western blot analysis mouse tissue was homogenized in glass tubes containing 5 µl lysis buffer (150 mM NaCl, 20 mM Tris pH 7.5, 1 mM EDTA, 1 mM EGTA, 1% Triton X-100, 1x complete protease inhibitor cocktail (Roche Applied Science, Germany), 0.5 mM PMSF, 1 mM sodium fluoride, 1 mM sodium orthovanadate, 20mM ß-glycerophosphate) per mg tissue with 15-20 strokes at 800 rpm of the PotterS (Sartorius, Göttingen, Germany). Lysates were clarified by centrifugation at 16.000 x *g* and 4°C for 15 minutes. Protein concentrations were determined by the Bradford method using a BioRad protein assay solution (Bio-Rad, München). Equal amounts of proteins were subjected to SDS-PAGE and blotted onto nitrocellulose membranes (Pall, Germany). After blocking with 1% blocking reagent (Roche Applied Science,

Germany), filters were probed with specific antibodies. Proteins were visualized with IRdye-coupled secondary antibodies. Quantitative analysis was performed with the Odyssey software (Licor-Biosciences, Germany).

Voluntary wheel running

To determine voluntary wheel running behaviour mice were housed individually in type 3 cages (23 x 27 x 43 cm) supplemented with running wheels 20 cm in diameter (Robowheel). Wheel-running performance was measured by recording wheel revolutions continuously with the help of magnetic reed switches. Animals were maintained on a 12:12-h light-dark cycle and provided with standard chow ad libidum. Female mice of 5-7 weeks age were used for voluntary wheel running experiments. After 2.5 weeks of voluntary wheel running all mice were sacrificed and hindlimb crural muscles were dissected for biochemical analysis or cryosectioning and determination of fiber type composition.

Indirect immunofluorescence

Freshly prepared mouse tissue was snap frozen in liquid nitrogen-cooled isopentane. Frozen sections (10-16 µm) were cut in a cryostat (Leica) and transferred to microscope slides (Polysine, Menzel-Gläser, Braunschweig) by thaw mounting. Slides were fixed in 4% paraformaldehyde (Electron Microscopy Science, PA, USA) in PBS for 15 minutes. For immunofluo-rescence staining slides were washed in PBS two times for 5 minutes each and permeabilized in 0.3% Triton-X-100 in PBS for 5 minutes. After washing with PBS another two times, the slides were blocked with 5% goat serum in PBS for 1 hour at room temperature, followed by incubation with a myosin heavy chain I specific antibody (BA-D5) in 5% goat serum at 4°C overnight. Slides were washed three times for five minutes each in PBS and incubated for 1 hour at room temperature with Alexa546 coupled goat anti-mouse IgG diluted 1:500 in 5% goat serum in PBS. The slides were washed three times for 5 minutes each in PBS, once again fixed in 4% PFA in PBS at 4°C for 10 minutes and sequentially treated as described above with a second primary antibody specific for myosin heavy chain IIa (SC-71) and a NL637 coupled donkey anti-mouse IgG as respective secondary antibody diluted 1:500 in 5% goat serum in PBS. Finally, slides were washed two times for 5 minutes each in PBS and mounted with Fluoromount-G (SouthernBiotech, AL, USA). To stain F-Actin, slides were incu-bated with Alexa546 coupled phalloidin (Invitrogen, Karlsruhe, Germany) and washed two times for 5 minutes each in PBS, before mounting. For nuclear counterstaining a 1:2000 dilu-tion of DRAQ5 in PBS was applied on the sections directly before mounting and incubated for 10 minutes at room temperature.

Microscopy, software and statistical analysis

Confocal images were acquired using a confocal laser scanning microscope (TCS SP2; Leica Microsystems GmbH, Heidelberg) equipped with a 100/1.4 HCX PlanAPO oil immersion objective. GFP was excited with an argon laser (488-nm line), whereas Alexa546 was excited with a helium-neon laser (543-nm line). DRAQ5 and Cy5 were excited with a helium-neon laser at (633-nm line). Widefield fluorescence and mosaic pictures were recorded using a widefield microscope (Zeiss Axio Observer.Z1) equipped with the AxioCam MR3 (Carl Zeiss AG, Jena) and a Plan-Apochromat 20x/0.8 M27 or an EC Plan-Neofluar 10x/0.30 M27 objective (Carl Zeiss AG, Jena). For quantitative image analysis microscopic pictures were further processed with Adobe Photoshop and the open source software *ImageJ* using the plugin *Cell Counter*. Quantification of fiber types (type I Alexa546 stained; type IIa NL637 stained; type IIb unstained) was performed by a person who had no knowledge of the coding system. Results of voluntary wheel running and fibertyping are presented as mean values ± SEM. Significance of differences was calculated by an unpaired student's *t*-test. $p<0.05$ was accepted as statistically significant.

Results and discussion

Generation of a conditional transgenic system for inducible expression of dominant-negative PKD1kd-GFP

There is substantial evidence that the individual PKD isoforms are functional redundant in skeletal muscle and heart (Fielitz et al., 2008; Kim et al., 2008b). In line with that, all three isoforms are expressed in skeletal muscle and cardiac tissue (Fig. 1A). To create a functional PKD knockout we therefore decided to generate transgenic mice, which express a kinase-dead (kd) PKD1-GFP protein, known to act dominant-negative on all three isoforms. The PKD1kd protein harbors a point mutation at position 612, which leads to disruption of kinase activity (Johannes et al., 1995). PKD1kd mediated dominant-negative effect on endogenous PKD signaling has been demonstrated in membrane fission and secretion (Fugmann et al., 2007; Liljedahl et al., 2001), cell migration (Eiseler et al., 2007), and phosphorylation of HDAC5 and 7, respectively (Parra et al., 2005; Vega et al., 2004). To express PKD1kd-GFP in an inducible and conditional manner, we made use of the tetracycline-dependent gene expression system originally described by Gossen and Bujard (Gossen and Bujard, 1992). In this system, the tet-activator protein (rtTA) is expressed constitutively from the activator transgene. In the presence of the tetracycline analog doxycycline, the rtTA protein binds to the tetracycline-responsive promoter element (TRE) thus inducing the expression of the trans-

gene (Fig. 1B). The activator transgene used in this study was driven by the CMV enhancer/β-actin promoter, which has been described to induce strong rtTA expression in skeletal muscle tissue, and moderate expression in heart, skin, kidney, thymus and lung (Wiekowski et al., 2001). 6 independent transgenic mouse lines were generated from founder animals carrying the reporter transgene, which contained the TRE element and the gene encoding human PKD1kd-GFP (Fig. 1B). Integration of the transgene into the genome was confirmed by Southern blot analysis using a GFP-specific probe (Fig. 1C, transgenic line 1 is exemplarily shown). Transgene heredity among offsprings was analyzed by PCR of genomic DNA using PKD1-specific oligonucleotides (Fig. 1D). One of these lines (line 1) demonstrated high expression of the transgene (Fig. 2A) and was selected for further experiments. Double-transgenic animals (referred to as CMV/PKD1kd-GFP tg) were created by crossing animals from the activator line to animals from the rtTA responsive mouse line and were indistinguishable from their single transgenic littermates.

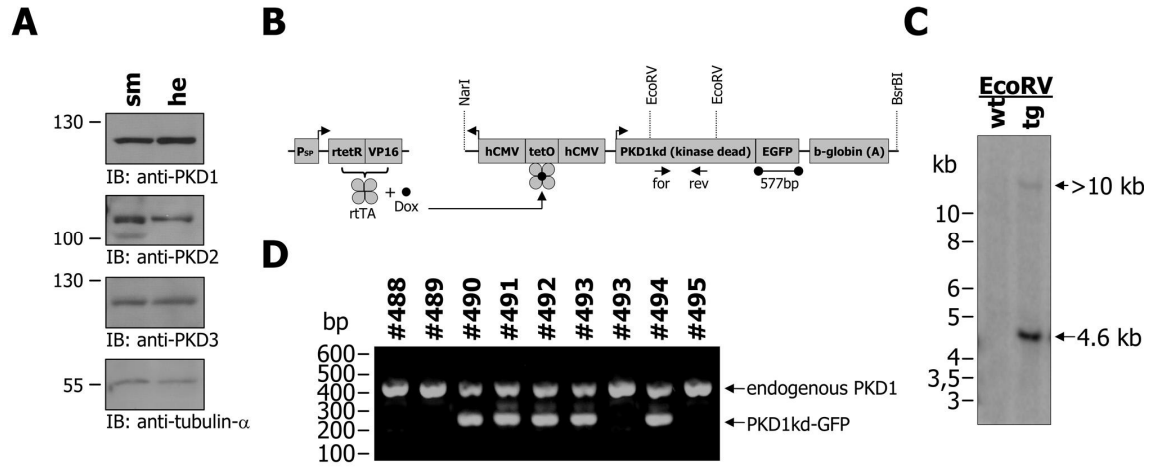

Figure 1 – Generation of transgenic tetO-PKD1kd-GFP mice. (A) Western blots illustrating endogenous expression of PKD1, PKD2 and PKD3 in skeletal muscle (sm) and heart (he) of wildtype mice. (B) Outline of the rtTA dependent unit and tetR-VP16 fusion protein. rtTA requires dox for binding to tetO in order to activate transcription. For Tg(tetO-PKD1kd-GFP) the construct used for the generation of transgenic animals is depicted. Restriction enzyme digestion sites that are critical for cloning and for Southern blot analysis are illustrated as well as the binding site of the 577bp GFP probe (handle) and the primer binding sites for PCR genotyping (for/rev, arrows). (C) Southern blot analysis of founder genomic DNA demonstrating the presence of the transgenic construct tetO-PKD1kd-GFP integrated as a head-to-tail array. After EcoRV digestion and hybridization with a GFP specific probe two fragments are detected: a fragment of predictable size (4.6 kb) due to tandem integration and a junction fragment (>10 kb) with an individual size depending on EcoRV sites flanking the position of transgenic integration. (D) PCR genotyping demonstrating the presence of the transgenic construct Tg(tetO-PKD1kd-GFP) among offsprings. Amplification of a specific 246 bp fragment indicates transgenity. As internal control a 399 bp fragment of the endogenous PKD1 sequence is amplified.

Induction of PKD1kd-GFP expression is dependent on doxycycline and occurs predominantly in skeletal muscle tissue

Administration of doxycycline rapidly induces transgene expression, with induction being complete within 24 hours in most organs (Kistner et al., 1996). First, to analyze whether expression of the PKD1kd-GFP transgene is inducible, double transgenic animals were treated with doxycycline for one week. Western blot analysis of double transgenic animals demonstrated high levels of transgene expression in skeletal muscle and additionally, low expression levels in heart, thymus, skin and stomach (Fig. 2A). This is in line with the reported expression pattern of rtTA in the respective transactivator line (Wiekowski et al., 2001). To demonstrate that the transgene expression is doxycycline-dependent, double transgenic animals were treated with doxycycline for different time points and PKD1kd-GFP expression was analyzed in lysates of skeletal muscle tissue by Western blotting (Fig. 2B). Transgene expression was already detectable within 3 hours after the onset of doxycycline administration and increased over time reaching a maximum within 1-3 weeks of treatment. Moreover, PKD1kd-GFP protein was not detectable in control mice, indicating that expression is strictly doxycycline-dependent and tightly controlled. A prerequisite for dominant-negative action of PKD1kd-GFP is a considerable overexpression compared to endogenous PKD levels. We therefore analyzed expression of endogenous and transgenic PKD1 in skeletal muscle tissue of CMV/PKD1kd-GFP tg and control mice. Quantitative Western blotting using a PKD1-specific antibody revealed a 13 fold higher expression level of PKD1kd-GFP compared to endogenous PKD1 (Fig. 2C), which displays the highest expression level in skeletal muscle among the PKD isoforms (Kim et al., 2008b). Furthermore, we investigated the expression of PKD1kd-GFP in skeletal muscle tissue on a single cell level. Fluorescence microscopy of cryosections revealed an uniform expression of PKD1kd-GFP in soleus and plantaris muscle (Fig. 2D). Confocal laser scanning microscopy revealed that in addition to a cytoplasmic distribution, the catalytically inactive PKD1 was strongly enriched in the nuclei (Fig. 2E). Interestingly, active PKD phosphorylates class IIa HDAC proteins in the nucleus, thereby mediating nuclear export and MEF2 activation (Vega et al., 2004). Localization of dominant-negative PKD1kd to this compartment allows the inhibition of active endogenous PKD in the nucleus and thus a dominant-negative effect towards class IIa HDAC phosphorylation. Of note, although PKD1kd-GFP was expressed at high levels after 3 weeks of doxycycline treatment (Fig. 2B), mice did not demonstrate apparent phenotypic changes. Body weight, heart and hindlimb crural skeletal muscle size as well as fiber type content of CMV/PKD1kd-GFP tg were not altered compared to control animals (data not shown). Conversely, animals expressing a constitutive-active PKD1 (caPKD1) protein in skeletal muscle tissue demonstrated a lean phenotype

accompanied by reduced body weight. This phenotype does not result from an altered metabolism but rather from an increase in type I fibers and a reduction in myofiber size (Kim et al., 2008b). However, taking into account that skeletal muscle remodeling is induced in response to environmental demands such as exercise and electrical stimulation (Potthoff et al., 2007a), one can assume that the activation of the PKD signaling pathways also

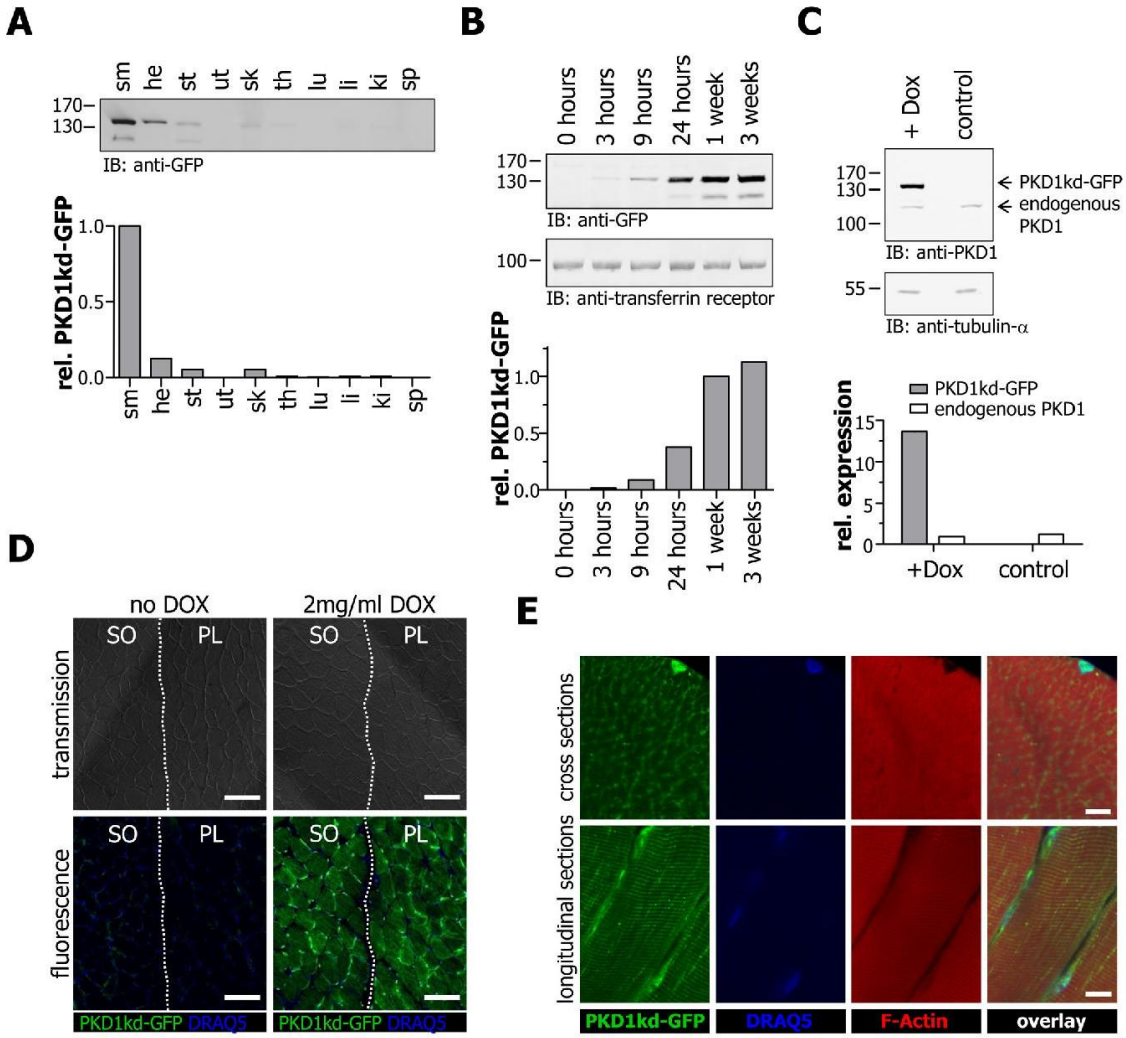

Figure 2 – Doxycycline-dependent expression of PKD1kd-GFP in double-transgenic mice carrying tetO-PKD1kd-GFP and CMV/β-actin rtTA. (A) Tissue specificity of transgene expression. sm: skeletal muscle, he: heart, st: stomach, ut: uterus, sk: skin, th: thymus, lu: lung, li: liver, ki: kidney, sp: spleen. The densitometry of the skeletal muscle sample was arbitrarily set to 1.0. (B) Kinetic of induction upon doxycycline treatment in skeletal muscle. The densitometry of the one week-induction sample was arbitrarily set to 1.0. (C) Overexpression level of transgenic PKD1kd-GFP versus endogenous PKD1 in skeletal muscle. Skeletal muscle from doxycycline-treated single transgenic animals carrying tetO-PKD1kd-GFP served as control. The densitometry of endogenous PKD in the control sample was arbitrarily set to 1.0. Shown are representative Western blots and graphs (A-C). (D) PKD1kd-GFP expression pattern in hindlimb crural muscle. Bright-field and wide-field fluorescence images, nuclei were stained with DRAQ5, SO: soleus, PL: plantaris, scale bar: 100 µm. (E) Subcellular localization of PKD1kd-GFP in skeletal muscle fibers. Nuclei were stained with DRAQ5, F-Actin was stained with Alexa546 coupled phalloidin. Projections of confocal sections, scale bars: 10 µm.

requires such an external stimulation. Therefore, expression of PKD1kd-GFP will only result in a dominant-negative phenotype upon induction of skeletal muscle remodeling whereas expression of caPKD1 bypasses external signaling. Whether long-term expression of PKD1kd-GFP might have an effect on skeletal muscle tissues independent of external signals has to be further investigated.

Expression of PKD1kd-GFP decreases running performance and inhibits skeletal muscle remodeling

Wu and colleagues could demonstrate that the transcriptional activity of MEF2 in mice is enhanced by voluntary wheel running and dependent on the activity of the phosphatase calcineurin (Wu et al., 2001). The response is accompanied by an increase in myoglobin expression resulting in a transformation of myofibers from type IIb to type IIa in plantaris muscle of running mice. Furthermore, calcineurin enhances the activity of PKD1 to activate slow-twitch- and oxidative-myofiber-specific gene expression thus acting synergistically with PKD1 (Kim et al., 2008b). It is therefore feasible to speculate that a functional knockout of endogenous PKD interferes with exercise-induced skeletal muscle remodeling. To address this point, we provided mice access to a running wheel. As already described (Wu et al., 2001) mice voluntarily exercised almost continuously mainly during the nocturnal phase of their day-night cycle. Activity was monitored and quantified by counting wheel revolutions. Running performance of control mice without transgene expression increased steadily within 17.5 days, reaching an absolute running distance of 191.5 ± 15.0 km (Fig. 3B) and an average daily running distance of 15.0 ± 2.1 km (Fig. 3C). This is in line with previous observations (Waters et al., 2004). Western blot analysis of skeletal muscle tissue revealed an exercise-induced activation of endogenous PKD evident from an enhanced autophosphorylation signal (Fig. 3A). Interestingly, mice expressing PKD1kd-GFP demonstrated a significantly decreased ($p < 0.005$) running performance with an absolute running distance of 74.8 ± 22.3 km (Fig. 3B) and an average daily running distance of 6.3 ± 1.7 km (Fig. 3C). This indicates that expression of the dominant-negative PKD1kd-GFP interferes with the ability of muscles to power exercise-induced contractions. In sedentary, cage-bound mice MEF2 activity is only detectable in soleus muscle, which is used to support the skeleton against gravity and predominantly contains slow-twitch type I fibers (Wu et al., 2001). Wheel running induced muscle contractions require the power of soleus, plantaris and white vastus muscles (Wu et al., 2001). In plantaris muscle, exercise induces fiber type transformation from type IIb to IIa whereas the amount of type I fibers is low and remains unchanged (Waters et al., 2004).

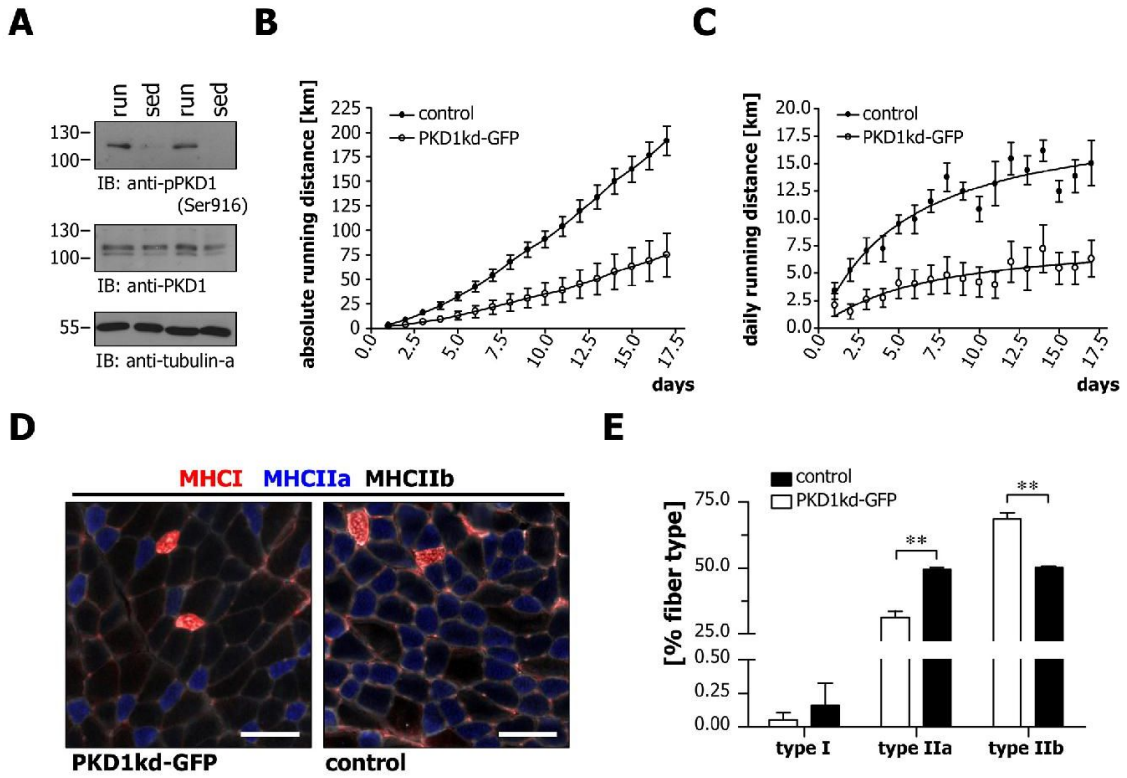

Figure 3 – Mice expressing PKD1kd-GFP show decreased voluntary wheel running performance and impaired muscle remodeling. (A) Western blot on skeletal muscle lysates isolated from two mice after 3 weeks voluntary wheel running (run) and two sedentary mice (sed) showing an exercise-induced increase of autophosphorylated PKD (pSer916) levels. (B) absolute running distance and (C) daily running distance of mice expressing PKD1kd-GFP (○) and control mice without transgene expression (●), mean values (n=9 for each group) ± SEM ($p<0.005$). (D) Indirect immunofluorescence staining of myosin heavy chain (MHC) type I (red) and type IIa (blue) on plantaris sections from mice expressing PKD1kd-GFP and control mice without transgene expression after 17.5 days voluntary wheel running. Unstained fibers are type IIb. Scale bars: 100 µm (E) Quantitative fiber type analysis of plantaris from mice expressing PKD1kd-GFP (□) and control mice without transgene expression (■) after 17.5 days of voluntary wheel running, mean values (n=3 for each group) ± SEM (**, $p<0.005$).

Therefore, we analyzed the fiber type composition in plantaris muscle of mice after 18 days of voluntary wheel running using indirect immunofluorescence staining of myosin heavy chain type I and type IIa (Fig. 3D). Interestingly, PKD1kd-GFP expressing mice contained a significantly higher amount of type IIb fibers (68.58 ± 1.88 % vs. 50.22 ± 0.26 %, $p<0.005$), whereas the amount of type IIa fibers was decreased (31.37 ± 1.91 % vs. 49.61 ± 0.13, $p<0.005$) compared to control animals (Fig. 3E). The percentage of type I fibers in plantaris was low and remained unchanged (0.53 ± 0.5 in PKD1kd-GFP mice vs. 0.16 ± 0.1 in control mice) (Fig. 3E). Of note, soleus muscle fiber type composition was not affected by voluntary wheel running or expression of PKD1kd-GFP (data not shown). Taken together, our data indicate that the expression of PKD1kd-GFP is sufficient to block exercise-induced transformation of type IIb fibers to type IIa fibers in plantaris muscle thus decreasing running performance.

All three PKD isoforms are expressed in skeletal muscle tissue (Fig. 1A). Therefore, PKD1kd-GFP most likely acts by blocking activation of all endogenous PKD isoforms. In addition, competition for common substrates might contribute to some extend. In the latter case, one would also have to consider that other kinases, such as CaMK and Sik1, can mediate class IIa HDAC phosphorylation and MEF2 activation and substrate access could thus potentially be impacted by PKD1kd-GFP. Sik1 was reported to promote survival of skeletal myocytes via class IIa HDAC phosphorylation (Berdeaux et al., 2007). Likewise, several studies addressed the role of CaMK in skeletal muscle. Using transgenic mice overexpressing a constitutive-active CaMKIV a role for the kinase in exercise-induced mitochondrial biogenesis and oxidative metabolism was demonstrated (Wu et al., 2002). Although it has been shown that CaMKI and IV directly phosphorylate and regulate HDAC5 (McKinsey et al., 2000b), these kinases are not endogenously expressed in skeletal muscle (Rose et al., 2006), making a role in fiber type remodeling unlikely. The major CaMK expressed in skeletal muscle is CaMKII (Rose et al., 2006). Recent studies demonstrated that CaMKII directly phosphorylates and interacts with HDAC4 via a unique binding motif (Backs et al., 2006). Interestingly, although HDAC5 is not a direct target it gains CaMKII responsiveness by formation of hetero-oligomers with HDAC4 (Backs et al., 2008). However, whether CaMKII and Sik1 signaling are involved in physiological, exercise-induced skeletal muscle remodeling is presently unclear. In conclusion, our *in vivo* model of muscle-specific, inducible interference with PKD activity clearly demonstrates the important physiologic role of PKD as a key regulator of skeletal muscle fiber type composition and thus muscle function in general.

Acknowledgements

We are grateful to Elke Gerlach for production and purification of BA-D5 and SC-71 antibodies. The laboratory of Angelika Hausser is supported by grants from the Deutsche Forschungsgemeinschaft DFG (HA3557/2-1 and 4-1), Deutsche Krebshilfe (107545) and Center Systems Biology, Stuttgart.

References

Backs, J., Backs, T., Bezprozvannaya, S., McKinsey, T. A., and Olson, E. N. (2008). Histone deacetylase 5 acquires calcium/calmodulin -dependent kinase II responsiveness by oligomerization with histone deacetylase 4. Mol Cell Biol *28*, 3437-3445.

Backs, J., Song, K., Bezprozvannaya, S., Chang, S., and Olson, E. N. (2006). CaM kinase II selectively signals to histone deacetylase 4 during cardiomyocyte hypertrophy. J Clin Invest *116*, 1853-1864.

Baron, U., Freundlieb, S., Gossen, M., and Bujard, H. (1995). Co-regulation of two gene activities by tetracycline via a bidirectional promoter. Nucleic Acids Res *23*, 3605-3606.

Berdeaux, R., Goebel, N., Banaszynski, L., Takemori, H., Wandless, T., Shelton, G. D., and Montminy, M. (2007). SIK1 is a class II HDAC kinase that promotes survival of skeletal myocytes. Nat Med *13*, 597-603.

Chang, S., Bezprozvannaya, S., Li, S., and Olson, E. N. (2005). An expression screen reveals modulators of class II histone deacetylase phosphorylation. Proc Natl Acad Sci U S A *102*, 8120-8125.

Dequiedt, F., Van Lint, J., Lecomte, E., Van Duppen, V., Seufferlein, T., Vandenheede, J. R., Wattiez, R., and Kettmann, R. (2005). Phosphorylation of histone deacetylase 7 by protein kinase D mediates T cell receptor-induced Nur77 expression and apoptosis. J Exp Med *201*, 793-804.

Dressel, U., Bailey, P. J., Wang, S. C., Downes, M., Evans, R. M., and Muscat, G. E. (2001). A dynamic role for HDAC7 in MEF2-mediated muscle differentiation. J Biol Chem *276*, 17007-17013.

Eiseler, T., Schmid, M. A., Topbas, F., Pfizenmaier, K., and Hausser, A. (2007). PKD is recruited to sites of actin remodelling at the leading edge and negatively regulates cell migration. FEBS Lett *581*, 4279-4287.

Ellwanger, K., Pfizenmaier, K., Lutz, S., and Hausser, A. (2008). Expression patterns of protein kinase D 3 during mouse development. BMC Dev Biol *8*, 47.

Fielitz, J., Kim, M. S., Shelton, J. M., Qi, X., Hill, J. A., Richardson, J. A., Bassel-Duby, R., and Olson, E. N. (2008). Requirement of protein kinase D1 for pathological cardiac remodeling. Proc Natl Acad Sci U S A *105*, 3059-3063.

Fugmann, T., Hausser, A., Schoffler, P., Schmid, S., Pfizenmaier, K., and Olayioye, M. A. (2007). Regulation of secretory transport by protein kinase D-mediated phosphorylation of the ceramide transfer protein. J Cell Biol *178*, 15-22.

Gossen, M., and Bujard, H. (1992). Tight control of gene expression in mammalian cells by tetracycline-responsive promoters. Proc Natl Acad Sci U S A *89*, 5547-5551.

Harrison, B. C., Kim, M. S., van Rooij, E., Plato, C. F., Papst, P. J., Vega, R. B., McAnally, J. A., Richardson, J. A., Bassel-Duby, R., Olson, E. N., and McKinsey, T. A. (2006). Regulation of cardiac stress signaling by protein kinase d1. Mol Cell Biol *26*, 3875-3888.

Hausser, A., Link, G., Bamberg, L., Burzlaff, A., Lutz, S., Pfizenmaier, K., and Johannes, F. J. (2002). Structural requirements for localization and activation of protein kinase C mu (PKC mu) at the Golgi compartment. J Cell Biol *156*, 65-74.

Huynh, Q. K., and McKinsey, T. A. (2006). Protein kinase D directly phosphorylates histone deacetylase 5 via a random sequential kinetic mechanism. Arch Biochem Biophys *450*, 141-148.

Johannes, F. J., Prestle, J., Dieterich, S., Oberhagemann, P., Link, G., and Pfizenmaier, K. (1995). Characterization of activators and inhibitors of protein kinase C mu. Eur J Biochem *227*, 303-307.

Kim, M. S., Fielitz, J., McAnally, J., Shelton, J. M., Lemon, D. D., McKinsey, T. A., Richardson, J. A., Bassel-Duby, R., and Olson, E. N. (2008). Protein kinase D1 stimulates MEF2 activity in skeletal muscle and enhances muscle performance. Mol Cell Biol *28*, 3600-3609.

Kistner, A., Gossen, M., Zimmermann, F., Jerecic, J., Ullmer, C., Lubbert, H., and Bujard, H. (1996). Doxycycline-mediated quantitative and tissue-specific control of gene expression in transgenic mice. Proc Natl Acad Sci U S A *93*, 10933-10938.

Liljedahl, M., Maeda, Y., Colanzi, A., Ayala, I., Van Lint, J., and Malhotra, V. (2001). Protein kinase D regulates the fission of cell surface destined transport carriers from the trans-Golgi network. Cell *104*, 409-420.

Liu, Y., Randall, W. R., and Schneider, M. F. (2005). Activity-dependent and -independent nuclear fluxes of HDAC4 mediated by different kinases in adult skeletal muscle. J Cell Biol *168*, 887-897.

Matthews, S. A., Liu, P., Spitaler, M., Olson, E. N., McKinsey, T. A., Cantrell, D. A., and Scharenberg, A. M. (2006). Essential role for protein kinase D family kinases in the regulation of class II histone deacetylases in B lymphocytes. Mol Cell Biol *26*, 1569-1577.

McKinsey, T. A., Zhang, C. L., Lu, J., and Olson, E. N. (2000a). Signal-dependent nuclear export of a histone deacetylase regulates muscle differentiation. Nature *408*, 106-111.

McKinsey, T. A., Zhang, C. L., and Olson, E. N. (2000b). Activation of the myocyte enhancer factor-2 transcription factor by calcium/calmodulin-dependent protein kinase-stimulated binding of 14-3-3 to histone deacetylase 5. Proc Natl Acad Sci U S A *97*, 14400-14405.

Nagy, A. (2003). Manipulating the mouse embryo : a laboratory manual, 3rd edn (Cold Spring Harbor, N.Y.: Cold Spring Harbor Laboratory Press).

Parra, M., Kasler, H., McKinsey, T. A., Olson, E. N., and Verdin, E. (2005). Protein kinase D1 phosphorylates HDAC7 and induces its nuclear export after T cell receptor activation. J Biol Chem *280*, 13762-13770.

Potthoff, M. J., and Olson, E. N. (2007). MEF2: a central regulator of diverse developmental programs. Development *134*, 4131-4140.

Potthoff, M. J., Olson, E. N., and Bassel-Duby, R. (2007a). Skeletal muscle remodeling. Curr Opin Rheumatol *19*, 542-549.

Potthoff, M. J., Wu, H., Arnold, M. A., Shelton, J. M., Backs, J., McAnally, J., Richardson, J. A., Bassel-Duby, R., and Olson, E. N. (2007b) . Histone deacetylase degradation and MEF2 activation promote the formation of slow-twitch myofibers. J Clin Invest *117*, 2459-2467.

Rose, A. J., Kiens, B., and Richter, E. A. (2006). Ca2+-calmodulin-dependent protein kinase expression and signalling in skeletal muscle during exercise. J Physiol *574*, 889-903.

Vega, R. B., Harrison, B. C., Meadows, E., Roberts, C. R., Papst, P. J., Olson, E. N., and McKinsey, T. A. (2004). Protein kinases C and D mediate agonist-dependent cardiac hypertrophy through nuclear export of histone deacetylase 5. Mol Cell Biol *24*, 8374-8385.

Wang, Q. J. (2006). PKD at the crossroads of DAG and PKC signaling. Trends Pharmacol Sci *27*, 317-323.

Waters, R. E., Rotevatn, S., Li, P., Annex, B. H., and Yan, Z. (2004). Voluntary running induces fiber type-specific angiogenesis in mouse skeletal muscle. Am J Physiol Cell Physiol *287*, C1342-1348.

Wiekowski, M. T., Chen, S. C., Zalamea, P., Wilburn, B. P., Kinsley, D. J., Sharif, W. W., Jensen, K. K., Hedrick, J. A., Manfra, D., and Lira, S. A. (2001). Disruption of neutrophil migration in a conditional transgenic model: evidence for CXCR2 desensitization in vivo. J Immunol *167*, 7102-7110.

Wu, H., Kanatous, S. B., Thurmond, F. A., Gallardo, T., Isotani, E., Bassel-Duby, R., and Williams, R. S. (2002). Regulation of mitochondrial biogenesis in skeletal muscle by CaMK. Science *296*, 349-352.

Wu, H., Rothermel, B., Kanatous, S., Rosenberg, P., Naya, F. J., Shelton, J. M., Hutcheson, K. A., DiMaio, J. M., Olson, E. N., Bassel-Duby, R., and Williams, R. S. (2001). Activation of MEF2 by muscle activity is mediated through a calcineurin-dependent pathway. Embo J *20*, 6414-6423.

Zhang, C. L., McKinsey, T. A., Chang, S., Antos, C. L., Hill, J. A., and Olson, E. N. (2002). Class II histone deacetylases act as signal-responsive repressors of cardiac hypertrophy. Cell *110*, 479-488.

Protein kinase D controls the integrity of Golgi apparatus and the maintenance of dendritic arborization in hippocampal neurons

Katalin Czöndör[1,2], Kornelia Ellwanger[2], Yannick F. Fuchs[2], Sylke Lutz[2], Isabelle M. Mansuy[3], Angelika Hausser[2], Klaus Pfizenmaier[2], Katalin Schlett[1,2*]

[1]Department of Physiology and Neurobiology, Eötvös Loránd University, Budapest, Hungary
[2]Institute of Cell Biology and Immunology, University Stuttgart, Stuttgart, Germany
[3]Brain Research Institute, Medical Faculty of University of Zürich, and Department of Biology of the Swiss Federal Institute of Technology, Zürich, Switzerland

*corresponding author

Summary

Protein kinase D (PKD) is known to participate in various cellular functions, including secretory vesicle fission from the Golgi and plasma membrane directed transport. We here report on expression and function of PKD in hippocampal neurons. Introducing a GFP-tagged PKD reporter into mouse embryonal hippocampal neurons revealed high endogenous PKD activity at the Golgi complex and in the dendrites, while PKD activity was excluded from the axon in parallel with axonal maturation. Expression of fluorescently tagged wild type PKD1 and constitutive active PKD1$^{S738/742E}$ (caPKD1) in neurons revealed that both proteins were slightly enriched at the trans-Golgi network (TGN) and did not interfere with its thread-like morphology. By contrast, expression of dominant-negative kinase-inactive PKD1^{K612W} (kdPKD1) led to the disruption of the neuronal Golgi complex, with kdPKD1 strongly localized to the TGN fragments. Similar findings were obtained from transgenic mice with inducible, neuron specific expression of kdPKD1-EGFP. As a prominent functional consequence, kdPKD1 expression led to severe shrinkage of the dendritic tree, while caPKD1 increased dendritic arborization. Our results thus provide direct evidence that PKD activity is selectively involved in the maintenance of dendritic arborization and Golgi structure of hippocampal neurons.

Introduction

Neurons are non-dividing and extremely polarized cells, with enormous membrane surface compared to the size of the soma. These features assume a highly specialized secretory machinery, which resembles in certain parts the directed transport mechanisms described in polarized non-neuronal cells (Horton and Ehlers, 2004; Winckler and Mellman, 1999). The vast neuronal membrane surface is functionally and structurally divided into axonal and somatodendritic compartments, possessing specific lipid and protein components required for the spatially different functions, e.g. for pre- or postsynaptic activity (Bresler et al., 2004; Dresbach et al., 2001; Sheng, 2001). The constitutive and precisely directed supply of surface membrane components is indispensable for the function of neurons, especially when consid-ering that postmitotic neurons normally serve throughout the life span of the organism. Up to now, we are far from understanding how the extreme polarization has been evolved and is maintained in neurons.

Despite a likely central role in neuronal morphogenesis and membrane trafficking, little is known about the special structure and transport features of the neuronal Golgi apparatus. A thread-like and reticular structure of the Golgi apparatus has been already described in many neuronal types (Fujita and Okamoto, 2005; Horton et al., 2005; Takamine et al., 2000). Central neuronal Golgi complex is localized in the soma and often extends into the principal dendrites, but Golgi elements were also found as discontinuous structures in the distal dendrites, often near synaptic contacts or in dendritic spines, as well (Gardiol et al., 1999; Horton and Ehlers, 2003; Pierce et al., 2001; Sytnyk et al., 2002). The dispersed localization of the Golgi apparatus indicates unique spatial regulation of the neuronal secretory pathway compared to other mammalian cells. Recent investigations on hippocampal pyramidal cells indicated that Golgi outposts located in the dendritic shafts (Horton and Ehlers, 2003; Sytnyk et al., 2002) and the perinuclear Golgi apparatus oriented towards the longest dendrite (Horton et al., 2005) can provide the necessary membrane supply for intensive dendritic growth. In case of axonal outgrowth and extension, increasing amount of data suggests that membrane supply and targeting of proteins are regulated in a different way compared to dendritic elongation (Horton et al., 2005; Lein et al., 2007; Silverman et al., 2001; Takemoto-Kimura et al., 2007; Ye et al., 2007).

Based on studies in non-neuronal cells, protein kinase D (PKD) is known to play a key regulatory role in secretory pathways. The PKD family has recently become a separate family among the serine-threonine kinases and comprises three isoforms, PKD1, PKD2 and PKD3

(Van Lint et al., 2002). PKD can link several intracellular signaling cascades, indicating a role of the kinase in diverse cellular functions including immune responses, apoptosis or cell proliferation (Rykx et al., 2003; Wang, 2006). Moreover, in resting cells, PKD is mainly cytoplasmic, but a smaller fraction is recruited to the Golgi apparatus where it can direct the fission of vesicles specifically destined to the cell surface (Hausser et al., 2005; Liljedahl et al., 2001). Furthermore, studies in polarized epithelial cells revealed that PKD is selectively involved in basolateral membrane protein transport (Yeaman et al., 2004). PKD was also reported to regulate lipid transfer between the endoplasmic reticulum and the Golgi apparatus (Fugmann et al., 2007).

All 3 PKD isoforms are expressed in the central nervous system already at embryonic stages in mice (Ellwanger et al., 2008; Oster et al., 2006). PKD activity has been recently implicated in regulating early neuronal polarization (Yin et al., 2008), early dendritic development (Horton et al., 2005) or selective transport of dendritic proteins (Bisbal et al., 2008). In the present work, we have used a newly developed reporter of PKD activity and studied transgenic mice with neuron-specific, inducible expression of a dominant-negative acting PKD mutant to unravel the role of PKD1 in mature hippocampal neurons, both *in vitro* and *in vivo*. We show that active PKD is present at the trans-Golgi network (TGN) and in the somatoden-dritic compartments, and regulates the integrity of the Golgi complex and the maintenance of the dendritic tree. Importantly, PKD activity is excluded from the axons, indicating a polarized action of PKD in the somatodendritic compartment of mature neurons.

Materials and Methods

Animals

CD1, CaMKIIαrtTA2 (Michalon et al., 2005) or kdPKD1-EGFP transgenic mice were housed in the Animal Facility of the Biological Institute, Eotvos Lorand University or of the Institute of Cell Biology and Immunology, University of Stuttgart at 22±1° C with 12h light/dark cycles and with ad libitum access to food and water. All procedures were performed under the supervision of Local Animal Care Comittee, in agreement with the European Union and Hungarian legislation (Budapest) or approved by the Regierungspräsidium Stuttgart. All experiments were complied with local guidelines and regulations for the use of experimental animals (35-9185.81/0209, 35-9185.81/0247 and #878/003/2004 for the experiments carried out in Stuttgart or in Budapest, respectively).

Generation of kdPKD1-EGFP transgenic mouse line

An EGFP-tagged version of human kinase-dead (kd) PKD1 (K612W) cDNA was inserted into the multiple cloning site of pBI-5 (Baron et al., 1995) next to the tet-operator and hCMV promoter sequences. The construct contained a downstream rabbit β-globin intron/polyadenylation signal. Vector sequences were excised by digestion with NarI and BsrBI. Pronucleus microinjection was performed by standard procedures (Nagy, 2003). Tail DNA from founder mice was digested with HindIII and analyzed by Southern blotting with a 577bp EGFP probe. The 4.7 kb fragment indicated the integration of the transgene as head-to-tail array of multiple copies into the genome, while the appox. 5.8 kb fragment denoted adjacent integration into the original genome. PCR genotyping was performed with PKD1 specific primers (forward: 5'- TTG GTC GTG AGA AGA GGT CAA ATT C -3'; reverse: 5'- CAC CAA GGC AGT TGT TTG GTA CTT T -3') giving an amplification product of 246 bp for transgenic kdPKD1 and a fragment of 399 bp for endogenous PKD1. Frequency of transgenic littermates occurred in Mendelian fashion.

To create a neuron-specific transgene expressing pattern, kdPKD1-EGFP mice were bred with mice carrying rtTA2 under the control of CaMKIIαpromoter (Michalon et al., 2005). Genotyping for rtTA2 was carried out as described in Michalon et al (2005). To induce kdPKD1-EGFP expression *in vivo*, doxycycline (Dox) was administrated in wet food at 6mg/g dose. Doxycycline-containing food was prepared daily and pellets were covered to protect from light. 10 - 14 weeks old animals received doxycycline-containing food for 8 days to 4 weeks.

Expression constructs

Fluorescently tagged human wtPKD1-GFP, kdPKD1-GFP (PKCμ^{K612W}-EGFP) or caPKD1-GFP (PKD1$^{S738/742E}$) plasmids have been described previously (Hausser et al., 2002; Hausser et al., 1999; Hausser et al., 2005). pEGFP-N1 and pmCherry-N1 vectors were from Clontech and A. Jeromin, Texas, USA, respectively. Generation and characterization of Golgi targeted and non-targeted PKD1 reporter constructs are described in detail elsewhere (Fuchs et al., under review).

Primary hippocampal neuronal cultures

Primary cultures of embryonal hippocampal cells were prepared from CD1 mice on embryonic day 18. After aseptically removing hippocampus from the skull, tissue was freed from men-

inges and incubated in 0.05% trypsin-EDTA (Gibco, Hungary) solution with 0.05% DNaseI in PBS for 15 min at 37° C. After a brief centrifugation, cells were triturated in NeuroBasal (NB) supplemented with B27 (Gibco) containing 5% Fetal Calf Serum (FCS; Sigma, Hungary), 0.5 mM glutamax (Gibco), 40 µg/ml gentamicin (Hungaropharma) and 2.5 µg/ml amphotericin B and filtered through a sterile polyester mesh with 42 µm pore size (EmTek Ltd, Hungary). Cell number was determined by trypan blue exclusion, and cells were seeded in NB culture medium onto poly-L-lysine (Sigma, Hungary) – 1 mg/cm^2 laminin (Sigma, Hungary) coated glass coverslips (13 mm diameter) in 24-well plates for microscopic observations. For Western blot analysis, cells were seeded into 12 well plates at 4x10^5 cells/well cell density, while in case of live cell imaging experiments, 4x10^5 cells were plated onto PLL-laminin coated glass-bottom 35 mm petri dishes (Greiner, Germany). Cytosin-arabinofuranoside (CAR, 10 µM) was added to the cultures 48 h after plating, then culture medium was changed to NeuroBasal supplemented with B27 without FCS on the fourth day of cultivation. One third of the medium was replaced every 3-4 days afterwards. Cells were cultivated for 10 days at 37° C in 5% CO_2/95% air atmosphere.

9 days after plating, transfection of hippocampal cells was carried out using Lipofectamine2000 (Invitrogen, Csertex, Hungary) according to the manufacturer's instructions. In 24-well plates, 0.3-0.5 µg plasmid DNA was mixed with Lipofectamine in a 1µg:2µl ratio. Medium was changed 5-8 hours after the transfection to the original cultivation medium, and cells were analyzed 20-24 hours after transfection.

Immunocytochemistry

Hippocampal cultures were fixed on the tenth day after plating (DIV10) for 20 min with cold 4% paraformaldehyde - 4% sucrose in PBS. After rinsing, cells were permeabilized with 0.1% Triton X-100 for 5 minutes. Non-specific antibody binding was blocked by incubation with 2% BSA - 0.1% Na azide in PBS (PBS-BSA) for 1 hour at room temperature. Primary antibodies like a-GM130 (mouse IgG1, 1:250, BD Transduction Laboratories), a-VAMP4 (rabbit, 1:300, Sigma) and a-pSer294 (rabbit, 1:750; (Hausser et al., 2002)) were diluted in PBS-BSA and used at 4° C overnight. Anti-mouse IgGs conjugated with Alexa 633 (1:500, Molecular Probes) or anti-rabbit-Alexa 546 (1:500, Molecular Probes) was employed for 1.5 hour at room temperature. Cultures were mounted with Mowiol 4.88 (Polysciences, Germany, supplemented with bis-benzimide). Control samples were processed as above, except that the first layer antibodies were omitted.

Immunohistological stainings

Wild-type or double transgenic mice were deeply anaesthetized with Isoflurane and were transcardially perfused with 4% paraformaldehyde (Taab; w/v in PBS). Brains were postfixed overnight and cryoprotected in 30% sucrose. 30 µm coronal sections from the area between Bregma -3 to -1.5 mm were incubated with 0.5 % Triton X-100 -PBS for 30 min and non-specific antibody binding was blocked by incubating the sections with 2% BSA (bovine serum albumin) - 0.3 % Triton X-100 - 0.1% Na-azide in PBS (blocking solution) for 1 hour at room temperature. anti-VAMP4 diluted in blocking solution (rabbit, 1:300, Sigma) was applied for 1 day at 4° C. After washing with PBS (4x15 min), sections were incubated with anti-rabbit IgGs conjugated with Alexa-546 (1:300, Molecular Probes) in blocking solution for 1.5 h at room temperature. Sections were mounted onto poly-L-lysine coated slides and covered with Mowiol supplemented with bis-benzimide. Control samples were processed as above, except that the first layer antibodies were omitted.

Microscopy

Pictures were taken with Zeiss HS CellObserver inverse microscope equipped with the Apotome system with Plan Neofluar 10x/0.3 M27, Plan Apochromat 20x/0.8 M27 or Plan Apochromat 63x/1.4 oil DIC M27 objective lenses. 3D reconstructions of the Golgi structure were made out of 28 to 33 z-stacks using the Inside 4D tool of the AxioVision 4.6 software. In this case, adjacent z-stacks were recorded by 0.15 µm steps. Confocal microscopy was performed with a Leica (TCS SP2) confocal scanning microscope at Airy pinhole using 488, 543, and 633 nm excitation and a 100/1.4 HCX PL APO objective lens.

Live cell imaging observations were carried out with the Zeiss HS CellObserver and with a 488 nm blue led illumination by the Colibri system. Neurons were observed by the Plan Apochro-mat 63x/1.4 oil DIC M27 objective lense and with the AxioCam HR camera with 200 msec frame rate and 2x2 binning. During imaging, cultures were kept in imaging buffer (142 mM NaCl, 5.4 mM KCl, 1.8 mM $CaCl_2$, 1 mM NaH_2PO_4, 25 mM HEPES, 5 mM glucose, 0.8 mM $MgCl_2$, pH 7.4) and at 37° C. In case of PDBu treatment, 1 µM PDBu was applied to the observed petri dish directly on the stage of the microscope.

Quantitative analysis of microscopy data

Golgi morphology was analyzed in 3 independent cultures, transfected with the indicated constructs in parallel. In total, Apotome recordings were made from 34 EGFP, 46 wtPKD1-

EGFP, 37 kdPKD1-EGFP and 53 caPKD1-EGFP transfected neurons, using the Plan Apochromat 63x/1.4 oil DIC M27 objective lens. Only those cells were taken into account where VAMP4 immunostaining of the Golgi complex was clearly detectable. Neuronal Golgi morphology was regarded as thread-like when cis- and trans-Golgi structures appeared as reticular networks with mostly continuous filaments. Abnormal Golgi structure had much shorter (if any) reticular structures and many small fragments, all labeled with VAMP4 and GM130, as well. Pictures were analyzed by a person unaware of the constructs used for the transfection. Dendritic tree morphology of 27 EGFP, 23 PKD1-EGFP, 28 kdPKD1-EGFP and 27 caPKD1-EGFP transfected cells was analyzed by a modified Sholl analysis. A template consisting of circles with consecutively increasing diameter (with 40 µm steps) was placed on the inverted pictures of the transfected neurons and the number of intersections was determined at every level. Student t-test was used for statistical evaluation in both cases ($p<0.05$).

Western blot

Whole cell extracts were obtained by harvesting cells from 12-well plates in 100 µl lysis buffer/well (1% Triton-X100, 20 mM Tris, pH 7.5, 150 mM NaCl, 1mM EGTA, 1 mM EDTA, 1 mM sodium orthovanadate, 10 mM sodium fluoride, 20 mM β-glycerophosphate and Com-plete protease inhibitors [Roche]). Lysates were centrifuged at 16,000 g for 10 min. Protein content of the supernatant was determined by the Bradford reagent (BioRad, Germany). Cell extracts were subjected to SDS-PAGE, and proteins were blotted onto nitrocellulose mem-branes (Pall Corporation). After blocking with 0.5% blocking reagent (Roche) in PBS contain-ing 0.1% Tween 20, filters were probed with specific antibodies as follows: anti-PKD1 (C20 rabbit, 1:2000; Santa Cruz), anti-pSer910 (rabbit, 1:2000; (Hausser et al., 2005)); anti-IIIβ tubulin (mouse, 1:5000; Exbio). Proteins were visualized with HRP-coupled secondary anti-bodies (Dianova) using the ECL system (Pierce Chemical Co.). Stripping of membranes was performed in 62.5 mM Tris, pH 6.8, 2% SDS, and 100 mM β-mercaptoethanol for 30 min at 55° C. Membranes were then reprobed with the indicated antibodies.

Results

PKD is localized at the trans-Golgi network in neurons

We have visualized neuronal Golgi apparatus in cultured mouse hippocampal neurons using GM130 as a cis-Golgi and VAMP4 (Vesicle Associated Membrane Protein 4) as a trans-Golgi

network (TGN) marker (Figure 1). GM130 has been widely used both in nonneuronal and neuronal cells to label cis-Golgi (Horton et al., 2005; Nakamura et al., 1995) while VAMP4, a member of the SNARE (soluble N-ethyl maleimide sensitive factor adaptor receptor) complex, is known to be highly enriched at the TGN and regulate the traffic and sorting of recycling endosomes (Steegmaier et al., 1999; Tran et al., 2007). Both GM130 and VAMP4 highlighted filamentous, perinuclear staining in cultivated neurons (Figure 1A) revealing side-by-side localization of cis- and trans-Golgi compartments. Additionally, 3D reconstruction of the immunostained neurons confirmed that VAMP4 and GM130 positive structures were located in close vicinity and formed a reticular structure located in the soma and with elongated filaments entering one or two dendrites (data not shown).

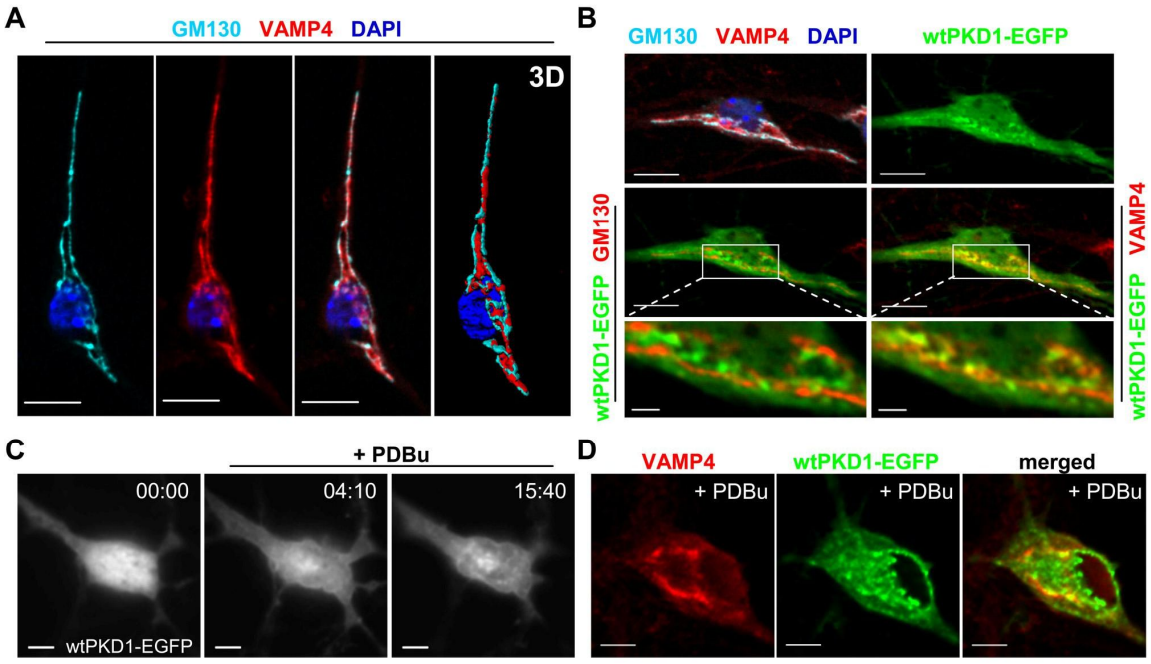

Figure 1 – Golgi structure and localization of wtPKD1-GFP in hippocampal neurons. (A) cultured hippocampal neuron immunostained for GM130, a cis-Golgi (cyan) and for VAMP4, a trans-Golgi marker (red). Nucleus is labeled by DAPI (dark blue). Fixation was carried out 10 days after plating (DIV10). Pictures on the left show individual z-stacks, while the right-most picture is a 3D reconstruction made from 29 z-stacks. (B) Single z-stacks from a hippocampal neuron transfected by wtPKD1-EGFP and immunostained for GM130 and VAMP4. Indicated perinuclear regions are enlarged on the bottom pictures where for the sake of better comparison, GM130 and VAMP4 are similarly displayed in red color. While wtPKD1-EGFP showed side-by-side localization with GM130, it strongly colocalized with VAMP4-stained structures. (C) Live cell imaging recording from a hippocampal neuron transfected with wtPKD1-EGFP and treated with 1 µM PDBu. Elapsed time is indicated as min:sec in the upper right corner. PDBu treatment induced the recruitment of wtPD1-EGFP to the plasma membrane and to internal structures. (D) Single z-stacks from a transfected neuron treated with 1 µM PDBu for 15 minutes and immunostained with anti-VAMP4. Bars indicate 10 µm (A and upper pictures on B), 2 µm (enlarged regions on B) or 5 µm (C, D).

In epithelial cells, TGN localized PKD regulates transport processes and vesicle fission (Diaz Anel and Malhotra, 2005; Ghanekar and Lowe, 2005; Maeda et al., 2001). Hippocampal neurons already possessing elaborate axonal arborization and well developed dendrites were transfected with EGFP-tagged human wild-type PKD1 (wtPKD1-EGFP) 9 days after plating (DIV9). Cultures were fixed 22 - 24 hours after transfection and were processed for GM130 and VAMP4 immunocytochemistry (Figure 1B). Golgi structure of wtPKD1-EGFP transfected neurons was indistinguishable from non-transfected neurons (see Figure 1A) or from control, vector-only transfected neurons (data not shown), as GM130 and VAMP4 staining confirmed the presence of thread-like Golgi apparatus. Besides a rather homogenous, cytoplasmic distribution, wtPKD1-EGFP was slightly enriched at the Golgi apparatus. On closer examination, wtPKD1-EGFP was localized side-by-side with GM130 but showed partially overlapping localization with VAMP4-stained structures (Figure 1B, enlargements).

Phorbol ester treatment is known to cause plasma membrane translocation and activation of PKD (Chiu and Rozengurt, 2001; Matthews et al., 1999a; Rey et al., 2004; Waldron et al., 2001; Zugaza et al., 1996). In live cell imaging of hippocampal neurons, 1 mM PDBu treatment led to a rapid recruitment of wtPKD1-EGFP to the plasma membrane, followed by the intracellular accumulation of the fluorescently tagged protein (Figure 1, C and D). Immunocytochemical staining with VAMP4 confirmed that 15 minutes of PDBu treatment enhanced the translocation of wtPKD1-EGFP to the TGN as well as to the nuclear membrane and to other intracellular structures (Figure 1D). These results indicate that fluorescently labeled PKD1 behaved similarly in transfected neurons as endogenous PKD in non-neuronal cells.

Endogenous PKD is selectively active at the Golgi complex and in the dendritic compartments

In hippocampal neuronal cultures, endogenous PKD1 was detectable already from the first day of plating (Figure 2H). PKD1 protein level increased in parallel with neuronal development and neurite elongation, demonstrated by the increasing level of neuron-specific IIIβ-tubulin signal during cultivation (Figure 2H). It is known that PKD activation leads to autophosphorylation on serine 910 in human PKD1 (Matthews et al., 1999b; Vertommen et al., 2000), therefore an antibody specific for the phosphorylated form of Ser910 in PKD1 can be successfully used to demonstrate endogenous PKD1 activation (Hausser et al., 2002; Haworth and Avkiran, 2001). In our mouse hippocampal cultures, the pS910-specific antibody gave a clear signal in DIV7 and DIV10 lysates, which could be detected also with PKD1-specific antibody (Figure 2I). Additionally, autophosphorylation of endogenous mouse PKD1

was greatly increased by 10 minutes of phorbol ester treatment in DIV10 hippocampal neuronal cultures (Figure 2I). These results confirm that endogenous PKD1 is present and active in cultured hippocampal neurons at time points when axons and main dendrites are already formed.

The consensus PKD target site has been mapped (Nishikawa et al., 1997) and antibodies raised against the phosphorylated serine of the consensus PKD target site have been suc-

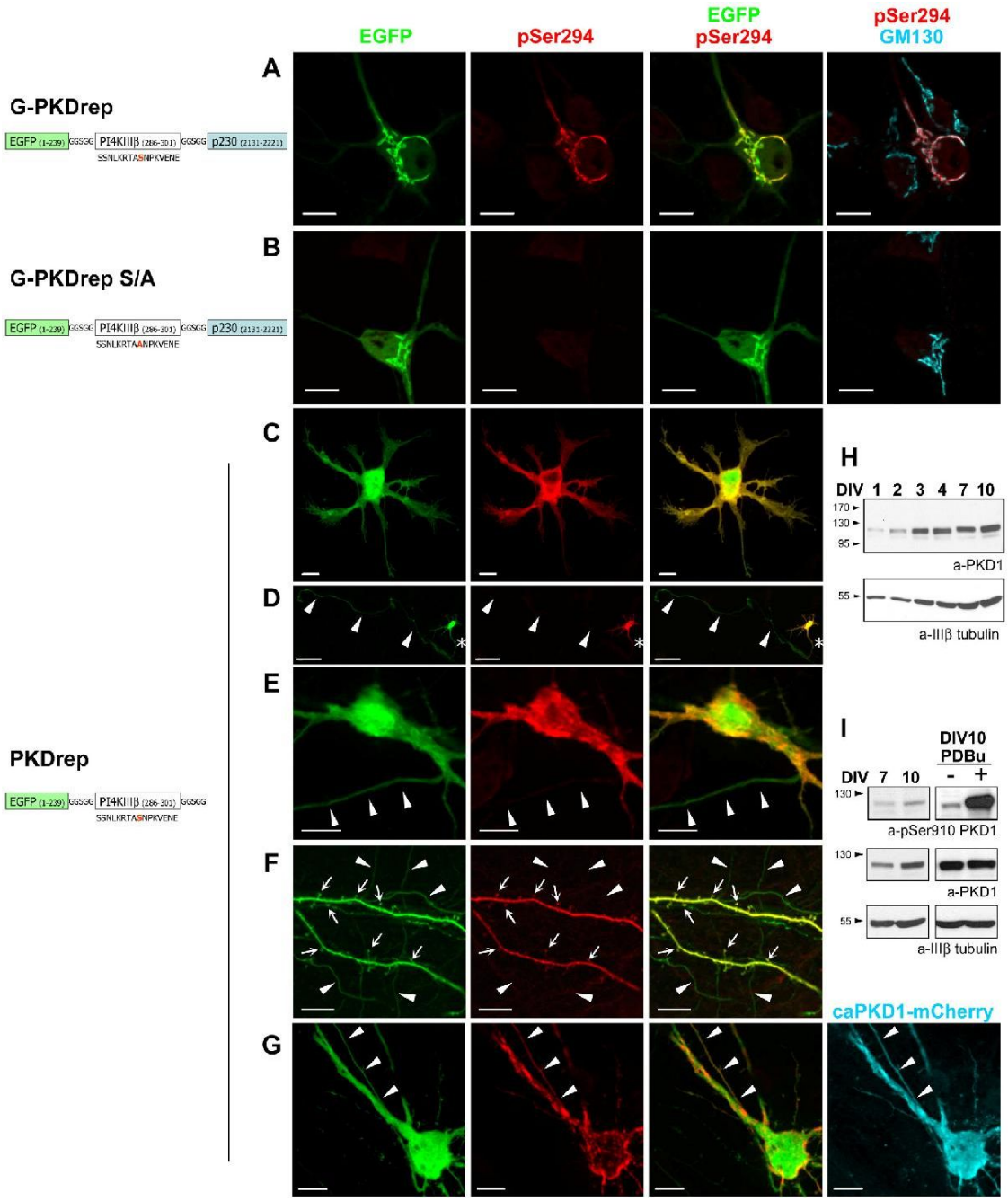

Figure 4 – see next page for legend

cessfully used to demonstrate PKD-mediated phosphorylation of various substrate molecules (Doppler et al., 2005; Hausser et al., 2005). Phosphatidylinositol 4-kinase IIIβ(PI4KIIIβ) is a known target of PKD and gets selectively phosphorylated by PKD on Ser294 (Hausser et al., 2005). In order to visualize endogenous PKD activity in cultured hippocampal neurons, different EGFP-tagged PKD reporter constructs were created using the PKD specific substrate sequence of PI4KIIIβat Ser294 (see cartoons on Figure 2). In case of Golgi-targeted PKD reporter (G-PKDrep), the GRIP domain of p230, a known trans-Golgi localized protein was fused to the PKD target site, providing selective enrichment of the construct at the TGN (Fig-ure 2A). PKD-mediated phosphorylation of the transfected constructs can be detected by immunocytochemistry using an antibody specific for phosphorylated Ser294 (Hausser et al., 2005). Specificity of the immunostaining was proven by transfecting constructs containing a serine to alanine mutation inside the PKD target sequence (G-PKDrep S/A; Figure 2B).

The GRIP domain of p230 led to enrichment of the EGFP-tagged constructs containing either serine or alanine in the PKD target site at the Golgi complex, the latter visualized by GM130 staining (Figure 2, A and B). As expected, pSer294 antibody staining was detected only in those cells which were transfected with the PKD reporter containing the original serine site. GM130 immunostaining revealed a side-by-side localization with the pSer294 signal, in accordance with the TGN-directed localization of the PKD reporter. Importantly, PKD reporter was highly phosphorylated at the TGN in transfected neurons, even without applying phorbol ester into the culture medium.

Figure 2 – PKD activity in cultivated hippocampal neurons. Cultivated hippocampal neurons were transfected either by Golgi-targeted (A, B) or non-targeted (C-G) PKD reporter constructs containing the PKD specific substrate sequence of PI4KIIIβaround Ser294. Golgi targeting was achieved by fusing the GRIP domain of p230 to the target sequence (A, B) and Ser294 was mutated to alanine in the control construct (B). PKD-mediated phosphorylation of the reporter was detected by using an antibody specific to the phosphorylated state of Ser294 (pSer294). Endogenous PKD activity was detected around the Golgi structure, highlighted by GM130 immunostaining (A, B). (C) PKD activity is uniformly detected in the developing neurites of stage 2 hippocampal neurons. (D) Parallel to axonal development, PKDrep phosphorylation is excluded from the distal axon (indicated by arrowheads) and is restricted to the proximal axonal segment (asterisk) as well as to the soma and dendrites of a stage 3 neuron. (E-F) In DIV10 neurons, PKDrep phosphorylation was absent from the initial axonal segment and thin axon collaterals (arrowheads) but was highly detected in the soma, in the dendrites and in the dendritic spines (see arrowheads). (G) When neurons were cotransfected with the constitutive active PKD1$^{S738/742E}$-mCherry mutant (caPKD1-mCherry), non-targeted PKD reporter was also phosphorylated in the axon (arrowheads). Note the increased surface localization of the pSer294 signal in the soma of the cotransfected neuron on G, as well. Pictures are projection images of 4-6 adjacent z-stacks taken by the Zeiss Apotome system. Bars indicate 50 µm (D) or 10 µm (A-C and E-G). (H) Endogenous PKD1 level increased during *in vitro* development of hippocampal neuronal cultures. (I) Ser910 autophosphorylation of endogenous PKD1 was detected both at DIV7 and DIV10 cultures. 10 minutes of 1 µM PDBu treatment highly increased endogenous PKD1 autophosphorylation in DIV10 neurons. Neuron-specific IIIβ-tubulin detection was used to follow *in vitro* neuronal development (H) or equal protein loading (I).

The intracellular activation of endogenous PKD was additionally investigated using the non-targeted version of the PKD reporter (PKDrep). Both the control, alanine containing construct (PKDrep S/A; data not shown) and PKDrep (Figure 2, C-G) were evenly distributed in the cytoplasm of the transfected neurons. In non-polarized, stage 2 neurons, PKDrep phosphorylation was evident in all neurites and in the soma (Fig. 2C). On the other hand, phosphorylation of PKDrep was gradually diminished in the course of axonal maturation: stage 3 neurons with already elongated axons possessed endogenous PKD activity only in the proximal axon (Figure 2D; see asterisk). In mature neurons, pSer294 signal was excluded from the axons, already from the axonal initial segment which originates usually from one of the main dendrites or directly from the soma (Figure 2E). Phosphorylation of PKDrep was also absent from the thinner axon collaterals (Figure 2F; see arrowheads) but was evident in the soma and in the main dendrites (Figure 2E), as well as in the smaller dendritic branches and dendritic spine heads (see small arrows on Figure 2F). When neurons were cotransfected with PKDrep and the constitutive active human PKD1 mutant, PKD1$^{S738/742E}$-mCherry (caPKD1-mCherry), phosphorylation of PKDrep was detected in axons co-expressing caPKD1 (see arrowheads on Figure 2G). These results prove that the lack of pSer294 staining in the axons is due to the lack of endogenous PKD activity under normal conditions and indicate that endogenous PKD has a polarized activity in the somatodendritic compartment of cultured hippocampal neurons.

Expression of dominant-negative kinase-inactive PKD leads to the disruption of the Golgi complex

In non-neuronal cells, disruption of PKD's kinase activity leads to impaired secretory vesicle fission and tubulation of the TGN (Liljedahl et al., 2001). In order to investigate the effects of different PKD mutations on neuronal Golgi complex morphology, DIV9 hippocampal neurons were transfected with EGFP-tagged wild-type, constitutive active and dominant-negative kinase-inactive (kdPKD1-EGFP; PKD1^{K612W}-EGFP) forms of human PKD1-GFP or the EGFP vec-tor. 24 hours after transfection, caPKD1-GFP showed similar distribution pattern to wtPKD1-GFP (see Figure 3A versus Figure 1B), being evenly distributed in the cytoplasm and slightly enriched around the neuronal Golgi complex. caPKD1-EGFP expression did not disturb the thread-like structure of the neuronal Golgi complex, either (Figure 3A).

Transfection with the kinase-inactive PKD1 mutant, on the other hand, led to evident changes in neuronal Golgi morphology (Figure 3, B and C). VAMP4 and GM130 immunostaining re-vealed that Golgi complex of the transfected neurons was disrupted into several small frag-ments containing both cis- and trans-Golgi elements (see enlarged area in Figure 3C).

Besides some weak cytoplasmic distribution, kdPKD1-EGFP was strongly localized to these fragments, and showed colocalization especially with the VAMP4-positive regions. In many cases, a sandwich-like arrangement between GM130 and VAMP4 positive structures and kdPKD1-EGFP was observed, with VAMP4-labeled trans-Golgi parts being in the middle (Figure 3C). 3D reconstruction further supported that kdPKD1-EGFP was trapped mostly at the trans-Golgi regions.

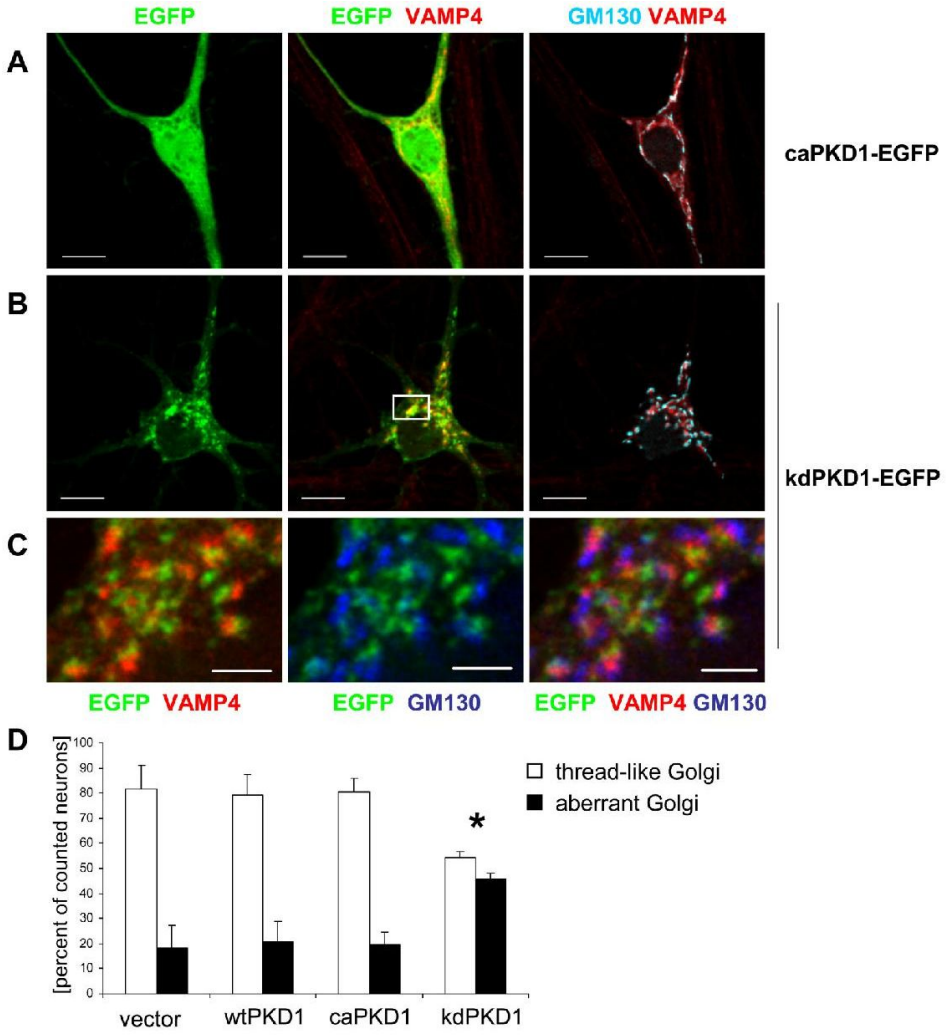

Figure 3 – Golgi morphology in transfected hippocampal neurons. Hippocampal neurons were transfected with constitutive active (caPKD1-EGFP; A) or kinase-inactive (kdPKD1-EGFP; B-C) mutant PKD1 constructs and were immunostained for VAMP4 and GM130 as trans- and cis-Golgi markers, respectively. caPKD1-EGFP was distributed in the cytoplasma with slight enrichment at the Golgi structure and did not disturb thread-like neuronal Golgi structure (A). kdPKD1-EGFP formed patches in the perinuclear region and in the dendrites and led to the dispersal of the Golgi complex (B). (C) Confocal images of the boxed area on (B). kdPKD1-EGFP localized mainly to the VAMP4-positive, trans-Golgi side of the dispersed neuronal Golgi. Images are single z-stacks recorded by the Zeiss Apotome (A, B) or the Leica SP2 confocal (C) systems. Bars indicate 10 µm (A-B) or 2 µm (C). (D) Quantitative evaluation of the neuronal Golgi morphology in 34 EGFP, 46 wtPKD1-EGFP, 37 kdPKD1-EGFP and 53 caPKD1-EGFP transfected neurons. Data are shown as averages and s.e.m. *: $p<0.05$.

Quantitative analysis of Golgi morphology from 3 independent cultures additionally confirmed the above findings by showing that the ratio of transfected neurons possessing fragmented Golgi complex was significantly increased upon kdPKD1-EGFP expression but did not differ between the vector transfected neurons and wt-PKD1-EGFP or caPKD1-EGFP expressing neurons (Figure 3D). These data indicate that PKD1 plays an important role in the maintenance of the normal Golgi apparatus structure in neurons.

Doxycycline induced kdPKD1-EGFP expression in hippocampal neurons leads to dis-ruption of Golgi morphology in vivo

To confirm our *in vitro* results, we generated mice expressing human kdPKD1-EGFP under the control of the tetracycline-responsive (TetO) HCMV promoter by standard transgenic tech-niques and pronucleus injection (kdPKD1-EGFP mice; Figure 4, A-C). Several transgenic lines were established from founder animals. The presence of the transgene in the founder mice as well as in the offsprings was verified both by Southern analysis and with genomic PCR (Figure 4, B and C). kdPKD1-EGFP mice were crossed to mice carrying rtTA2 under the con-trol of CaMKIIαpromoter, known to provide a forebrain and hippocampus-specific expression pattern of the transactivator (Michalon et al., 2005). Double transgenic animals from these breedings were readily identified by PCR (data not shown). Neither single transgenic, nor double transgenic mice showed any signs of abnormal development or behavioural effects (data not shown).

kdPKD1-EGFP expression was induced in adult CaMKIIαrtTA2 x kdPKD1-EGFP mice by administration of doxycycline (Dox) in the food. The appearance of kdPKD1-EGFP signal was already visible upon 5 days of Dox treatment (data not shown). By 2 weeks of feeding the animals with Dox, kdPKD1-EGFP expression was evident in the perinuclear region and in the proximal dendrites of CA3 neurons (Figure 4E). As expected, no EGFPexpressing cells were found in wild-type animals (Figure 4F). 4-week-long Dox treatment led to high level of transgene expression in the dentate gyrus (DG) and CA3, with somewhat lower signal in the CA1 region of double transgenic hippocampus (Figure 4G). Interestingly, our observations did not reveal homogenous expression patterns, as only a part of double transgenic hippocampal neurons were found to be kdPKD1-EGFP positive. Transgene expression was also detected in hippocampal lysates by Western blotting (Figure 4D).

To visualize neuronal Golgi structure *in vivo*, VAMP4 immunostaining was used. Besides weakly labelling small, dot-like structures in the dendrites, resembling most likely recycling endosomes, VAMP4 staining was highly enriched at the neuronal Golgi complex (Figure 4, I-J and L-M). In non-transgenic hippocampal sections, regardless of the length of Dox treatment, VAMP4 was localized to thread-like, perinuclear structures often extending into the apical

dendrites (Figure 4, H-J). These results show that even long-term Dox treatment did not disturb normal, thread-like TGN morphology in wild-type neurons. On the other hand, in CaMKIIαrtTA2 x kdPKD1-EGFP double transgenic mice treated with Dox for 4 weeks, kdPKD1-EGFP was enriched at VAMP4-positive TGN structures, which were strongly dispersed (Figure 4, K-M). Thus, *in vivo* observations are in close agreement with the findings obtained from transfected hippocampal neuronal cultures.

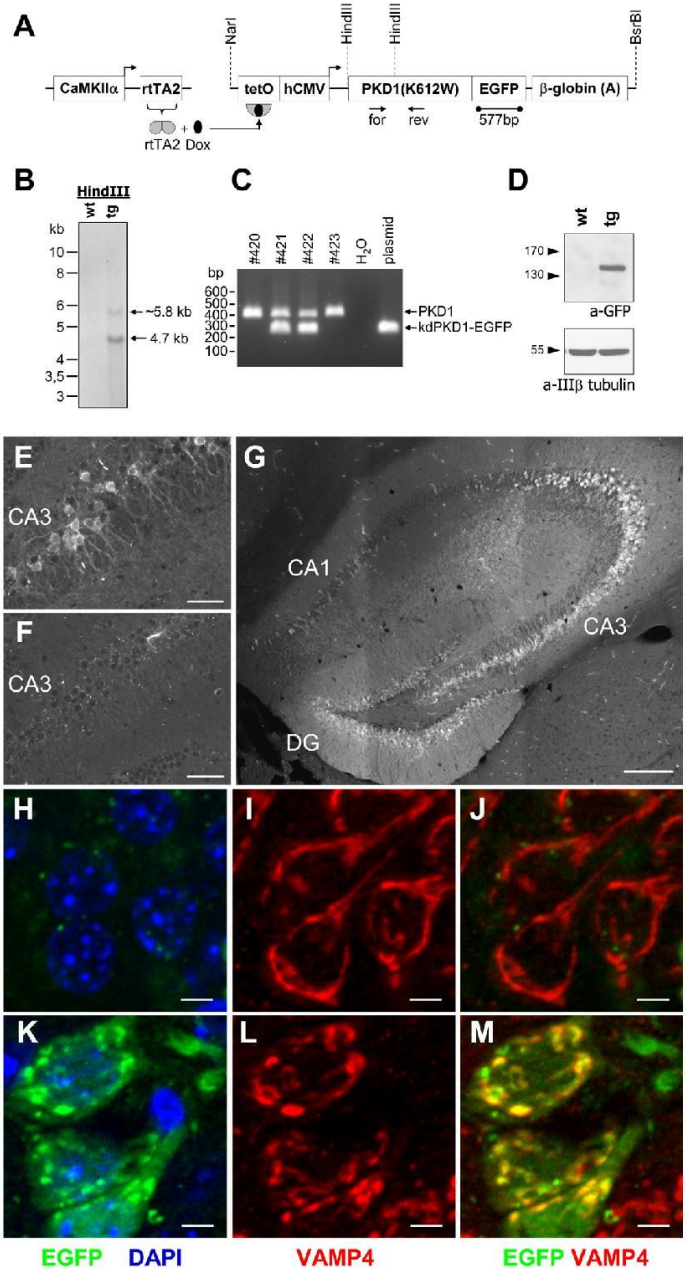

Figure 4 – see next page for legend

PKD activity regulates dendritic rearrangements in neurons

Our experiments have already shown that besides being active at the Golgi complex, endogenous PKD was selectively active in the dendrites (Figure 2). In order to investigate the effect of PKD1 mutants on dendritic arrangement, morphology of EGFP, wtPKD1-GFP, caPKD-GFP or kdPKD1-GFP transfected neurons was quantitatively analyzed in DIV10 hippocampal neurons, 22-24 hours after transfection. Modified Sholl analysis was carried out to determine the extent of dendritic branching by calculating the intersection numbers at concentric circles located over the soma of the transfected neurons with a 20 µm stepwise increase in radius (Figure 5A shows the outline and dendritic intersections of representative neurons). The average number of intersections as a function of distance from the soma characterizes well the dendritic arborization of the transfected neurons (Figure 5).

Control, vector-only transfected neurons had the highest number of intersections in the close (within 40 µm) vicinity of the soma, with dendrites reaching up to 300 µm distance from the soma. The extent of arborization gradually decreased in parallel with the increasing distance. The presence of kdPKD1-EGFP led to a significant decrease in the intersection numbers at almost all levels (indicated by asterisks on Figure 5B) and dendrites did not extend further than 200 µm distance. Introducing caPKD1-EGFP into transfected neurons, on the other hand, led to a significant increase in dendritic arborization. Not only did the distribution of the

Figure 4 – Characterization of the *in vivo* kdPKD1-EGFP expression in CaMKIIαrtTA2 x kdPKD1-EGFP transgenic mice. (A) Schematic diagram depicting the generation of CaMKIIα-rtTA2 x kdPKD1-EGFP double transgenic mice. Upon doxycycline (Dox) treatment, rtTA2 binds to the tetO responsive element and induces the expression of kdPKD1-EGFP. (B) Southern blot from wild-type (wt) and kdPKD1-EGFP transgenic (tg) mice, hybridized with the 577bp EGFP probe indicated on (A). (C) PCR genotyping of kdPKD1-EGFP transgenic animals from a heterozygous breeding, using the forward and reverse primers indicated on A. Due to an intron, endogenous PKD1 amplification gives a 399 bp fragment, while transgenic DNA yields a 246 bp amplification product. (D) Transgene expression was detected only in hippocampal lysates of kdPKD1-EGFP transgenic (tg) mice, after 4 weeks of Dox treatment. (E-F) In the CA3 region, kdPKD1-EGFP expression was already evident after 2 weeks of Dox treatment (E), while sections from non-transgenic littermates showed no expression (F). (G) 4 weeks of Dox treatment led to elevated hippocampal expression of kdPKD1-EGFP in double transgenic animals, especially in the dentate gyrus (DG) and CA3 region of the hippocampus. In CA1, weaker expression was also detected. (H-M) CA3 neurons of Dox-treated (4 weeks) wild-type (H-J) and double transgenic (K-M) sections. Neuronal TGN was visualized by VAMP4 staining, nuclei were stained by DAPI. Corresponding pictures from wild-type and double transgenic sections were recorded under identical settings. (G) is a mosaic image from 9 images taken by 10x objective and the Zeiss Apotome system. (E-F) pictures are projection images of 4-6 adjacent z-stacks obtained by a 20x objective, while (H-M) were recorded by a 63x objective and are the projections of 12-14 individual z-stacks. Corresponding wild type and double transgenic pictures were taken under identical settings and processed similarly. Bars indicate 200 µm (G), 50 µm (E-F) or 5 µm (H-M).

highest intersection numbers shift towards outer regions around the soma (60 - 80 µm), but the average number of cross-points was also significantly elevated (see + signs on Figure 5B). Expression of wtPKD1-EGFP led to similar changes, but to a lesser extent. Morphological changes observed within a day following transfection indicate that PKD1 activity rapidly influences the extent of dendritic arborization in neurons.

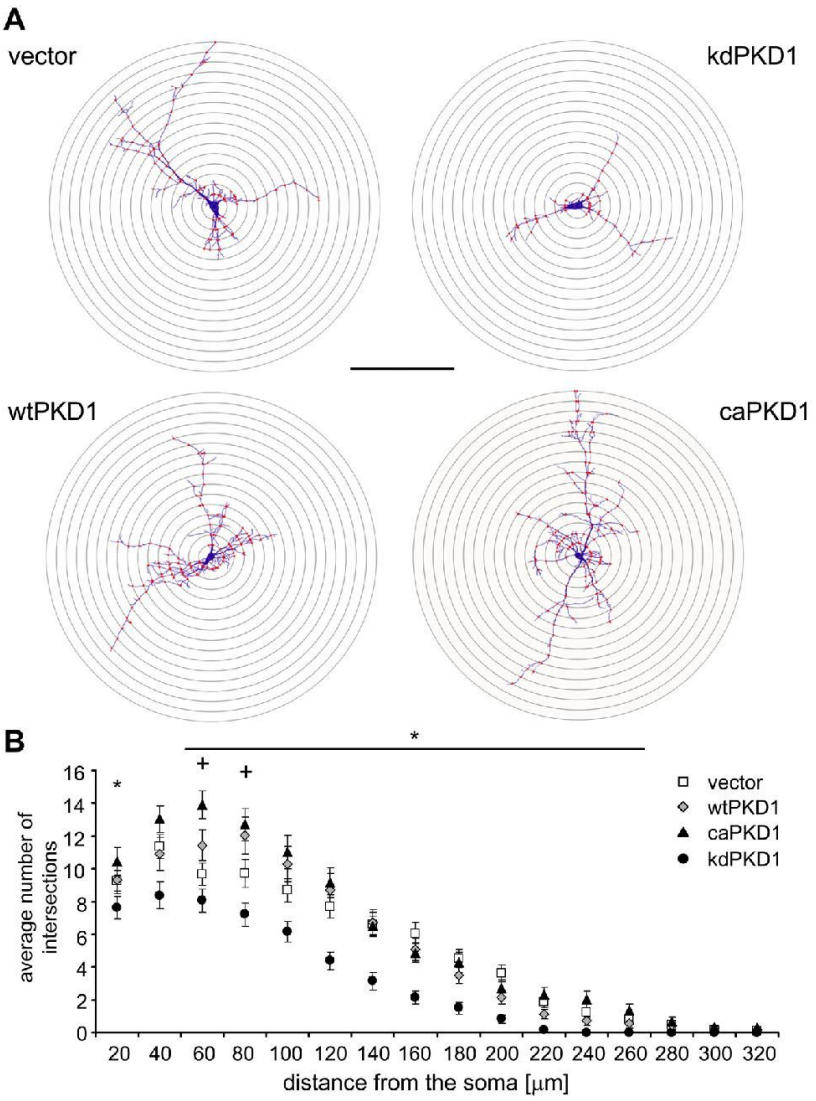

Figure 5 – Sholl analysis of transfected hippocampal neurons. (A) Representative Sholl analysis images of neurons transfected with different constructs as indicated at the sides. Dendritic intersections are labeled by red dots. Bar indicates 200 µm. (B) Average intersection numbers at certain distance from the soma in neurons transfected with EGFP vector (empty square), wtPKD1-EGFP (grey diamond), caPKD1-EGFP (filled triangle) or kdPKD1-EGFP (filled circle). 27 EGFP, 23 wtPKD1-EGFP, 28 kdPKD1-EGFP and 27 caPKD1-EGFP transfected neurons were used for the analysis. Data are presented as averages and s.e.m. * and +: $p<0.05$ for kdPKD1-EGFP (*) or for caPKD1-EGFP (+) expressing neurons.

Discussion

Studies in polarized epithelial cells revealed that PKD is selectively involved in the basolateral membrane protein transport (Yeaman et al., 2004). On the other hand, PKD-mediated effects and transport processes in neurons are still to be understood. In line with recent publications (Bisbal et al., 2008; Horton et al., 2005), our work provides additional evidences on the polarized, somatodendritic activity as well as on Golgi-localized action of PKD in neurons.

In our hands, endogenous PKD activity was gradually restricted to the somatodendritic compartment of developing hippocampal neurons, leading to a highly polarized activity in mature, DIV10 neurons. High level of PKDrep phosphorylation was detected in the soma, in the main dendrites as well as in dendritic filopodia and spines. In neurons coexpressing caPKD1 and PKDrep, pSer294 immunostaining was highly increased at the plasma membrane in the soma or at certain locations in the main dendrites, likely reflecting the local activity of PKD. Although pSer294 signal was excluded from the axons, axonal PKD activity could be restored upon cotransfection with the evenly distributed constitutive active PKD1.

To explain these findings, several mechanisms appear conceivable: First, lack of endogenous PKD activity might reflect the lack of the endogenous protein in the axonal cytoplasm. This possibility, however, can be ruled out as endogenous PKD was detected in the axons of cultivated hippocampal neurons (Bisbal et al., 2008; Yin et al., 2008). Second, PKD is evenly distributed, comprising the axonal compartment, too, but upstream activators of PKD, like PKCs or PLC, might not be present along the axon in sufficient amount to activate PKD there. However, because presynaptic PKC activity and the involvement of DAG-mediated signaling events were described to regulate axonal branching and extension (Rosner and Vacun, 1999; Schmidt et al., 2004; Wang and Wadsworth, 2002), this mechanism appears less likely. Last but not least, dephosphorylation of PKD and/or the reporter (Uetani et al., 2006) or inactivation of PKD, e.g. via sequestration by 14-3-3 adapter proteins (Hausser et al., 1999; Taya et al., 2007) could be selectively increased in the axons, thus preventing accumulation of phosphorylated PKD sensor. Irrespective of the underlying mechanisms, our findings are in accordance with recent data showing that kdPKD1 expression had no axonal effects in DIV5 hippocampal neurons (Horton et al., 2005) or on the localization of axonal membrane proteins (Bisbal et al., 2008).

A recent work reported the involvement of PKD during early neuronal polarization by showing that downregulating PKD1 and PKD2 levels led to the transformation of developing neurites into axons (Yin et al., 2008). At first sight, this data might fit to our results showing a gradual restriction of PKD activity to the somatodendritic compartments and could lead to the conclu-

sion that loss of PKD activity might be a prerequisite for axonal development. However, we have not found increased Tau1 positivity in kdPKD expressing young neurons (KC, KS, unpublished data). Multiple axon formation upon decreased PKD activity is also in contrast to previously published data (Horton et al., 2005) or to an elegant work showing the mistargeting of dendritic but not axonal membrane proteins in neurons with impaired PKD activity (Bisbal et al., 2008). Therefore it is a more feasible assumption that PKD activity is required predominantly for the selective maintenance of the dendritic membrane surface. Further work is needed to clarify these apparent inconsistencies.

Dendrite-specific action of PKD was also supported by the dramatic shrinkage of the dendritic tree within 24 hours upon the expression of kdPKD1 and by the enhancing effect of caPKD1 in transfected neurons. Golgi-mediated secretory processes play a highly important role in the supply of cargo necessary for the maintenance of the dendritic surface machinery (Hanus and Ehlers, 2008; Tang, 2008; Ye et al., 2007). Therefore, a possible explanation for the shrinkage of the dendritic tree in kdPKD1 transfected neurons is that the observed changes are, at least partly, the consequence of impaired dendrite-directed secretory transport. On the other hand, PKD-regulated dendritic endocytosis also serves as a potential mode of action. Decreasing PKD activity was reported to selectively increase endocytosis of dendritic proteins, leading to a missorting between dendritic versus axonal compartments (Bisbal et al., 2008). Consequently, endogenous PKD activity can be responsible for the maintenance of the dendritic membrane surface via regulating the rate of endocytosis. Thus, caPKD1-mediated increase in dendritic branching can be a consequence of inhibited dendritic endocytosis.

Golgi targeted PKD reporter also revealed endogenous PKD activity at the neuronal Golgi complex, and EGFP-tagged PKD1 constructs were shown to localize to the TGN. This is in accordance with findings in non neuronal cells, where a fraction of cytoplasmic PKD can be recruited to the TGN and participates in the fission of membrane destined transport carriers (Baron and Malhotra, 2002; Ghanekar and Lowe, 2005; Liljedahl et al., 2001; Maeda et al., 2001). Accumulation of kdPKD1-GFP at the VAMP4 positive TGN-fragments was observed both *in vitro*, in transfected neurons, and *in vivo*, upon Dox-induced PKD mutant expression in CaMKIIαrtTA2 x kdPKD1-EGFP double transgenic mice. Similar to what is known from non-neuronal cells, the K612W mutation in the kinase domain of PKD1 did not interfere with its substrate and membrane binding capacity (Hausser et al., 2002; Johannes et al., 1998), yet detachment from membranes appears impaired, resulting in an accumulation at the TGN (Bard and Malhotra, 2006).

Importantly, kdPKD accumulation led to the disruption of the neuronal Golgi apparatus via the formation of smaller fragments, still possessing cis- and trans-Golgi elements. This phenomenon resembles nocadozole-induced fragmentation of the Golgi complex and the forma-

tion of the so-called Golgi ministacks in epithelial cells (Cole et al., 1996; Yang and Storrie, 1998). At a first glance, these observations differ from that of the Caceres group, who did not report morphological changes in the Golgi apparatus upon interfering with neuronal PKD activity (Bisbal et al., 2008). However, as we waited 20 to 24 hours instead of 12 to 14 hours after the transfection, the observed fragmentation can be a consequence of the prolonged kdPKD1 effects at the Golgi complex. Fragmentation of the Golgi apparatus is at variance with the well-described tubulation of the TGN in kdPKD expressing non-neuronal cells, as well, which is widely accepted as a consequence of impaired vesicle fission (Bard and Malhotra, 2006; De Matteis and Luini, 2008). However, morphology of the Golgi complex in neuronal cells differs largely from those of the typical transformed cell lines of epithelial origin. Therefore, despite potential differences in phenotypical changes, it is important to note that the common finding in our studies with neuronal cells and in others with non-neuronal cells is that PKD activity is required for the maintenance of the cell type specific Golgi complex architecture and that interfering with PKD activity rapidly changes Golgi complex integrity.

In addition to its important role in secretory transport, a role of PKD in the regulation of cytoskeletal organization affecting cell migration and invasion was already shown in nonneuronal cells (Bowden et al., 1999; Eiseler et al., 2007; Prigozhina and Waterman-Storer, 2004; Qiang et al., 2004; Van Lint et al., 2002). PKD was also reported to interact with F-actin and cortactin (Eiseler et al., 2007) and to participate in nocodazole-mediated disruption of the Golgi complex (Fuchs et al., under review). As the morphology of the Golgi complex depends to a large extent on the integrity of the surrounding cytoskeletal elements (Bard and Malhotra, 2006; De Matteis and Luini, 2008; Egea et al., 2006), the observed fragmentation of the Golgi complex could be a consequence of altered cytoskeletal organization upon kdPKD expression, too. Cytoskeletal rearrangements fundamentally influence the formation and maintenance of dendritic structures, too, including elongation and branching of dendrites and spine formation (Gauthier-Campbell et al., 2004; Hayashi et al., 2007; Kim et al., 2006; Tada et al., 2007; Zhang and Macara, 2008). Accordingly, direct or indirect cytoskeletal effects of PKD can also participate in the observed dendritic rearrangements in transfected neurons, especially when taking into account that high level of PKD activity was observed not only around the neuronal Golgi, but also in the cytoplasm of dendrites and even in the dendritic spines.

Taken together, our investigations have provided evidence that PKD acts selectively in the somatodendritic compartment of polarized neurons and is needed for the integrity of Golgi apparatus and for the maintenance of dendritic arborization.

References

Bard, F., and Malhotra, V. (2006). The formation of TGN-to-plasma-membrane transport carriers. Annu Rev Cell Dev Biol *22*, 439-455.

Baron, C. L., and Malhotra, V. (2002). Role of diacylglycerol in PKD recruitment to the TGN and protein transport to the plasma membrane. Science *295*, 325-328.

Baron, U., Freundlieb, S., Gossen, M., and Bujard, H. (1995). Co-regulation of two gene activities by tetracycline via a bidirectional promoter. Nucleic Acids Res *23*, 3605-3606.

Bisbal, M., Conde, C., Donoso, M., Bollati, F., Sesma, J., Quiroga, S., Diaz Anel, A., Malhotra, V., Marzolo, M. P., and Caceres, A. (2008). Protein kinase d regulates trafficking of dendritic membrane proteins in developing neurons. J Neurosci *28*, 9297-9308.

Bowden, E. T., Barth, M., Thomas, D., Glazer, R. I., and Mueller, S. C. (1999). An invasion-related complex of cortactin, paxillin and PKCmu associates with invadopodia at sites of extracellular matrix degradation. Oncogene *18*, 4440-4449.

Bresler, T., Shapira, M., Boeckers, T., Dresbach, T., Futter, M., Garner, C. C., Rosenblum, K., Gundelfinger, E. D., and Ziv, N. E. (2004). Postsynaptic density assembly is fundamentally different from presynaptic active zone assembly. J Neurosci *24*, 1507-1520.

Chiu, T., and Rozengurt, E. (2001). PKD in intestinal epithelial cells: rapid activation by phorbol esters, LPA, and angiotensin through PKC. Am J Physiol Cell Physiol *280*, C929-942.

Cole, N. B., Sciaky, N., Marotta, A., Song, J., and Lippincott-Schwartz, J. (1996). Golgi dispersal during microtubule disruption: regeneration of Golgi stacks at peripheral endoplasmic reticulum exit sites. Mol Biol Cell *7*, 631-650.

De Matteis, M. A., and Luini, A. (2008). Exiting the Golgi complex. Nat Rev Mol Cell Biol *9*, 273-284.

Diaz Anel, A. M., and Malhotra, V. (2005). PKCeta is required for beta1gamma2/beta3gamma2- and PKD-mediated transport to the cell surface and the organization of the Golgi apparatus. J Cell Biol *169*, 83-91.

Doppler, H., Storz, P., Li, J., Comb, M. J., and Toker, A. (2005). A phosphorylation state-specific antibody recognizes Hsp27, a novel substrate of protein kinase D. J Biol Chem *280*, 15013-15019.

Dresbach, T., Qualmann, B., Kessels, M. M., Garner, C. C., and Gundelfinger, E. D. (2001). The presynaptic cytomatrix of brain synapses. Cell Mol Life Sci *58*, 94-116.

Egea, G., Lazaro-Dieguez, F., and Vilella, M. (2006). Actin dynamics at the Golgi complex in mammalian cells. Curr Opin Cell Biol *18*, 168-178.

Eiseler, T., Schmid, M. A., Topbas, F., Pfizenmaier, K., and Hausser, A. (2007). PKD is recruited to sites of actin remodelling at the leading edge and negatively regulates cell migration. FEBS Lett *581*, 4279-4287.

Ellwanger, K., Pfizenmaier, K., Lutz, S., and Hausser, A. (2008). Expression patterns of protein kinase D 3 during mouse development. BMC Dev Biol *8*, 47.

Fuchs, Y. F., Pimpl, S. A., Link, G., Schlicker, O., Bunt, G., Pfizenmaier, K., and Hausser, A. (under review). A Golgi PKD activity reporter reveals a crucial role of PKD in nocodazole-induced Golgi dispersal.

Fugmann, T., Hausser, A., Schoffler, P., Schmid, S., Pfizenmaier, K., and Olayioye, M. A. (2007). Regulation of secretory transport by protein kinase D-mediated phosphorylation of the ceramide transfer protein. J Cell Biol *178*, 15-22.

Fujita, Y., and Okamoto, K. (2005). Golgi apparatus of the motor neurons in patients with amyotrophic lateral sclerosis and in mice models of amyotrophic lateral sclerosis. Neuropathology *25*, 388-394.

Gardiol, A., Racca, C., and Triller, A. (1999). Dendritic and postsynaptic protein synthetic machinery. J Neurosci *19*, 168-179.

Gauthier-Campbell, C., Bredt, D. S., Murphy, T. H., and El-Husseini Ael, D. (2004). Regulation of dendritic branching and filopodia formation in hippocampal neurons by specific acylated protein motifs. Mol Biol Cell *15*, 2205-2217.

Ghanekar, Y., and Lowe, M. (2005). Protein kinase D: activation for Golgi carrier formation. Trends Cell Biol *15*, 511-514.

Hanus, C., and Ehlers, M. D. (2008). Secretory Outposts for the Local Processing of Membrane Cargo in Neuronal Dendrites. Traffic.

Hausser, A., Link, G., Bamberg, L., Burzlaff, A., Lutz, S., Pfizenmaier, K., and Johannes, F. J. (2002). Structural requirements for localization and activation of protein kinase C mu (PKC mu) at the Golgi compartment. J Cell Biol *156*, 65-74.

Hausser, A., Storz, P., Link, G., Stoll, H., Liu, Y. C., Altman, A., Pfizenmaier, K., and Johannes, F. J. (1999). Protein kinase C mu is negatively regulated by 14-3-3 signal transduction proteins. J Biol Chem *274*, 9258-9264.

Hausser, A., Storz, P., Martens, S., Link, G., Toker, A., and Pfizenmaier, K. (2005). Protein kinase D regulates vesicular transport by phosphorylating and activating phosphatidylinositol-4 kinase IIIbeta at the Golgi complex. Nat Cell Biol *7*, 880-886.

Haworth, R. S., and Avkiran, M. (2001). Inhibition of protein kinase D by resveratrol. Biochem Pharmacol *62*, 1647-1651.

Hayashi, K., Ohshima, T., Hashimoto, M., and Mikoshiba, K. (2007). Pak1 regulates dendritic branching and spine formation. Dev Neurobiol *67*, 655-669.

Horton, A. C., and Ehlers, M. D. (2003). Dual modes of endoplasmic reticulum-to-Golgi transport in dendrites revealed by live-cell imaging. J Neurosci *23*, 6188-6199.

Horton, A. C., and Ehlers, M. D. (2004). Secretory trafficking in neuronal dendrites. Nat Cell Biol *6*, 585-591.

Horton, A. C., Racz, B., Monson, E. E., Lin, A. L., Weinberg, R. J., and Ehlers, M. D. (2005). Polarized secretory trafficking directs cargo for asymmetric dendrite growth and morphogenesis. Neuron *48*, 757-771.

Johannes, F. J., Horn, J., Link, G., Haas, E., Siemienski, K., Wajant, H., and Pfizenmaier, K. (1998). Protein kinase Cmu downregulation of tumor-necrosis-factor-induced apoptosis correlates with enhanced expression of nuclear-factor-kappaB-dependent protective genes. Eur J Biochem *257*, 47-54.

Kim, Y., Sung, J. Y., Ceglia, I., Lee, K. W., Ahn, J. H., Halford, J. M., Kim, A. M., Kwak, S. P., Park, J. B., Ho Ryu, S.*, et al.* (2006) . Phosphorylation of WAVE1 regulates actin polymerization and dendritic spine morphology. Nature *442*, 814-817.

Lein, P. J., Guo, X., Shi, G. X., Moholt-Siebert, M., Bruun, D., and Andres, D. A. (2007). The novel GTPase Rit differentially regulates axonal and dendritic growth. J Neurosci *27*, 4725-4736.

Liljedahl, M., Maeda, Y., Colanzi, A., Ayala, I., Van Lint, J., and Malhotra, V. (2001). Protein kinase D regulates the fission of cell surface destined transport carriers from the trans-Golgi network. Cell *104*, 409-420.

Maeda, Y., Beznoussenko, G. V., Van Lint, J., Mironov, A. A., and Malhotra, V. (2001). Recruitment of protein kinase D to the trans-Golgi network via the first cysteine-rich domain. Embo J *20*, 5982-5990.

Matthews, S., Iglesias, T., Cantrell, D., and Rozengurt, E. (1999a). Dynamic re-distribution of protein kinase D (PKD) as revealed by a GFP-PKD fusion protein: dissociation from PKD activation. FEBS Lett *457*, 515-521.

Matthews, S. A., Rozengurt, E., and Cantrell, D. (1999b). Characterization of serine 916 as an in vivo autophosphorylation site for protein kinase D/Protein kinase Cmu. J Biol Chem *274*, 26543-26549.

Michalon, A., Koshibu, K., Baumgartel, K., Spirig, D. H., and Mansuy, I. M. (2005). Inducible and neuron-specific gene expression in the adult mouse brain with the rtTA2S-M2 system. Genesis *43*, 205-212.

Nagy, A. (2003). Manipulating the mouse embryo : a laboratory manual, 3rd edn (Cold Spring Harbor, N.Y.: Cold Spring Harbor Laboratory Press).

Nakamura, N., Rabouille, C., Watson, R., Nilsson, T., Hui, N., Slusarewicz, P., Kreis, T. E., and Warren, G. (1995). Characterization of a cis-Golgi matrix protein, GM130. J Cell Biol *131*, 1715-1726.

Nishikawa, K., Toker, A., Johannes, F. J., Songyang, Z., and Cantley, L. C. (1997). Determination of the specific substrate sequence motifs of protein kinase C isozymes. J Biol Chem *272*, 952-960.

Oster, H., Abraham, D., and Leitges, M. (2006). Expression of the protein kinase D (PKD) family during mouse embryogenesis. Gene Expr Patterns *6*, 400-408.

Pierce, J. P., Mayer, T., and McCarthy, J. B. (2001). Evidence for a satellite secretory pathway in neuronal dendritic spines. Curr Biol *11*, 351-355.

Prigozhina, N. L., and Waterman-Storer, C. M. (2004). Protein kinase D-mediated anterograde membrane trafficking is required for fibroblast motility. Curr Biol *14*, 88-98.

Qiang, Y. W., Yao, L., Tosato, G., and Rudikoff, S. (2004). Insulin-like growth factor I induces migration and invasion of human multiple myeloma cells. Blood *103*, 301-308.

Rey, O., Reeve, J. R., Jr., Zhukova, E., Sinnett-Smith, J., and Rozengurt, E. (2004). G protein-coupled receptor-mediated phosphorylation of the activation loop of protein kinase D: de-pendence on plasma membrane translocation and protein kinase Cepsilon. J Biol Chem *279*, 34361-34372.

Rosner, H., and Vacun, G. (1999). 1,2-dioctanoyl-s,n-glycerol-induced activation of protein kinase C results in striking, but reversible growth cone shape changes and an accumulation of f-actin and serine 41-phosphorylated GAP-43 in the axonal process. Eur J Cell Biol *78*, 698-706.

Rykx, A., De Kimpe, L., Mikhalap, S., Vantus, T., Seufferlein, T., Vandenheede, J. R., and Van Lint, J. (2003). Protein kinase D: a family affair. FEBS Lett *546*, 81-86.

Schmidt, J. T., Fleming, M. R., and Leu, B. (2004). Presynaptic protein kinase C controls maturation and branch dynamics of developing retinotectal arbors: possible role in activity-driven sharpening. J Neurobiol *58*, 328-340.

Sheng, M. (2001). Molecular organization of the postsynaptic specialization. Proc Natl Acad Sci U S A *98*, 7058-7061.

Silverman, M. A., Kaech, S., Jareb, M., Burack, M. A., Vogt, L., Sonderegger, P., and Banker, G. (2001) . Sorting and directed transport of membrane proteins during development of hippocampal neurons in culture. Proc Natl Acad Sci U S A *98*, 7051-7057.

Steegmaier, M., Klumperman, J., Foletti, D. L., Yoo, J. S., and Scheller, R. H. (1999). Vesicle-associated membrane protein 4 is implicated in trans-Golgi network vesicle trafficking. Mol Biol Cell *10*, 1957-1972.

Sytnyk, V., Leshchyns'ka, I., Delling, M., Dityateva, G., Dityatev, A., and Schachner, M. (2002). Neural cell adhesion molecule promotes accumulation of TGN organelles at sites of neuron-to-neuron contacts. J Cell Biol *159*, 649-661.

Tada, T., Simonetta, A., Batterton, M., Kinoshita, M., Edbauer, D., and Sheng, M. (2007). Role of Septin cytoskeleton in spine morphogenesis and dendrite development in neurons. Curr Biol *17*, 1752-1758.

Takamine, K., Okamoto, K., Fujita, Y., Sakurai, A., Takatama, M., and Gonatas, N. K. (2000). The involvement of the neuronal Golgi apparatus and trans-Golgi network in the human olivary hypertrophy. J Neurol Sci *182*, 45-50.

Takemoto -Kimura, S., Ageta-Ishihara, N., Nonaka, M., Adachi-Morishima, A., Mano, T., Okamura, M., Fujii, H., Fuse, T., Hoshino, M., Suzuki, S.*, et al.* (2007). Regulation of dendritogenesis via a lipid-raft-associated Ca2+/calmodulin-dependent protein kinase CLICK-III/CaMKIgamma. Neuron *54*, 755-770.

Tang, B. L. (2008). Emerging aspects of membrane traffic in neuronal dendrite growth. Biochim Biophys Acta *1783*, 169-176.

Taya, S., Shinoda, T., Tsuboi, D., Asaki, J., Nagai, K., Hikita, T., Kuroda, S., Kuroda, K., Shimizu, M., Hirotsune, S.*, et al.* (2007). DISC1 regulates the transport of the NUDEL/LIS1/14-3-3epsilon complex through kinesin-1. J Neurosci *27*, 15-26.

Tran, T. H., Zeng, Q., and Hong, W. (2007). VAMP4 cycles from the cell surface to the trans-Golgi network via sorting and recycling endosomes. J Cell Sci *120*, 1028-1041.

Uetani, N., Chagnon, M. J., Kennedy, T. E., Iwakura, Y., and Tremblay, M. L. (2006). Mammalian motoneuron axon targeting requires receptor protein tyrosine phosphatases sigma and delta. J Neurosci *26*, 5872-5880.

Van Lint, J., Rykx, A., Maeda, Y., Vantus, T., Sturany, S., Malhotra, V., Vandenheede, J. R., and Seufferlein, T. (2002). Protein kinase D: an intracellular traffic regulator on the move. Trends Cell Biol *12*, 193-200.

Vertommen, D., Rider, M., Ni, Y., Waelkens, E., Merlevede, W., Vandenheede, J. R., and Van Lint, J. (2000). Regulation of protein kinase D by multisite phosphorylation. Identification of phosphorylation sites by mass spectrometry and characterization by site-directed mutagenesis. J Biol Chem *275*, 19567-19576.

Waldron, R. T., Rey, O., Iglesias, T., Tugal, T., Cantrell, D., and Rozengurt, E. (2001). Activation loop Ser744 and Ser748 in protein kinase D are transphosphorylated in vivo. J Biol Chem *276*, 32606-32615.

Wang, Q., and Wadsworth, W. G. (2002). The C domain of netrin UNC-6 silences calcium/calmodulin-dependent protein kinase- and diacylglycerol-dependent axon branching in Caenorhabditis elegans. J Neurosci *22*, 2274-2282.

Wang, Q. J. (2006). PKD at the crossroads of DAG and PKC signaling. Trends Pharmacol Sci *27*, 317-323.

Winckler, B., and Mellman, I. (1999). Neuronal polarity: controlling the sorting and diffusion of membrane components. Neuron *23*, 637-640.

Yang, W., and Storrie, B. (1998). Scattered Golgi elements during microtubule disruption are initially enriched in trans-Golgi proteins. Mol Biol Cell *9*, 191-207.

Ye, B., Zhang, Y., Song, W., Younger, S. H., Jan, L. Y., and Jan, Y. N. (2007). Growing dendrites and axons differ in their reliance on the secretory pathway. Cell *130*, 717-729.

Yeaman, C., Ayala, M. I., Wright, J. R., Bard, F., Bossard, C., Ang, A., Maeda, Y., Seufferlein, T., Mellman, I., Nelson, W. J., and Malhotra, V. (2004). Protein kinase D regulates basolateral membrane protein exit from trans-Golgi network. Nat Cell Biol *6*, 106-112.

Yin, D. M., Huang, Y. H., Zhu, Y. B., and Wang, Y. (2008). Both the establishment and maintenance of neuronal polarity require the activity of protein kinase D in the Golgi apparatus. J Neurosci *28*, 8832-8843.

Zhang, H., and Macara, I. G. (2008). The PAR-6 polarity protein regulates dendritic spine morphogenesis through p190 RhoGAP and the Rho GTPase. Dev Cell *14*, 216-226.

Zugaza, J. L., Sinnett-Smith, J., Van Lint, J., and Rozengurt, E. (1996). Protein kinase D (PKD) activation in intact cells through a protein kinase C-dependent signal transduction pathway. Embo J *15*, 6220-6230.

Supplement

Generation and characterization of transgenic mice

INDEX

Transgenic animal technologies

All animal handling and experiments carried out in this study were approved by the Regierungspräsidium Stuttgart and complied with local guidelines and regulations for the use of experimental animals (35-9185.81/0209 and 35-9185.81/0247).

Genetic manipulation of mouse embryos

Choice of genetic background

Due to the poor reproductive performance of mice from inbred strains, outbred mice of the strain CD1 were used for the production of zygotes, the generation of transgenic mice, and their subsequent breedings. For vasectomy, male mice with a good plugging performance of the outbred strain NMRI were selected.

Preparation of glass capillaries for microinjection

Consumables:	Borosilicate Glass Capillaries TW120F-3 outer diameter 1.5 mm / inner diameter 1.12 mm / length 76 mm (World Precision Instruments Inc., FL, USA, http://www.wpiinc.com)
Devices:	Flaming/Brown Micropipette Puller P-87 (Sutter Instruments Inc, CA, USA)

Injection capillaries were prepared from borosilicate glass tubes with filament. The production was performed with a micropipette puller and the following settings:

Program 7	HEAT	PULL	VELOCITY	TIME	PRESSURE
1	710	-	30	200	500
2	650	40	40	150	500

Isolation and Purification of DNA for Microinjection

Kits:	QIAEX® II Gel Extraction Kit (Qiagen, Hilden) NucleoBond PC 500 (Macherey-Nagel, Düren)
reagents:	Agarose Ultra Pure (Invitrogen, Karlsruhe) Ethanol (Carl Roth GmbH + Co. KG, Karlsruhe) Isopropyl alcohol (Carl Roth GmbH + Co. KG, Karlsruhe) Potassium acetate (Carl Roth GmbH + Co. KG, Karlsruhe)
media	LB-Amp (10 g/l tryptone, 5 g/l yeast extrakt, 10 g/l NaCl, pH 7.2, 100 µg/ml ampicillin)
Plasmids or bacterial stocks:	pBI-5-PKD1kd-EGFP (plasmid #E369 or glycerin stock #748) pBI-5-PKD2kd-EGFP (plasmid #E370 or glycerin stock #746) pBI-5-PKD1kd-EGFP (plasmid #E371 or glycerin stock #825)
Enzymes:	AseI (New England BioLabs, Frankfurt) BsiWI (Fermentas, St. Leon-Rot) BsrBI (Fermentas, St. Leon-Rot) NarI (New England BioLabs, Frankfurt)
Buffers:	TAE 50x (2 M Tris, 1 M acetic acid, 50 mM EDTA, pH 8) microinjection buffer (5mM Tris pH 7.4, 0.1 mM EDTA, sterile filtered)

The purity of the DNA preparation is a very crucial factor affecting the successful outcome of pronuclear microinjections (Nagy, 2003). The slightest traces of contaminants as bacterial endotoxins, ethidiumbromide, agarose, solvents, or salts can harm the zygotes and lead to lysis.

The plasmid-containing bacteria were cultured over night in LB-Amp and harvested by centrifugation at 6000 x *g* and 4° C for 15 min. Plasmid DNA was purified using a NucleoBond Maxiprep Kit according to the manufacturer's instructions. As it is recommended to separate the transgenic construct from the vector sequences, 50 µg of isolated plasmid DNA from each constructs were consecutively digested in a total volume of 500 µl with 40 units of appropriate restriction enzymes (Supplementary Figure 1A) to release the transgenic sequences from prokaryotic sequences. Digestion was performed overnight at 37° C. Residual enzyme was inactivated by heat treatment (20 min, 65° C). In between the single restriction enzyme digestion steps DNA was precipitated by addition of salt and isopropyl alcohol (0.1 Vol 5 M Potassium acetate and 0.7 Vol isopropyl alcohol), sedimented by centrifugation (15 min, 16000 x *g*) and washed once with 70% ethanol. A small aliquot of each digest was controlled on an ethidium bromide stained agarose gel to verify complete digestion and DNA integrity. Finally, the digested plasmid DNAs were separated on a preparative 0.7% agarose gel in TAE by electrophoresis.

To avoid contaminations of ethidium bromide in the purified DNA, only a part of the gel containing a DNA ladder and an aliquot of the restriction enzyme digest as marker was stained with ethidium bromide. According to that, the fragment corresponding to the transgenic construct was excised from the agarose gel with a clean scalpel. The exposure of the plasmid DNA to UV light was kept as short as possible to avoid UV induced DNA damage. For recovery of the DNA from the agarose gel the QIAEX® II Gel Extraction Kit was used according to the manufacturer's protocol. Finally the eluted DNA was twice precipitated with salt and isopropyl alcohol (see above) and solved in microinjection buffer. DNA concentration was determined photometrically and integrity of DNA was reconfirmed by agarose gel electrophoresis.

The purified DNA was diluted to a final concentration of 50 ng/µl in prefiltered microinjection buffer and stored as stock at -20°C. For microinjection the stock was further diluted to a final concentration of 2 ng/µl in microinjection buffer and stored in 100 µl aliquots at -20°C. For each microinjection session one aliquot was thawed, clarified by centrifugation at 16000 x *g* and 4° C for 15 min and the supernatant was used for microinjection.

Superovulation of female mice

Mice:	prepubescent female mice (CD1, 4-5 weeks, own breeding) fertile stud male mice (CD1, >8 weeks, own breeding)
Hormones:	pregnant mare serum gonadotropin (Intervet GmbH, Unterschleißheim) human chorionic gonadotropin (Intervet GmbH, Unterschleißheim)
Consumables:	1ml syringes Omnifix-F (B.Braun, Melsungen) 26- gauge needles Sterican (B.Braun, Melsungen)

Immature (4-5 weeks old) female CD1 mice were kept on a 13:11 light-dark cycle (light period 3:00-16:00, dark period 16:00-3:00) and were primed by hormonal tratment. 5 IU PMSG were injected intraperitoneally (i.p.) to stimulate the development of the ovarian follicle in the females. 46.5 hours after PMSG stimulation each female was injected with 5 IU hCG to induce ovulation and placed in a cage with one CD1 stud male. The next morning the females were checked for a copulation plug and plug positive females were used to recover zygote stage mouse embryos.

Recovery of zygote stage embryos

Media:	M2 medium, mouse embryo tested (Sigma-Aldrich, Deisenhofen) M16 medium, mouse embryo tested (Sigma-Aldrich, Deisenhofen)
Reagents:	Ethanol (Carl Roth GmbH + Co. KG, Karlsruhe) mineral oil, embryo tested (Sigma-Aldrich, Deisenhofen)
Consumables:	35-mm Petri dishes (Greiner bio-one, Frickenhausen)
Equipment:	Fine forceps INOX #7 (Dumont&Fils, Switzerland)
Enzymes:	Hyaluronidase (Sigma-Aldrich, Deisenhofen)
Devices:	Stereomicroscope Highlight 3000 (Olympus, Hamburg)

To handle mouse embryos a mouth pipette device was used, consisting of an aspirator mouthpiece, latex tubings and a glass capillary pulled on a flame to create an appropriate opening.

Mice were humanely sacrificed by carbon dioxide asphyxiation, placed on their back and the fur was soaked thoroughly in 70% ethanol. A lateral skin incision was performed at the midline and by pulling the skin towards the head and the tail the abdomen was completely exposed. The peritoneum was opened and the alimentary tract was displaced to unveil the reproductive organs in the abdominal cavity. The oviduct was dissected by separating the uterus from the mesometrium and cutting between the oviduct and the uterus. The isolated oviducts and attached segments of uterus from several mice were collected in a 35-mm petri dish containing M2 medium. Under a stereomicroscope the zygotes surrounded by cumulus cells can be visualized in the swollen upper part of the oviduct, the ampulla. By tearing the ampulla with fine forceps the clutch of cumulus cells and zygotes was released. The zygotes with the surrounding cumulus cells were transferred to a fresh petri dish with M2 medium and 0.1% hyaluronidase and left there for a few minutes until the cumulus cells were fallen

apart. After release, the zygotes were immediately picked up and rinsed in a fresh petri dish with M2 medium. After that zygotes were equilibrated in M16 medium and transferred to a microdrop culture (small drops of M16 medium on the bottom of a plastic dish flooded with mineral oil to cover the drops and to avoid evaporation) and incubated at 37° C and 5% CO_2.

Microinjection of Zygotes

Media:	M2 medium, mouse embryo tested (Sigma-Aldrich, Deisenhofen)
Reagents:	mineral oil, embryo tested (Sigma-Aldrich, Deisenhofen) silicone oil (Sigma-Aldrich, Deisenhofen)
Consumables:	Glass slides (Carl Roth GmbH + Co. KG, Karlsruhe) Plasticine Glass holding pipette as per Zimmermann (BioMedical Instruments, Zöllnitz) Microloader (Eppendorf, Hamburg)
Devices:	Microscope Axiovert 200 (Carl Zeiss AG, Oberkochen) Micromanipulator (holding pipette) 471845-9901 (Carl Zeiss AG, Oberkochen) Micromanipulator (injection pipette) TransferMan NK (Eppendorf, Hamburg) Pressure controller (holding pipette) CellTram vario (Eppendorf, Hamburg) Microinjector FemtoJet (Eppendorf, Hamburg)

A microinjection chamber was prepared by fixing a circular plasticine wall on a glass slide, placing a drop of M2 medium in the center which was covered with mineral oil. The chamber was placed on the microscope stage. The holding pipette was filled with silicone oil and assembled into the left-hand-side micromanipulator. Carefully, the pipette was lowered into the medium drop until it started to slide forward on the bottom of the chamber.

The microinjection pipette was loaded with the DNA solution (in a final concentration of 2 ng/µl) through the wide back end with a Microloader and assembled into the handle of the right-hand-side micromanipulator. The microinjector settings (compensation pressure) were modified in a way to produce a slow constant flow of DNA through the tip of the pipette. The injection pipette was inserted into the microinjection drop and adjusted to face the holding pipette in an 180° angle.

With the help of the embryo transfer pipette a group of fertilized oozytes was placed in the microinjection chamber. The zygotes were examined under high magnification to make sure that two pronuclei are visible and that the morphology is good. By applying a negative pressure to the holding pipette the zygotes were slightly pulled into the opening via the zona pellucida and thereby fixed for microinjection. The pronucleus to be injected was refocused and the tip of the injection pipette was brought into the same focal plane. Finally, the injection pipette was pushed through the zona pellucida and the cytoplasm into the pronucleus. The swelling of the pronucleus was controlled via the microscope to prove successful microinjection. After that, the injection needle was pulled quickly out of the zygote and sorted into the group of injected zygotes. Zygotes that started to lyse after injection were shed separately.

The procedure was repeated for all zygotes of one group before the healthy zygotes were moved back into the microdrop culture and incubated at 37° C and 5% CO_2.

Surgical procedures

Anaesthetics:	Pentobarbital sodium salt (Sigma-Aldrich, Deisenhofen) Xyloneural forte 2% (Pharma Stroschein, Hamburg) Neocain solution 5% (WDT e.G., Garbsen)
Consumables:	1ml syringes Omnifix-F (B.Braun, Melsungen) 26-gauge needles Sterican (B.Braun, Melsungen)
Medicines:	Thilo tears ophthalmic ointment (Alcon Pharma, Freiburg)
Devices:	Infrared light source (Philips, Hamburg)

For surgical procedures (vasectomy and oviduct transfer) mice were weighted and anaesthetized by intraperitoneal pentobarbital injection in a dose of 100 mg/kg body weight.
To provide a prolonged intraoperative anesthesia and extended analgesia the site of skin incision was furthermore treated with local anaesthetics.
To prevent corneal drying during anesthesia the eyes of the mice were moistened with ophthalmic ointment.
The anaesthetized mice were placed on an isolated pad covered with paper towels to avoid decreasing body temperatures of the animals during surgery.
After surgery mice were placed in a clean cage and kept warm with infrared light and observed until recovery.

Vasectomy for generation of sterile males

mice	fertile stud male mice (NMRI, own breeding)
Reagents:	Ethanol (Carl Roth GmbH + Co. KG, Karlsruhe)
Equipment:	Fine forceps INOX #7 (Dumont&Fils, Switzerland) Micro-dissecting scissors (Sigma-Aldrich, Deisenhofen)
Consumables:	Absorbable surgical silk suture Dexon II (Davis & Geck, Danbury, CT, USA) Non-resorbable surgical silk suture Supramid (B.Braun, Melsungen)
Devices:	Small vessel cauterizer set #18000-00 (Fine Science Tools, Heidelberg)

For the generation of vasectomized males experienced NMRI stud males with optimal breeding performance were selected.
The mouse was anaesthetized and placed on its back. The abdomen was shaved in the area of skin incision and wiped with 70% ethanol. With fine dissection scissors the skin was transversally cut at a position in line with the top of the legs followed by a transverse incision in the body wall. On one side of the incision a stitch through the body wall was performed using a curved surgical needle and thereby leaving a piece of silk suture in place. By pulling out the testicular fat pad the associated testis and the vas deferens was exposed. One loop of the vas deferens was kept with forceps and was removed with a red-hot cauterizer. The proce-

dure was repeated with the vas deferens of the other testis before both testis were carefully placed back inside the body cavity. Finally, the body wall was sewn with three to four stitches of a resorbable silk suture and the skin was stitched with non-resorbable surgical silk.
One week after vasectomy the males were mated to fertile females to test the sterility.

Transfer of microinjected zygotes into the oviduct of foster mothers

mice	mature female mice (CD1, 6-12 weeks, own breeding) sterile stud male mice (NMRI, own breeding and vasectomy)
Equipment:	Fine spring scissors #15100-09 (Fine Science Tools, Heidelberg) Serrefine clamp (Fine Science Tools, Heidelberg) Fine forceps INOX #7 (Dumont&Fils, Switzerland) Micro-dissecting scissors (Sigma-Aldrich, Deisenhofen)
Reagents:	Ethanol p.a. (Carl Roth GmbH + Co. KG, Karlsruhe) Epinephrine (Sigma-Aldrich, Deisenhofen)
Consumables:	Absorbable surgical silk suture Dexon II (Davis & Geck, Danbury, CT, USA) Non-resorbable surgical silk suture Supramid (B.Braun, Melsungen)
Devices:	Stereomicroscope Highlight 3000 (Olympus, Hamburg)

Pseudopregnant recipient mice at 0.5 dpc were generated by mating CD1 females in natural estrus to vasectomized stud males on the day before microinjection and transfer. Successful matings were assessed by the detection of a vaginal plug on the next morning.
The designated foster mother was anaesthetized and placed prone on a paper towel with the mouses´ head to the left. The back was shaved in the area of skin incision and wiped with 70% ethanol-soaked tissue to remove any loose hairs.
A single cut was made in the skin at a level with the point where the hindleg meets the abdomen. The peritoneal cavity was opened by a second cut through the body wall and marked with a piece of surgical silk suture. By pulling at the ovarian fat pad the attached ovary, the oviduct and the uterine horn were lifted out and laid over the mouse´s back on a small piece of tissue. A Serrefine clamp was attached to the fat pad above the ovary, keeping the oviduct and ovary outside the body cavity. After that, the mouse was gently moved onto the stage of the stereomicroscope. To reduce subsequent bleeding a drop of epinephrine was placed on the bursa, the thin transparent membrane surrounding the ovary and the oviduct. Thereafter, the bursa was carefully cut with fine spring scissors, avoiding damage of large blood vessels. In the meanwhile, the embryos were transferred from the microdrop culture into M2 medium and loaded into a transfer pipette in a minimum possible volume.
Under the dissecting microscope the end of the oviduct (infundibulum) was located and the edge of the opening was held very gently with fine forceps. The tip of the transfer pipette with embryos was inserted into the infundibulum and the embryos were blown in the ampulla. An air bubble visible in the oviduct indicated successful transfer.

At the end of the procedure, the Serrefine clamp was unclipped and the fat pad, ovary, and oviduct were carefully placed back into the body cavity. Finally, the body wall was sewn with three to four stitches of a resorbable silk suture and the skin was stitched with non-resorbable surgical silk.

Caesarean section and cross fostering

Equipment:	Fine forceps INOX #7 (Dumont&Fils, Switzerland) Micro-dissecting scissors (Sigma-Aldrich, Deisenhofen)
Reagents:	Ethanol (Carl Roth GmbH + Co. KG, Karlsruhe)
Devices:	Infrared light source (Philips, Hamburg)

Caesarean section was required when a pregnant mouse has not given birth by the calculated delivery time. This occurred e.g. when only few embryos were present and they have grown too big to be born naturally.

First of all, it had to be made sure that a suitable foster mother was available. An ideal foster mother is a female mouse, which has successfully nurtured one or more litters of her own an has given birth on the same day or on one of the previous days.

The pregnant female was sacrificed by cervical dislocation, placed on her back and the fur was soaked thoroughly in 70% ethanol. The abdomen was quickly opened and the uterus was dissected out. The uterine wall and the embryonic membranes were carefully cut to expose the pups. The pups were gently pinched to stimulate breathing and warmed under an infrared lamp.

In the meanwhile the foster mother was removed from the cage and the size of her original litter was reduced. The foster pups were mixed with the remaining pups and with dirty bedding material from the foster mothers´ cage. While keeping the pups warm the foster mother was given back to the original cage.

Mouse labeling and collection of biopsies for genotyping

Reagents:	Ethanol (Carl Roth GmbH + Co. KG, Karlsruhe)
Consumables:	1.5 ml microcentrifuge tubes (Eppendorf, Hamburg)
Devices:	Ear punch pliers (Fine Science Tools, Heidelberg) Tail cauterizer Engel Type Kausto-Lux (Meyer + Kersting, Ettlingen)

The analysis of the DNA from individual mice is necessary for the identification of genetically manipulated mice. Mouse labeling and collection of biopsies for genotyping were carried out simultaneously. For marking the mouse was gripped by the scruff of the neck and was restrained so that the ears are easily accessible. With the help of ear punch pliers a margin was placed in the pinna at the desired location. To sanitize, the punch was thoroughly cleaned

with alcohol between the labeling of single animals. Mouse number and position of the ear-mark were recorded on the cage chart.

To obtain mouse tissue for genotyping the tail biopsy procedure was used. The tail tissue near the tip of the tail of a young mouse is still soft and the bones have not completely mineralized. Therefore the ablation of the tail tip of a young mouse is judged to cause only temporary pain for the animal. The mouse was restrained in a plastic tube and a cross-sectional cut was performed perpendicular to the long axis of the tail to minimize the surface area of traumatized tissue. To avoid bleeding problems a red-hot cauterizer was used to clip less than 5 mm of the tail tip. With clean forceps the biopsy was transferred to a labeled reaction tube.

Detection of transgenic sequences by genomic Southern hybridization

Isolation of high-molecular-weight genomic DNA from mouse tails

Reagents:	Proteinase K (Peqlab, Erlangen) Isopropyl alcohol (Carl Roth GmbH + Co. KG, Karlsruhe) Ethanol p.a. (Carl Roth GmbH + Co. KG, Karlsruhe)
Buffers and Solutions:	Tail buffer (100 mM NaCl, 50 mM Tris pH 8.0, 100 mM EDTA, 1% SDS) Saturated NaCl (>6 M NaCl) TE buffer (10 mM Tris pH 7.5, 1 mM EDTA)
Devices:	BioPhotometer (Eppendorf, Hamburg) Thermomixer (Eppendorf, Hamburg)

The tail biopsy (~0.5 cm) was placed in a tube containing 750 µl tail buffer. Proteinase K was added to a final concentration of 0.5 mg/ml. For complete lysis the samples were incubated over night at 56° C in the thermomixer. To precipitate protein, 250 µl saturated NaCl were added and the tubes were vigorously mixed for 5 min. After centrifugation for 10 min at 13000 rpm 750 µl of the cleared supernatant were transferred into a fresh tube containing 500 ml isopropyl alcohol. Samples were mixed carefully by inverting the tubes and precipitated DNA was pelleted by centrifugation (10 min at 13000 rpm) and washed with 500 µl of 70% ethanol. After an additional centrifugation step (5 min at 13000 rpm) the pellet of genomic DNA was briefly dried and dissolved in 200 µl TE buffer by gentle shaking at 42° C for one hour.

Genomic DNA concentrations were determined by measuring the absorbance at 260 nm.

Restriction enzyme digestion of genomic DNA

Enzymes:	BamHI, EcoRI, HindIII and restriction enzyme buffers (Fermentas, St. Leon-Rot)
Reagents:	Agarose Ultra Pure (Invitrogen, Karlsruhe)
Buffers:	10x TBE (1.337 M Tris, 445 mM boric acid, 25 mM EDTA)
Devices	Gel documentation system (Biostep, Jahnsdorf)

10-15 µg of genomic DNA were digested over night with 40 U of the appropriate restriction endonuclease at the required temperature in a final volume of 60 µl containing a final concentration of 1x of an appropriate restriction enzyme buffer. 2 µl of each reaction were analyzed on an analytical agarose gel to check for complete digestion of the genomic DNA.

Southern blot

Reagents:	Agarose Ultra Pure (Invitrogen, Karlsruhe)
Buffers and Solutions:	TAE 50x (2 M Tris, 1 M acetic acid, 50 mM EDTA, pH 8) acid depurination solution (0.25 M HCl in ddH_2O) denaturation solution (1.5 M NaCl, 0.5 M NaOH) neutralization buffer (0.5 M Tris, 1.5 M NaCl, pH 7.5) transfer buffer 20x SSC (3 M NaCl, 0.3 M Sodium citrate, pH 7.5)
Consumables:	Nylon membrane Hybond-N (GE Healthcare Bio-Sciences) Blotting Paper (Whatman International)

Samples were mixed with 12 µl DNA gel loading buffer and applied into the wells of 0.6-0.7% agarose, 0.2 µg/ml ethidium bromide, TAE Southern gels. Genomic DNA fragments were separated at 5 V/cm for several hours and visualized under UV illumination. In order to facilitate the transfer of larger DNA fragments Southern gels were further processed by acidic depurination for 15 min, followed by incubation in denaturation solution for 30 min and neutralization for 30 min. After equilibration in 10x SSC for 10min the DNA fragments were transferred onto a Nylon membrane by capillary blotting (Southern, 1975). Blotting was performed over night with 10x SSC as transfer buffer. After disassembling of the blot the membranes were dried and baked for 2 hours at 80° C to fix the DNA to the membrane.

Probe synthesis and labeling

Kits:	Rediprime II Random Prime Labelling System (GE Healthcare, München) PCR DIG probe synthesis kit (Roche Applied Science, Mannheim)	
Reagents:	[α-^{32}P] dCTP (GE Healthcare, München)	
Primer:	EGFP for	(#583) 5'- TAA ACG GCC ACA AGT TCA GCG TGT C -3'
	EGFP rev	(#584) 5'- CTT CTC GTT GGG GTC TTT GCT CAG G -3'
Consumables:	ProbeQuant G-50 Micro Columns (GE Healthcare, München)	
Devices:	Scintillation Analyzer 1600 TR (Packard Instrument Company, Meriden, CT, USA)	

For radioactively labelled hybridization probes, a specific sequence was amplified via PCR and purified with gel extraction. The labelling was performed with the Rediprime II Random Prime Labelling System and [α-^{32}P] dCTP according to the manufacturer's protocol. Probes were purified from unincorporated labelled nucleotides with ProbeQuant G-50 Micro Columns. The cpm/µl of the labelled probes was determined by measuring the Cerenkov radiation in a scintillation counter.

In an alternative, non-radioactive approach, DIG-labelled probes were produced with a PCR DIG Probe Synthesis Kit.

Southern hybridization

Buffers and Solutions:	Church Buffer (250 mM Na phosphate buffer pH 7.2, 1 mM EDTA, 7% SDS, 1% BSA) Low stringency washing solution (2x SSC, 0.1% SDS) Medium stringency washing solution (0.5x SSC, 0.1% SDS)
Devices:	Hybridization oven (GE Healthcare, München) Geiger Counter (Berthold Technologies, Bad Wildbad)

Southern membranes were rolled along their length, placed in glass hybridization tubes and prehybridized with 15 ml Church buffer per tube for at least 1 hour at 65° C. For use in hybridization the labelled probes were denatured by heating to 95° C for 5min and snap cooling on ice. After that, an appropriate volume of the labelled probe was added into the hybridization tubes containing membrane and Church buffer resulting in a final activity of $0.5\text{-}2.0 \cdot 10^6$ cpm per ml of the hybridization solution. Hybridization was carried out over night at 65° C under constant rolling of the tubes.

Membranes were washed two times with 50ml of low stringency washing solution and two times with 50 ml of high stringency washing solution, 30 min each. The washing steps were carried out at 60° C under constant rolling with preheated washing solutions.

Southern detection

Reagents:	Blocking Reagent (Roche Applied Science, Mannheim) CDP Star (Roche Applied Science, Mannheim) Tween 20 (Carl Roth GmbH + Co. KG, Karlsruhe)
Antibodies:	Anti-DIG-AP conjugate, Fab fragments (Roche Applied Science, Mannheim)
Buffers and Solutions:	MN buffer (100 mM maleic acid, 150 mM NaCl, pH 7.5) AP detection buffer (100 mM Tris, 100 mM NaCl, pH 9.5)
Devices:	Phosphoreader Storm 860 (Molecular Dynamics, Krefeld) Film processor X-OMAT 1000 (Kodak, Stuttgart)
Software:	Image Quant (Molecular Dynamics, Krefeld)

For radioactively labelled Southern blots the membranes were wrapped in plastic, exposed to Phosphoscreens and analyzed by quantitative phosphoimage analysis.

For DIG-labelled probes membranes were equilibrated for 10 min in MN buffer, blocked in 1x Roche blocking in MN buffer and incubated for 1 hour with an anti-DIG-AP Fab fragment 1:2500 in blocking solution. After washing two times for 15 min in MN buffer with 0.3% Tween 20 for 15 min the membrane was equilibrated for 5 min in AP detection buffer and finally incubated for 5 min with the ultra-sensitive and fast chemiluminescent substrate for alkaline phosphatase CDP-Star 1:100 in AP detection buffer. The membrane was wrapped in plastic and exposed to X-ray films that were developed by an X-OMAT 1000 film processor.

Detection of transgenic sequences by genomic PCR amplification

Preparation of lysates for PCR genotyping

Reagents:	Proteinase K (Peqlab, Erlangen)
Buffers and Solutions:	Tail lysis buffer (10 mM Tris pH 8.5, 5 mM EDTA, 0.3 M Na acetate, 1% Triton X-100) 10 mM Tris pH 8.0
Devices:	Thermomixer (Eppendorf, Hamburg)

To extract genomic DNA for PCR genotyping, small tissue samples (e.g. tail tips from adult mice, tails or limbs from mouse embryos) were taken and incubated with 100 µl tail lysis buffer containing 0.5 mg/ml Proteinase K for several hours in a thermomixer at 65° C (for embryonic tissue) or over night at 56° C (for adult tissue). Samples were briefly centrifuged to spin down large debris. Genomic DNA from the lysates was diluted by mixing 5µl of each lysate with 95 µl of 10 mM Tris pH 8.0 and heat inactivated at 95° C for 10 min. Samples were stored at 4° C until used in PCR. A volume of 2µl of the diluted lysates was used for a 20 µl PCR reaction.

PCR amplification of transgene specific sequences

Reagents:	100 mM dNTP Set (Invitrogen, Karlsruhe) Agarose Ultra Pure (Invitrogen, Karlsruhe) Ethidium bromide (Sigma-Aldrich, Deisenhofen)
Enzymes:	Taq DNA polymerase (5 Prime GmbH, Hamburg)
Buffers and Solutions:	10x self-adjusting Mg^{2+} Taq buffer advanced (5 Prime GmbH, Hamburg) 25 mM $MgCl_2$ TBE 10x (90 mM Tris, 89 mM Boric acid, 20 mM EDTA, pH8.9)
Consumables:	PCR softstrips and capstrips (Biozym, Hess. Oldendorf)
Devices:	Mastercycler gradient (Eppendorf, Hamburg) Robocycler (Stratagene)

For genotyping of CMV/β-actin rtTA- and CMV rtTA-transgenic mice a multiplex touchdown PCR protocol was used as follows:

multiplex reaction mix	final conc.	touchdown PCR program		
2 µl 10x taq buffer	1x	Eppendorf Mastercycler (gradient)		
0.8 µl 25 mM $MgCl_2$	1 mM (extra)	94° C	– 3 min	
2 µl 2 mM dNTPs	200 µM	94° C	– 20 sec	x12
0,25 µl 10 µM Primer #618	125 nM	64° C (-0.5° C/cycle)	– 20 sec	
0,25 µl 10 µM Primer #619	125 nM	72° C	– 35 sec	
1 µl 10 µM Primer #620	500 nM	94° C	– 20 sec	x25
1 µl 10 µM Primer #621	500 nM	58° C	– 30 sec	
10,5 µl ddH_2O		72° C	– 35 sec	
0.2 µl taq polymerase	1 U/reaction	72° C	– 2 min	
2 µl tail dilution (1:20)				

For the genotyping of all other mouse strains the following standard PCR protocol was used:

standard reaction mix	Final conc.	standard PCR program		
2 µl 10x taq buffer	1x	Stratagene RoboCycler		
2 µl 2 mM dNTPs	200 µM			
1 µl 10 µM Primer for	500 nM	94° C	– 2 min	
1 µl 10 µM Primer rev	500 nM	94° C	– 45 sec	x36
11.8 µl ddH_2O		60° C-66° C [1]	– 45 sec	
0.2 µl taq polymerase	1 U/reaction	72° C	– 1 min	
2 µl tail dilution (1:20)		72° C	– 10 min	

[1] Annealing temperatures were adapted individually for different PCRs and primer combinations. Op-timized conditions are listed in Supplementary Table 1.

Supplementary Table 1 – Oligonucleotide combinations and sequences for PCR genotyping of different transgenic mouse lines. Annealing temperatures ($T_{Annealing}$) and predicted sizes of specific ampli-fication products are listed.

CMV/β-actin rtTA and CMV rtTA [1]		**$T_{Annealing}$=60°C**	**product [4]**
rtTA for	#622	5'- CGG GTC TAC CAT CGA GGG CCT GCT -3'	242 bp (tg)
rtTA rev	#623	5'- CCC GGG GAA TCC CCG TCC CCC AAC -3'	
CMV/β-actin rtTA and CMV rtTA [2]		**touchdown (see above)**	**products [4]**
CMV rtTA for	#620	5'- CGC TGT GGG GCA TTT TAC TTT AG -3'	469 bp (tg)
CMV rtTA rev	#621	5'- CAT GTC CAG ATC GAA ATC GTC -3'	
WT for	#618	5'- CAA ATG TTG CTT GTC TGG TG -3'	206 bp (ic)
WT rev	#619	5'- GTC AGT CGA GTG CAC AGT TT -3'	
CaMKIIa rtTA [3]		**$T_{Annealing}$=62°C**	**product [4]**
rtTA2 for	#741	5'- TGC CTT TCT CTC CAC AGG TGT CC -3'	341 bp (tg)
rtTA2 rev	#740	5'- GAG AGC ACA GCG GAA TGA C -3'	
PKD1kd-EGFP		**$T_{Annealing}$=60°C**	**product [4]**
muPKD1 Ex6/7 for	#593	5'- TTG GTC GTG AGA AGA GGT CAA ATT C -3'	246 bp (tg)
muPKD1 Ex6/7 rev	#594	5'- CAC CAA GGC AGT TGT TTG GTA CTT T -3'	399 bp (ic)
muPKD1 Ex15/16 for	#591	5'- AAC CCT CAT CAC CCT GGT GTT GTA A -3'	223 bp (tg)
muPKD1 Ex15/16 rev	#592	5'- CTG GTT TGA GGT CAC AGT GAA CGA T -3'	812 bp (ic)
PKD2kd-EGFP		**$T_{Annealing}$=66°C**	**product [4]**
PKD2kd for	#572	5'- AGA GCT GGA GGG GAA GAT GGG AGA G -3'	294 bp (tg)
EGFP rev	#574	5'- GAC ACG CTG AAC TTG TGG CCG TTT A -3'	
PKD3kd-EGFP		**$T_{Annealing}$=60°C**	**products [4]**
muPKD3 Ex5/6 for	#595	5'- TTG GTC GTG AGA AGA GGT CAA ATT C -3'	204 bp (tg)
muPKD3 Ex5/6 rev	#596	5'- CAC CAA GGC AGT TGT TTG GTA CTT T -3'	766 bp (ic)
muPKD3 Ex14/15 for	#597	5'- TTT GCA CCA TCC TGG GAT TGT AAA C -3'	245 bp (tg)
muPKD3 Ex14/15 rev	#598	5'- CTG CTG ATG CAA GCA GCA CAT TTT C -3'	766 bp (ic)

[1] Genotyping protocol modified from (Wiekowski et al., 2001), [2] genotyping strategy adapted from http://jaxmice.jax.org/strain/003273.html, [3] genotyping protocol modified from (Michalon et al., 2005). [4] Sizes of amplification products for transgenic (tg) or internal control (ic) sequences were calculated on the basis of the underlying transgenic or genomic sequences.

PCR products were mixed with 5 µl DNA gel loading buffer, applied together with an appropriate molecular weight marker to the wells of 1.5% agarose, 0.2 µg/ml ethidium bromide, TBE gels, separated at 8 V/cm for 20-30 min and visualized under UV illumination.

Strategy for the establishment of a PKD mouse model

Transgenic approach

The aim of this work was to establish an appropriate mouse model to characterize the physiological role of members of the PKD family *in vivo*. All three PKD isoforms are very similar in their overall structure and share highly homologous domains. Moreover they are expressed partly in overlapping but also in differentiated patterns during mouse development and in adult organism (Ellwanger et al., 2008; Oster et al., 2006). Furthermore, recent studies about PKD function in skeletal muscle and heart support the idea that the individual PKDs are at least in part functionally redundant. Therefore, loss of one PKD isoform, e.g. by insertion of a knockout-allele via gene targeting, could be compensated by the other two isoforms. Both, the fact that gene targeting in embryonic stem cells by homologous recombination is a very complicated procedure that requires expert knowledge and the realization that PKD ge-nomic sequences are rather difficult to target, due to very large introns (Dr. Angelika Hausser, University of Stuttgart, personal communication), brought us to the idea to concen-trate on a transgenic mouse approach.

From *in vitro* studies it is known that kinase-dead PKD versions, mutants of wildtype PKD which harbor an amino acid exchange that leads to the disruption of kinase activity, can exert a dominant-negative effect. Overexpression of kinase-dead PKD has been demonstrated to interrupt endogenous PKD signaling and to interfere with PKD functions, e.g. membrane fission, secretion and cell migration (Eiseler et al., 2007; Fugmann et al., 2007; Liljedahl et al., 2001). To obtain a functional PKD knockout *in vivo* we therefore decided to construct transgenic mice, which overexpress kinase-dead PKD isoforms. Compared to a classical knockout approach, we claim that by the expression of one kinase-dead PKD isoform we can exert not only a dominant-negative effect on this isoform, but also on the other isoforms that might have redundant functions.

To express dominant-negative PKD versions in an inducible and conditional manner in mice, we made use of the tetracycline-dependent gene expression system originally described by Gossen and Bujard (Gossen and Bujard, 1992; Gossen and Bujard, 2002; Kistner et al., 1996). In this system, the reverse Tetracyclin transactivator protein (rtTA) is expressed constitutively from the activator transgene. In the presence of the tetracycline analog doxycycline, the rtTA protein binds to the tetracycline-responsive promoter element (TRE) thus inducing the expression of the transgene. Mouse lines expressing rtTA are published and

available for different specific promoters[1]. Moreover, by selecting mouse strains expressing rtTA in a tissue specific manner it is possible to achieve a spatio-temporal expression of transgenic constructs.

Transgene design

The constructs for the generation of transgenic animals were designed as follows: cDNA sequences of human PKD1, 2 and 3 were modified in a way to inactivate the kinase activity by inserting a point mutation in the ATP-binding domain. The resulting kinase-dead (kd) PKD mutants (PKD1-K612W, PKD2-K580W and PKD3-K605W, respectively) were N-terminally fused to EGFP, which served as a reporter to visualize the gene products *in vivo.* Conditional expression was achieved by insertion of the PKDkd-EGFP constructs into the multiple cloning site of pBI-5 (Baron et al., 1995). To eliminate inhibitory effects of prokaryotic sequences on transgene expression (Townes et al., 1985) the vector sequences were excised by digestion with appropriate restriction enzymes (Supplementary Figure 1A). Finally, the constructs used for pronuclear injection were composed of heptamerized tet-operator (tetO) sequences flanked by two divergently orientated hCMV minimal promoters whereof one controls the expression of PKDkd-EGFP followed by a rabbit ß-globin intron/polyadenylation signal.

Generation and genetic characterization of transgenic mice

Pronucleus microinjection and embryo transfer

Gene transfer into the mouse was performed by pronuclear microinjection using standard techniques (Nagy, 2003; Rülicke, 2004). In general, the use of zygotes from inbred strains is advisable. An inbred genetic background enables a more precise evaluation of the effects caused by transgene expression, as transgenic and nontransgenic animals are genetically identical (isogenic) and essentially homozygous at all loci, except for the allele of the newly inserted genetic modification by the transgene (Beck et al., 2000). Nevertheless, it has to be taken into account that inbred strains are less profitable in nearly all crucial aspects of pronuclear injection. As outbred strains are characterized by a higher viability and fertility, improved response to hormonally induced superovulation and zygotes are easy to inject and survive the microinjection procedure well we selected mice from the outbred strain CD1 as eligible oocyte donors and stud males. Superovulation induced with the gonadotropins (hCG and PMSG) before mating of the animals led to an average yield of 19 isolated oozytes per donor female (Supplementary Table 2). Oozyte quality determined by the accurate appear-

[1] List of up-to-date available mouse lines expressing Tet-transactivators under the control of various promoters and responsive mouse lines carrying target genes under Tet-control on http://www.tetsystems.com/

ance of pronuclei was also sufficient to obtain an adequate number of injectable zygotes (averaging 69% of isolated zygotes).

Microinjection of a 2 ng/µl DNA solution was performed with a constant compensation pressure causing swelling of the pronucleus in case of successful injection. Hereunder, several hundred copies of the transgenic construct are introduced into the nucleus of a microinjected zygote (Brinster et al., 1985). However this procedure can also injure the plasma membrane of the zygote which results in immediate lysis of the cell (Voncken, 2002). During the microinjection sessions performed in this study in average only 23% of injected oocytes lysed after pronuclear injection, which indicates that all conditions and settings were well adjusted, DNA was highly pure and microinjection was carried out carefully.

As *in vitro* culture in generally might decrease embryo viability, healthy zygotes were transferred into the oviduct of a pseudopregnant foster mother as soon as possible after injection. However, overnight cultivation was performed in case there was a lack of available recipient mice. In this instance over night culture provides a control of quality determined by the number of healthy embryos developed to the two-cell stage. In our hands about 50-75% of microinjected zygotes reached the two-cell stage after over night culture.

From literature it is known, that approximately 30% of the microinjected zygotes will develop to term after transferred into the oviduct of pseudopregnant foster mothers (Nagy, 2003). To avoid the occurrence of very small litters that might not be optimally fostered by the surrogate mother, the number of embryos retransferred after microinjection should be approximately double that of natural ovulations (Rülicke, 2004). We transferred 25 up to 35 oozytes unilaterally into only one oviduct of each foster mother and thereby obtained sufficient litter sizes. Moreover pregnancies of foster mothers were most often stable and lactation and parental care were satisfactory.

To sum up, we can conclude that mice from the outbred strain CD1 are in every respect suitable for the generation of transgenic animals, as they provide good zygotes and serve as adequate surrogate mothers.

Identification of transgenic animals

The initial screening for potential transgenic founders among the mice produced by pronuclear injection was performed by Southern blot analysis (Southern, 1975) and PCR genotyping. Altogether 20 transgenic founders were identified, six animals each carrying Tg(tetO-PKD1kd-EGFP) and Tg(tetO-PKD3kd-EGFP), respectively, and eight animals carrying Tg(tetO-PKD2kd-EGFP) (Supplementary Table 2). This corresponds to an overall frequency of 13.3% transgenic animals among the offsprings after pronucleus microinjection and retransfer of the

injected zygotes, which is in accordance with literature data (Brinster et al., 1985; Nagy, 2003). There was no sign of general toxicity mediated by the integration of the transgenic constructs as most (92%) pups born after microinjection and retransfer survived until weaning. Among the 13 animals that died during the first 4 weeks only one was transgenic which corresponds to a frequency of 7.6%.

The differences in the yields of transgenic animals for PKD1kd-, PKD2kd- and PKD3kd-EGFP constructs (8.2%, 14.0% and 30.0% respectively) can rather be explained by differences in DNA quality and microinjection settings than in any unspecific functional consequences mediated by the integration of the different constructs.

Supplementary Table 2 – Generation of transgenic mice

construct	**PKD1kd**	**PKD2kd**	**PKD3kd**	**total**
microinjection sessions	**7**	**7**	**5**	**19**
donor females	72	61	61	194
oocytes isolated	1369	1317	1007	3693
oocytes injected	1023	933	601	2557
oocytes retransfered	866	669	424	1959
oocyte yield [number/donor]	19	22	17	19
oocyte quality [% injectable]	75%	71%	60%	69%
oocyte lysis rate [%] (1)	**15%**	**28%**	**29%**	**23%**
foster mothers	29	25	16	70
pregnant foster mothers	21	18	8	47
offsprings born	77	61	25	163
offsprings survived	**73**	**57**	**20**	**150**
transgenic founders born	6	8	7	21
transgenic founders	**6**	**8**	**6**	**20**
transgenic offspring [%]	8.2%	14.0%	30.0%	13.3%

(1) mechanical damage during the microinjection procedure can result in oocyte lysis.

Expansion of transgenic mouse lines and genetic characterization

Transgenic animals were backcrossed to non-transgenic wildtype animals in order to establish transgenic lines for each individual founder. We selected wildtype mice from the outbred strain CD1 for subsequent breedings of the transgenic founder animals, as they have an excellent reproductive capacity with highest litter sizes and best breeding performance, compared to inbred strains. Though, the use of mice from inbred strains would allow a more defined evaluation of the effect of transgene expression as the single genetic difference between transgenic and non-transgenic control mice is the transgene (Yoshiki and Moriwaki, 2006).

After the first backcrossing, offsprings were genotyped by PCR and Southern blot. In contrast to PCR amplification of transgene-specific sequences, the Southern hybridization technique is

less error-prone and provides additional information about the structure, integrity and copy number of the inserted DNA sequences. When integration patterns of the original founder and its offsprings are compared the Southern technique can additionally specify the type of inheritance of the genetic modification (Deatly et al., 1998).

The combination of the restriction enzyme for digestion of genomic DNA and the probe used for detection is crucial to make a conclusion from the experimental readout upon the integration properties (Supplementary Figure 1A, Supplementary Table 3). As all transgenic constructs used for the generation of transgenic mice in this study contained an EGFP cassette and as there is no homology of the EGFP sequence to wildtype mouse genomic DNA, this sequence was selected as an optimal target site for the Southern hybridization probe. Therefore, a 577 bp sequence of EGFP was amplified via PCR, purified, labelled and used as transgene specific Southern probe.

Most often, transgenic constructs inserted by pronuclear injection integrate in a head-to-tail array (Bishop and Smith, 1989; Palmiter and Brinster, 1985; Shaw-White et al., 1993). In this case, the selection of an enzyme with a unique restriction digestion site within the transgene will yield fragments that are equivalent to the size of the whole transgene. Equally, an enzyme, which cuts at several positions upstream or downstream of the probe binding site within the transgenic sequence leads to fragments of predictable size. For each individual integration site additional junction fragments occur. The size of these fragments depends on the position of endogenous restriction enzyme digestion sites flanking the point of transgenic integration. As the integration of the transgene into the genome occurs randomly, the size of these junction fragments differs among the founder animals and can not be predicted. Occasionally, head-to-head or tail-to-tail joints can be formed which further complicates the band patterns by predictable sizes (Supplementary Figure 1C).

Supplementary Table 3 – Restriction enzymes for used for digestion of genomic DNA and expected fragment sizes after Southern hybridization with an EGFP probe

	tetO-PKD1kd-EGFP	**tetO-PKD2kd-EGFP**	**tetO-PKD3kd-EGFP**
BamHI	2.8 kb [(b)]	2.9 kb [(b)]	2.9 kb [(b)]
	>2.2 kb [(c)]	>2.2 kb [(c)]	>2.1 kb [(c)]
HindIII	4.8 kb [(b)]	4.4 kb [(b)]	5.5 kb [(b)]
	>4.0 kb [(c)]	>3.2 kb [(c)]	>4.7 kb [(c)]
EcoRI	4.5 kb [(a)]	4.1 kb [(a)]	3.4 kb [(a)]

[(a)] internal fragment of predictable size
[(b)] concatamer fragment of predictable size (in case of tandem integration)
[(c)] junction fragment (minimal size)

Alternatively, by the use of an enzyme that cuts upstream and downstream of the probe binding site only one type of fragments of known size is produced. However this strategy gives no further information about the type and pattern of transgenic integration.

To characterize Tg(tetO-PKDkd-EGFP) founder animals and their offsprings genomic DNA was digested with EcoRI, HindIII and BamHI respectively (Supplementary Table 3). EcoRI digestion of genomic DNA produced an internal fragment of known length, which could be visualized by Southern hybridization with the labelled EGFP probe, for all three transgenic constructs. In case of tandem integration of the transgene, HindIII and BamHI digestion led to fragments of predictable sizes and junction fragments which were individual for the different founder animals (Supplementary Figure 1B).

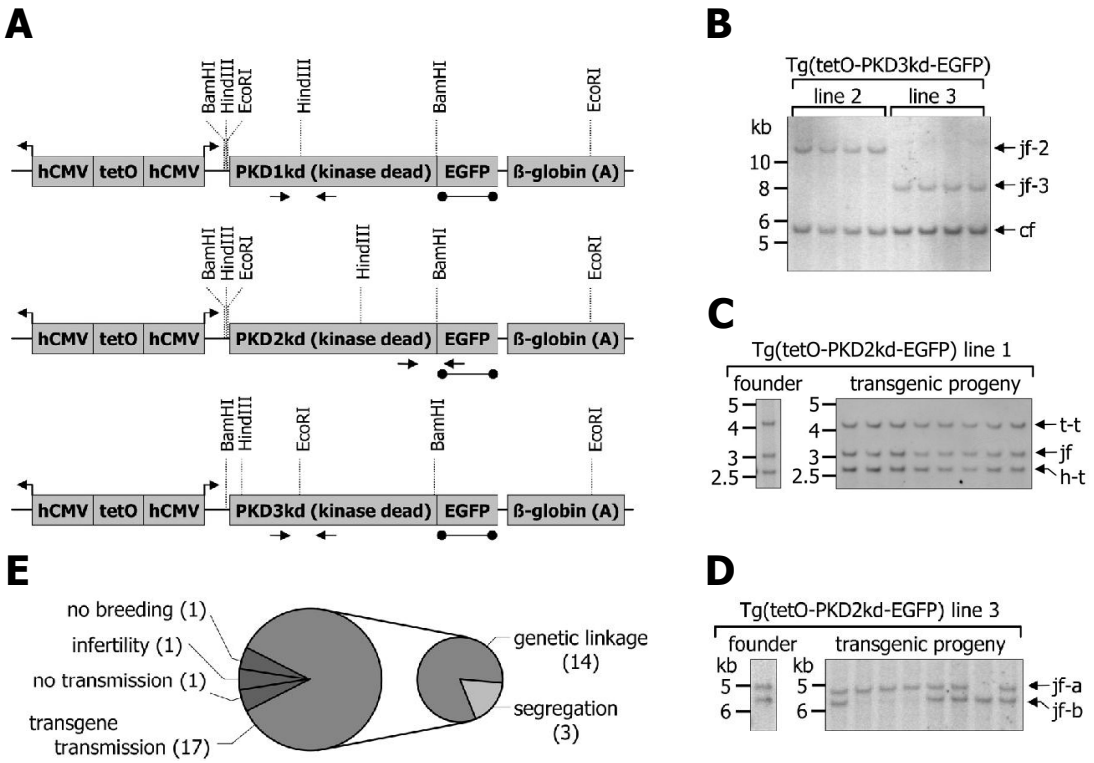

Supplementary Figure 1 – Southern strategy and representative results. (A) genetic constructs used for the generation of transgenic animals in this study with restriction enzyme digestion sites that are criticial for Southern blot analysis. The binding site of the 577 bp EGFP probe is illustrated (handle) as well as the primer binding sites for PCR genotyping (arrows). (B) Southern blot after HindIII digestion of genomic DNA from animals of two different founder lines of Tg(tetO-PKD3kd-EGFP). For both lines concatamer fragments (cf) of predictable size and individual junction fragments (jf-2 and jf-3) are detected. (C) Southern blot after HindIII digestion of genomic DNA from the initial founder animal and its transgenic offsprings of Tg(tetO-PKD2kd-EGFP) line 1. tail-to-tail (t-t) and head-to-tail (h-t) fragments of predictable size are detected as well as a junction fragment. The integration pattern of the transgene is transmitted to the following generation. (D) Southern blot after BamHI digestion of genomic DNA from the initial founder animal and its transgenic offsprings of Tg(tetO-PKD2kd-EGFP) line 3. Two individual junction fragments are detected which segregate among the offsprings. (E) Summary of genetic characterization of transgene integration and transmission of genetic alterations on offsprings. (E) Pie chart summarizing the genetic characterization of transgenic lines established in this work.

Sometimes, double integration events occur (Wagner et al., 1983), whereby the transgene integrates into different chromosomes (Lacy et al., 1983). This is becoming obvious after the first backcrossing of transgenic animals. We compared the integration pattern of the transgenic progeny and of the original founder animal by genomic Southern blot analysis.

Multiple integration sites within a founder transgenic mouse line were identified by comparing the fragment pattern visualized by Southern blot analysis of the transgenic offspring and the original founder animal. In case that the individual junction fragments generated by each integration event occur separated among the progeny when compared to the DNA of the original founder it becomes evident that the DNA of the original founder comprises multiple independent integration sites (Supplementary Figure 1D).

Among the transgenic founder animals generated in this work, three were identified to show segregation of the Southern fragments after the first backcrossing (Supplementary Figure 1E, Supplementary Table 4). This corresponds to a frequency of occurrence of multiple integration of 15% among the founder animals, which is consistent with results from other groups (Rülicke, 2004). Founder animals with multiple non-linked integration sites are moreover attributed to have significantly more than 50% transgenic progeny due to the segregation the F1 generation. However this was not evident in this study, maybe due to the fact, that each founder was backcrossed only once and the number of animals from the F1 generation analyzed was therefore to low to obtain statistically relevant data (data not shown). In general, the segregation of multiple independent integration sites from one transgenic founder after backcrossing facilitates the establishment of distinct transgenic lines from one founder animal. However, in this study we obtained sufficient independent transgenic lines for each construct and thus limited the amount of transgenic lines established from one founder to one.

85% (n=17) of the transgenic founder animals generated in this work successfully inherited the transgene through the germline (Supplementary Table 4, Supplementary Figure 1E). The remaining three animals (15%) were not able to produce transgenic offspring due to different reasons (Supplementary Table 4, Supplementary Figure 1E): one female founder animal showed insufficient breeding performance and maternal cannibalism, one founder was just infertile and did not produce any litters and the third produced litters but without transmitting the transgene through the germline. A possible explanation for the latter case is the formation of a chimeric mouse resulting from a delayed integration of the transgene after the first round of chromosomal DNA replication. In mosaics resulting from integration after the first division the germline is sometimes deficient or entirely lacks transgenic cells. In about 20-30% of transgenic mice obtained by microinjection of plasmids into pronuclei mosaicism in the germline can occur (Wilkie et al., 1986).

Interestingly, all three founder animals that failed to transmit the transgene to the next generation, were female, which supports the fact that female founder animals are more challenging than male founders for the establishment of transgenic lines (Nagy, 2003).

Statistical analysis of PCR genotyping results revealed that in further breedings of the transgenic lines the genetic modifications were transmitted to ~50% of their offspring, as expected for backcrossing of hemizygous animals. This is in agreement with the Mendelian laws of inheritance (Mendel, 1865). Considering the error rate of PCR genotyping, we conclude that the distribution of determined genotypes and the expected distribution of genotypes calculated on the basis of Mendelian laws of inheritance are according to χ^2-tests not significantly different (data not shown).

Supplementary Table 4 – Analysis of transgene integration and transmission by Southern blot

[tetO-PKD1kd-EGFP] transgenic mouse lines					**characteristics**	
founder	sex	date of birth	strain nomenclature	short code	integration	transmission
#31887	♂	*21.12.2005	Tg(tetO-PKD1kd-EGFP)1Izi	PKD1kd L1	(2b), (3)	
#32001	♀	*02.01.2006	Tg(tetO-PKD1kd-EGFP)2Izi	PKD1kd L2	(1)	
#32013	♂	*04.01.2006	Tg(tetO-PKD1kd-EGFP)3Izi	PKD1kd L3	(2b)	
#32021	♀	*02.01.2006	Tg(tetO-PKD1kd-EGFP)4Izi	PKD1kd L4	(2b), (3)	(E)
#32482	♂	*22.02.2006	Tg(tetO-PKD1kd-EGFP)5Izi	PKD1kd L5	(1)	
#32483	♀	*22.02.2006	Tg(tetO-PKD1kd-EGFP)6Izi	PKD1kd L6	(1)	
[tetO-PKD2kd-EGFP] transgenic mouse lines						
founder	sex	date of birth	strain nomenclature	short code	integration	transmission
#31793	♂	*07.12.2005	Tg(tetO-PKD2kd-EGFP)1Izi	PKD2kd L1	(2b), (2c)	
#31800	♂	*05.12.2005	Tg(tetO-PKD2kd-EGFP)2Izi	PKD2kd L2	(1)	
#32033	♂	*10.01.2006	Tg(tetO-PKD2kd-EGFP)3Izi	PKD2kd L3	(2a)	(E)
#32135	♀	*01.02.2006	Tg(tetO-PKD2kd-EGFP)4Izi	PKD2kd L4	n.d.	(A), (X)
#32190	♀	*07.02.2006	Tg(tetO-PKD2kd-EGFP)5Izi	PKD2kd L5	(1)	
#32195	♀	*07.02.2006	Tg(tetO-PKD2kd-EGFP)6Izi	PKD2kd L6	n.d.	(B), (X)
#32197	♂	*07.02.2006	Tg(tetO-PKD2kd-EGFP)7Izi	PKD2kd L7	(2b), (3)	(D)
#32208	♂	*07.02.2006	Tg(tetO-PKD2kd-EGFP)8Izi	PKD2kd L8	(1)	
[tetO-PKD3kd-EGFP] transgenic mouse lines						
founder	sex	date of birth	strain nomenclature	short code	integration	transmission
#30995	♀	*13.09.2005	Tg(tetO-PKD3kd-EGFP)1Izi	PKD3kd L1	(2b), (3)	
#31601	♂	*09.11.2005	Tg(tetO-PKD3kd-EGFP)2Izi	PKD3kd L2	(2b), (3)	
#31611	♀	*14.11.2005	Tg(tetO-PKD3kd-EGFP)3Izi	PKD3kd L3	(2b), (3)	
#31613	♀	*14.11.2005	Tg(tetO-PKD3kd-EGFP)4Izi	PKD3kd L4	(2a)	(E)
#31614	♀	*14.11.2005	Tg(tetO-PKD3kd-EGFP)5Izi	PKD3kd L5	n.d.	(C), (X)
#31620	♀	*15.11.2005	Tg(tetO-PKD3kd-EGFP)6Izi	PKD3kd L6	(1)	

(1) one single copy integration, (2a) two independent integration sites each comprising one copy, (2b) multiple copies integrated in tandem or head-to-tail orientation, (2c) multiple copies integrated in tail-to-tail orientation, (3) integration of high copy numbers of the transgenic construct.
(A) no successful breeding of offsprings, (B) infertility of founder mouse, (C) no germline transmission of transgene, (D) after breeding to transactivator strain, transgene expression can only be induced in a proportion of double transgenic offsprings, (E) segregation of transgenic integration sites due to multiple independent integration events, (X) extinction of transgenic line.

Establishment of homozygous transgenic mouse lines:

Homozygous transgenic animals can be obtained by setting up hemizygous intercrosses. According to Mendelians´ laws of inheritance 25% of the progeny should be homozygous, 50% hemizygous and 25% non-transgenic.

However, as DNA integration proceeds randomly, in approximately 5-20% insertional mutations of endogenous genes may occur (Nagy, 2003; Palmiter and Brinster, 1985; Woychik et al., 1985). Recessive embryonic lethal mutations created by random insertion are inconspicuous in hemizygous mice but can be identified by inbreeding of hemizygous mice and noting that homozygous offsprings are not viable (Jaenisch et al., 1983; Wagner et al., 1983).

A comfortable method to distinguish among hemizygous and heterozygous animals is quantitative real time PCR on genomic DNA templates (Aigner and Brem, 1995). As this technique was not implemented in our lab we made some efforts in identifying homozygous transgenic animals by testbreedings and analysis of the distribution of genotypes among the progeny. Since this procedure is very labour-intensive, we made an attempt only for transgenic lines which were frequently used in our lab.

For the mouse lines Tg(tetO-PKD1kd-EGFP)1Izi, Tg(tetO-PKD1kd-EGFP)4Izi, Tg(tetO-PKD2kd-EGFP)1Izi, Tg(CMV/β-actin-rtTA) (Wiekowski et al., 2001) and Tg(CaMKIIa rtTA2) (Michalon et al., 2005) ,it was possible to obtain homozygous animals without any apparent problems due to insertional mutations. As we didn´t try to establish homozygous animals from all strains we can not make a comment on the percentage of lethal recessive mutations among the mice generated in this work.

However, due to the fact that the animals were kept in an inhomogeneous genetic background, successive breeding of related individuals was also accompanied with inbreeding depression. For that reason it was not possible to maintain transgenic lines exclusively by homozygous breedings.

Analysis of transgene expression

Analysis of transgene expression and integrity

To analyze the capacity to induce transgene expression by doxycycline treatment double transgenic animals were generated by crossing hemizygous Tg(tetO-PKDkd-EGFP) animals from the different transgenic lines with hemizygous animals of the strain Tg(CMV/β-actin-rtTA) (Wiekowski et al., 2001). At an age of 6-8 weeks double transgenic animals were exposed for 1 week to 2mg/ml doxycycline and 5% sucrose in the drinking water. Transgene expression and integrity were analyzed by Western blotting in lysates from different tissues

and organs from these mice. To control the leakiness of the system we analyzed either single or non-transgenic animals treated with doxycycline-drinking water or double transgenic animals treated with drinking water containing 5% sucrose without doxycycline.

The transactivator mouse line used in this study was described to induce a strong rtTA expression in skeletal muscle tissue and a moderate expression in kidney, liver, heart and skin (Wiekowski et al., 2001). Therefore, we performed Western blot analysis of skeletal muscle lysates and quantitatively analyzed the PKDkd-EGFP levels to compare the Doxycycline-induced upregulation of transgene expression in different mouse lines (Supplementary Figure 2 and 3). Quantification of transgene expression was revealed by setting the signal intensity of the transgene relative to the signal obtained for tubulin-α. Six independent tetO-PKD1kd-EGFP-transgenic lines were generated and analyzed in the CMV/β-actin-rtTA-background. The highest level of transgene expression was found in double transgenic animals from line 1, moderate levels of transgene expression were detected in line 3 and line 4, whereas lines 2, 5 and 6 demonstrated only very low levels of PKD1kd-EGFP-expression (Supplementary Fig-ure 2A, Supplementary Table 5). Additionally, six different founder lines carrying tetO-PKD2kd-EGFP were tested for the CMV/β-actin-rtTA-dependent doxycycline-induced trans-gene expression. Again, the highest level of transgene expression was found in line 1, fol-lowed by line 2 and line 5. Moderate levels of PKD2kd-EGFP expression were detectable in line 3 and line 7 and only very low levels were found in line 8 (Supplementary Figure 3A, Supplementary Table 5). In double transgenic animals carrying tetO-PKD3kd-EGFP and CMV/β-actin-rtTA the levels of doxycycline-induced transgene expression were very low (Supplementary Table 5). In lysates from skeletal muscle PKD3kd-EGFP was hardly detect-able (line 4) or not detectable at all (line 1-3 and 6) (Supplementary Table 5). This is in ac-cordance with previous experiments, where it became obvious that after transfection of cells PKD3kd-EGFP showed lower expression levels compared to PKD1kd-EGFP and PKD2kd-EGFP (Dr. Angelika Hausser, University of Stuttgart, personal communication). For that reason, all following experiments and analysis were performed either with PKD1kd-EGFP or PKD2kd-EGFP expressing mouse lines.

Further investigations concerning transgene induction, biodistribution and overexpression levels were carried out with the transgenic lines that have been demonstrated to show the highest levels of transgene expression in skeletal muscle upon doxycycline stimulation (Tg(tetO-PKD1kd-EGFP)1Izi and Tg(tetO-PKD2kd-EGFP)1Izi, respectively).

To analyze the biodistribution of transgene expression tetO-PKDkd-EGFP/ CMV/β-actin-rtTA double transgenic animals were treated with doxycycline for one week. Western blot analysis of lysates from different tissues or organs demonstrated high levels of transgene expression

Supplementary Table 5 – Levels of doxycycline induced transgene expression: Tg(tetO-PKDkd-EGFP) transgenic lines analyzed in the CMV/β-actin-rtTA-background

construct	line	strain identification	level of transgene expression	
PKD1kd-EGFP	#1	Tg(tetO-PKD1kd-EGFP)1Izi	++++	(1)
	#2	Tg(tetO-PKD1kd-EGFP)2Izi	+	
	#3	Tg(tetO-PKD1kd-EGFP)3Izi	++	
	#4	Tg(tetO-PKD1kd-EGFP)4Izi	++	
	#5	Tg(tetO-PKD1kd-EGFP)5Izi	+	
	#6	Tg(tetO-PKD1kd-EGFP)6Izi	+	
PKD2kd-EGFP	#1	Tg(tetO-PKD1kd-EGFP)1Izi	++++	(1)
	#2	Tg(tetO-PKD1kd-EGFP)2Izi	+++	
	#3	Tg(tetO-PKD1kd-EGFP)3Izi	++	
	#5	Tg(tetO-PKD1kd-EGFP)4Izi	+++	
	#7	Tg(tetO-PKD1kd-EGFP)5Izi	+	
	#8	Tg(tetO-PKD1kd-EGFP)6Izi	-	
PKD3kd-EGFP	#1	Tg(tetO-PKD1kd-EGFP)1Izi	-	
	#2	Tg(tetO-PKD1kd-EGFP)2Izi	-	
	#3	Tg(tetO-PKD1kd-EGFP)3Izi	-	
	#4	Tg(tetO-PKD1kd-EGFP)4Izi	+	
	#6	Tg(tetO-PKD1kd-EGFP)5Izi	-	

(1) transgenic strains used for subsequent analysis of transgene induction, biodis-tribution and overexpression levels.

in skeletal muscle and moderate expression levels in heart and stomach for both Tg(tetO-PKD1kd-EGFP)1Izi mice and Tg(tetO-PKD2kd-EGFP)1Izi mice analyzed in the CMV/β-actin-rtTA-background (Supplementary Figure 2B and 3B). This is in line with the reported expression pattern of rtTA in the respective transactivator line (Wiekowski et al., 2001). Moreover, tetO-PKD1kd-EGFP/ CMV/β-actin-rtTA double transgenic animals showed a moderate expression in the skin and low expression levels in thymus, liver and kidney (Supplementary Figure 2B). In contrast, tetO-PKD2kd-EGFP/CMV/β-actin-rtTA double transgenic mice showed a moderate expression in the thymus and low expression levels in the skin, lung and kidney (Supplementary Figure 3B).

These variations of the biodistribution among different transgenic lines might be due to the differences in the individual transgene integration sites. The spatial distribution of the transgene does not only depend on the promoter controlling rtTA expression, but can also depend on the transgene integration site (Krumlauf et al., 1985). Therefore, level and biodistribution of transgene expression can be different for various founder lines though the same transactivator line is used.

To study the kinetic of doxycycline-induced transgene expression double transgenic animals were kept without any drinking water over night, treated with doxycycline drinking water for different timepoints and finally isolated skeletal muscle tissue was analyzed for transgene expression by Western blotting (Supplementary Figure 2C and 3C). PKD1kd-EGFP expression was already detectable within 3 hours after the onset of doxycycline administration and in-

creased over time reaching a maximum within 1-3 weeks of treatment (Supplementary Figure 2C). In the uninduced state (control) PKD1kd-EGFP was not detectable, indicating that transgene expression is strictly doxycycline dependent and tightly regulated.

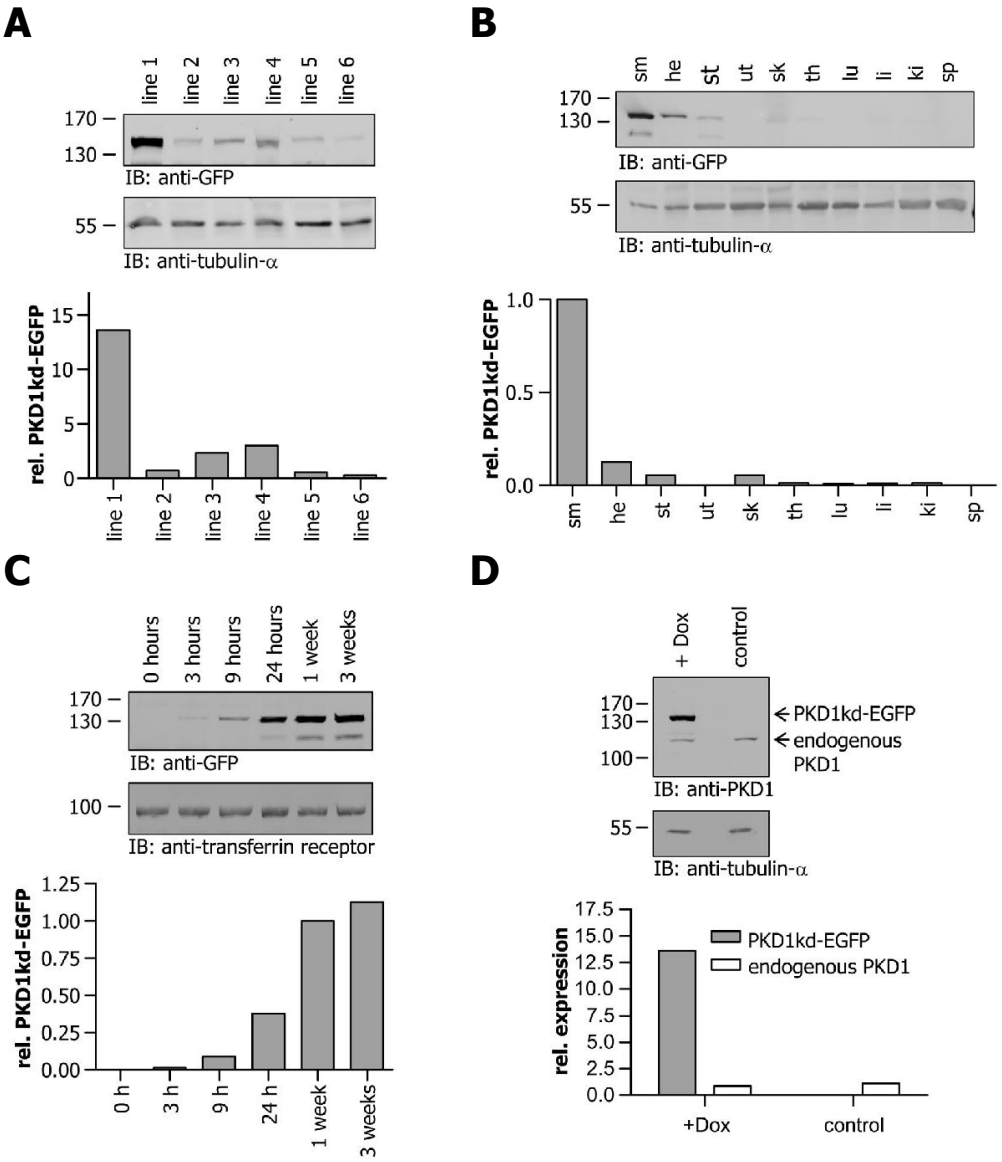

Supplementary Figure 2 – Doxycycline-dependent expression of PKD1kd-GFP in double-transgenic mice carrying tetO-PKD1kd-GFP and CMV/β-actin rtTA. Representative quantitative Western blots and graphs showing (A) relative expression levels of PKD1kd-EGFP upon doxycycline treatment in skeletal muscle from different PKD1kd -EGFP-transgenic lines and (B)-(D) further characteristics of transgene expression analyzed for mice from the transgenic line Tg(tetO-PKD1kd-EGFP)1Izi. (B) Tissue specificity and biodistribution of transgene expression (sm: skeletal muscle, he: heart, st: stomach, ut: uterus, sk: skin, th: thymus, lu: lung, li: liver, ki: kidney, sp: spleen). The densitometry of the skeletal muscle sample was arbitrarily set to 1.0. (C) Kinetic of induction upon doxycycline treatment in skeletal muscle. The densitometry of the one week-induction sample was arbitrarily set to 1.0. (D) Overexpression level of transgenic PKD1kd-EGFP versus endogenous PKD1 in skeletal muscle. Skeletal muscle from doxycycline-treated single transgenic animals carrying tetO-PKD1kd-EGFP served as control. The densitometry of endogenous PKD1 in the control sample was arbitrarily set to 1.0.

The kinetic of doxycycline induced PKD2kd-EGFP (Supplementary Figure 3C) looks very similar to that of PKD1kd-EGFP. According to literature the limiting parameter for the induction of transcription is the delivery of the effector molecule (doxycycline) to the target sites within

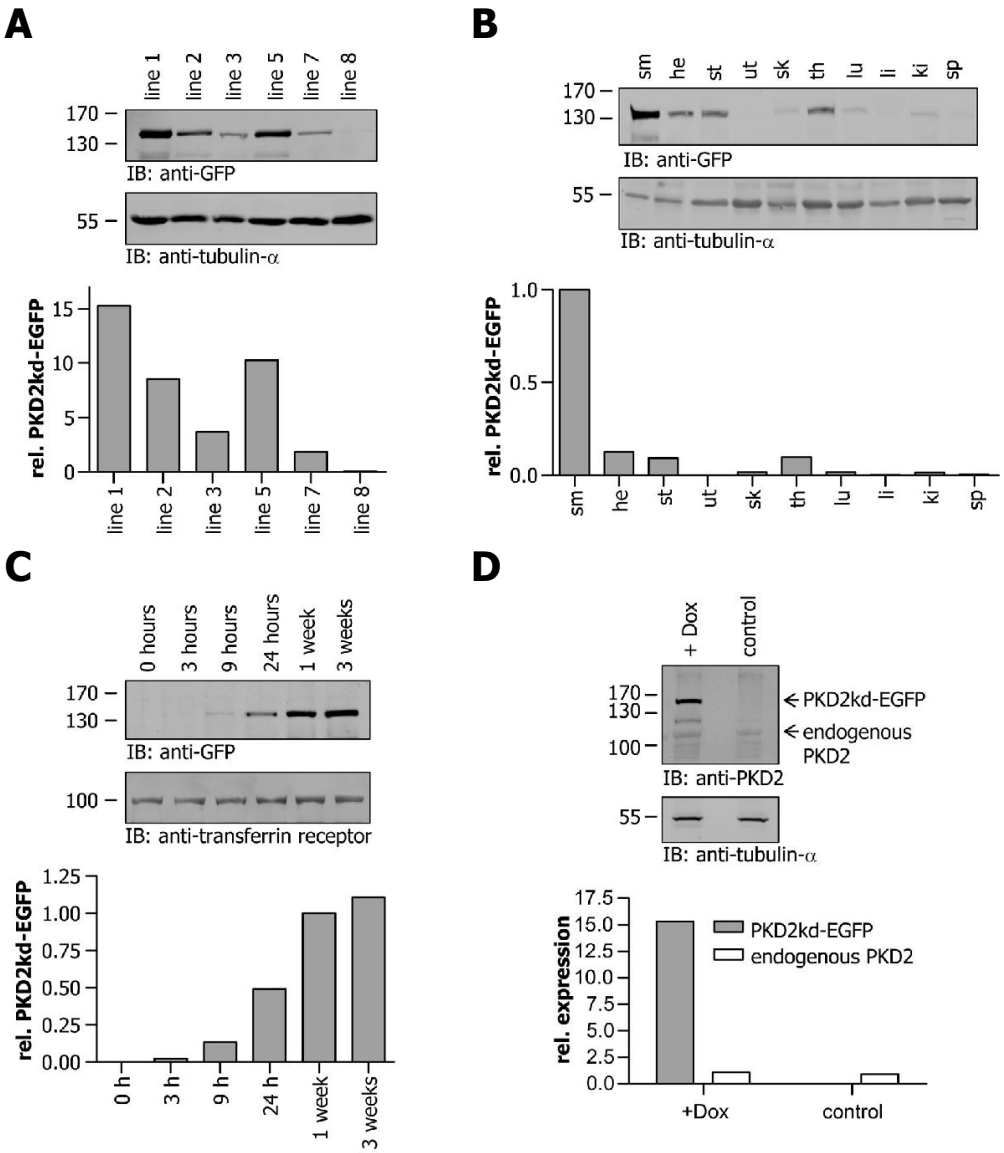

Supplementary Figure 3 – Doxycycline-dependent expression of PKD2kd-GFP in double-transgenic mice carrying tetO-PKD1kd-GFP and CMV/β-actin rtTA. Representative quantitative Western blots and graphs showing (A) relative expression levels of PKD2kd-EGFP upon doxycycline treatment in skeletal muscle from different PKD2kd -EGFP-transgenic lines and (B)-(D) further characteristics of transgene expression analyzed for mice from the transgenic line Tg(tetO-PKD2kd-EGFP)1Izi. (B) Tissue specificity and biodistribution of transgene expression (sm: skeletal muscle, he: heart, st: stomach, ut: uterus, sk: skin, th: thymus, lu: lung, li: liver, ki: kidney, sp: spleen). The densitometry of the skeletal muscle sample was arbitrarily set to 1.0. (C) Kinetic of induction upon doxycycline treat-ment in skeletal muscle. The densitometry of the one week-induction sample was arbitrarily set to 1.0. (D) Overexpression level of transgenic PKD2kd-EGFP versus endogenous PKD2 in skeletal muscle. Skeletal muscle from doxycycline-treated single transgenic animals carrying tetO-PKD2kd-EGFP served as control. The densitometry of endogenous PKD2 in the control sample was arbitrarily set to 1.0.

the specific compartment of the animal (Hofker and Deursen, 2003). In conclusion skeletal muscle belongs to a group of tissues with very fast kinetics of doxycycline induction (Hasan et al., 2001).

An important requirement for dominant-negative action of a kinase-dead PKD is a considerable overexpression compared to endogenous PKD levels. We therefore analyzed and compared the expression levels of endogenous and transgenic PKDs in skeletal muscle tissue of double transgenic animals treated with doxycycline for one week and untreated control animals. Quantitative Western blotting using a monoclonal PKD1-specific antibody revealed a 13.6 fold higher expression level of PKD1kd-EGFP compared to endogenous PKD1 (Supplementary Figure 2D). Similarly analysis of tetO-PKD2kd-EGFP/CMV/β-actin-rtTA double transgenic mice demonstrated a 15.3 fold overexpression of transgenic PKD2kd-EGFP versus endogenous PKD2 (Supplementary Figure 3D).

As there was no appropriate pan-PKD antibody available in this study, it was not possible to conclude from these findings on the overexpression level of dominant-negative PKD versus the total expression of endogenous PKD isoforms. However, according to literature data (Kim et al., 2008b), in skeletal muscle all three PKD isoforms are expressed whereas PKD1 displays the highest expression level. Therefore, we claim that the level of transgene expression is sufficient to mediate dominant-negative effects in skeletal muscle.

Analysis of tissue specific and isoform dependent localization of the transgenes

PKD can be recruited to various subcellular compartments to carry out different cellular functions (Wang, 2006). Thus, analysis of the localization of overexpressed kinase-dead PKD transgenes is essential for the evaluation of dominant-negative effects on putative endogenous PKD functions. Therefore we investigated the spatial distribution of transgene expression in different tissues and organs by fluorescence microscopy. PKDkd-EGFP x CMV/β-actin-rtTA double transgenic animals were provided with doxycycline drinking water for one week before different organs and tissues were dissected for further analysis. Confocal laser scanning microscopy of cryosections counterstained with Alexa-546 phalloidin (for F-Actin) and DRAQ5 (for DNA) revealed tissue dependent and isoform specific localization of the transgenic proteins (Supplementary Figure 4 and 5).

In skeletal muscle PKD1kd-EGFP expression was very obvious and uniformly distributed throughout the muscle. On a single cell level PKD1kd-EGFP was found in the cytoplasma of skeletal muscle fibers where it was associated with the myofilament substructure. Careful investigation of the stripe pattern on longitudinal sections revealed an enrichment of PKD1kd-

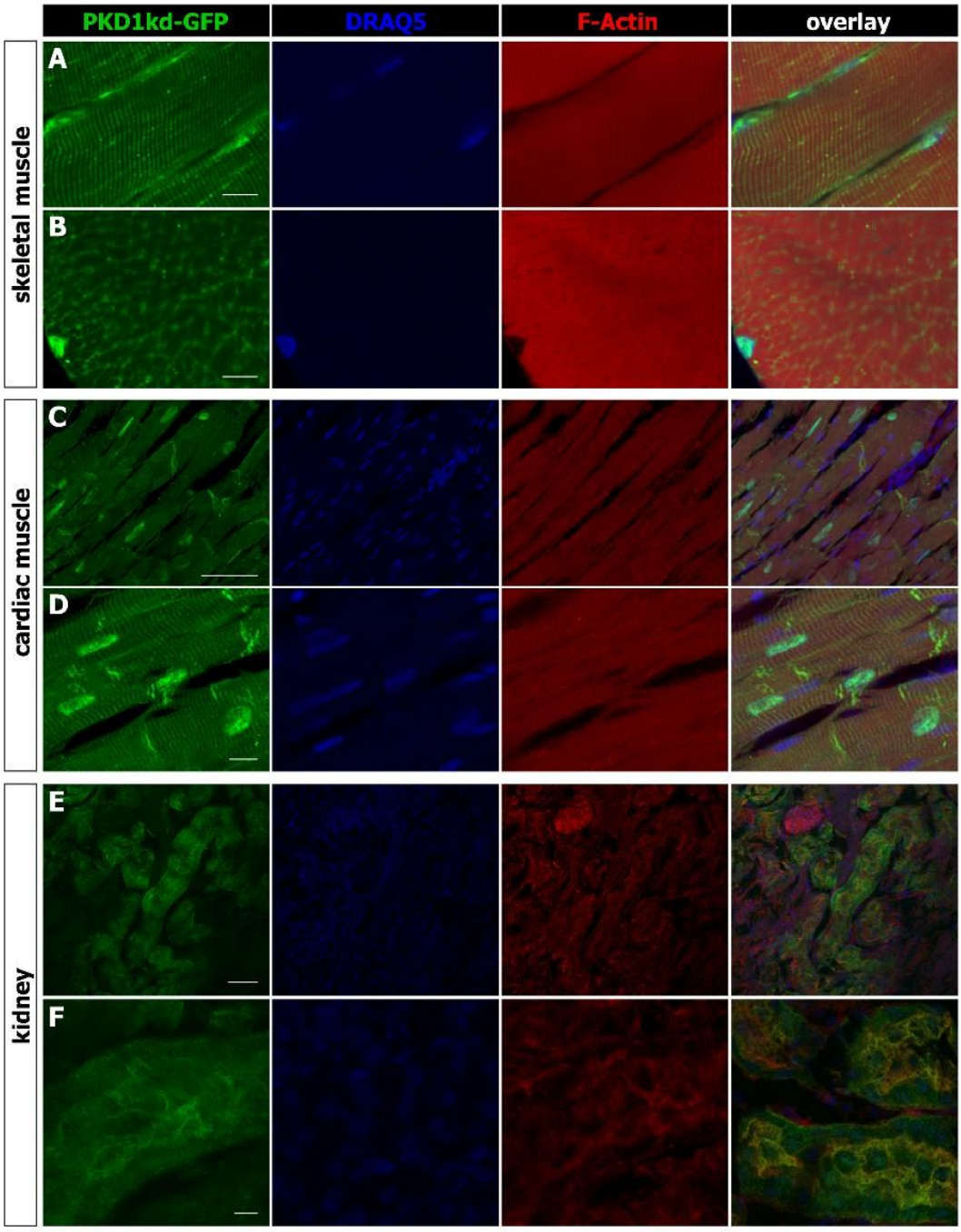

Supplementary Figure 4 – Tissue specific expression and localization patterns of PKD1kd-EGFP. Organs from double-transgenic mice carrying tetO-PKD1kd-EGFP (line1) and CMV/β-actin rtTA were isolated after 1 week of doxycycline stimulation and processed for cryo-sectioning. 16 µm frozen sections were cut, fixed in 4% PFA in PBS and treated with Alexa-546 phalloidin to visualize F-Actin and with DRAQ5 for nuclear staining. (A) Longitudinal and (B) cross sections of skeletal muscle fibers indicate localization of the transgene in the nuclei and associated with the sarcomeric structure. (C, D) In sections from cardiac muscle PKD1kd-EGFP was localized at the central nuclei of cardiac muscle fibers, at the intercalated discs and associated with the sarcomeric structure. (E, F) In sections from kidney PKD1kd-EGFP expression was evident in patches of epithelial cells lining proximal convoluted tubules. Shown are projections of z-stacks recorded by confocal microscopy. Scale bars indicate 10 µm (A, B, D, F) or 50µm (C, E).

EGFP in the H-band, a region which lacks actin filaments but is mainly composed of thick my osin filaments (Supplementary Figure 4A). As PKD has been shown to phosphorylate cardiac myofilament proteins (Cuello et al., 2007; Haworth et al., 2004) a function of the kinase in the regulation of myocyte contraction is supposed. Until now it is unknown whether PKD-mediated myofilament phosphorylation is restricted to cardiac myocytes or whether it represents a general mechanism in the regulation of contractile functions.

Microscopic analysis of cross sections from skeletal muscle revealed that a proportion of the catalytically inactive PKD1 is localized to the sarcoplasmatic reticulum and to transverse tubules (Supplementary Figure 4B) which are deep invaginations of the skeletal muscle plasma membrane and which are both involved in the coupling of excitation and contraction (Siegel, 1999). In addition to the cytoplasmic distribution, PKD1kd-EGFP was strongly enriched in the nuclei of skeletal muscle fibers (Supplementary Figure 4A, B). From *in vitro* studies it is known that in cardiomyocytes active PKD phosphorylates class IIa HDAC proteins in the nucleus, thereby mediating nuclear export and MEF2 activation (Vega et al., 2004). Thus, shuttling of kinase-dead PKD1 into the nucleus allows the inhibition of endogenous PKD in this compartment and might mediate dominant-negative effects towards HDAC phosphorylation.

Fluorescence microscopy of cryosections from cardiac muscle demonstrated a homogeneous expression of PKD1kd-EGFP, an association with the myofilament substructures and a dominant localization of the protein in the big, central nuclei of the cardiomyocytes (Supplementary Figure 4C, D). Interestingly, PKD1kd-EGFP was also prominently localized at the intercalated discs, which are junction sites between adjacent cardiac muscle cells. Intercalated discs contain anchoring desmosomes and gap junctions arranged in a way to allow the heart to act as a functional syncytium (Berg et al., 2002).

In contrast to the uniform distribution of PKD1kd-EGFP in skeletal and cardiac muscle we observed a very patchy expression of the transgene in the kidney (Supplementary Figure 4E, F). This result is in accordance with the Western blot obtained from whole organ lysates, showing a rather low expression level of PKD1kd-EGFP in the kidney compared to muscle tissue (Supplementary Figure 2B). Microscopic imaging revealed that transgene expression is confined to individual areas of the renal cortex. In some patches of epithelial cells lining proximal convoluted tubules the transgene expression was detectable (Supplementary Figure 4E, F) but it was completely absent from other regions of the kidney, e.g. from the glomerulus and its surrounding Bowman's capsule. On a subcellular level PKD1kd-EGFP seemed to be localized rather in the cytoplasma and at the membrane than in the nuclei of kidney cells (Supplementary Figure 4F). However, due to the low expression level and the patchy localization of PKD1kd-EGFP in the kidney dominant-negative effects resulting in an obvious phenotype are rather unlikely.

Analysis of skeletal muscle specimens of doxycycline induced PKD2kd-EGFP/CMV/β-actin-rtTA double transgenic animals revealed that the dominant-negative protein is also expressed uniformly throughout the skeletal muscle and that it is highly accumulated in the nuclei of myofibers (Supplementary Figure 5A, B). In contrast to PKD1kd-EGFP, where a proportion of the transgene was found at cytoplasmic structures (Supplementary Figure 4A, B), PKD2kd-EGFP is slightly enriched at the sarcolemma of the skeletal muscle fibers (Supplementary Figure 5B). A similar distribution of PKD2kd-EGFP was observed in cardiac muscle fibers. Here, the localization of PKD2kd-EGFP to the central nuclei of cardiomyocytes was also most evident (Supplementary Figure 5C, D). An accumulation of PKD2kd-EGFP at the intercalated discs or at other membranes was not detected.

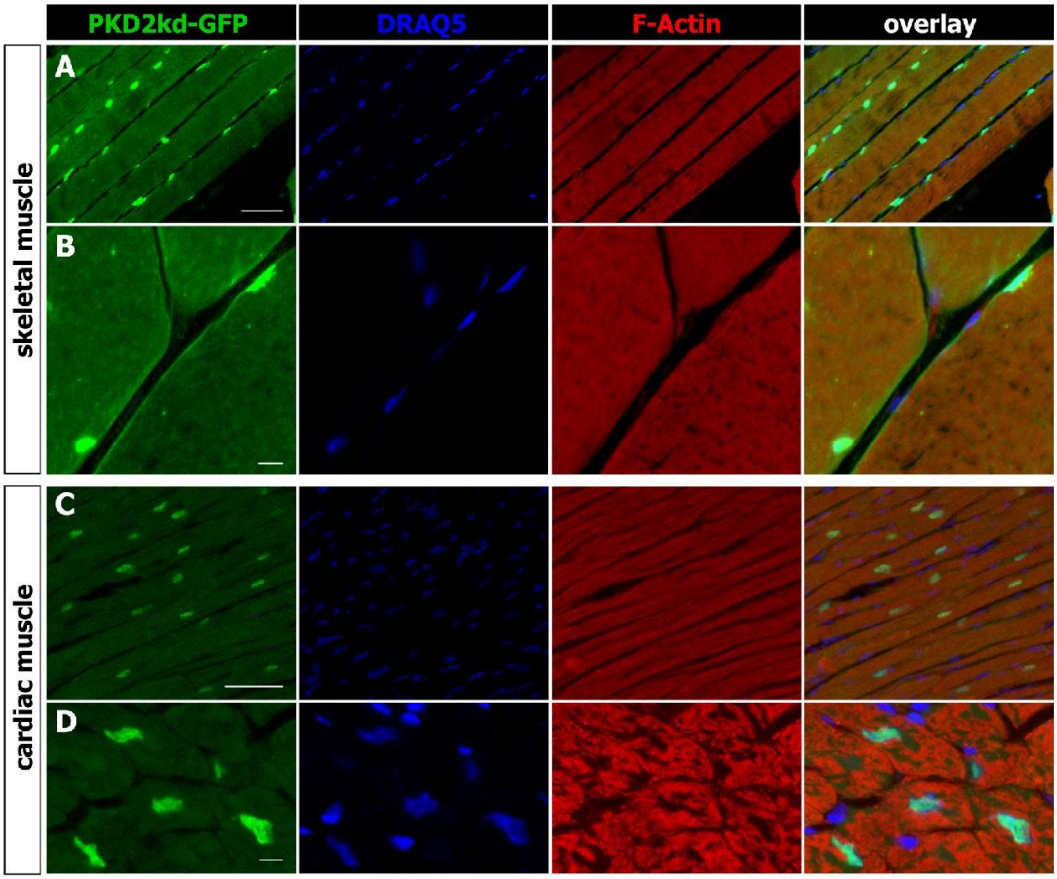

Supplementary Figure 5 – Tissue specific expression and localization patterns of PKD2kd-EGFP. Organs from double-transgenic mice carrying tetO-PKD2kd-EGFP (line1) and CMV/β-actin rtTA were isolated after 1 week of doxycycline stimulation and processed for cryo-sectioning. 12-20 µm frozen sections were cut, fixed in 4% PFA in PBS and treated with Alexa-546 phalloidin to visualize F-Actin and with DRAQ5 for nuclear staining. (A) Longitudinal and (B) cross sections of skeletal muscle fibers indicate localization of the transgene in the nuclei and sarcolemma. (C) Longitudinal and (D) cross sections from cardiac muscle PKD1kd-EGFP show PKD2kd-EGFP localized in the central nuclei of cardiac muscle fibers. Shown are projections of z-stacks recorded by confocal microscopy. Scale bars indicate 50 µm (A, C) or 10µm (B, D).

Interestingly, fluorescence microscopy of kidney specimens detected only very weak and patchy expression of PKD2kd-EGFP but also a nuclear localization of the dominant-negative protein (data not shown).

In sum, PKD1kd-EGFP was localized to cytoplasmic, membrane and nuclear compartments in the analyzed tissues and organs, whereas PKD2kd-EGFP was predominantly found in nuclei. We conclude that the expression levels and the biodistribution of transgene expression depend on the transactivator line used and on the site and frequency of transgene integration. Patchy expression might be a result of position effect variegation (PEV)[2] (Kioussis and Festenstein, 1997; Opsahl et al., 2002). The subcellular localization of a transgene depends on the protein properties (e.g. presence of nuclear localization or export sequences) and on the potential function of the endogenous protein in the respective cell type (e.g. availability of adapter or scaffolding proteins).

Induction and analysis of transgene expression in embryogenesis

To analyze transgene inducibility and expression during embryonic development hemizygous Tg(tetO-PKDkd-EGFP) animals were bred to hemizygous Tg(CMV/β-actin rtTA) animals. Plug-positive females were identified and treated with 2mg/ml doxycycline in the drinking water starting at 0.5 dpc. From literature it is known that doxycycline passes the placenta in quantities that are sufficient to activate gene expression in the embryo. Furthermore, doxycycline is transmitted to the breast milk and activates expression in newborn mice (Ray et al., 1997). Thus, the Tet regulatory system has been used as a tool for the regulation of gene expression during embryogenesis and development (Fedorov et al., 2001; Shin et al., 1999).

To analyze transgene expression, embryos were dissected at stage E14.5-E16.5. They were screened for morphological abnormalities and the genotypes were determined by PCR. Altogether 161 embryos from mothers which were supplied with doxycycline during pregnancy were analyzed. In general the appearance of the single genotypes was very similar to the expected Mendelian frequencies (Supplementary Figure 6A). However a notable proportion of fetuses was either already resorbed (n=36) or showed neural tube closure defects like spina bifida (n=12) or exencephaly (n=2) which would certainly lead to fetal death in the later development. When we considered the distribution of genotypes separately for the viable (Supplementary Figure 6B) and for the non-viable embryos (Supplementary Figure 6C) it became obvious that the proportion of genetic individuals carrying Tg(CMV/β-actin rtTA) was significantly ($p<0.001$) reduced among the viable embryos. Conversely, for the non-viable fetuses individuals carrying Tg(CMV/β-actin rtTA) appear with a significantly ($p<0.001$) increased

[2] Position effect variegation is a variegation caused by the inactivation of a gene in some cells through its specific juxtaposition with heterochromatin.

frequency. The result points towards an off target effect of the rtTA in these animals. The appearance of neural tube closure defects or other abnormalities leading to embryo resorption did not depend on whether the kinase-dead PKD isoforms were expressed or not, and must therefore be regarded as unspecific. Similarly, toxic effects of doxycycline can be excluded, as only embryos carrying Tg(CMV/β-actin rtTA) were affected.

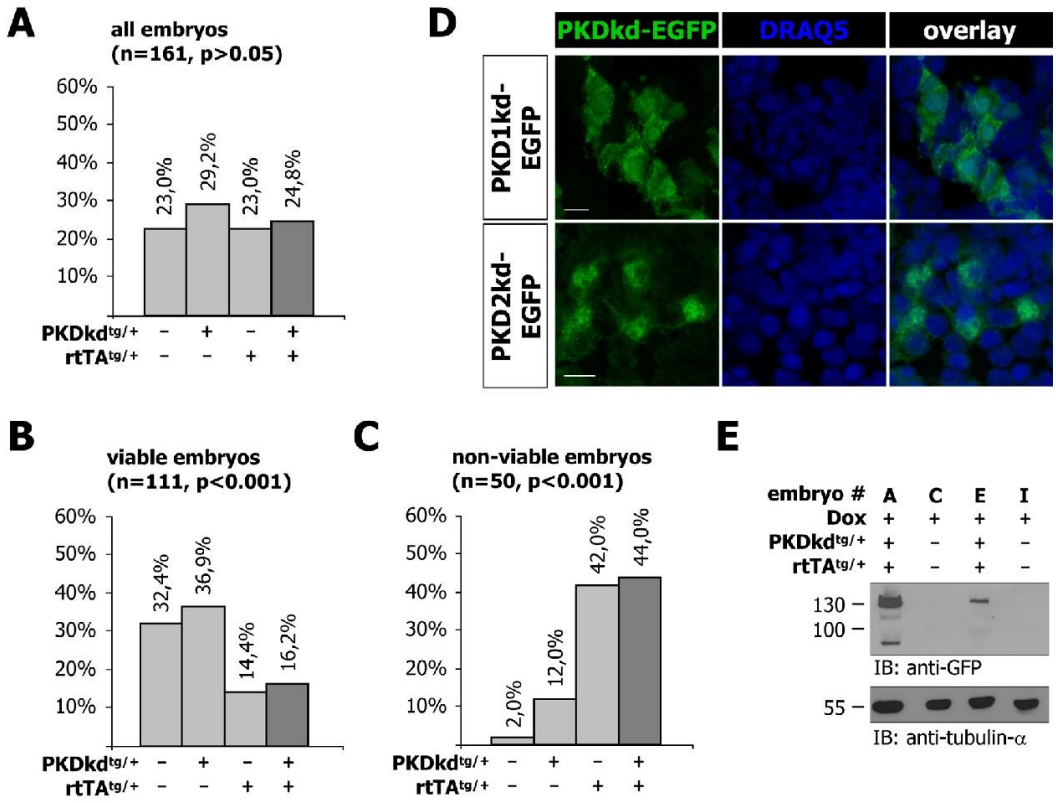

Supplementary Figure 6 – CMV/β-actin rtTA-dependent transgene expression during embryogenesis. (A-C) Genotype distribution of embryos derived from breedings of hemizygous Tg(tetO-PKDkd-EGFP) mice with hemizygous Tg(CMV/β-actin rtTA) mice. Pregnant mothers were treated with 5mg/ml doxycycline and 5% sucrose in the drinking water starting from 0.5 dpc. Embryos were dissected at stage E14.5 to E16.5. Considering all embryos (A) the frequency of occurrence for the single genotype combinations is not significantly different from the expected ratios ($p>0.05$). Regarding only the proportion of viable embryos (B) or non-viable embryos (C) respectively, the genotype distribution diverges significantly from the expected values ($p<0.001$). Statistical significance was assessed using χ^2-tests. (D) Distribution and subcellular localization of PKD1kd-EGFP or PKD2kd-EGFP expressed via CMV/β-actin rtTA during embryogenesis. 12-20 µm frozen sections were cut, fixed in 4% PFA in PBS and treated with DRAQ5 for nuclear staining. Shown are projections of z-stacks recorded by confocal microscopy. Scale bars indicate 10 µm. (E) Representative Western blot showing variations of the transgene expression level between embryo littermates with equal genotype.

Nevertheless we analyzed the expression of PKD1kd-EGFP and PKD2kd-EGFP in viable double transgenic embryos, after in utero treatment with doxycycline. Microscopic analysis of cryo-sections revealed a very patchy expression confined to individual areas for both kinase-dead PKD isoforms (Supplementary Figure 6D). However, the localization to specific embryonic substructures was not further analyzed. At the subcellular level PKD1kd-EGFP was distributed rather uniformly in the cells (Supplementary Figure 6D upper panel) whereas PKD2kd-EGFP localization was more dominant in the nuclear compartment (Supplementary Figure 6D lower panel). This subcellular localization pattern of PKD1kd-EGFP and PKD2kd-EGFP is in agreement with microscopic observations in adult tissue (Supplementary Figure 4 and 5). Western blot analysis of whole embryo lysates demonstrated variations of transgene expression levels between embryo littermates with equal genotype for PKD1kd-EGFP (Supplementary Figure 6E) and for PKD2kd-EGFP (data not shown). A possible explanation for the variablilty of transgene expression might be the heterogeneous genetic background of the animals.

Recapitulating, these experiments demonstrated that in general it is possible to induce transgene expression during embryonic development with the provided mouse lines. However, we observed unspecific effects due to rtTA expression in this study, which were highly undesirable and difficult to interpret. Furthermore, the spatially very restricted expression and the variations in the expression levels among genetically identical and equally treated embryos convinced us to discontinue further analysis.

Functional consequences of transgene expression

Genetically manipulated mice often show phenotypes that differ from our expectations. To get a first impression, it is important to carry out extensive examinations using behavioural tests as well as macroscopic and microscopic analysis. Ideally, standard operation procedures have to be established for all tests in the primary screening (Gailus-Durner et al., 2005).

Most of the experiments carried out in this study were performed with PKDkd-EGFP x CMV/β-actin rtTA double transgenic animals. Of note, although expression of PKDkd-EGFP was highly upregulated upon doxycycline treatment in skeletal muscle and moderately upregulated in a variety of other tissues (Supplementary Figure 2 and 3), mice did not demonstrate any apparent phenotypical changes. Body weight, heart and skeletal muscle size as well as muscle fiber type content were not altered compared to control animals. Moreover, histological analysis of H&E sections from tissues or organs with transgene expression showed no obvious alterations in the gross morphology (data not shown).

In cardiomyocytes PKD has been reported to activate myocyte enhancer factor 2 (MEF2) dependent transcription via phosphorylation of the repressor histone deacetylase 5 (HDAC5) *in*

vitro (Vega et al., 2004). To analyze whether PKD is involved in MEF2 dependent skeletal muscle remodeling *in vivo,* we subjected doxycycline treated PKDkd-EGFP x CMV/β-actin rtTA double transgenic mice to voluntary wheel running, an exercise which has been shown to activate MEF2 (Wu et al., 2001). Interestingly, PKD1kd-EGFP expressing mice achieved significantly decreased absolute running distances and relative velocities compared to control mice. Accordingly, overexpression of PKD1kd-EGFP inhibited fiber type transformation in these mice. Therefore we propose an essential role of PKD in exercise-induced skeletal muscle remodeling *in vivo*. Experimental results and argumentations supporting this hypothesis are given on page 50 et seq. (publication manuscript II – PKD controls skeletal muscle remodeling).

The group of Dr. Sandra Beer (Institute of Medical Microbiology and Hospital Hygiene, Heinrich-Heine-University Düsseldorf, Germany) recently received PKD2kd-EGFP x CMV/β-actin rtTA double transgenic mice from us to make use of the expression of dominant-negative PKD2 in the thymus. The group is working with Sly1, a protein which has recently been shown to be a potential PKD substrate (Reis, 2007). Sly1 is specifically expressed in lymphocytes and was proposed to play a role in antigene receptor mediated activation of T lymphocytes (Beer et al., 2005; Beer et al., 2001). A reduction of the Sly1 phosphorylation in lymphocytes from mice expressing dominant-negative PKD2 would support the hypothesis of a physiological role of PKD in the regulation T cell activity via Sly1.

Apart from Tg(CMV/β-actin rtTA) mice we also used other transactivator strains to drive PKDkd-EGFP expression. In an independent study carried out in our lab Tg(PKDkd-EGFP) mice were crossed with transactivator mice, expressing the reverse tetracycline transactivator under the control of a human CMV early promoter rtTA (Kistner et al., 1996). Transgene expression and localization was analyzed and compared with the pattern obtained in the CMV/β-actin rtTA background. Moreover an assay for the analysis of potential phenotypes caused by impaired insulin secretion was established (Krenkler, 2008).

From *in vitro* studies with transfected primary hippocampal neurons we suggested a role of PKD in the maintenance of the neuronal Golgi structure. To confirm these findings *in vivo* we made use of a transactivator line which expresses a reverse tetracycline transactivator under the control of the forebrain-specific calcium-calmodulin-dependent kinase IIα promoter termed Tg(CaMKIIαrtTA) (Michalon et al., 2005). To improve the use of the Tet system for *in vitro* and *in vivo* applications, in this mouse a new version of the rtTA (rtTA2) is used which is characterized by an increased mRNA stability, optimized codon-use for mammals, lower background activity, and higher affinity for doxycycline (Urlinger et al., 2000). A detailed characterization of the doxycycline induced PKD1kd-EGFP expression in the CaMKIIαrtTA

background as well as a description and discussion of the functional consequences are provided on page 66 et seq. (publication manuscript III – PKD controls dendritic arborization). In subsequent investigations we studied the effect of the duration of doxycycline treatment on transgene expression in the brain. In adult animals we found a very strong expression in the hippocampus, mainly in CA1, CA3 and DG, but also a clear expression in the amygdala and very weak and rare signals in cortical cells after 4 weeks induction. However, we also identified variations of the expression intensity and localization between double transgenic littermates (Katalin Schlett, unpublished data).

Concerning the physiological role of PKD in neurons, we await further insights from an ongoing collaboration with Dr. Ingrid Nijholt from the laboratory of Prof. Dr. U. L. M. Eisel (Department of Molecular Neurobiology, University of Groningen, Haren, the Netherlands) who is going to perform behavioral experiments with PKDkd-EGFP expressing mice. To measure learning performance it is planned to carry out fear conditioning studies. Furthermore, other learning tasks like elevated plus maze will give us an impression on possible changes in anxiety in the mice with transgene expression.

Bibliography

Abedi, H., Rozengurt, E., and Zachary, I. (1998). Rapid activation of the novel serine/threonine protein kinase, protein kinase D by phorbol esters, angiotensin II and PDGF-BB in vascular smooth muscle cells. FEBS Lett *427*, 209-212.

Aigner, B., and Brem, G. (1995). Detection of homozygous individuals in gene transfer experiments by semiquantitative PCR. Biotechniques *18*, 754-756, 758.

Akimoto, T., Li, P., and Yan, Z. (2008). Functional interaction of regulatory factors with the Pgc-1alpha promoter in response to exercise by in vivo imaging. Am J Physiol Cell Physiol *295*, C288-292.

Arevalo, J. C., Pereira, D. B., Yano, H., Teng, K. K., and Chao, M. V. (2006). Identification of a switch in neurotrophin signaling by selective tyrosine phosphorylation. J Biol Chem *281*, 1001-1007.

Arnold, R., Patzak, I. M., Neuhaus, B., Vancauwenbergh, S., Veillette, A., Van Lint, J., and Kiefer, F. (2005). Activation of hematopoietic progenitor kinase 1 involves relocation, autophosphorylation, and transphosphorylation by protein kinase D1. Mol Cell Biol *25*, 2364-2383.

Auer, A., von Blume, J., Sturany, S., von Wichert, G., Van Lint, J., Vandenheede, J., Adler, G., and Seufferlein, T. (2005). Role of the regulatory domain of protein kinase D2 in phorbol ester binding, catalytic activity, and nucleocytoplasmic shuttling. Mol Biol Cell *16*, 4375-4385.

Avkiran, M., Rowland, A. J., Cuello, F., and Haworth, R. S. (2008). Protein kinase d in the cardiovascular system: emerging roles in health and disease. Circ Res *102*, 157-163.

Backs, J., Backs, T., Bezprozvannaya, S., McKinsey, T. A., and Olson, E. N. (2008). Histone deacetylase 5 acquires calcium/calmodulin-dependent kinase II responsiveness by oligomerization with histone deacetylase 4. Mol Cell Biol *28*, 3437-3445.

Backs, J., and Olson, E. N. (2006). Control of cardiac growth by histone acetylation/deacetylation. Circ Res *98*, 15-24.

Backs, J., Song, K., Bezprozvannaya, S., Chang, S., and Olson, E. N. (2006). CaM kinase II selectively signals to histone deacetylase 4 during cardiomyocyte hypertrophy. J Clin Invest *116*, 1853-1864.

Bagowski, C. P., Stein-Gerlach, M., Choidas, A., and Ullrich, A. (1999). Cell-type specific phosphorylation of threonines T654 and T669 by PKD defines the signal capacity of the EGF receptor. Embo J *18*, 5567-5576.

Bankaitis, V. A. (2002). Cell biology. Slick recruitment to the Golgi. Science *295*, 290-291.

Bard, F., and Malhotra, V. (2006). The formation of TGN-to-plasma-membrane transport carriers. Annu Rev Cell Dev Biol *22*, 439-455.

Baron, C. L., and Malhotra, V. (2002). Role of diacylglycerol in PKD recruitment to the TGN and protein transport to the plasma membrane. Science *295*, 325-328.

Baron, U., Freundlieb, S., Gossen, M., and Bujard, H. (1995). Co-regulation of two gene activities by tetracycline via a bidirectional promoter. Nucleic Acids Res *23*, 3605-3606.

Bassel-Duby, R., and Olson, E. N. (2006). Signaling pathways in skeletal muscle remodeling. Annu Rev Biochem *75*, 19-37.

Baubonis, W., and Sauer, B. (1993). Genomic targeting with purified Cre recombinase. Nucleic Acids Res *21*, 2025-2029.

Beck, J. A., Lloyd, S., Hafezparast, M., Lennon-Pierce, M., Eppig, J. T., Festing, M. F., and Fisher, E. M. (2000). Genealogies of mouse inbred strains. Nat Genet *24*, 23-25.

Beer, S., Scheikl, T., Reis, B., Huser, N., Pfeffer, K., and Holzmann, B. (2005). Impaired immune responses and prolonged allograft survival in Sly1 mutant mice. Mol Cell Biol *25*, 9646-9660.

Beer, S., Simins, A. B., Schuster, A., and Holzmann, B. (2001). Molecular cloning and characterization of a novel SH3 protein (SLY) preferentially expressed in lymphoid cells. Biochim Biophys Acta *1520*, 89-93.

Berdeaux, R., Goebel, N., Banaszynski, L., Takemori, H., Wandless, T., Shelton, G. D., and Montminy, M. (2007). SIK1 is a class II HDAC kinase that promotes survival of skeletal myocytes. Nat Med *13*, 597-603.

Berg, J. M., Tymoczko, J. L., Stryer, L., and Stryer, L. (2002). Biochemistry, 5th edn (New York: W.H. Freeman).

Besirli, C. G., and Johnson, E. M., Jr. (2006). The activation loop phosphorylation of protein kinase D is an early marker of neuronal DNA damage. J Neurochem *99*, 218-225.

Biliran, H., Jan, Y., Chen, R., Pasquale, E. B., and Ruoslahti, E. (2008). Protein kinase D is a positive regulator of bit1 apoptotic function. J Biol Chem in Press published on August 14, 2008 as doi:10.1074/jbc.M803139200.

Bisbal, M., Conde, C., Donoso, M., Bollati, F., Sesma, J., Quiroga, S., Diaz Anel, A., Malhotra, V., Marzolo, M. P., and Caceres, A. (2008). Protein kinase d regulates trafficking of dendritic membrane proteins in developing neurons. J Neurosci *28*, 9297-9308.

Bishop, J. O., and Smith, P. (1989). Mechanism of chromosomal integration of microinjected DNA. Mol Biol Med *6*, 283-298.

Bliss, J. M., Venkatesh, B., and Colicelli, J. (2006). The RIN family of Ras effectors. Methods Enzymol *407*, 335-344.

Bollag, W. B., Dodd, M. E., and Shapiro, B. A. (2004). Protein kinase D and keratinocyte proliferation. Drug News Perspect *17*, 117-126.

Bolli, R. (2007). Preconditioning: a paradigm shift in the biology of myocardial ischemia. Am J Physiol Heart Circ Physiol *292*, H19-27.

Bossard, C., Bresson, D., Polishchuk, R. S., and Malhotra, V. (2007). Dimeric PKD regulates membrane fission to form transport carriers at the TGN. J Cell Biol *179*, 1123-1131.

Bossuyt, J., Helmstadter, K., Wu, X., Clements-Jewery, H., Haworth, R. S., Avkiran, M., Martin, J. L., Pogwizd, S. M., and Bers, D. M. (2008). Ca2+/calmodulin-dependent protein kinase IIdelta and protein kinase D overexpression reinforce the histone deacetylase 5 redistribution in heart failure. Circ Res *102*, 695-702.

Bowden, E. T., Barth, M., Thomas, D., Glazer, R. I., and Mueller, S. C. (1999). An invasion-related complex of cortactin, paxillin and PKCmu associates with invadopodia at sites of extracellular matrix degradation. Oncogene *18*, 4440-4449.

Bracale, A., Cesca, F., Neubrand, V. E., Newsome, T. P., Way, M., and Schiavo, G. (2007). Kidins220/ARMS is transported by a kinesin-1-based mechanism likely to be involved in neuronal differentiation. Mol Biol Cell *18*, 142-152.

Bradford, M. D., and Soltoff, S. P. (2002). P2X7 receptors activate protein kinase D and p42/p44 mitogen-activated protein kinase (MAPK) downstream of protein kinase C. Biochem J *366*, 745-755.

Bradley, A., Evans, M., Kaufman, M. H., and Robertson, E. (1984). Formation of germ-line chimaeras from embryo-derived teratocarcinoma cell lines. Nature *309*, 255-256.

Brandlin, I., Hubner, S., Eiseler, T., Martinez-Moya, M., Horschinek, A., Hausser, A., Link, G., Rupp, S., Storz, P., Pfizenmaier, K., and Johannes, F. J. (2002). Protein kinase C (PKC)eta-mediated PKC mu activation modulates ERK and JNK signal pathways. J Biol Chem *277*, 6490-6496.

Bresler, T., Shapira, M., Boeckers, T., Dresbach, T., Futter, M., Garner, C. C., Rosenblum, K., Gundelfinger, E. D., and Ziv, N. E. (2004). Postsynaptic density assembly is fundamentally different from presynaptic active zone assembly. J Neurosci *24*, 1507-1520.

Brinster, R. L., Braun, R. E., Lo, D., Avarbock, M. R., Oram, F., and Palmiter, R. D. (1989). Targeted correction of a major histocompatibility class II E alpha gene by DNA microinjected into mouse eggs. Proc Natl Acad Sci U S A *86*, 7087-7091.

Brinster, R. L., Chen, H. Y., Trumbauer, M. E., Yagle, M. K., and Palmiter, R. D. (1985). Factors affecting the efficiency of introducing foreign DNA into mice by microinjecting eggs. Proc Natl Acad Sci U S A *82*, 4438-4442.

Brooks, G., Goss, M. W., Rozengurt, E., and Galinanes, M. (1997). Phorbol ester, but not ischemic preconditioning, activates protein kinase D in the rat heart. J Mol Cell Cardiol *29*, 2273-2283.

Buch, P. K., Bainbridge, J. W., and Ali, R. R. (2008). AAV-mediated gene therapy for retinal disorders: from mouse to man. Gene Ther *15*, 849-857.

Celil, A. B., and Campbell, P. G. (2005). BMP-2 and insulin- like growth factor-I mediate Osterix (Osx) expression in human mesenchymal stem cells via the MAPK and protein kinase D signaling pathways. J Biol Chem *280*, 31353-31359.

Chang, S., Bezprozvannaya, S., Li, S., and Olson, E. N. (2005). An expression screen reveals modulators of class II histone deacetylase phosphorylation. Proc Natl Acad Sci U S A *102*, 8120-8125.

Chang, S., McKinsey, T. A., Zhang, C. L., Richardson, J. A., Hill, J. A., and Olson, E. N. (2004). Histone deacetylases 5 and 9 govern responsiveness of the heart to a subset of stress signals and play redundant roles in heart development. Mol Cell Biol *24*, 8467-8476.

Chen, J., Deng, F., Singh, S. V., and Wang, Q. J. (2008). Protein kinase D3 (PKD3) contributes to prostate cancer cell growth and survival through a PKCepsilon/PKD3 pathway downstream of Akt and ERK 1/2. Cancer Res *68*, 3844-3853.

Chen, J., Lu, G., and Wang, Q. J. (2005). Protein kinase C-independent effects of protein kinase D3 in glucose transport in L6 myotubes. Mol Pharmacol *67*, 152-162.

Chiu, T., and Rozengurt, E. (2001) . PKD in intestinal epithelial cells: rapid activation by phorbol esters, LPA, and angiotensin through PKC. Am J Physiol Cell Physiol *280*, C929-942.

Cole, N. B., Sciaky, N., Marotta, A., Song, J., and Lippincott-Schwartz, J. (1996). Golgi dispersal during microtubule disruption: regeneration of Golgi stacks at peripheral endoplasmic reticulum exit sites. Mol Biol Cell *7*, 631-650.

Cortes, R. Y., Arevalo, J. C., Magby, J. P., Chao, M. V., and Plummer, M. R. (2007). Developmental and activity-dependent regulation of ARMS/Kidins220 in cultured rat hippocampal neurons. Dev Neurobiol *67*, 1687-1698.

Crawley, J. N. (2007). What's wrong with my mouse? : behavioral phenotyping of transgenic and knockout mice, 2nd edn (Hoboken, N.J.: Wiley-Interscience).

Cuello, F., Bardswell, S. C., Haworth, R. S., Yin, X., Lutz, S., Wieland, T., Mayr, M., Kentish, J. C., and Avkiran, M. (2007). Protein kinase D selectively targets cardiac troponin I and regulates myofilament Ca2+ sensitivity in ventricular myocytes. Circ Res *100*, 864-873.

De Matteis, M. A., and Luini, A. (2008). Exiting the Golgi complex. Nat Rev Mol Cell Biol *9*, 273-284.

Deatly, A. M., Taffs, R. E., McAuliffe, J. M., Nawoschik, S. P., Coleman, J. W., McMullen, G., Weeks-Levy, C., Johnson, A. J., and Racaniello, V. R. (1998). Characterization of mouse lines transgenic with the human poliovirus receptor gene. Microb Pathog *25*, 43-54.

Deininger, K., Eder, M., Kramer, E. R., Zieglgansberger, W., Dodt, H. U., Dornmair, K., Colicelli, J., and Klein, R. (2008). The Rab5 guanylate exchange factor Rin1 regulates endocytosis of the EphA4 receptor in mature excitatory neurons. Proc Natl Acad Sci U S A *105*, 12539-12544.

Dequiedt, F., Kasler, H., Fischle, W., Kiermer, V., Weinstein, M., Herndier, B. G., and Verdin, E. (2003). HDAC7, a thymus-specific class II histone deacetylase, regulates Nur77 transcription and TCR-mediated apoptosis. Immunity *18*, 687-698.

Dequiedt, F., Van Lint, J., Lecomte, E., Van Duppen, V., Seufferlein, T., Vandenheede, J. R., Wattiez, R., and Kettmann, R. (2005). Phosphorylation of histone deacetylase 7 by protein kinase D mediates T cell receptor-induced Nur77 expression and apoptosis. J Exp Med *201*, 793-804.

Dhaka, A., Costa, R. M., Hu, H., Irvin, D. K., Patel, A., Kornblum, H. I., Silva, A. J., O'Dell, T. J., and Colicelli, J. (2003). The RAS effector RIN1 modulates the formation of aversive memories. J Neurosci *23*, 748-757.

Diaz Anel, A. M., and Malhotra, V. (2005). PKCeta is required for beta1gamma2/beta3gamma2- and PKD-mediated transport to the cell surface and the organization of the Golgi apparatus. J Cell Biol *169*, 83-91.

Doppler, H., and Storz, P. (2007). A novel tyrosine phosphorylation site in protein kinase D contributes to oxidative stress-mediated activation. J Biol Chem *282*, 31873-31881.

Doppler, H., Storz, P., Li, J., Comb, M. J., and Toker, A. (2005). A phosphorylation state-specific antibody recognizes Hsp27, a novel substrate of protein kinase D. J Biol Chem *280*, 15013-15019.

Dresbach, T., Qualmann, B., Kessels, M. M., Garner, C. C., and Gundelfinger, E. D. (2001). The presynaptic cytomatrix of brain synapses. Cell Mol Life Sci *58*, 94-116.

Dressel, U., Bailey, P. J., Wang, S. C., Downes, M., Evans, R. M., and Muscat, G. E. (2001). A dynamic role for HDAC7 in MEF2-mediated muscle differentiation. J Biol Chem *276*, 17007-17013.

Egea, G., Lazaro-Dieguez, F., and Vilella, M. (2006). Actin dynamics at the Golgi complex in mammalian cells. Curr Opin Cell Biol *18*, 168-178.

Eiseler, T. (2006) Role of Protein Kinase D (PKD) in migration, invasion and cell adhesion of pancreas ductal adenocarcinoma cells, PhD Thesis. Institute of Cell Biology and Immunology, University of Stuttgart, Germany.

Eiseler, T., Schmid, M. A., Topbas, F., Pfizenmaier, K., and Hausser, A. (2007). PKD is recruited to sites of actin remodelling at the leading edge and negatively regulates cell migration. FEBS Lett *581*, 4279-4287.

Ellwanger, K. (2004) Expression and potential function of protein kinase D (PKD) during mouse development, Diploma Thesis. Institute of Cell Biology and Immunology, University of Stuttgart, Germany.

Ellwanger, K., Pfizenmaier, K., Lutz, S., and Hausser, A. (2008). Expression patterns of protein kinase D 3 during mouse development. BMC Dev Biol *8*, 47.

Endo, K., Oki, E., Biedermann, V., Kojima, H., Yoshida, K., Johannes, F. J., Kufe, D., and Datta, R. (2000). Proteolytic cleavage and activation of protein kinase C [micro] by caspase-3 in the apoptotic response of cells to 1-beta -D-arabinofuranosylcytosine and other genotoxic agents. J Biol Chem *275*, 18476-18481.

Erickson, R. P. (1999). Antisense transgenics in animals. Methods *18*, 304-310.

Ernest Dodd, M., Ristich, V. L., Ray, S., Lober, R. M., and Bollag, W. B. (2005). Regulation of protein kinase D during differentiation and proliferation of primary mouse keratinocytes. J Invest Dermatol *125*, 294-306.

Evans, I. M., Britton, G., and Zachary, I. C. (2008). Vascular endothelial growth factor induces heat shock protein (HSP) 27 serine 82 phosphorylation and endothelial tubulogenesis via protein kinase D and independent of p38 kinase. Cell Signal *20*, 1375-1384.

Fedorov, L. M., Tyrsin, O. Y., Krenn, V., Chernigovskaya, E. V., and Rapp, U. R. (2001). Tet-system for the regulation of gene expression during embryonic development. Transgenic Res *10*, 247-258.

Feng, H., Ren, M., and Rubin, C. S. (2006a). Conserved domains subserve novel mechanisms and functions in DKF-1, a Caenorhabditis elegans protein kinase D. J Biol Chem *281*, 17815-17826.

Feng, H., Ren, M., Wu, S. L., Hall, D. H., and Rubin, C. S. (2006b). Characterization of a novel protein kinase D: Caenorhabditis elegans DKF-1 is activated by translocation-phosphorylation and regulates movement and growth in vivo. J Biol Chem *281*, 17801-17814.

Fielitz, J., Kim, M. S., Shelton, J. M., Qi, X., Hill, J. A., Richardson, J. A., Bassel-Duby, R., and Olson, E. N. (2008). Requirement of protein kinase D1 for pathological cardiac remodeling. Proc Natl Acad Sci U S A *105*, 3059-3063.

Fuchs, Y. F., Pimpl, S. A., Link, G., Schlicker, O., Bunt, G., Pfizenmaier, K., and Hausser, A. (under review). A Golgi PKD activity reporter reveals a crucial role of PKD in nocodazole-induced Golgi dispersal.

Fugmann, T., Hausser, A., Schoffler, P., Schmid, S., Pfizenmaier, K., and Olayioye, M. A. (2007). Regulation of secretory transport by protein kinase D-mediated phosphorylation of the ceramide transfer protein. J Cell Biol *178*, 15-22.

Fujita, Y., and Okamoto, K. (2005). Golgi apparatus of the motor neurons in patients with amyotrophic lateral sclerosis and in mice models of amyotrophic lateral sclerosis. Neuropathology *25*, 388-394.

Funakoshi, Y., Ichiki, T., Takeda, K., Tokuno, T., Iino, N., and Takeshita, A. (2002). Critical role of cAMP-response element-binding protein for angiotensin II-induced hypertrophy of vascular smooth muscle cells. J Biol Chem *277*, 18710-18717.

Gailus-Durner, V., Fuchs, H., Becker, L., Bolle, I., Brielmeier, M., Calzada-Wack, J., Elvert, R., Ehrhardt, N., Dalke, C., Franz, T. J.*, et al.* (2005). Introducing the German Mouse Clinic: open access platform for standardized phenotyping. Nat Methods *2*, 403-404.

Gardiol, A., Racca, C., and Triller, A. (1999). Dendritic and postsynaptic protein synthetic machinery. J Neurosci *19*, 168-179.

Gautel, M., Furst, D. O., Cocco, A., and Schiaffino, S. (1998). Isoform transitions of the myosin binding protein C family in developing human and mouse muscles: lack of isoform transcomplementation in cardiac muscle. Circ Res *82*, 124-129.

Gauthier-Campbell, C., Bredt, D. S., Murphy, T. H., and El-Husseini Ael, D. (2004). Regulation of dendritic branching and filopodia formation in hippocampal neurons by specific acylated protein motifs. Mol Biol Cell *15*, 2205-2217.

Gerlai, R. (1996). Gene-targeting studies of mammalian behavior: is it the mutation or the background genotype? Trends Neurosci *19*, 177-181.

Ghanekar, Y., and Lowe, M. (2005). Protein kinase D: activation for Golgi carrier formation. Trends Cell Biol *15*, 511-514.

Gordon, J. W., Scangos, G. A., Plotkin, D. J., Barbosa, J. A., and Ruddle, F. H. (1980). Genetic transformation of mouse embryos by microinjection of purified DNA. Proc Natl Acad Sci U S A *77*, 7380-7384.

Gossen, M., and Bujard, H. (1992). Tight control of gene expression in mammalian cells by tetracycline-responsive promoters. Proc Natl Acad Sci U S A *89*, 5547-5551.

Gossen, M., and Bujard, H. (2002). Studying gene function in eukaryotes by conditional gene inactivation. Annu Rev Genet *36*, 153-173.

Gossen, M., Freundlieb, S., Bender, G., Muller, G., Hillen, W., and Bujard, H. (1995). Transcriptional activation by tetracyclines in mammalian cells. Science *268*, 1766-1769.

Gossler, A., Doetschman, T., Korn, R., Serfling, E., and Kemler, R. (1986). Transgenesis by means of blastocyst-derived embryonic stem cell lines. Proc Natl Acad Sci U S A *83*, 9065-9069.

Gschwendt, M., Johannes, F. J., Kittstein, W., and Marks, F. (1997). Regulation of protein kinase Cmu by basic peptides and heparin. Putative role of an acidic domain in the activation of the kinase. J Biol Chem *272*, 20742-20746.

Ha, C. H., Wang, W., Jhun, B. S., Wong, C., Hausser, A., Pfizenmaier, K., McKinsey, T. A., Olson, E. N., and Jin, Z. G. (2008). Protein kinase D-dependent phosphorylation and nuclear export of histone deacetylase 5 mediates vascular endothelial growth factor-induced gene expression and angiogenesis. J Biol Chem *283*, 14590-14599.

Hanks, M., Wurst, W., Anson-Cartwright, L., Auerbach, A. B., and Joyner, A. L. (1995). Rescue of the En-1 mutant phenotype by replacement of En-1 with En-2. Science *269*, 679-682.

Hanus, C., and Ehlers, M. D. (2008). Secretory Outposts for the Local Processing of Membrane Cargo in Neuronal Dendrites. Traffic.

Harrison, B. C., Kim, M. S., van Rooij, E., Plato, C. F., Papst, P. J., Vega, R. B., McAnally, J. A., Richardson, J. A., Bassel-Duby, R., Olson, E. N., and McKinsey, T. A. (2006). Regulation of cardiac stress signaling by protein kinase d1. Mol Cell Biol *26*, 3875-3888.

Hasan, M. T., Schonig, K., Berger, S., Graewe, W., and Bujard, H. (2001). Long-term, noninvasive imaging of regulated gene expression in living mice. Genesis *29*, 116-122.

Hausser, A., Link, G., Bamberg, L., Burzlaff, A., Lutz, S., Pfizenmaier, K., and Johannes, F. J. (2002). Structural requirements for localization and activation of protein kinase C mu (PKC mu) at the Golgi compartment. J Cell Biol *156*, 65-74.

Hausser, A., Link, G., Hoene, M., Russo, C., Selchow, O., and Pfizenmaier, K. (2006). Phospho-specific binding of 14-3-3 proteins to phosphatidylinositol 4-kinase III beta protects from dephosphorylation and stabilizes lipid kinase activity. J Cell Sci *119*, 3613-3621.

Hausser, A., Storz, P., Hubner, S., Braendlin, I., Martinez-Moya, M., Link, G., and Johannes, F. J. (2001). Protein kinase C mu selectively activates the mitogen-activated protein kinase (MAPK) p42 pathway. FEBS Lett *492*, 39-44.

Hausser, A., Storz, P., Link, G., Stoll, H., Liu, Y. C., Altman, A., Pfizenmaier, K., and Johannes, F. J. (1999). Protein kinase C mu is negatively regulated by 14-3-3 signal transduction proteins. J Biol Chem *274*, 9258-9264.

Hausser, A., Storz, P., Martens, S., Link, G., Toker, A., and Pfizenmaier, K. (2005). Protein kinase D regulates vesicular transport by phosphorylating and activating phosphatidylinositol-4 kinase IIIbeta at the Golgi complex. Nat Cell Biol *7*, 880-886.

Haussermann, S., Kittstein, W., Rincke, G., Johannes, F. J., Marks, F., and Gschwendt, M. (1999). Proteolytic cleavage of protein kinase Cmu upon induction of apoptosis in U937 cells. FEBS Lett *462*, 442-446.

Haworth, R. S., and Avkiran, M. (2001). Inhibition of protein kinase D by resveratrol. Biochem Pharmacol *62*, 1647-1651.

Haworth, R. S., Cuello, F., Herron, T. J., Franzen, G., Kentish, J. C., Gautel, M., and Avkiran, M. (2004). Protein kinase D is a novel mediator of cardiac troponin I phosphorylation and regulates myofilament function. Circ Res *95*, 1091-1099.

Haworth, R. S., Goss, M. W., Rozengurt, E., and Avkiran, M. (2000). Expression and activity of protein kinase D/protein kinase C mu in myocardium: evidence for alpha1-adrenergic receptor- and protein kinase C-mediated regulation. J Mol Cell Cardiol *32*, 1013-1023.

Haworth, R. S., Roberts, N. A., Cuello, F., and Avkiran, M. (2007). Regulation of protein kinase D activity in adult myocardium: novel counter-regulatory roles for protein kinase Cepsilon and protein kinase A. J Mol Cell Cardiol *43*, 686-695.

Hayashi, A., Seki, N., Hattori, A., Kozuma, S., and Saito, T. (1999). PKCnu, a new member of the protein kinase C family, composes a fourth subfamily with PKCmu. Biochim Biophys Acta *1450*, 99-106.

Hayashi, K., Ohshima, T., Hashimoto, M., and Mikoshiba, K. (2007). Pak1 regulates dendritic branching and spine formation. Dev Neurobiol *67*, 655-669.

Hofker, M. H., and Deursen, J. v. (2003). Transgenic mouse : methods and protocols (Totowa, N.J.: Humana Press).

Hollander, J. M., Martin, J. L., Belke, D. D., Scott, B. T., Swanson, E., Krishnamoorthy, V., and Dillmann, W. H. (2004). Overexpression of wild-type heat shock protein 27 and a nonphosphorylatable heat shock protein 27 mutant protects against ischemia/reperfusion injury in a transgenic mouse model. Circulation *110*, 3544-3552.

Horton, A. C., and Ehlers, M. D. (2003). Dual modes of endoplasmic reticulum-to-Golgi transport in dendrites revealed by live-cell imaging. J Neurosci *23*, 6188-6199.

Horton, A. C., and Ehlers, M. D. (2004). Secretory trafficking in neuronal dendrites. Nat Cell Biol *6*, 585-591.

Horton, A. C., Racz, B., Monson, E. E., Lin, A. L., Weinberg, R. J., and Ehlers, M. D. (2005). Polarized secretory trafficking directs cargo for asymmetric dendrite growth and morphogenesis. Neuron *48*, 757-771.

Hrabe de Angelis, M. H., Flaswinkel, H., Fuchs, H., Rathkolb, B., Soewarto, D., Marschall, S., Heffner, S., Pargent, W., Wuensch, K., Jung, M.*, et al.* (2000). Genome-wide, large-scale production of mutant mice by ENU mutagenesis. Nat Genet *25*, 444-447.

Hurd, C., and Rozengurt, E. (2001). Protein kinase D is sufficient to suppress EGF-induced c-Jun Ser 63 phosphorylation. Biochem Biophys Res Commun *282*, 404-408.

Hurd, C., Waldron, R. T., and Rozengurt, E. (2002). Protein kinase D complexes with C-Jun N-terminal kinase via activation loop phosphorylation and phosphorylates the C-Jun N-terminus. Oncogene *21*, 2154-2160.

Huynh, Q. K., and McKinsey, T. A. (2006). Protein kinase D directly phosphorylates histone deacetylase 5 via a random sequential kinetic mechanism. Arch Biochem Biophys *450*, 141-148.

Iglesias, T., Cabrera-Poch, N., Mitchell, M. P., Naven, T. J., Rozengurt, E., and Schiavo, G. (2000). Identification and cloning of Kidins220, a novel neuronal substrate of protein kinase D. J Biol Chem *275*, 40048-40056.

Iglesias, T., Matthews, S., and Rozengurt, E. (1998a). Dissimilar phorbol ester binding properties of the individual cysteine-rich motifs of protein kinase D. FEBS Lett *437*, 19-23.

Iglesias, T., and Rozengurt, E. (1998). Protein kinase D activation by mutations within its pleckstrin homology domain. J Biol Chem *273*, 410-416.

Iglesias, T., and Rozengurt, E. (1999). Protein kinase D activation by deletion of its cysteine-rich motifs. FEBS Lett *454*, 53-56.

Iglesias, T., Waldron, R. T., and Rozengurt, E. (1998b). Identification of in vivo phosphorylation sites required for protein kinase D activation. J Biol Chem *273*, 27662-27667.

Iwata, M., Maturana, A., Hoshijima, M., Tatematsu, K., Okajima, T., Vandenheede, J. R., Van Lint, J., Tanizawa, K., and Kuroda, S. (2005). PKCepsilon-PKD1 signaling complex at Z-discs plays a pivotal role in the cardiac hypertrophy induced by G-protein coupling receptor agonists. Biochem Biophys Res Commun *327*, 1105-1113.

Jaenisch, R., Harbers, K., Schnieke, A., Lohler, J., Chumakov, I., Jahner, D., Grotkopp, D., and Hoffmann, E. (1983). Germline integration of moloney murine leukemia virus at the Mov13 locus leads to recessive lethal mutation and early embryonic death. Cell *32*, 209-216.

Jaggi, M., Du, C., Zhang, W., and Balaji, K. C. (2007). Protein kinase D1: a protein of emerging translational interest. Front Biosci *12*, 3757-3767.

Jaggi, M., Rao, P. S., Smith, D. J., Wheelock, M. J., Johnson, K. R., Hemstreet, G. P., and Balaji, K. C. (2005). E-cadherin phosphorylation by protein kinase D1/protein kinase C{mu} is associated with altered cellular aggregation and motility in prostate cancer. Cancer Res *65*, 483-492.

Jamora, C., Yamanouye, N., Van Lint, J., Laudenslager, J., Vandenheede, J. R., Faulkner, D. J., and Malhotra, V. (1999). Gbetagamma- mediated regulation of Golgi organization is through the direct activation of protein kinase D. Cell *98*, 59-68.

Jareb, M., and Banker, G. (1997) . Inhibition of axonal growth by brefeldin A in hippocampal neurons in culture. J Neurosci *17*, 8955-8963.

Johannes, F. J., Horn, J., Link, G., Haas, E., Siemienski, K., Wajant, H., and Pfizenmaier, K. (1998). Protein kinase Cmu downregulation of tumor-necrosis-factor-induced apoptosis correlates with enhanced expression of nuclear-factor-kappaB-dependent protective genes. Eur J Biochem *257*, 47-54.

Johannes, F. J., Prestle, J., Dieterich, S., Oberhagemann, P., Link, G., and Pfizenmaier, K. (1995). Characterization of activators and inhibitors of protein kinase C mu. Eur J Biochem *227*, 303-307.

Johannes, F. J., Prestle, J., Eis, S., Oberhagemann, P., and Pfizenmaier, K. (1994). PKCμ is a novel, atypical member of the protein kinase C family. J Biol Chem *269*, 6140-6148.

Johannessen, M., Delghandi, M. P., Rykx, A., Dragset, M., Vandenheede, J. R., Van Lint, J., and Moens, U. (2007). Protein kinase D induces transcription through direct phosphorylation of the cAMP-response element-binding protein. J Biol Chem *282*, 14777-14787.

Keverne, E. B., Fundele, R., Narasimha, M., Barton, S. C., and Surani, M. A. (1996). Genomic imprinting and the differential roles of parental genomes in brain development. Brain Res Dev Brain Res *92*, 91-100.

Kim, M., Jang, H. R., Kim, J. H., Noh, S. M., Song, K. S., Cho, J. S., Jeong, H. Y., Norman, J. C., Caswell, P. T., Kang, G. H., *et al.* (2008a). Epigenetic inactivation of protein kinase D1 in gastric cancer and its role in gastric cancer cell migration and invasion. Carcinogenesis *29*, 629-637.

Kim, M. S., Fielitz, J., McAnally, J., Shelton, J. M., Lemon, D. D., McKinsey, T. A., Richardson, J. A., Bassel-Duby, R., and Olson, E. N. (2008b). Protein kinase D1 stimulates MEF2 activity in skeletal muscle and enhances muscle performance. Mol Cell Biol *28*, 3600-3609.

Kim, M. S., Wang, F., Puthanveetil, P., Kewalramani, G., Hosseini-Beheshti, E., Ng, N., Wang, Y., Kumar, U., Innis, S., Proud, C. G., *et al.* (2008c). Protein kinase D is a key regulator of cardiomyocyte lipoprotein lipase secretion after diabetes. Circ Res *103*, 252-260.

Kim, Y., Phan, D., van Rooij, E., Wang, D. Z., McAnally, J., Qi, X., Richardson, J. A., Hill, J. A., Bassel-Duby, R., and Olson, E. N. (2008d). The MEF2D transcription factor mediates stress-dependent cardiac remodeling in mice. J Clin Invest *118*, 124-132.

Kim, Y., Sung, J. Y., Ceglia, I., Lee, K. W., Ahn, J. H., Halford, J. M., Kim, A. M., Kwak, S. P., Park, J. B., Ho Ryu, S., *et al.* (2006). Phosphorylation of WAVE1 regulates actin polymerization and dendritic spine morphology. Nature *442*, 814-817.

Kioussis, D., and Festenstein, R. (1997). Locus control regions: overcoming heterochromatin-induced gene inactivation in mammals. Curr Opin Genet Dev *7*, 614-619.

Kistner, A. (1996) Etablierung Tetrazyklin-kontrollierter Expressionssysteme in transgenen Mäusen, PhD Thesis. University of Heidelberg, Germany.

Kistner, A., Gossen, M., Zimmermann, F., Jerecic, J., Ullmer, C., Lubbert, H., and Bujard, H. (1996). Doxycycline-mediated quantitative and tissue-specific control of gene expression in transgenic mice. Proc Natl Acad Sci U S A *93*, 10933-10938.

Knight, Z. A., and Shokat, K. M. (2007). Chemical genetics: where genetics and pharmacology meet. Cell *128*, 425-430.

Krenkler, J. (2008) Induzierbare und gewebespezifische Expression dominant-negativer PKD-Isoformen in vivo, Studienarbeit. Institute of Cell Biology and Immunology, University of Stuttgart, Germany.

Krumlauf, R., Hammer, R. E., Tilghman, S. M., and Brinster, R. L. (1985). Developmental regulation of alpha-fetoprotein genes in transgenic mice. Mol Cell Biol *5*, 1639-1648.

Kühn, R., and Schwenk, F. (2002). Conditional Knockout Mice, In Transgenic Mouse: Methods and Protocols, M. H. Hofker, and J. van Deursen, eds., pp. 159-185.

Lacy, E., Roberts, S., Evans, E. P., Burtenshaw, M. D., and Costantini, F. D. (1983). A foreign beta-globin gene in transgenic mice: integration at abnormal chromosomal positions and expression in inappropriate tissues. Cell *34*, 343-358.

Lein, P. J., Guo, X., Shi, G. X., Moholt-Siebert, M., Bruun, D., and Andres, D. A. (2007). The novel GTPase Rit differentially regulates axonal and dendritic growth. J Neurosci *27*, 4725-4736.

Lemonnier, J., Ghayor, C., Guicheux, J., and Caverzasio, J. (2004). Protein kinase C-independent activation of protein kinase D is involved in BMP-2-induced activation of stress

mitogen-activated protein kinases JNK and p38 and osteoblastic cell differentiation. J Biol Chem *279*, 259-264.

Lewandoski, M. (2001). Conditional control of gene expression in the mouse. Nat Rev Genet *2*, 743-755.

Li, J., Chen, L. A., Townsend, C. M., Jr., and Evers, B. M. (2008). PKD1, PKD2, and their substrate Kidins220 regulate neurotensin secretion in the BON human endocrine cell line. J Biol Chem *283*, 2614-2621.

Liljedahl, M., Maeda, Y., Colanzi, A., Ayala, I., Van Lint, J., and Malhotra, V. (2001). Protein kinase D regulates the fission of cell surface destined transport carriers from the trans-Golgi network. Cell *104*, 409-420.

Liu, Y., Randall, W. R., and Schneider, M. F. (2005). Activity-dependent and -independent nuclear fluxes of HDAC4 mediated by different kinases in adult skeletal muscle. J Cell Biol *168*, 887-897.

Lu, G., Chen, J., Espinoza, L. A., Garfield, S., Toshiyuki, S., Akiko, H., Huppler, A., and Wang, Q. J. (2007). Protein kinase D 3 is localized in vesicular structures and interacts with vesicle-associated membrane protein 2. Cell Signal *19*, 867-879.

Luiken, J. J., Vertommen, D., Coort, S. L., Habets, D. D., El Hasnaoui, M., Pelsers, M. M., Viollet, B., Bonen, A., Hue, L., Rider, M. H., and Glatz, J. F. (2008). Identification of protein kinase D as a novel contraction-activated kinase linked to GLUT4-mediated glucose uptake, independent of AMPK. Cell Signal *20*, 543-556.

Madeddu, P., Kraenkel, N., Barcelos, L. S., Siragusa, M., Campagnolo, P., Oikawa, A., Caporali, A., Herman, A., Azzolino, O., Barberis, L.*, et al.* (2008). Phosphoinositide 3-kinase gamma gene knockout impairs postischemic neovascularization and endothelial progenitor cell functions. Arterioscler Thromb Vasc Biol *28*, 68-76.

Maeda, Y., Beznoussenko, G. V., Van Lint, J., Mironov, A. A., and Malhotra, V. (2001). Recruitment of protein kinase D to the trans-Golgi network via the first cysteine-rich domain. Embo J *20*, 5982-5990.

Maier, D., Hausser, A., Nagel, A. C., Link, G., Kugler, S. J., Wech, I., Pfizenmaier, K., and Preiss, A. (2006). Drosophila protein kinase D is broadly expressed and a fraction localizes to the Golgi compartment. Gene Expr Patterns *6*, 849-856.

Maier, D., Nagel, A. C., Gloc, H., Hausser, A., Kugler, S. J., Wech, I., and Preiss, A. (2007). Protein kinase D regulates several aspects of development in Drosophila melanogaster. BMC Dev Biol *7*, 74.

Malleret, G., Haditsch, U., Genoux, D., Jones, M. W., Bliss, T. V., Vanhoose, A. M., Weitlauf, C., Kandel, E. R., Winder, D. G., and Mansuy, I. M. (2001). Inducible and reversible enhancement of learning, memory, and long-term potentiation by genetic inhibition of calcineurin. Cell *104*, 675-686.

Mandell, J. W., and Banker, G. A. (1996). A spatial gradient of tau protein phosphorylation in nascent axons. J Neurosci *16*, 5727-5740.

Manning, G., Whyte, D. B., Martinez, R., Hunter, T., and Sudarsanam, S. (2002). The protein kinase complement of the human genome. Science *298*, 1912-1934.

Mansour, S. L., Thomas, K. R., and Capecchi, M. R. (1988). Disruption of the proto-oncogene int-2 in mouse embryo-derived stem cells: a general strategy for targeting mutations to non-selectable genes. Nature *336*, 348-352.

Mansuy, I. M., and Bujard, H. (2000). Tetracycline-regulated gene expression in the brain. Curr Opin Neurobiol *10*, 593-596.

Mansuy, I. M., Mayford, M., Jacob, B., Kandel, E. R., and Bach, M. E. (1998a). Restricted and regulated overexpression reveals calcineurin as a key component in the transition from short-term to long-term memory. Cell *92*, 39-49.

Mansuy, I. M., Winder, D. G., Moallem, T. M., Osman, M., Mayford, M., Hawkins, R. D., and Kandel, E. R. (1998b). Inducible and reversible gene expression with the rtTA system for the study of memory. Neuron *21*, 257-265.

Mao, X., Fujiwara, Y., and Orkin, S. H. (1999). Improved reporter strain for monitoring Cre recombinase-mediated DNA excisions in mice. Proc Natl Acad Sci U S A *96*, 5037-5042.

Markel, P., Shu, P., Ebeling, C., Carlson, G. A., Nagle, D. L., Smutko, J. S., and Moore, K. J. (1997). Theoretical and empirical issues for marker-assisted breeding of congenic mouse strains. Nat Genet *17*, 280-284.

Marklund, U., Lightfoot, K., and Cantrell, D. (2003). Intracellular location and cell context-dependent function of protein kinase D. Immunity *19*, 491-501.

Matthews, S., Iglesias, T., Cantrell, D., and Rozengurt, E. (1999a). Dynamic re-distribution of protein kinase D (PKD) as revealed by a GFP-PKD fusion protein: dissociation from PKD activation. FEBS Lett *457*, 515-521.

Matthews, S. A., Dayalu, R., Thompson, L. J., and Scharenberg, A. M. (2003). Regulation of protein kinase Cnu by the B-cell antigen receptor. J Biol Chem *278*, 9086-9091.

Matthews, S. A., Iglesias, T., Rozengurt, E., and Cantrell, D. (2000a). Spatial and temporal regulation of protein kinase D (PKD). Embo J *19*, 2935-2945.

Matthews, S. A., Liu, P., Spitaler, M., Olson, E. N., McKinsey, T. A., Cantrell, D. A., and Scharenberg, A. M. (2006). Essential role for protein kinase D family kinases in the regulation of class II histone deacetylases in B lymphocytes. Mol Cell Biol *26*, 1569-1577.

Matthews, S. A., Pettit, G. R., and Rozengurt, E. (1997). Bryostatin 1 induces biphasic activation of protein kinase D in intact cells. J Biol Chem *272*, 20245-20250.

Matthews, S. A., Rozengurt, E., and Cantrell, D. (1999b). Characterization of serine 916 as an in vivo autophosphorylation site for protein kinase D/Protein kinase Cmu. J Biol Chem *274*, 26543-26549.

Matthews, S. A., Rozengurt, E., and Cantrell, D. (2000b). Protein kinase D. A selective target for antigen receptors and a downstream target for protein kinase C in lymphocytes. J Exp Med *191*, 2075-2082.

McCaffrey, A. P., Meuse, L., Pham, T. T., Conklin, D. S., Hannon, G. J., and Kay, M. A. (2002). RNA interference in adult mice. Nature *418*, 38-39.

McKinsey, T. A. (2007). Derepression of pathological cardiac genes by members of the CaM kinase superfamily. Cardiovasc Res *73*, 667-677.

McKinsey, T. A., Zhang, C. L., Lu, J., and Olson, E. N. (2000a). Signal-dependent nuclear export of a histone deacetylase regulates muscle differentiation. Nature *408*, 106-111.

McKinsey, T. A., Zhang, C. L., and Olson, E. N. (2000b). Activation of the myocyte enhancer factor-2 transcription factor by calcium/calmodulin-dependent protein kinase-stimulated binding of 14-3-3 to histone deacetylase 5. Proc Natl Acad Sci U S A *97*, 14400-14405.

Mendel, G. (1865). Versuche über Pflanzen-Hybriden. Verhandlungen des Naturforschenden Vereines in Brünn *Bd. IV.*, 3-47.

Metsaranta, M., Garofalo, S., Decker, G., Rintala, M., de Crombrugghe, B., and Vuorio, E. (1992). Chondrodysplasia in transgenic mice harboring a 15-amino acid deletion in the triple helical domain of pro alpha 1(II) collagen chain. J Cell Biol *118*, 203-212.

Michalon, A., Koshibu, K., Baumgartel, K., Spirig, D. H., and Mansuy, I. M. (2005). Inducible and neuron-specific gene expression in the adult mouse brain with the rtTA2S-M2 system. Genesis *43*, 205-212.

Mikkers, H., and Berns, A. (2003). Retroviral insertional mutagenesis: tagging cancer pathways. Adv Cancer Res *88*, 53-99.

Mochizuki, H., Miura, M., Shimada, T., and Mizuno, Y. (2002). Adeno-associated virus-mediated antiapoptotic gene delivery: in vivo gene therapy for neurological disorders. Methods *28*, 248-252.

Montagutelli, X. (2000). Effect of the genetic background on the phenotype of mouse mutations. J Am Soc Nephrol *11 Suppl 16*, S101-105.

Murphy, T. R., Legere, H. J., 3rd, and Katz, H. R. (2007). Activation of protein kinase D1 in mast cells in response to innate, adaptive, and growth factor signals. J Immunol *179*, 7876-7882.

Nagy, A. (2000). Cre recombinase: the universal reagent for genome tailoring. Genesis *26*, 99-109.

Nagy, A. (2003). Manipulating the mouse embryo : a laboratory manual, 3rd edn (Cold Spring Harbor, N.Y.: Cold Spring Harbor Laboratory Press).

Nakamura, N., Rabouille, C., Watson, R., Nilsson, T., Hui, N., Slusarewicz, P., Kreis, T. E., and Warren, G. (1995). Characterization of a cis-Golgi matrix protein, GM130. J Cell Biol *131*, 1715-1726.

Nishikawa, K., Toker, A., Johannes, F. J., Songyang, Z., and Cantley, L. C. (1997). Determination of the specific substrate sequence motifs of protein kinase C isozymes. J Biol Chem *272*, 952-960.

Novak, A., Guo, C., Yang, W., Nagy, A., and Lobe, C. G. (2000). Z/EG, a double reporter mouse line that expresses enhanced green fluorescent protein upon Cre-mediated excision. Genesis *28*, 147-155.

Opsahl, M. L., McClenaghan, M., Springbett, A., Reid, S., Lathe, R., Colman, A., and Whitelaw, C. B. (2002). Multiple effects of genetic background on variegated transgene expression in mice. Genetics *160*, 1107-1112.

Oster, H., Abraham, D., and Leitges, M. (2006). Expression of the protein kinase D (PKD) family during mouse embryogenesis. Gene Expr Patterns *6*, 400-408.

Palmiter, R. D., and Brinster, R. L. (1985). Transgenic mice. Cell *41*, 343-345.

Papazyan, R., Doche, M., Waldron, R. T., Rozengurt, E., Moyer, M. P., and Rey, O. (2008). Protein kinase D isozymes activation and localization during mitosis. Exp Cell Res *314*, 3057-3068.

Park, J. E., Kim, Y. I., and Yi, A. K. (2008). Protein kinase D1: a new component in TLR9 signaling. J Immunol *181*, 2044-2055.

Parra, M., Kasler, H., McKinsey, T. A., Olson, E. N., and Verdin, E. (2005). Protein kinase D1 phosphorylates HDAC7 and induces its nuclear export after T-cell receptor activation. J Biol Chem *280*, 13762-13770.

Peters, K., Werner, S., Liao, X., Wert, S., Whitsett, J., and Williams, L. (1994). Targeted expression of a dominant negative FGF receptor blocks branching morphogenesis and epithelial differentiation of the mouse lung. Embo J *13*, 3296-3301.

Pierce, J. P., Mayer, T., and McCarthy, J. B. (2001). Evidence for a satellite secretory pathway in neuronal dendritic spines. Curr Biol *11*, 351-355.

Potthoff, M. J., and Olson, E. N. (2007). MEF2: a central regulator of diverse developmental programs. Development *134*, 4131-4140.

Potthoff, M. J., Olson, E. N., and Bassel-Duby, R. (2007a). Skeletal muscle remodeling. Curr Opin Rheumatol *19*, 542-549.

Potthoff, M. J., Wu, H., Arnold, M. A., Shelton, J. M., Backs, J., McAnally, J., Richardson, J. A., Bassel-Duby, R., and Olson, E. N. (2007b). Histone deacetylase degradation and MEF2 activation promote the formation of slow-twitch myofibers. J Clin Invest *117*, 2459-2467.

Prestle, J., Pfizenmaier, K., Brenner, J., and Johannes, F. J. (1996). Protein kinase C mu is located at the Golgi compartment. J Cell Biol *134*, 1401-1410.

Prigozhina, N. L., and Waterman-Storer, C. M. (2004). Protein kinase D-mediated anterograde membrane trafficking is required for fibroblast motility. Curr Biol *14*, 88-98.

Qiang, Y. W., Yao, L., Tosato, G., and Rudikoff, S. (2004). Insulin-like growth factor I induces migration and invasion of human multiple myeloma cells. Blood *103*, 301-308.

Qin, L., Zeng, H., and Zhao, D. (2006). Requirement of protein kinase D tyrosine phosphorylation for VEGF-A165-induced angiogenesis through its interaction and regulation of phospholipase Cgamma phosphorylation. J Biol Chem *281*, 32550-32558.

Ray, P., Tang, W., Wang, P., Homer, R., Kuhn, C., 3rd, Flavell, R. A., and Elias, J. A. (1997). Regulated overexpression of interleukin 11 in the lung. Use to dissociate development-dependent and -independent phenotypes. J Clin Invest *100*, 2501-2511.

Reis, B. (2007) SLY1-Charakterisierung der Funktion und Rolle im Immunsystem, PhD Thesis. Institute of Medical Microbiology and Hospital Hygiene, Heinrich-Heine-University Düsseldorf, Germany.

Rennecke, J., Rehberger, P. A., Furstenberger, G., Johannes, F. J., Stohr, M., Marks, F., and Richter, K. H. (1999). Protein-kinase-Cmu expression correlates with enhanced keratinocyte proliferation in normal and neoplastic mouse epidermis and in cell culture. Int J Cancer *80*, 98-103.

Rey, O., Reeve, J. R., Jr., Zhukova, E., Sinnett-Smith, J., and Rozengurt, E. (2004). G protein-coupled receptor-mediated phosphorylation of the activation loop of protein kinase D: dependence on plasma membrane translocation and protein kinase Cepsilon. J Biol Chem *279*, 34361-34372.

Rey, O., Sinnett-Smith, J., Zhukova, E., and Rozengurt, E. (2001a). Regulated nucleocytoplasmic transport of protein kinase D in response to G protein-coupled receptor activation. J Biol Chem *276*, 49228-49235.

Rey, O., Young, S. H., Cantrell, D., and Rozengurt, E. (2001b). Rapid protein kinase D translocation in response to G protein-coupled receptor activation. Dependence on protein kinase C. J Biol Chem *276*, 32616-32626.

Rey, O., Yuan, J., Young, S. H., and Rozengurt, E. (2003). Protein kinase C nu/protein kinase D3 nuclear localization, catalytic activation, and intracellular redistribution in response to G protein-coupled receptor agonists. J Biol Chem *278*, 23773-23785.

Riol-Blanco, L., Iglesias, T., Sanchez -Sanchez, N., de la Rosa, G., Sanchez-Ruiloba, L., Cabrera-Poch, N., Torres, A., Longo, I., Garcia-Bordas, J., Longo, N.*, et al.* (2004). The neuronal protein Kidins220 localizes in a raft compartment at the leading edge of motile immature dendritic cells. Eur J Immunol *34*, 108-118.

Roberts, N. A., Haworth, R. S., and Avkiran, M. (2005). Effects of bisindolylmaleimide PKC inhibitors on p90RSK activity in vitro and in adult ventricular myocytes. Br J Pharmacol *145*, 477-489.

Robertson, E., Bradley, A., Kuehn, M., and Evans, M. (1986). Germ-line transmission of genes introduced into cultured pluripotential cells by retroviral vector. Nature *323*, 445-448.

Rose, A. J., Kiens, B., and Richter, E. A. (2006). Ca2+-calmodulin-dependent protein kinase expression and signalling in skeletal muscle during exercise. J Physiol *574*, 889-903.

Rosner, H., and Vacun, G. (1999). 1,2-dioctanoyl-s,n-glycerol-induced activation of protein kinase C results in striking, but reversible growth cone shape changes and an accumulation of f-actin and serine 41-phosphorylated GAP-43 in the axonal process. Eur J Cell Biol *78*, 698-706.

Rozengurt, E., Rey, O., and Waldron, R. T. (2005). Protein kinase D signaling. J Biol Chem *280*, 13205-13208.

Rülicke, T. (2004). Pronuclear Microinjection of Mouse Zygotes, In Germ Cell Protocols: Volume 2: Molecular Embryo Analysis, Live Imaging, Transgenesis, and Cloning (Humana Press), pp. 165-194.

Rykx, A., De Kimpe, L., Mikhalap, S., Vantus, T., Seufferlein, T., Vandenheede, J. R., and Van Lint, J. (2003). Protein kinase D: a family affair. FEBS Lett *546*, 81-86.

Sakai, K., and Miyazaki, J. (1997). A transgenic mouse line that retains Cre recombinase activity in mature oocytes irrespective of the cre transgene transmission. Biochem Biophys Res Commun *237*, 318-324.

Sanchez-Ruiloba, L., Cabrera -Poch, N., Rodriguez-Martinez, M., Lopez-Menendez, C., Jean-Mairet, R. M., Higuero, A. M., and Iglesias, T. (2006). Protein kinase D intracellular localization and activity control kinase D-interacting substrate of 220-kDa traffic through a postsynaptic density-95/discs large/zonula occludens-1-binding motif. J Biol Chem *281*, 18888-18900.

Schmidt, J. T., Fleming, M. R., and Leu, B. (2004). Presynaptic protein kinase C controls maturation and branch dynamics of developing retinotectal arbors: possible role in activity-driven sharpening. J Neurobiol *58*, 328-340.

Schönig, K., and Bujard, H. (2002). Generating Conditional Mouse Mutants via Tetracycline-Controlled Gene Expression, In Transgenic Mouse: Methods and Protocols, M. H. Hofker, and J. van Deursen, eds., pp. 69-104.

Shaw-White, J. R., Denko, N., Albers, L., Doetschman, T. C., and Stringer, J. R. (1993). Expression of the lacZ gene targeted to the HPRT locus in embryonic stem cells and their derivatives. Transgenic Res *2*, 1-13.

Sheng, M. (2001). Molecular organization of the postsynaptic specialization. Proc Natl Acad Sci U S A *98*, 7058-7061.

Shin, M. K., Levorse, J. M., Ingram, R. S., and Tilghman, S. M. (1999). The temporal requirement for endothelin receptor-B signalling during neural crest development. Nature *402*, 496-501.

Sidorenko, S. P., Law, C. L., Klaus, S. J., Chandran, K. A., Takata, M., Kurosaki, T., and Clark, E. A. (1996). Protein kinase C mu (PKC mu) associates with the B cell antigen receptor complex and regulates lymphocyte signaling. Immunity *5*, 353-363.

Siegel, G. J. (1999). Basic neurochemistry : molecular, cellular and medical aspects, 6th edn (Philadelphia: Lippincott-Raven Publishers).

Silverman, M. A., Kaech, S., Jareb, M., Burack, M. A., Vogt, L., Sonderegger, P., and Banker, G. (2001). Sorting and directed transport of membrane proteins during development of hippocampal neurons in culture. Proc Natl Acad Sci U S A *98*, 7051-7057.

Sinnett-Smith, J., Zhukova, E., Hsieh, N., Jiang, X., and Rozengurt, E. (2004) . Protein kinase D potentiates DNA synthesis induced by Gq-coupled receptors by increasing the duration of ERK signaling in swiss 3T3 cells. J Biol Chem *279*, 16883-16893.

Sokol, D. L., and Murray, J. D. (1996). Antisense and ribozyme constructs in transgenic animals. Transgenic Res *5*, 363-371.

Southern, E. M. (1975). Detection of specific sequences among DNA fragments separated by gel electrophoresis. J Mol Biol *98*, 503-517.

Spankuch, B., and Strebhardt, K. (2005). RNA interference -based gene silencing in mice: the development of a novel therapeutical strategy. Curr Pharm Des *11*, 3405-3419.

Spitaler, M., Emslie, E., Wood, C. D., and Cantrell, D. (2006). Diacylglycerol and protein kinase D localization during T lymphocyte activation. Immunity *24*, 535-546.

Srinivas, S., Watanabe, T., Lin, C. S., William, C. M., Tanabe, Y., Jessell, T. M., and Costantini, F. (2001). Cre reporter strains produced by targeted insertion of EYFP and ECFP into the ROSA26 locus. BMC Dev Biol *1*, 4.

Stacey, A., Bateman, J., Choi, T., Mascara, T., Cole, W., and Jaenisch, R. (1988). Perinatal lethal osteogenesis imperfecta in transgenic mice bearing an engineered mutant pro-alpha 1(I) collagen gene. Nature *332*, 131-136.

Stafford, M. J., Watson, S. P., and Pears, C. J. (2003). PKD: a new protein kinase C-dependent pathway in platelets. Blood *101*, 1392-1399.

Stanford, W. L., Cohn, J. B., and Cordes, S. P. (2001). Gene-trap mutagenesis: past, present and beyond. Nat Rev Genet *2*, 756-768.

Steegmaier, M., Klumperman, J., Foletti, D. L., Yoo, J. S., and Scheller, R. H. (1999). Vesicle-associated membrane protein 4 is implicated in trans-Golgi network vesicle trafficking. Mol Biol Cell *10*, 1957-1972.

Storz, P. (2007). Mitochondrial ROS--radical detoxification, mediated by protein kinase D. Trends Cell Biol *17*, 13-18.

Storz, P., Doppler, H., Johannes, F. J., and Toker, A. (2003). Tyrosine phosphorylation of protein kinase D in the pleckstrin homology domain leads to activation. J Biol Chem *278*, 17969-17976.

Storz, P., Doppler, H., and Toker, A. (2004). Protein kinase Cdelta selectively regulates protein kinase D-dependent activation of NF-kappaB in oxidative stress signaling. Mol Cell Biol *24*, 2614-2626.

Storz, P., Doppler, H., and Toker, A. (2005). Protein kinase D mediates mitochondrion-to-nucleus signaling and detoxification from mitochondrial reactive oxygen species. Mol Cell Biol *25*, 8520-8530.

Storz, P., and Toker, A. (2003). Protein kinase D mediates a stress-induced NF-kappaB activation and survival pathway. Embo J *22*, 109-120.

Sturany, S., Van Lint, J., Gilchrist, A., Vandenheede, J. R., Adler, G., and Seufferlein, T. (2002). Mechanism of activation of protein kinase D2(PKD2) by the CCK(B)/gastrin receptor. J Biol Chem *277*, 29431-29436.

Sturany, S., Van Lint, J., Muller, F., Wilda, M., Hameister, H., Hocker, M., Brey, A., Gern, U., Vandenheede, J., Gress, T. *, et al.* (2001). Molecular cloning and characterization of the human protein kinase D2. A novel member of the protein kinase D family of serine threonine kinases. J Biol Chem *276*, 3310-3318.

Sytnyk, V., Leshchyns'ka, I., Delling, M., Dityateva, G., Dityatev, A., and Schachner, M. (2002). Neural cell adhesion molecule promotes accumulation of TGN organelles at sites of neuron-to-neuron contacts. J Cell Biol *159*, 649-661.

Tada, T., Simonetta, A., Batterton, M., Kinoshita, M., Edbauer, D., and Sheng, M. (2007). Role of Septin cytoskeleton in spine morphogenesis and dendrite development in neurons. Curr Biol *17*, 1752-1758.

Takamine, K., Okamoto, K., Fujita, Y., Sakurai, A., Takatama, M., and Gonatas, N. K. (2000). The involvement of the neuronal Golgi apparatus and trans-Golgi network in the human olivary hypertrophy. J Neurol Sci *182*, 45-50.

Takeda, J., Keng, V. W., and Horie, K. (2007). Germline mutagenesis mediated by Sleeping Beauty transposon system in mice. Genome Biol *8 Suppl 1*, S14.

Takemoto -Kimura, S., Ageta-Ishihara, N., Nonaka, M., Adachi -Morishima, A., Mano, T., Okamura, M., Fujii, H., Fuse, T., Hoshino, M., Suzuki, S.*, et al.* (2007). Regulation of dendritogenesis via a lipid-raft-associated Ca2+/calmodulin-dependent protein kinase CLICK-III/CaMKIgamma. Neuron *54*, 755-770.

Tan, M., Xu, X., Ohba, M., and Cui, M. Z. (2004). Angiotensin II-induced protein kinase D activation is regulated by protein kinase Cdelta and mediated via the angiotensin II type 1 receptor in vascular smooth muscle cells. Arterioscler Thromb Vasc Biol *24*, 2271-2276.

Tan, M., Xu, X., Ohba, M., Ogawa, W., and Cui, M. Z. (2003). Thrombin rapidly induces protein kinase D phosphorylation, and protein kinase C delta mediates the activation. J Biol Chem *278*, 2824-2828.

Tang, B. L. (2008). Emerging aspects of membrane traffic in neuronal dendrite growth. Biochim Biophys Acta *1783*, 169-176.

Taya, S., Shinoda, T., Tsuboi, D., Asaki, J., Nagai, K., Hikita, T., Kuroda, S., Kuroda, K., Shimizu, M., Hirotsune, S.*, et al.* (2007). DISC1 regulates the transport of the NUDEL/LIS1/14-3-3epsilon complex through kinesin-1. J Neurosci *27*, 15-26.

Thomas, W., McEneaney, V., and Harvey, B. J. (2008). Aldosterone-induced signalling and cation transport in the distal nephron. Steroids *73*, 979-984.

Townes, T. M., Lingrel, J. B., Chen, H. Y., Brinster, R. L., and Palmiter, R. D. (1985). Erythroid-specific expression of human beta-globin genes in transgenic mice. Embo J *4*, 1715-1723.

Tran, T. H., Zeng, Q., and Hong, W. (2007). VAMP4 cycles from the cell surface to the trans-Golgi network via sorting and recycling endosomes. J Cell Sci *120*, 1028-1041.

Trauzold, A., Schmiedel, S., Sipos, B., Wermann, H., Westphal, S., Roder, C., Klapper, W., Arlt, A., Lehnert, L., Ungefroren, H.*, et al.* (2003). PKCmu prevents CD95-mediated apoptosis and enhances proliferation in pancreatic tumour cells. Oncogene *22*, 8939-8947.

Tsybouleva, N., Zhang, L., Chen, S., Patel, R., Lutucuta, S., Nemoto, S., DeFreitas, G., Entman, M., Carabello, B. A., Roberts, R., and Marian, A. J. (2004). Aldosterone, through novel signaling proteins, is a fundamental molecular bridge between the genetic defect and the cardiac phenotype of hypertrophic cardiomyopathy. Circulation *109*, 1284-1291.

Uetani, N., Chagnon, M. J., Kennedy, T. E., Iwakura, Y., and Tremblay, M. L. (2006). Mammalian motoneuron axon targeting requires receptor protein tyrosine phosphatases sigma and delta. J Neurosci *26*, 5872-5880.

Urlinger, S., Baron, U., Thellmann, M., Hasan, M. T., Bujard, H., and Hillen, W. (2000). Exploring the sequence space for tetracycline-dependent transcriptional activators: novel mutations yield expanded range and sensitivity. Proc Natl Acad Sci U S A *97*, 7963-7968.

Valdar, W., Solberg, L. C., Gauguier, D., Cookson, W. O., Rawlins, J. N., Mott, R., and Flint, J. (2006). Genetic and environmental effects on complex traits in mice. Genetics *174*, 959-984.

Valverde, A. M., Sinnett-Smith, J., Van Lint, J., and Rozengurt, E. (1994). Molecular cloning and characterization of protein kinase D: a target for diacylglycerol and phorbol esters with a distinctive catalytic domain. Proc Natl Acad Sci U S A *91*, 8572-8576.

Van Lint, J., Ni, Y., Valius, M., Merlevede, W., and Vandenheede, J. R. (1998). Platelet-derived growth factor stimulates protein kinase D through the activation of phospholipase Cgamma and protein kinase C. J Biol Chem *273*, 7038-7043.

Van Lint, J., Rykx, A., Maeda, Y., Vantus, T., Sturany, S., Malhotra, V., Vandenheede, J. R., and Seufferlein, T. (2002). Protein kinase D: an intracellular traffic regulator on the move. Trends Cell Biol *12*, 193-200.

Van Lint, J. V., Sinnett- Smith, J., and Rozengurt, E. (1995) . Expression and characterization of PKD, a phorbol ester and diacylglycerol-stimulated serine protein kinase. J Biol Chem *270*, 1455-1461.

Vantus, T., Vertommen, D., Saelens, X., Rykx, A., De Kimpe, L., Vancauwenbergh, S., Mikhalap, S., Waelkens, E., Keri, G., Seufferlein, T.*, et al.* (2004). Doxorubicin-induced activation of protein kinase D1 through caspase-mediated proteolytic cleavage: identification of two cleavage sites by microsequencing. Cell Signal *16*, 703-709.

Vega, R. B., Harrison, B. C., Meadows, E., Roberts, C. R., Papst, P. J., Olson, E. N., and McKinsey, T. A. (2004). Protein kinases C and D mediate agonist-dependent cardiac hypertrophy through nuclear export of histone deacetylase 5. Mol Cell Biol *24*, 8374-8385.

Vertommen, D., Rider, M., Ni, Y., Waelkens, E., Merlevede, W., Vandenheede, J. R., and Van Lint, J. (2000). Regulation of protein kinase D by multisite phosphorylation. Identification of phosphorylation sites by mass spectrometry and characterization by site-directed mutagenesis. J Biol Chem *275*, 19567-19576.

von Blume, J., Knippschild, U., Dequiedt, F., Giamas, G., Beck, A., Auer, A., Van Lint, J., Adler, G., and Seufferlein, T. (2007). Phosphorylation at Ser244 by CK1 determines nuclear localization and substrate targeting of PKD2. Embo J *26*, 4619-4633.

von Wichert, G., Edenfeld, T., von Blume, J., Krisp, H., Krndija, D., Schmid, H., Oswald, F., Lother, U., Walther, P., Adler, G., and Seufferlein, T. (2008). Protein kinase D2 regulates chromogranin A secretion in human BON neuroendocrine tumour cells. Cell Signal *20*, 925-934.

Voncken, J. W. (2002). Genetic Modification of the Mouse, In Transgenic Mouse: Methods and Protocols, M. H. Hofker, and J. van Deursen, eds., pp. 9-34.

Wagner, E. F., Covarrubias, L., Stewart, T. A., and Mintz, B. (1983). Prenatal lethalities in mice homozygous for human growth hormone gene sequences integrated in the germ line. Cell *35*, 647-655.

Waldron, R. T., Rey, O., Iglesias, T., Tugal, T., Cantrell, D., and Rozengurt, E. (2001). Activation loop Ser744 and Ser748 in protein kinase D are transphosphorylated in vivo. J Biol Chem *276*, 32606-32615.

Waldron, R. T., Rey, O., Zhukova, E., and Rozengurt, E. (2004). Oxidative stress induces protein kinase C-mediated activation loop phosphorylation and nuclear redistribution of protein kinase D. J Biol Chem *279*, 27482-27493.

Waldron, R. T., and Rozengurt, E. (2000). Oxidative stress induces protein kinase D activation in intact cells. Involvement of Src and dependence on protein kinase C. J Biol Chem *275*, 17114-17121.

Waldron, R. T., and Rozengurt, E. (2003). Protein kinase C phosphorylates protein kinase D activation loop Ser744 and Ser748 and releases autoinhibition by the pleckstrin homology domain. J Biol Chem *278*, 154-163.

Wang, L., and Wang, D. H. (2005). TRPV1 gene knockout impairs postischemic recovery in isolated perfused heart in mice. Circulation *112*, 3617-3623.

Wang, Q., and Wadsworth, W. G. (2002). The C domain of netrin UNC- 6 silences calcium/calmodulin-dependent protein kinase- and diacylglycerol-dependent axon branching in Caenorhabditis elegans. J Neurosci *22*, 2274-2282.

Wang, Q. J. (2006). PKD at the crossroads of DAG and PKC signaling. Trends Pharmacol Sci *27*, 317-323.

Wang, S., Li, X., Parra, M., Verdin, E., Bassel-Duby, R., and Olson, E. N. (2008). Control of endothelial cell proliferation and migration by VEGF signaling to histone deacetylase 7. Proc Natl Acad Sci U S A *105*, 7738-7743.

Wang, Y., Kedei, N., Wang, M., Wang, Q. J., Huppler, A. R., Toth, A., Tran, R., and Blumberg, P. M. (2004). Interaction between protein kinase Cmu and the vanilloid receptor type 1. J Biol Chem *279*, 53674-53682.

Wang, Y., Waldron, R. T., Dhaka, A., Patel, A., Riley, M. M., Rozengurt, E., and Colicelli, J. (2002). The RAS effector RIN1 directly competes with RAF and is regulated by 14-3-3 proteins. Mol Cell Biol *22*, 916-926.

Waters, R. E., Rotevatn, S., Li, P., Annex, B. H., and Yan, Z. (2004). Voluntary running induces fiber type-specific angiogenesis in mouse skeletal muscle. Am J Physiol Cell Physiol *287*, C1342-1348.

Wiekowski, M. T., Chen, S. C., Zalamea, P., Wilburn, B. P., Kinsley, D. J., Sharif, W. W., Jensen, K. K., Hedrick, J. A., Manfra, D., and Lira, S. A. (2001). Disruption of neutrophil migration in a conditional transgenic model: evidence for CXCR2 desensitization in vivo. J Immunol *167*, 7102-7110.

Wilkie, T. M., Brinster, R. L., and Palmiter, R. D. (1986). Germline and somatic mosaicism in transgenic mice. Dev Biol *118*, 9-18.

Winckler, B., and Mellman, I. (1999). Neuronal polarity: controlling the sorting and diffusion of membrane components. Neuron *23*, 637-640.

Wong, C., and Jin, Z. G. (2005). Protein kinase C-dependent protein kinase D activation modulates ERK signal pathway and endothelial cell proliferation by vascular endothelial growth factor. J Biol Chem *280*, 33262-33269.

Wong, G. T. (2002). Speed congenics: applications for transgenic and knock-out mouse strains. Neuropeptides *36*, 230-236.

Woychik, R. P., and Alagramam, K. (1998). Insertional mutagenesis in transgenic mice generated by the pronuclear microinjection procedure. Int J Dev Biol *42*, 1009-1017.

Woychik, R. P., Stewart, T. A., Davis, L. G., D'Eustachio, P., and Leder, P. (1985). An inherited limb deformity created by insertional mutagenesis in a transgenic mouse. Nature *318*, 36-40.

Wu, H., Kanatous, S. B., Thurmond, F. A., Gallardo, T., Isotani, E., Bassel-Duby, R., and Williams, R. S. (2002). Regulation of mitochondrial biogenesis in skeletal muscle by CaMK. Science *296*, 349-352.

Wu, H., Rothermel, B., Kanatous, S., Rosenberg, P., Naya, F. J., Shelton, J. M., Hutcheson, K. A., DiMaio, J. M., Olson, E. N., Bassel-Duby, R., and Williams, R. S. (2001). Activation of MEF2 by muscle activity is mediated through a calcineurin-dependent pathway. Embo J *20*, 6414-6423.

Xu, X., Ha, C. H., Wong, C., Wang, W., Hausser, A., Pfizenmaier, K., Olson, E. N., McKinsey, T. A., and Jin, Z. G. (2007). Angiotensin II stimulates protein kinase D-dependent histone deacetylase 5 phosphorylation and nuclear export leading to vascular smooth muscle cell hypertrophy. Arterioscler Thromb Vasc Biol *27*, 2355-2362.

Yamamura, K., and Araki, K. (2008). Gene trap mutagenesis in mice: new perspectives and tools in cancer research. Cancer Sci *99*, 1-6.

Yang, W., and Storrie, B. (1998). Scattered Golgi elements during microtubule disruption are initially enriched in trans-Golgi proteins. Mol Biol Cell *9*, 191-207.

Ye, B., Zhang, Y., Song, W., Younger, S. H., Jan, L. Y., and Jan, Y. N. (2007). Growing dendrites and axons differ in their reliance on the secretory pathway. Cell *130*, 717-729.

Yeaman, C., Ayala, M. I., Wright, J. R., Bard, F., Bossard, C., Ang, A., Maeda, Y., Seufferlein, T., Mellman, I., Nelson, W. J., and Malhotra, V. (2004). Protein kinase D regulates basolateral membrane protein exit from trans-Golgi network. Nat Cell Biol *6*, 106-112.

Yin, D. M., Huang, Y. H., Zhu, Y. B., and Wang, Y. (2008). Both the establishment and maintenance of neuronal polarity require the activity of protein kinase D in the Golgi apparatus. J Neurosci *28*, 8832-8843.

Yoshiki, A., and Moriwaki, K. (2006). Mouse phenome research: implications of genetic background. Ilar J *47*, 94-102.

Yuan, J., Rey, O., and Rozengurt, E. (2005). Protein kinase D3 activation and phosphorylation by signaling through G alpha q. Biochem Biophys Res Commun *335*, 270-276.

Yuan, J., Rey, O., and Rozengurt, E. (2006). Activation of protein kinase D3 by signaling through Rac and the alpha subunits of the heterotrimeric G proteins G12 and G13. Cell Signal *18*, 1051-1062.

Yuan, J., Slice, L., Walsh, J. H., and Rozengurt, E. (2000). Activation of protein kinase D by signaling through the alpha subunit of the heterotrimeric G protein G(q). J Biol Chem *275*, 2157-2164.

Zhang, C. L., McKinsey, T. A., Chang, S., Antos, C. L., Hill, J. A., and Olson, E. N. (2002). Class II histone deacetylases act as signal-responsive repressors of cardiac hypertrophy. Cell *110*, 479-488.

Zhang, H., and Macara, I. G. (2008). The PAR-6 polarity protein regulates dendritic spine morphogenesis through p190 RhoGAP and the Rho GTPase. Dev Cell *14*, 216-226.

Zhang, W., Zheng, S., Storz, P., and Min, W. (2005). Protein kinase D specifically mediates apoptosis signal-regulating kinase 1-JNK signaling induced by H2O2 but not tumor necrosis factor. J Biol Chem *280*, 19036-19044.

Zhukova, E., Sinnett-Smith, J., and Rozengurt, E. (2001). Protein kinase D potentiates DNA synthesis and cell proliferation induced by bombesin, vasopressin, or phorbol esters in Swiss 3T3 cells. J Biol Chem *276*, 40298-40305.

Zmuda, J. F., and Rivas, R. J. (1998). The Golgi apparatus and the centrosome are localized to the sites of newly emerging axons in cerebellar granule neurons in vitro. Cell Motil Cytoskeleton *41*, 18-38.

Zugaza, J. L., Sinnett-Smith, J., Van Lint, J., and Rozengurt, E. (1996). Protein kinase D (PKD) activation in intact cells through a protein kinase C-dependent signal transduction pathway. Embo J *15*, 6220-6230.

Zugaza, J. L., Waldron, R. T., Sinnett-Smith, J., and Rozengurt, E. (1997). Bombesin, vasopressin, endothelin, bradykinin, and platelet-derived growth factor rapidly activate protein kinase D through a protein kinase C-dependent signal transduction pathway. J Biol Chem *272*, 23952-23960.

Abbreviations

Abl	Abelson tyrosine kinase
Amp	Ampicillin
Ang II	Angiotensin II
AP	Alkaline phosphatase
APC	Antigen-presenting cell
APS	Ammonium persulfate
ARMS	Ankyrin repeat-rich membrane spanning
ASK	Apoptosis signal-regulating kinase
ATP	Adenosine triphosphate
Bcl-2	B cell lymphoma 2
BCR	B cell receptor
Bit1	Bcl-2 inhibitor of transcription
BMP	Bone morphogenic protein
bp	Base pairs
BSA	Bovine serum albumin
ca	Constitutively active mutant
CA	Cornu Ammonis area
CaMK	calcium/calmodulin-dependent protein kinase
cAMP	Cyclic adenosine monophosphate
cDNA	complementary DNA
CERT	Ceramide Transport Protein
c-FLIP	Cellular FLICE (caspase 8)-like inhibitory protein
CMV	Cytomegalovirus
cMyBP-C	Cardiac myosin-binding protein C
cpm	Counts per minute
CRD	Cystein rich domain
CREB	cAMP-response element-binding
cTnI	cardiac troponin I
DAG	Diacylglycerol
dCTP	Deoxycytidine triphosphate
ddH_2O	Double distilled H_2O
DG	Dentate gyrus
DIG	Digoxigenin
DIV	Days *in vitro*
DNA	Deoxyribonucleic acid
dNTP	Deoxynucleotide
Dox	Doxycycline
dpc	days post coitum
ECL	Enhanced chemiluminescence
EDTA	Ethylendiamintetraacetate
EGF	Epidermal growth factor
EGFP	Enhanced green fluorescent protein
EGTA	ethylene glycol tetraacetic acid

ERK	extracellular signal-regulated kinases
ES	Embryonic stem
Fab	Fragment of antigen binding
FCS	Fetal calf serum
Fig	Figure
g	gravity
GFP	Green fluorescent protein
GPCR	G-protein coupled receptor
h	Hour
hCG	human chorionic gonadotropin
hCMV	Human cytomegalovirus
HDAC	Histone deacetylase
HPK1	Hematopoietic progenitor kinase 1
HRP	Horseradish peroxidase
HSP	Heat shock protein
HUVEC	Human umbilical vein endothelial cells
IB	Immunoblot
Ig	Immunoglobulin
IGF-I	Insulin growth factor I
IHC	Immunohistochemistry
IκB	Inhibitor of NF-κB
IKK	IκB kinase
IL	Interleukin
i.p.	Intraperitoneal
IP_3	Inositol-1,4,5-triphosphate
IU	Injection unit
JNK	c-Jun N-terminal kinase
kb	Kilo base pairs
kd	Kinase-dead mutant
kDa	Kilodalton
Kidins220	Kinase D-interacting substrate of 220 kDa
Lab	Laboratory
LB	Lysogeny broth
M	Molar [mol/l]
MAPK	mitogen activated protein kinase
MEF2	Myocyte enhancer factor-2
MEK	mitogen activated protein kinase/ERK kinase
min	Minute(s)
MnSOD	Manganese-dependent superoxide dismutase
mRNA	Messenger ribonucleic acid
MyD88	Myeloid differentiation primary response gene 88
NES	Nuclear export signals
NF-κB	Nuclear factor kappaB
NLS	Nuclear localization sequence
NR4A1	Nuclear receptor subfamily 4, group A, member 1
Nur77	Nerve Growth factor IB

Osx	Osterix
P2X7	Purinergic receptor P2X ligand-gated ion channel 7
PAGE	Polyacrylamide gel electrophoresis
PBS	Phosphate buffered saline
PCR	Polymerase chain reaction
PdBU	phorbol 12,13-dibutyrate
PDGF	Platelet derived growth factor
PDZ	postsynaptic density-95/discs large/zonula occludens-1-binding motif
PEV	Position-effect variegation
PFA	para-formaldehyde
PH	Pleckstrin homology
PI4KIIIβ	Phosphatidylinositol 4-kinase IIIβ
PIP_2	Phosphatidylinositol-4,5-bisphosphate
PKC	Protein kinase C
PKD	Protein kinase D
PLC	Phospholipase C
PLL	Poly-L-lysine
PMSG	Pregnant mare serum gonadotropin
RIN1	Ras and Rab interactor 1
RNA	Ribonucleic acid
RNAi	RNA interference
ROS	Reactive oxygen species
rpm	Revolutions per minute
rtetR	Reverse tetracycline repressor
rtTA	Reverse tetracycline transactivator
SDS	Sodium Dodecyl Sulfate
Sly	SH3 Protein expressed in lymphocytes
SNARE	Soluble N-ethyl maleimide sensitive factor adaptor receptor
TCR	T cell receptor
Tet	Tetracycline
tetO	Tetracycline operator
TetR	Tetracycline repressor
tg	Transgenic
TGN	Trans Golgi network
TLR	Toll-like receptor
TNF	Tumor necrosis factor
TRAF	TNF Receptor Associated Factor
tTA	Tetracycline transactivator
UV	Ultraviolet
VAMP4	Vesicle Associated Membrane Protein 4
VEGF	Vascular endothelial growth factor
Vol	Volume
VP16	Herpes simplex virus protein 16
VSMC	Vascular smooth muscle cell
wt	Wild type